Coláiste na Tríonóide, Baile Átha Cliath
Trinity College Dublin
Ollscoil Átha Cliath | The University of Dublin

Peat bogs as archives of atmospheric metal pollution from natural and anthropogenic sources - A case study from Ireland

Ph.D. thesis

2018

Carolina Rosca

EU FP7 Marie Curie Training Network under REA grant agreement no. [608069] - Project ISONOSE (Isotopic Tools as Novel Sensors of Earth Surface Resources)

I declare that this thesis had not been submitted as an exercise for a degree at this or any other university and it is entirely my own work.

I agree to deposit this in the University's open access institutional repository or allow the library to do so on my behalf, subject to Irish Copyright Legislation and Trinity College Library condition of use and acknowledgement.

Carolina Rosca,

Dublin, September 12th, 2018

Peat bogs as archives of atmospheric metal pollution from natural and anthropogenic sources - A case study from Ireland

Carolina Rosca

Abstract

This research project combines various geochemical techniques to identify and characterise historic and recent sources of atmospheric metal pollution recorded in ombrotrophic peat bogs across Ireland.

In a first subproject, trace element concentrations and Pb isotope signatures are used to investigate a peat monolith from the Liffey Head bog in the Wicklow Mountains (Co. Wicklow, eastern Ireland). The results show significant heavy metal (Cu, Zn, Pb, Ag, Sb, Sn, Cd) perturbance during the local Pb-Zn mining and smelting activities (19^{th}-20^{th} century), with concentrations exceeding crustal abundances by far (e.g., 40-fold Pb, 80-fold Sb). Lead isotopes display the composition of the local lithology during the mining period of the 19^{th} century ($^{206}Pb/^{207}Pb$=1.183±0.013) but shift towards significantly less radiogenic values ($^{206}Pb/^{207}Pb$=1.138±0.011) in 1980, reflecting the wider use of leaded petrol in the northern hemisphere. Remarkably, the highest Pb pollution at this site is not associated with the use of leaded petrol rather than the historic metalliferous activity in the Wicklow uplands.

In the second subproject, evolution and sources of recent atmospheric metal pollution with emphasis on Zn are examined and compared in a near-urban environment (Liffey Head bog, Co. Wicklow, east coast) and a rural area (Brackloon wood, Co. Mayo, west coast of Ireland). A combination of trace metal systematics, radiogenic Pb- and stable Zn isotopes allows to distinguish pollution sources. A dominant influence from solid fossil fuel combustion (coal) can be inferred for west Ireland (Cr/Cd=12, Zn/Cd=96, at 0-1 cm) whereas increasing emissions from the wider deployment of liquid fossil fuels (oil, diesel, petrol) are recorded close to the urban area of Dublin in east Ireland (oil: Cu/Cd=57, Zn/Cd=300 at 0-1 cm). This interpretation is further supported by increasingly light Zn isotope signatures with sallower peat bog horizons ($\delta^{66}Zn/^{64}Zn$= from 0.53 to 0.18 ±0.03‰), readily explained by stronger traffic emissions through recent time.

In a third subproject, the geochemical record of the historic Laki 1783-4 volcanic eruption was identified and further examined in Brackloon wood peat bog horizons from western Ireland. This eruption record is expressed in excess metal concentrations of V, Ti, and Fe. Although these cannot unequivocally be attributed to an addition of basaltic cryptotephra at this depth, the higher concentrations of these elements in the separately investigated tephra shards compared to background peat support this hypothesis. Moreover, remarkably systematic correlations are observed for metal ratios such as Cu/Cd, Pb/Cd, Pb/Zn, Cu/Zn between the tephra-bearing layer and Laki aerosols previously detected in Greenland ice. These correlations point to a common volcanic aerosol signal originating from the Laki eruption. Although the high background in the peat monolith complicates a deconvolution of the S signal, subtle S enrichments at the depth of tephra deposition are attributed to addition of Laki 1783-4 volcanic aerosols. Altogether, the potential of peat bog archives to record volcanogenic metal deposition is demonstrated and dependent on background concentration levels.

Acknowledgements

The research leading to these results has received funding from the People Programme (Marie Curie Actions) of the European Union's Seventh Framework Programme FP7/2007-2013/ under REA grant agreement n° [608069].

I am grateful to my project supervisors Emma L Tomlinson and Balz S Kamber for obtaining the funding for this research investigation, and for giving me the opportunity to aspire to a PhD degree. This has been a life changing opportunity, and I would like to thank Emma and Balz for everything I learned from our journey together.

Several people have contributed significantly to this project with lab assistance, guidance, support, and discussions. A special thank you to Cora McKenna, Ronny Schoenberg, Walter Geibert, Michael Babechuk, Teresa Ubide, John Caulfield, Elaine Treacy, Paul Albert, Victoria Cullen, and David Chew. Further, I would like to express my gratitude to my PhD panel members: Quentin Crowley and Fraser Mitchell for their input and ideas to the project. I would also like to thank the geology department's technical and administrative staff Francis Hendron, Neil Kearney, Maura Morgan, and Sarah Guerin, for their constant support.

I am thankful to a bunch of amazing colleagues that made these three years at Trinity College Dublin memorable: Isadora, Clare, Hilde, Maurice, Brendan, Nils, Sabrina, Daniel, Paul, Claire, Meabh, Gary, Tadhg, Oakley, and especially Thomas for his friendship and help towards the end.

My sincere gratitude to my family; my parents Liudmila and Igor, my grandmother Maria, as well as my extended family members Elena, Vadim, Daniela, Galina, Vasile and Aliona, for their unconditional support in all my life and professional choices, understanding, and patience. I am extremely thankful for having them in my life.

Finally, I would like to thank Stephan for his time, encouragement, endurance, optimism, scientific discussions, and for believing in me whenever I failed at it. Without his moral support, I would have not completed this journey.

Table of Contents *page*

Abstract I

Acknowledgements II

Chapter 1: Introduction and motivation of the study 1

1. Introduction 1
2. Aims and objectives of this research investigation 3
3. Layout and themes of the thesis 4
4. Co-Author statement 6
5. References 8

Chapter 2: Context of the thesis 11

1. Processes of metal transfer to the atmosphere 11
2. Origin of metal input into the atmosphere 13
2.1. Natural sources of metals to the atmosphere 13
2.2. Anthropogenic sources of metals to the atmosphere 14
3. A summary of metallurgical activities in Ireland 16
3.1. Historical metallurgical activities (until the first half of the 20th century) 16
3.2. Recent metallurgical and non-metallurgical activities (20th century - today) 17
4. Geochemical tools to fingerprint atmospheric metal enrichment 17
4.1. The use of enrichment factors with respect to conservative elements 17
4.2. Lead isotope composition 18
4.3. Zinc isotope composition 21
5. General characteristics of peat as archive of atmospheric composition 25
5.1. The definition of peatlands 25
5.2. Mechanisms of metal retention in ombrotrophic peat bogs 27
5.3. Dating techniques applied for peat bogs 28
6. Peat bogs in Ireland 29
7. Mechanisms of metal retention using biomaterials 32
References 33

Chapter 3: Sampling sites and physical properties of the extracted monoliths 45

1. Geographical location and environmental setting of the sampling sites 45
1.1. Liffey Head bog, Co. Wicklow 45
1.2. Brackloon Wood, Co. Mayo 46
2. Sampling procedure 47
2.1. Methods applied for physical properties determination
2.1.1. Moisture, ash content, loss on ignition, and bulk density 48
2.1.2. Core scanning via ITRAX XRF 49

3. Physical properties of the two monoliths – results **50**
3.1. *The decomposition status of the bogs* 50
3.2. Moisture, ash content & bulk density of the LHB and BW peat monoliths *53*
3.3. ITRAX-XRF element intensities in LHB 54
4. Previous works and their findings on these sites **56**
4.1. Liffey Head bog, Co. Wicklow 56
4.2. Brackloon wood, Co. Mayo 57
References 59

Chapter 4: Trace element and Pb isotope fingerprinting of atmospheric pollution sources: A case study from the east coast of Ireland **61**

Abstract **62**
1. Introduction **63**
2. Background and methods **64**
2.1. Study area and sample collection 64
2.2. Analytical methods 65
2.2.1. Radiometric data and analysis 65
2.2.2. Moisture content, density, and LOI 67
2.2.3. Trace element and Pb isotope analyses 67
3. Results **68**
3.1. Peat properties 68
3.2. Radionuclide chronology reconstruction 70
3.3. Trace element data treatment 71
3.3.1. Principal component analysis (PCA) 71
3.3.2. Enrichment factors (EF) 72
3.4. Lead isotope compositions 73
4. Discussion **75**
4.1. Temporal patterns in metal enrichments and implications for element mobility within Liffey Head bog 75
4.2. Sources of metal pollution deposited into the LHB 76
4.2.1. Local background composition (100-62 cm) 77
4.2.2. Pollution phase 1 (62-25 cm, pre-1900 AD) 77
4.2.3. Pollution phase 2a (25-5 cm, ~1900-2000 AD) 78
4.2.4. Pollution phase 2b (4-0 cm, 2000-2015 AD) 81
4.3. Timing of Pb pollution and synthesis of Pb isotope information from other relevant peat archives 83
5. Summary and conclusions **84**
References 86
Appendices 95

Chapter 5: Combined zinc-lead isotope and trace-metal assessment of recent atmospheric pollution sources recorded in peat bogs from Ireland **107**

Abstract **108**
1. Introduction **109**
2. Background and site descriptions **112**
3. Methodology **112**
3.1. Liffey Head bog (LHB) - near-urban site 112
3.2. Brackloon wood (BW) - rural site 116
4. Results **117**
4.1. Morphological and physical properties of the peat profiles 117
4.2. Chronological constraints on the peat records 117
4.3. Geochemical characteristics of the peat profiles 118
5. Discussion **122**
5.1. Constraints on Zn mobility within the two archives 123
5.1.1. Liffey Head Bog 123
5.1.2. Brackloon wood 124
5.2. Defining sources of Zn and accompanying metals 125
5.2.1. Sources of metals onto LHB - near urban site 126
5.2.2. Sources of metals onto BW - rural site 130
5.3. The impact of road transport on the increasing atmospheric Zn pollution in Ireland 131
5.4. Comparison to other archives of geographic relevance and identification of long-range pollution fingerprints 132
6. Summary and concluding remarks **134**
References 135
Appendices 143

Chapter 6: Deposition of atmospheric heavy metals to the Irish peat following the Icelandic Laki 1783-1784 volcanic eruption **145**

Abstract **145**
1. Introduction **146**
2. Brackloon wood - area of investigation **147**
3. Anthropogenic activity in the area relevant for this study **147**
4. Methodology **148**
4.1. Tephra separation 148
4.2. Major element investigation via EDS-SEM and WDS-EMPA 148
4.2.1. In-situ major oxide analysis via WDS-EMPA 149
4.2.2. In-situ major element analysis via FE-SEM-EDS 149

4.3. Trace element investigation of tephra via LA-ICP-MS 150
4.4. Trace element investigation of peat via Qs-ICP-MS 153
4.5. Carbon-Nitrogen-Sulphur analyses 155
5. Results and Discussion **155**
5.1. Element mobility along the peat profile 155
5.2. Location and geochemical composition of the investigated tephra 156
5.3. The background composition of the peat 160
5.4. Calculating excess metal enrichment 162
5.5. The role of tephra in modifying bulk peat signatures 164
5.6. Composition of the Laki 1783-4 volcanic aerosols deposited onto Brackloon wood peat at the west coast of Ireland 165
5.6.1. Sulphur enrichment patterns along the peat monolith 165
5.6.2. Enrichments of other metals by Laki aerosol deposition 167
6. Summary and conclusions **171**
References 173

Chapter 7: Synthesis **177**

1. Summary and major findings of the thesis **177**
2. Suggestions for future studies **179**

CHAPTER 1

Introduction and motivation of the study

1. Introduction

Anthropogenic activity is linked to continuing disturbance of metal cycles at the Earth's surface since prehistoric times (Martínez Cortizas et al., 2005). Activities such as mining, smelting, fossil fuel burning, intensification of agricultural practices, urbanisation, and in a general sense, recent globalisation are linked to ongoing landscape modification and deterioration with significant accumulations of heavy metals (e.g., As, Hg, Pb, Cu, Cd, Ni, Co, Zn) in hydrologic, lithologic, and atmospheric systems close to the pollution source (Shotyk, 1988). The concentrations of these metals can sometimes exceed their natural abundance by several orders of magnitude, with potentially toxic or even vital effects for humans and ecosystems (Pacyna and Pacyna, 2001). Yet, not only low-latitude sites are affected by human activities; Long-range metal pollution is also evident from depositions onto distal ice and sediment archives of Antarctica (Wolff et al., 1999), the Arctic (McConnell and Edwards, 2008), Samoa (Arimoto et al., 1987), and New Zealand (Marx et al., 2014). The atmospheric metal enrichment load in these areas has increased by several orders of magnitude during the course of the past two centuries, with some metals (Zn, Cd, Cu) showing continuing aggravation in their concentration in upward trajectory.

Episodic natural events such as volcanic eruptions may also lead to punctuated enrichments in trace elements at the Earth's surface. Volcanic ejecta which is composed of aerosols and particulates (termed hereafter as particulate matter: PM) is associated with significant atmospheric release of volatile and semi-volatile elements such as S, Se, Hg, Zn, Pb, Cd, and Ag (e.g., Hong et al., 1996). These volcanic particulates are often preserved as well-defined layers in natural archives such as ice cores, snow cumulates, lake sediments and peat bogs. They are a robust chronostratigraphic marker and enable a correlation between sites (Lowe, 2011; Swindles et al., 2010). In addition, volcanic products which have a negative effect on our climate are used for qualitative and semi-quantitative investigations of environmentally significant volcanic eruptions throughout the Holocene. This is important for understanding the societal impact following massive volcanic eruptions and for assessing adequate preparatory measures for future natural hazards. Up to now, compositions of historic volcanic aerosols have been studied from ice core records only (e.g., Clausen et al., 1997; Dunbar, 2003; Hammer et al., 1980;

Pearce et al., 2004; Zielinski et al., 1997) which are very important for the study of such events at hemispheric scale, but do not give a view of dispersal away from the pole, e.g., above a certain area such a country or a continent.

Ombrotrophic (rain fed) peat bogs have become increasingly recognized as valuable archives of atmospheric metal deposition from natural and anthropogenic sources. Three pivotal characteristics make them ideal: i) the hydrological isolation from local ground- and surface waters, ensuring that their surface layers are exclusively fed by atmospheric inputs (i.e., dust, rain, snow, fog; ii) high abundance of natural complex-forming organic acids, enabling the preservation of metal-bearing particles despite their prevailing reducing pore-water pH (e.g., Roux and Shotyk, 2006), and iii) overall low hydro-conductivity which ensures minimised mobility of particles. Previous studies of peat cores from all around the world including Canada (e.g.,Kylander et al., 2009; Shotyk, 1992; Weiss et al., 2002), Europe (e.g., (Aubert et al., 2006; De Vleeschouwer et al., 2007 and references therein; Krachler et al., 2002; Le Roux et al., 2004; Martinez Cortizas et al., 2002; Shotyk, 1988; Shotyk et al., 2002), and South America (De Vleeschouwer et al., 2014) China (e.g.,Ferrat et al., 2012) and Australia (e.g., Marx et al., 2010) have linked the temporal variations in atmospheric metal records (Cu, Pb, Sb) to the industrial history and advances from the antiquity (e.g., Roman Empire, Chineze Bronze Age) to modern times. The pollution trajectories further demonstrate that the periods of Industrial Revolution (1800's - 1900's) and leaded petrol (1900's - 2000) have caused significant atmospheric heavy metal perturbations at hemispheric scale. Studies of more recent depositions, i.e., past 100 years (e.g., Marx et al., 2010; Weiss et al., 2007) have shown that while the pollution load of some elements, such as Pb and Cu, decreased over the course of 21st century, some others such as Zn, Cd, V, Mo are at their maximum level today. This implies either enhanced emissions from known origin, or a proliferation of new and relatively uncharacterised anthropogenic sources. In general, the behaviour of metals in ombrotrophic peat bogs is still poorly understood, which is due to a scarcity of studies investigating a broader range of elements in a given archive.

Pioneering studies of PM from anthropogenic activities recorded within the Irish peat bogs are relatively scarce and mainly focused on questions at a regional scale, often attributable to a single point source of contamination (e.g., mining from one-point source; Shell et al., 1997, Mighall et al., 2013). Further investigation is therefore required, particularly because the island is exposed to a complex weather system with both North Atlantic and North European influence, potentially carrying aerosols from as far as North America, Iceland and the UK.

Ireland's geographic position at Europe's north western periphery with dominating westerly Atlantic winds is prone to frequent atmospheric influx of volcanic PM from the active volcanoes of Iceland. Abundant rainfall facilitates near-continuous deposition of these particles at the surface, which are the ultimately incorporated into growing peat bogs. Existing peat core studies have identified a rich record of tephra (e.g., Hall and Pilcher, 2002), spanning the entire Holocene. However, relatively little work has been conducted into deciphering the details of tephra chemistry and none have attempted to measure volcanic aerosols of known eruptions preserved in peat archives.

2. Aims and objectives of this research investigation

The main research question of this PhD is to identify the main sources of metals in the Irish atmosphere and how these have changed over time. For this, various physical and geochemical tools are combined to assess the origin of historic and recent metal deposition from natural and anthropogenic sources onto actively growing ombrotrophic peat bogs from Ireland.

The first aim is set on reconstructing pollution excursions associated with the historically important Pb and Zn mining and smelting in the Wicklow uplands (east Ireland) operating during the 18th century until ca. 1940 (Rynne, 2015). For this, a peat monolith extracted from the Liffey Head bog in the Wicklow mountains is investigated for its trace element and Pb isotope composition. The second aim is the characterisation and comparison of recent (past ~150 years) pollution in a near-urban environment (Liffey Head bog, Co. Wicklow) and a rural site (Brackloon wood, Co. Mayo) at the west coast of Ireland. These investigations commonly aim at gaining new insights into the historic and recent atmospheric pollution over Ireland and complement the finding of related studies from relevant distance (Ireland, North America, North Europe). Here, we explore the possibility to combined trace element – radiogenic Pb – and stable Zn isotopes to trace sources of pollution.

Additionally, this research investigates the aerosol signal following the Icelandic Lakagígar (also known as Laki) eruption in 1783-1784 from its depositions onto the peat archive on the west coast of Ireland (Brackloon wood, Co. Mayo). This significant volcanic event and its aftermath was estimated to have emitted ca. 120 million tons of sulphur dioxide and hydrofluoric acid to the atmosphere, which ultimately decimated the Icelandic population by 25% (Grattan et al., 2003; Jacoby et al., 1999; Witham and Oppenheimer, 2004). Furthermore, a drop in the global temperatures resulted in two extreme winters in

Europe and North America and caused thousands of other fatalities related to famine due to crop failure.

The tephra layer at Brackloon wood has been initially described by Reilly and Mitchell (2015) who interpreted it as the ejecta of Lakagígar (Laki) 1783-1784 volcanic eruption on the basis of major oxide composition and cross-calibrations with Radiocarbon ages. Before that, it was believed that the ejecta of Lakagígar 1783-4 had not travelled as far south to reach Ireland. Here, we investigate the aerial deposits of this volcanic eruption in terms of its major and trace element composition as well as sulphur content, deposited in a peat archive from the west coast of Ireland. The main aim of this investigation is estimate the metal contribution to the peat bog following this eruption, and to explore the suitability of volcanic aerosols to serve as chronostratigraphic markers in peat archives.

3. Layout and themes of the thesis

The thesis is arranged to start with the background information and processes necessary for a general understanding of peat bogs as natural archives of atmospheric composition. The second chapter provides detailed site descriptions, as well as physical characteristics of the two monoliths from the Liffey Head bog, Co. Wicklow, and Brackloon wood, Co. Mayo. The core of this PhD thesis consists of two research manuscripts which build up the chapters 4, and 5, and a pilot study in manuscript form which forms Chapter 6. The thesis is closed with a synopsis (Chapter 7) of all major findings of this PhD research investigation together with suggestions for future works.

The first manuscript (**Chapter 4**), entitled: "**Trace element and Pb isotope fingerprinting of atmospheric pollution sources: A case study from the east coast of Ireland**" is currently under revision in the journal "*Applied Geochemistry"*. Main aims addressed in this study are:

- To evaluate the geochemical signal associated with the environmental pollution during the historic mining period of the 19^{th}-20^{th} century in the Wicklow uplands.
- To discriminate between aerial metal pollution originating from the mining and smelting activity from other sources, such as combustion of fossil fuels and agricultural activities.

Objectives:

1) *To extract an undisturbed peat sequence from the Liffey Head peat bog from the Wicklow mountains.*

2) *To reconstruct the chronology of the extracted peat core with a particular focus on the uppermost segment relevant for this study. The method based on the ^{210}Pb-^{241}Am radionuclide activity was considered most appropriate.*
3) *To obtain a high-quality data set of trace- and ultra-trace metal concentrations in the peat profile at high resolution (1 cm) via solution analyses (quadrupole-solution inductively coupled plasma mass spectrometry, Qs-ICP-MS).*
4) *To analyse the Pb composition of peat sub-samples via Qs-ICP-Ms with the main focus on the uppermost 20 cm.*

The second manuscript (**Chapter 5**), entitled "**Combined zinc-lead isotope and trace-metal assessment of recent atmospheric pollution sources recorded in peat bogs from Ireland**" is currently under review to the journal "*Science of the Total Environment".* Main aims of this research investigations are:

- To decipher sources of present day anthropogenic pollution in an urban and rural area of Ireland, with a special focus on increasing atmospheric Zn pollution during the past century.
- To explore the feasibility of the stable isotopic system of Zn to represent a tool of atmospheric pollution identification.
- To discuss implications of recent heavy metal pollution at hemispheric level.

Objectives:

1) *To extract two monoliths from different parts of the country with different anthropogenic histories. A near-urban site: Liffey Head bog, Co. Wicklow; and a rural site, Brackloon wood, Co. Mayo.*
2) *To produce a high-quality dataset of heavy metal composition in the uppermost sections of both monoliths via Qs-ICP-MS.*
3) *To analyse the Zn isotope composition of peat subsamples from the pre-polluted, near-urban site via double spike and multi-collector inductively coupled plasma mass spectrometry (MC-ICP-MS), and discuss the results in conjunction with the Pb isotopes.*

The pilot study (**Chapter 6**), entitled: "**Deposition of atmospheric heavy metals to the Irish peat following the Icelandic Laki 1783-1784 volcanic eruption**" was conducted with the following aims:

- To investigate whether the geochemical signal of the volcanic tephra can be identified in bulk peat from Ireland.
- To explore whether the aerosols emitted during this eruption were preserved in bulk peat.

- To explore the possibilities and limitations of using the volcanic aerosol signal as a chronostratigraphic marker in peat.

Objectives:

1) *To extract a peat monolith from the Brackloon wood site where this tephra layer was previously identified by Reilly and Mitchel (2015).*
2) *To separate the tephra from the peat via the method of* Blockley et al. (2005).
3) *To analyse the major oxide composition of the tephra shards via electron microprobe (EMPA) and additionally with scanning electron microscope with energy dispersive spectroscopy (SEM-EDS) for the extremely small shards.*
4) *To analyse the trace element assemblage of the tephra shards via laser ablation inductively coupled plasma mass spectrometry (LA-ICP-MS)*
5) *To analyse the trace element composition of bulk peat containing the tephra and without the tephra at high resolution via solution-ICP-MS.*
6) *To investigate the sulphur concentrations in the peat profile using a combustion elemental analyser (TruMac-Leco).*

4. Co-author statement

The core chapters (4-6) of this thesis were designed as research papers and are built as entities. Chapter 4 is currently under revision, and 5 is currently under review in scientific journals, while chapter 6 is presented as a manuscript draft. All manuscripts are multi-authored, with myself being the leader of these works. I wrote the manuscripts entirely. The role of the co-authors was to provide help and expert advice with sample collection and analytical procedures, as well as guidance for the data interpretation. Detailed contributions are explained below:

Walter Geibert, Institute for Marine and Polar research, Bremerhaven, Germany, provided guidance, analytical support, and interpretation of the radionuclide data of subsamples from the Liffey Head bog, Co. Wicklow.

Cora Anne McKenna, Trinity College Dublin, Ireland provided support for the trace-element analyses and data reduction.

Michael Babechuk, Laurentian University, Canada, provided support for the data reduction and interpretation of the trace elements.

Ronny Schoenberg, Eberhard Wilhelms University Tuebingen, Germany, provided all facilities for the chemical purification and analyses of zinc isotopes, as well as their interpretation.

Teresa Ubide and *John Caulfield*, University of Queensland, Brisbane, Australia were involved in the volcanic tephra analyses via SEM-EDX and LA-ICP-MS, conducted at the Trinity College, Dublin.

Balz Kamber, my second supervisor, provided guidance for the lead isotope analyses and reduction, as well as interpretation. Balz also provided editorial comments to the manuscripts.

Emma Tomlinson, my first supervisor, was the main discussion partner for the interpretation of the data and provided scientific and editorial comments to all manuscripts.

References

Arimoto, R., Duce, R. a., Ray, B.J., Hewitt, A.D., Williams, J., 1987. Trace elements in the atmosphere of American Samoa: Concentrations and deposition to the tropical South Pacific. J. Geophys. Res. 92, 8465. https://doi.org/10.1029/JD092iD07p08465

Aubert, D., Le Roux, G., Krachler, M., Cheburkin, A., Kober, B., Shotyk, W., Stille, P., 2006. Origin and fluxes of atmospheric REE entering an ombrotrophic peat bog in Black Forest (SW Germany): Evidence from snow, lichens and mosses. Geochim. Cosmochim. Acta 70, 2815–2826. https://doi.org/10.1016/j.gca.2006.02.020

Blockley, S.P.E., Pyne-O'Donnell, S.D.F., Lowe, J.J., Matthews, I.P., Stone, A., Pollard, A.M., Turney, C.S.M., Molyneux, E.G., 2005. A new and less destructive laboratory procedure for the physical separation of distal glass tephra shards from sediments. Quat. Sci. Rev. 24, 1952–1960. https://doi.org/10.1016/j.quascirev.2004.12.008

Clausen, H.B., Hammer, C.U., Hvidberg, C.S., Dahl-Jensen, D., Steffensen, J.P., Kipfstuhl, J., Legrand, M., 1997. A comparison of the volcanic records over the past 4000 years from the Greenland Ice Core Project and Dye 3 Greenland ice cores. J. Geophys. Res. Ocean. 102, 26707–26723. https://doi.org/10.1029/97JC00587

De Vleeschouwer, F., Gérard, L., Goormaghtigh, C., Mattielli, N., Le Roux, G., Fagel, N., 2007. Atmospheric lead and heavy metal pollution records from a Belgian peat bog spanning the last two millenia: Human impact on a regional to global scale. Sci. Total Environ. 377, 282–295. https://doi.org/10.1016/j.scitotenv.2007.02.017

De Vleeschouwer, F., Vanneste, H., Mauquoy, D., Piotrowska, N., Torrejón, F., Roland, T., Stein, A., Le Roux, G., 2014. Emissions from pre-Hispanic metallurgy in the South American atmosphere. PLoS One 9. https://doi.org/10.1371/journal.pone.0111315

Dunbar, N.W., 2003. Tephra layers in the Siple Dome and Taylor Dome ice cores, Antarctica: Sources and correlations. J. Geophys. Res. 108, 2374. https://doi.org/10.1029/2002JB002056

Ferrat, M., Weiss, D.J., Dong, S., Large, D.J., Spiro, B., Sun, Y., Gallagher, K., 2012. Lead atmospheric deposition rates and isotopic trends in Asian dust during the last 9.5kyr recorded in an ombrotrophic peat bog on the eastern Qinghai-Tibetan Plateau. Geochim. Cosmochim. Acta 82, 4–22. https://doi.org/10.1016/j.gca.2010.10.031

Grattan, J., Durand, M., Taylor, S., 2003. Illness and elevated human mortality in Europe coincident with the Laki Fissure eruption. Geol. Soc. London, Spec. Publ. 213, 401–414. https://doi.org/10.1144/GSL.SP.2003.213.01.24

Hall, V.A., Pilcher, J.R., 2002. Late-Quaternary Icelandic tephras in Ireland and Great Britain: Detection, characterization and usefulness. Holocene 12, 223–230. https://doi.org/10.1191/0959683602h1538rr

Hammer, C.U., Clausen, H.B., Dansgaard, W., 1980. Greenland ice sheet evidence of post-glacial volcanism and its climatic impact. Nature 288, 230–235. https://doi.org/10.1038/288230a0

Hong, S., Candelone, J.-P., Boutron, C.F., 1996. Deposition of atmospheric heavy metals to the

Greenland ice sheet from the 1783–1784 volcanic eruption of Laki, Iceland. Earth Planet. Sci. Lett. 144, 605–610. https://doi.org/10.1016/S0012-821X(96)00171-9

Jacoby, G.C., Workman, K.W., D'Arrigo, R.D., 1999. Laki eruption of 1783, tree rings, and disaster for northwest Alaska Inuit. Quat. Sci. Rev. 18, 1365–1371. https://doi.org/10.1016/S0277-3791(98)00112-7

Krachler, M., Mohl, C., Emons, H., Shotyk, W., 2002. Analytical procedures for the determination of selected trace elements in peat and plant samples by inductively coupled plasma mass spectrometry. Spectrochim. Acta - Part B At. Spectrosc. 57, 1277–1289. https://doi.org/10.1016/S0584-8547(02)00068-X

Kylander, M.E., Weiss, D.J., Kober, B., 2009. Two high resolution terrestrial records of atmospheric Pb deposition from New Brunswick, Canada, and Loch Laxford, Scotland. Sci. Total Environ. 407, 1644–1657. https://doi.org/10.1016/j.scitotenv.2008.10.036

Le Roux, G., Weiss, D., Grattan, J., Givelet, N., Krachler, M., Cheburkin, A., Rausch, N., Kober, B., Shotyk, W., 2004. Identifying the sources and timing of ancient and medieval atmospheric lead pollution in England using a peat profile from Lindow bog, Manchester. J. Environ. Monit. 6, 502–510. https://doi.org/10.1039/B401500B

Lowe, D.J., 2011. Tephrochronology and its application: A review. Quat. Geochronol. 6, 107–153. https://doi.org/10.1016/j.quageo.2010.08.003

Martinez Cortizas, A., Garcia-Rodeja, E., Pontevedra Pombal, X., Novoa Munoz, J.C., Weiss, D., Cheburkin, A., 2002. Atmospheric Pb deposition in Spain during the last 4600 years recorded by two ombrotrophic peat bogs and implications for the use of peat as archive. Sci. Total Environ. 292, 33–44. https://doi.org/10.1016/S0048-9697(02)00031-1

Martínez Cortizas, A., Mighall, T., Pontevedra Pombal, X., Nóvoa Muñoz, J.C., Peiteado Varela, E., Piñeiro Rebolo, R., 2005. Linking changes in atmospheric dust deposition, vegetation change and human activities in northwest Spain during the last 5300 years. Holocene 15, 698–706. https://doi.org/10.1191/0959683605hl834rp

Marx, S.K., Kamber, B.S., McGowan, H.A., Zawadzki, A., 2010. Atmospheric pollutants in alpine peat bogs record a detailed chronology of industrial and agricultural development on the Australian continent. Environ. Pollut. 158, 1615–1628. https://doi.org/10.1016/j.envpol.2009.12.009

Marx, S.K., Lavin, K.S., Hageman, K.J., Kamber, B.S., O'Loingsigh, T., McTainsh, G.H., 2014. Trace elements and metal pollution in aerosols at an alpine site, New Zealand: Sources, concentrations and implications. Atmos. Environ. 82, 206–217. https://doi.org/10.1016/j.atmosenv.2013.10.019

McConnell, J.R., Edwards, R., 2008. Coal burning leaves toxic heavy metal legacy in the Arctic. Proc. Natl. Acad. Sci. 105, 12140–12144. https://doi.org/10.1073/pnas.0803564105

Pacyna, J.M., Pacyna, E.G., 2001. An assessment of global and regional emissions of trace metals to the atmosphere from anthropogenic sources worldwide. Environ. Rev. 9, 269–298. https://doi.org/10.1139/er-9-4-269

Pearce, N.J.G., Westgate, J.A., Preece, S.J., Eastwood, W.J., Perkins, W.T., 2004. Identification of Aniakchak (Alaska) tephra in Greenland ice core challenges the 1645 BC date for

Minoan eruption of Santorini. Geochemistry, Geophys. Geosystems 5. https://doi.org/10.1029/2003GC000672

Reilly, E., Mitchell, F.J.G., 2015. Establishing chronologies for woodland small hollow and mor humus deposits using tephrochronology and radiocarbon dating. https://doi.org/10.1177/0959683614557571

Roux, G. Le, Shotyk, W., 2006. Chapter 9 Weathering of inorganic matter in bogs. Dev. Earth Surf. Process. https://doi.org/10.1016/S0928-2025(06)09009-2

Rynne, C., 2015. Industrial Ireland - An Archaeology. The Collins Press (9. Juli 2015), Cork.

Shell et al., 1997 Polution in USA, Ireland and Czech republic.pdf, n.d.

Shotyk, W., 1992. Natural and anthropogenic enrichments of arsenic through three Canadian ombrotrophic Sphagnum bog profiles. Arsen. Environ. Part I Cycl. Charact. 20, 381–401. https://doi.org/10.1016/0166-5162(92)90004-G

Shotyk, W., 1988. Review of the inorganic geochemistry of peats and peatland waters. Earth Sci. Rev. 25, 95–176. https://doi.org/10.1016/0012-8252(88)90067-0

Shotyk, W., Krachler, M., Martinez-Cortizas, A., Cheburkin, A.K., Emons, H., 2002. A peat bog record of natural, pre-anthropogenic enrichments of trace elements in atmospheric aerosols since 12 370 14C yr BP, and their variation with Holocene climate change. Earth Planet. Sci. Lett. 199, 21–37. https://doi.org/10.1016/S0012-821X(02)00553-8

Swindles, G., Vleeschouwer, F. De, Plunkett, G., 2010. Dating peat profiles using tephra: stratigraphy, geochemistry and chronology. Mires Peat 7, 1–9.

Weiss, D., Shotyk, W., Boyle, E.A., Kramers, J.D., Appleby, P.G., Cheburkin, A.K., 2002. Comparative study of the temporal evolution of atmospheric lead deposition in Scotland and eastern Canada using blanket peat bogs. Sci. Total Environ. 292, 7–18. https://doi.org/10.1016/S0048-9697(02)00025-6

Weiss, D.J., Rausch, N., Mason, T.F.D., Coles, B.J., Wilkinson, J.J., Ukonmaanaho, L., Arnold, T., Nieminen, T.M., 2007. Atmospheric deposition and isotope biogeochemistry of zinc in ombrotrophic peat. Geochim. Cosmochim. Acta 71, 3498–3517. https://doi.org/10.1016/j.gca.2007.04.026

Witham, C.S., Oppenheimer, C., 2004. Mortality in England during the 1783-4 Laki Craters eruption. Bull. Volcanol. 67, 15–26. https://doi.org/10.1007/s00445-004-0357-7

Wolff, E., Suttie, E., Peel, D., 1999. Antarctic snow record of cadmium, copper, and zinc content during the twen- tieth century. Atmos. Environ. 33, 1535–1541.

Zielinski, G.A., Mayewski, P.A., Meeker, L.D., Grönvold, K., Germani, M.S., Whitlow, S., Twickler, M.S., Taylor, K., 1997. Volcanic aerosol records and tephrochronology of the Summit, Greenland, ice cores. J. Geophys. Res. Ocean. 102, 26625–26640. https://doi.org/10.1029/96JC03547

CHAPTER 2

Context of the thesis

1. Processes of metal transfer to the atmosphere

Anthropogenic and natural sources both contribute metals to the atmosphere. Metals can be transported as aerosols and airborne particles, hereafter collectively termed as particulate matter (PM). Air suspended PM are removed from the atmosphere through wet and dry deposition processes. The emission-deposition path is illustrated in Figure 1 (Schroeder, 1987). The distance PM can travel through the atmosphere varies based on aspects such as the wind speed, altitude, precipitation, and most importantly, particle size (e.g., Zechmeister et al., 2003; Environmental Protection Agency, 2011).

Figure 1.

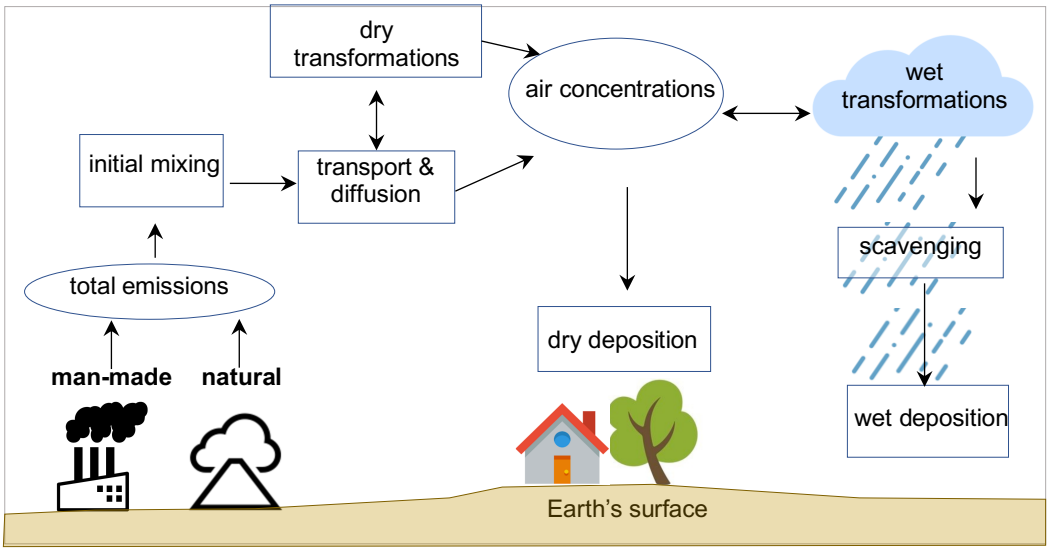


Fig. 1. Schematic illustration of the main atmospheric metal pathways from their initial emission to the deposition onto the surface. Picture modified after Schroeder (1987) and Cloy (2006).

In environmental geosciences, two particle sizes are widely monitored: PM_{10} and $PM_{2.5}$. PM_{10} are atmospheric particles with a diameter less than or equal to 10 micron (µm), while $PM_{2.5}$ is the subset of the PM_{10} particles with a diameter less than or equal to 2.5 µm. Particulate matter falling within the two size categories behaves differently in the atmosphere (Environmental Protection Agency, 2011). Coarse particles (>10 µm) have a relatively limited spatial impact and are thus expected to be deposited

close to their source. Small-size particles (10-0.1 µm) remain airborne for long periods and can be subjected to long-range transport, far from their original source. Figure 2 shows few examples of particle-sizes resulting from natural (sea salt nuclei, lithogenic dust) and anthropogenic activities (oil smoke, diesel emissions, Zn oxide fumes, metal fumes; modified after Muhlfeld et al., 2008), and the relative distance these particles can travel. Prominent examples of long-range metal transport from continental Europe to high-latitude areas are the depositions onto Greenland ice (Candelone et al., 1995; Hong et al., 1996; Rosman et al., 1997), and Arctic snow (Barrie, 1986; McConnell and Edwards, 2008). These archives show an increased PM load since the initiation of the Industrial Revolution in continental Europe until present. Another example is the increasing metal pollution in dry depositions near Bermuda, which reflects increasing PM transport from the North American continent (Arimoto et al., 2003). Thus, besides mirroring the increasing anthropogenic influence on pristine archives, the long-range metal transport also reflects pathways of air mass circulation (Martinez-Cortizas et al. 2002a).

Figure 2.

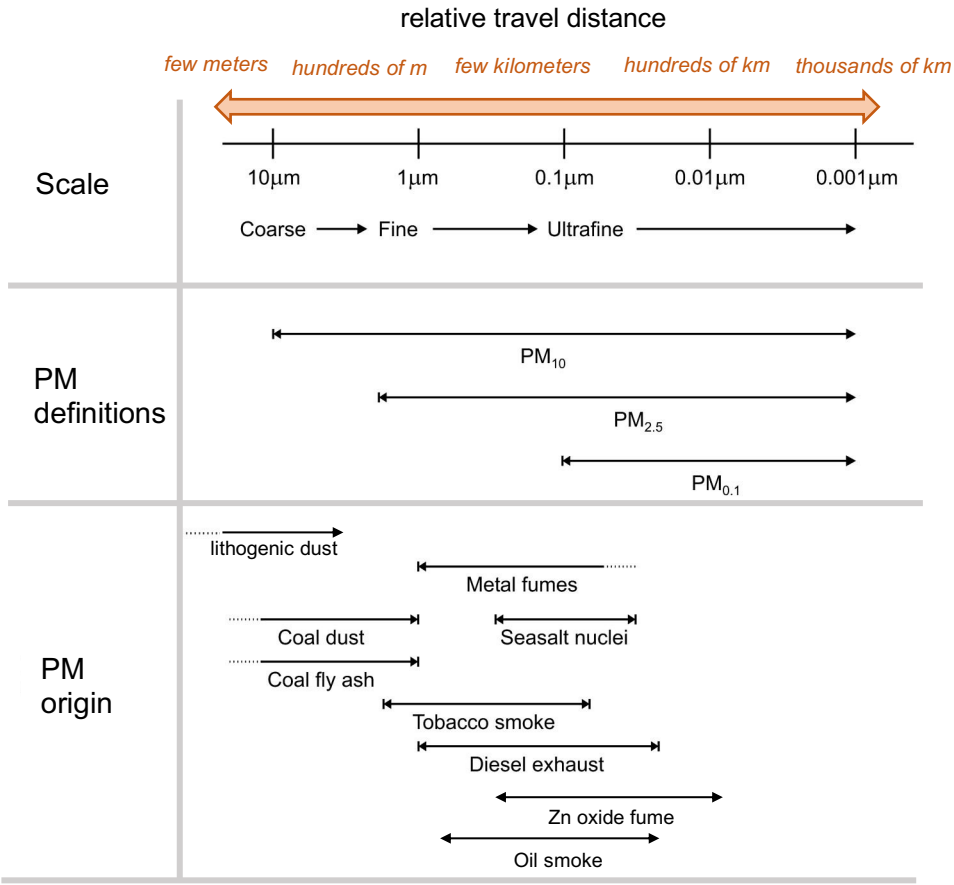


Fig. 2. Classification of particulate matter (PM) according to particle diameter, together with sources of the respective particles. Shown is also the relative distance these particles can travel. Figure slightly modified after Hinds (1999) and Mühlfeld et al. (2008).

2. Origin of metal input into the atmosphere

2.1. Natural sources of metals to the atmosphere

Detritus and soil dust represent the main lithogenic sources of metals to the atmosphere. Their availability and transport depend on several factors such as the degree of lithogenic erosion, vegetation cover, and wind. A prominent example of long-range dust circulation is the periodic transport of Saharan sand as far as South America (Brazil, every year, Formenti et al., 2001), North Europe and Australia (every couple of years, Guieu et al., 2002). Saharan dust circulation plays an important role for giant ecosystems such as the Amazon rainforest, where diversions from the annual particulate input are linked to significant biological changes (Rizzolo et al., 2016; Yu et al., 2015). Soil and sediment dust is the major supplier of lithogenic elements such as Al, Ti, Sc, Zr, Sr, and Y to the atmosphere, and their use in environmental studies is discussed in detail in section 4.1.

Volcanoes, i.e., volcanic eruptions and fumaroles are another significant episodic source of metals to the atmosphere, and especially of Hg and S (Oppenheimer, 2003; Pyle and Mather, 2003). It has been estimated that the annual amount of human released sulphur is higher than volcanic emissions during dormant periods (Mather et al., 2003). However, the load of anthropogenic S is almost insignificant if compared to the amount of sulphur released over the course of an eruption. In a recent study of the 2014 Bardarbunga volcanic eruption, Schmidt et al. (2015) have reported significant SO_2 injections in the lowermost troposphere transported to monitoring stations situated up to 2750 km away, as far as Ireland and central Europe. The volcanic burden was estimated to be at least a factor of 2 greater than the average atmospheric S cargo calculated from anthropogenic emissions from the entire Europe between 2007 and 2009. Another relevant example is the eruption of the Icelandic LAKI (as part of the volcanic suture centred around Grimsvötn) volcano in 1783-1784, which is considered to have been the most violent, extensive, and prolonged volcanic eruption in the northern hemisphere in the modern era (Grattan and Pyatt, 1994). Strong sulphuric acid signals in Greenland and Svalbard ice-cores associated with the Laki eruption were reported in several studies (Fiacco et al., 1994; Thordarson, 2003). Besides Hg and S, volcanic eruptions can be a significant source of other heavy metals such as Pb, Cd, Ag, Cu, and Zn (Hong et al., 1996). Volcanic ash particles and greenhouse gases (CO_2, SO_2, H_2S) bearing the metals during these events can have a significant impact on terrestrial ecosystems, climate change, and human health (e.g., Sigl et al., 2015).

Oceanic aerosols are an important geochemical source of Cl, Na, Ca, Mg, P, S, and Se to the atmosphere and coastal environments (Pernigotti et al., 2016). Their

concentration and composition can vary depending on the nature of the prevailing winds, as well as the composition or nature of the waters (i.e., aged or fresh waters), which are in turn dependant on the hydrological exchange between reservoirs.

2.2. Anthropogenic sources of metals to the atmosphere

Human activities are linked to metal release to the atmosphere since prehistoric times (Nriagu, 1989). Identifying and quantifying anthropogenically induced metal emissions to the atmosphere became progressively more difficult during the last century due to a rapid increase in the number of "diffuse" sources, such as various fuel products, advancements in modern technology, waste processing, and agricultural development. For a general idea about the magnitude of anthropogenic influence, world-wide metal emissions from human sources during the late 1990s are listed in Table 1. These are calculated based on statistical reports from different continents and compiled by Pacyna and Pacyna (2001). The principal anthropogenic sources of metals are considered to be:

1) *pyrometallurgical non-ferrous metal production* (such as mining, Pb production, Zn-Cd-, Cu-Ni -, REE production)
2) *steel and iron manufacturing*
3) *solid fossil fuel combustion* (such as coal, wood, peat)
4) *liquid fossil fuel combustion* (crude oil, and oil products such as heating oil, domestic utilities, kerosene, petrol, diesel)
5) *waste incineration* (municipal and industrial)
6) *phosphate fertilisers*
7) *cement production*
8) *urbanisation*

Table 1. Worldwide emissions of metals to the atmosphere from anthropogenic sources in the mid-1990s (in tons/year) from Pacyna and Pacyna (2001)

Source category	As	Cd	Cr	Cu	Hg	In	Mn	Mo	Ni	Pb	Sb	Se	Sn	Tl	V	Zn
Stationary fossil fuel combustion	809	691	10 145	7 081	1 475		9 417	2 642	86 110	11 690	730	4 101	3 517	1 824	240 084	9 417
Vehicular traffic										88 739						
Non-ferrous metal production	3 457	2 171	—	18 071	164	45	59	—	8 878	14 815	552	466	319	—	77	40 872
Iron and steel production	353	64	2 825	142	29	—	1 060	—	36	2 926	7	7	—	—	71	2 118
Cement production	268	17	1 335	—	133	—	—	—	134	268	—	3	—	—	—	2 670
Waste disposal	124	40	425	621	109	—	511	—	129	821	272	24	115	—	23	1 933
Other					325[a]											
Total	5 011	2 983	14 730	25 915	2 235	45	11 047	2 642	95 287	119 259	1 561	4 601	3 951	1 824	240 255	57 010
1983 emission[b]	18 820	7 570	30 480	35 370	3 560	25	38 270	3 270	55 650	332 350	3 510	3 510	3 790	5 140	86 000	131 880

[a] Emission of Hg from gold production.
[b] Nriagu and Pacyna (1988).

Metals such as Pb, Cu, Zn, Ni, Co, and Cd occur in high concentrations in sulphide ore deposits at the Earth's surface. These are often also enriched in elements such as Hg, Ag, Sb, Se, and As. During metal processing involving high temperature steps, a

fraction of these elements will enter the vapour phase and ultimately the ambient air (Nriagu and Pacyna, 1988). The volatility of elements plays an important role and governs the proportional distribution of the elements between the gas phase and the residuum or the end product. At the beginning of the 21st century, non-ferrous metal production continued to be the largest source of atmospheric As (69%), Cd (73%), Cu (70%), In (100%), and Zn (72%). Stationary fossil fuel combustion is considered the dominating atmospheric source, with coal specifically dominating emission of Cr (69%), Hg (66%), Mn (85%), Sb (47%), Se (89%), Sn (89%), and Tl (almost 100%), and oil combustion being the major source of V (almost 100%) and Ni (90%) (Pacyna and Pacyna, 2001). Not all metal enrichments occur naturally in these sources. A prominent example is the worldwide addition of tetraalkyl-Pb to gasoline during the 20th century to serve as an anti-knock agent. However, despite the abolition of leaded petrol in most of the countries of the world at the end of the 20th century, combustion of leaded- (parts of Asia), low-leaded, and unleaded gasoline continues to be a major source of Pb to the aerial environment today. Another "modern" example is the use of Zn-phosphates as oil lubricants and anti-wear additives in the automobile industry (Johnson and Hils, 2013). The magnitude of Zn emissions from this source has not been assessed yet. Nevertheless, depositions of heavy metals and especially Zn have been shown to strongly correlate with the population and traffic density of the areas of e.g., Florida, US (Callender and Rice, 2000), or Ulsan South Korea (Duong and Lee, 2011). Other studies have shown that street furniture, brake linings, rubber tyres, and tyre wear particles, collectively termed as "street dust" (Nriagu, 1989) also represent a major source of Zn of an unprecedented order (e.g., Councell et al., 2004; Falahi-Ardakani, 1984; Gonzalez et al., 2016; Legret and Pagotto, 1999; Muschack, 1990). This altogether points towards increasing pollution in urban and per urban areas with potential long-term effects for human health.

Emissions from phosphate fertilisers, cement production, and waste incineration are generally difficult to quantify at global scale due to lack of information from most countries, ultimately leading to an underestimation of the magnitude of their environmental impact (Pacyna et al., 2007). At continental scale, these sources are associated with high emissions of As, Cd, Pb, Sn, and Zn.

Road traffic is considered a very important source of heavy metals, inorganic particles and organic compounds to the atmosphere and immediate environment. A significant proportion of the heavy metal emissions, and especially Cd, Pb, Cu, Zn, Ni, Cr, and Hg originates from the combustion of fossil fuels (e.g., Beelen et al. 2008; Biswas et al. 2009; Walsh 2011). A variety of inorganic, metal-rich particles (steel, plastic, glass fibers) such as those resulting from vehicle wear (tire, body, clutch plates, erosion of the active layer of the catalytic converter, brake linings) and road

paint are usually deposited and accumulated up to toxic levels along the road margins and can be of significant threat to humans and ecosystems (e.g., Chan and Stachowiak 2004, Pagotto et al., 2001). For example, it is now well-recognized that tire wear dust is associated with significant release of Zn, Cd, As, Co, Cr, Cu, Hg, Mo, Ni, and Pb (Fukuzaki et al., 1986, Fauser et al., 1999, Adachia and Tainoshob, 2004, Schauer et al., 2006, and Hjortenkrans et al., 2007). In particular, Zn is the most abundant heavy metal resulting from tire wear because of its addition in form of ZnO and ZnS during vulcanization. Focused studies have shown that tires contain 1.3 - 1.7 % Zn (Ozaki et al., 2004), or 0.4 - 4.3 % Zn (Smolders and Degryse, 2002), and that on average 10 - 20 % of rubber enters the environment over a 3 years period due to abrasion (Baekken 1993; Lee et al. 1997; Legret and Pagotto 1999). The metal concentration levels in the immediate road environment depends on several aspects such as i) road features (roundabouts, motorway roads, and traffic lights, average speed allowed, Duong and Lee 2011), ii) the distance from the road edge, the iii) the investigated depth, and iv) type of material (soil, wetland, sediment, asphalt) serving as natural sink following wet and dry atmospheric deposition.

3. A summary of metallurgical activities in Ireland

3.1. Historical metallurgical activities (until the first half of the 20th century)

Earliest evidence of Cu activity in the south and south-eastern part of Ireland reaches back as far as the Bronze Age (2.400 and 2.000 BC, O'Brien, 1996) at Ross Island in Co. Kerry, and Co. Clare. These metallurgical activities are recognised as some of the oldest human activities in north-west Europe. However, it was not until the 17th and 18th centuries when the mining activities intensified significantly through the mining of Fe from the Carboniferous strata of the Midland basin and from bog ores (Rynne, 2015). As long as the charcoal resources permitted, smelting of Fe and, to a lesser extent, of Cu and Zn took place at the furnaces south of the Araglin River and Tallow (Co. Waterford), Drumshambo and Arigna Valley (Co. Roscommon), as well as Neath, near Swansea in Wales (UK). Triggered by the Industrial Revolution in the UK, the decades between the 18th and 19th century resulted in the discovery and opening of significant Cu, Pb-Zn, Ag, Au, Mn, barite ($BaSO_4$), and stibnite (Sb_2S_3) mines within the Wicklow uplands and surrounding valleys such as Avoca. Smelting of Pb and Ag ores took place at Ballycorus (Co. Dublin) and Glenmalure (Wicklow mountains), and although some of these extractions were short-lived, the Wicklow mountains were considered the centre of the Irish mining industry for approximately two centuries (Rynne, 2015). Sub-economic conditions resulted in the decommissioning of all mining activities in the area by 1940 AD. Today, Wicklow uplands are a cultural heritage area.

3.2. Recent metallurgical and non-metallurgical activities (20th century - today)

The political involvement of the state in the mineral exploitation sector, expressed by new tax reforms and the introduction of the "Minerals Development Act" at the beginning of the 20th century attracted a number of foreign exploration companies (mostly Canadian and Swedish) into the country (Rynne, 2015). This resulted in the discovery of several high-grade Pb-Zn deposits in Lower Carboniferous strata (as part of the Iapetus suture zone formed during the Caledonian orogeny, ca. 390 million years ago) at Abbeytown (Co. Sligo) and Tynagh (Co. Galway), the Cu-Ag-Hg deposits at Gortdrum, and the barite deposit at Ballynoe (Rynne, 2015). The climax of the Irish exploitation sector is represented by the discoveries of numerous first-class Zn-Pb deposits (Navan, Galmoy, and Lisheen) between 1970's and 1990. These resources, which covered 40% of the Zn and almost 20% of the European Pb production in 2003 placed Ireland on the international supplier map. Current Zn mining takes place only at Europe's largest Zn mine – Boliden Tara mines (Swedish company), with ore concentrates being exported to Sweden for smelting. Further significant, non-metallurgical exploitations are focused on gypsum (Co. Monaghan), dolomite (Co. Kilkenny), salt (Co. Antrim), marble (Connemara), fireclay, and silica.

4. Geochemical tools to fingerprint atmospheric metal enrichment

The following section offers information on the fundamentals of the geochemical techniques applied in this research, intended to provide the reader with the necessary background to understand their use in the succeeding chapters. More detailed and example related information is given in the respective chapter.

4.1. The use of enrichment factors with respect to conservative elements

A general understanding of the upper continental crust (UCC) elemental composition is essential for the interpretation of metal sources to the aerial environment. Although the local geology and its weathered products might vary significantly between sites, efforts have been made to calculate the element abundances at the Earth's surface (e.g., McLennan, 2001). In environmental forensics, crustal values are used as baseline to calculate the enrichment factors (EF) and proportion of metals originated from anthropogenic activities. In doing so, metal enrichments are discussed relative to the enrichment of lithophile elements (X), such as Ti, Sc, Sr, Zr, Al, Si, Y, or Ta (e.g., Espi et al., 1997; Kempter et al., 1997; Marx et al., 2010; Shotyk, 1996):

$$EF = (Metal/X)_{unknown} / (Metal/X)_{UCC} \quad [1]$$

Lithophile elements are generally accepted to maintain their initial state upon transport and re-deposition onto natural archives and are therefore considered conservative. Moreover, they do not originate, *per se*, from anthropogenic activities; the only indirect effects which promote lithogenic exposure and erosional processes emerge through activities such as open cast mining and landscape clearance for agricultural expansion and deforestation (e.g., Kylander et al., 2005; Lomas-Clarke and Barber, 2007; Martínez Cortizas et al., 2002; Weiss et al., 2002).

The use of the estimated UCC values as a measure for lithogenic input has been, however, intensively debated in several studies (e.g., Martínez Cortizas et al., 2002; Reimann and De Caritat, 2005). The main critical argument is that the calculated UCC values represent an average composition of rocks present at the Earth's surface, which does not necessarily consider the local lithology. This can ultimately result in an under- or overestimation of the lithogenic budget transported into an archive. To overcome this issue, some authors suggested a determination of the element EF's relative to a local "background", representative for the area of interest (e.g., Martínez Cortizas et al., 2002). In environmental archives covering a specific period, the background is represented by the segment displaying the lowest element concentrations which can be attributed to lithogenic dust input only (usually the deepest sections of an archive). Since concentrations of these elements are a quantitative indicator of lithogenic dust transport into the bog, an $EF_{backgr.}$ >1 will represent a change in the source of the elements (e.g., anthropogenic). This baseline proved more accurate than EF_{UCC}>1 which has been shown to be representative for areas dominated by long-range dust transport only (Martínez-Cortizas et al., 1997).

In view of the EF discrepancy and the complex Irish geology, element enrichment factors presented in this research study are calculated with respect to the background in the respective areas. Moreover, as element concentrations alone are incapable of disclosing information about the source(s), likewise background corrected metal ratios are presented.

4.2. Lead isotope composition

Metallurgical processing such as mining, smelting, and refining of Pb from metal sulphides together with the combustion of solid (e.g. wood, coal, peat) and liquid (e.g., oil, petrol) fossil fuels, municipal solid waste processing, and the use of mineral fertilisers are the major contributors of Pb to the atmosphere (e.g., Boutron, 1995; Ng and Patterson, 1981; Nriagu and Pacyna, 1988; Rosman et al., 1993). Emission

estimates have shown that anthropogenic Pb input is at least 1-2 orders of magnitude greater than inputs from natural sources (Komárek et al., 2008). Identifying sources and quantifying inputs of Pb pollution to the atmosphere is important for assessing the level of pollution and toxicity and for the initiation of regulatory actions.

Lead has four naturally occurring isotopes: ^{204}Pb (1.4%), ^{206}Pb (24.1%), ^{207}Pb (22.1%), and ^{208}Pb (52.4%). The isotopes 206, 207, and 208 are formed by the radioactive decay of the mother nuclides ^{238}U, ^{235}U, and ^{232}Th, respectively, while 204 is a primordial isotope. As this isotopic system is composed of three different decay chains, with i) significant differences in the half lives: 4.47×10^9, 7.04×10^8, and 1.4×10^{10}, respectively, and ii) different geochemical behaviours of U, Th, and Pb, the resulting Pb isotope ratio of the Pb bearing minerals and rocks will carry the individual genetic fingerprint of the original protolith.

Because the isotopic system of Pb contains only one stable isotope (^{204}Pb), there is no suitable isotope ratio that can be used for mass-bias correction necessary for isotope ratio determination using the Thermal ionisation mass spectrometry (TIMS). A possibility to overcome this issue is to enrich the sample with a double (e.g., Woodhead and Hergt, 1997) or triple (e.g., Galer, 1999) spike of known ratio in order to obtain accurate and precise data (e.g., Baker et al., 2004). Yet, due to the significant variability in ^{206}Pb/^{204}Pb, ^{207}Pb/^{204}Pb, and ^{208}Pb/^{204}Pb which emerge from large fractionation of U/Pb and Th/Pb at the Earth's surface, the analytical precision of multi-collector inductively coupled plasma mass spectrometry (MC-ICP-MS), without the addition of an isotopically enriched spike, is considered sufficient for addressing terrestrial research questions (e.g., Collerson et al., 2002). Alternatively, in order to correct for mass fractionation during the measurements, all sample unknowns and standards are doped with a ^{205}Tl/^{203}Tl enriched solution (e.g., NIST 997). Owing to the facts that i) both Tl isotopes are stable, ii) Tl shows a similar mass fractionation behaviour as Pb (e.g., Rehkämper and Metzger, 2000), and iii) their masses lie interleaved between the (204, 206, 207, and 208) Pb isotopes, an on-line internal drift correction can be successfully conducted.

In environmental geosciences, the isotope composition of Pb is commonly expressed through the ratios ^{206}Pb/^{207}Pb, ^{208}Pb/^{206}Pb, and ^{208}Pb/^{207}Pb (e.g., Monna et al., 1997). Among these, the ratio ^{206}Pb/^{207}Pb has been used the most because of its higher analytical precision and because it is the most sensitive to change; Thus, it can be used to distinguish between natural and anthropogenic sources (e.g., Komárek et al., 2008). Table 2 shows a compilation of Pb isotope ratios of relevant origins. In general, geologically old rocks and ores will carry a smaller proportion of radiogenic to non-radiogenic Pb, and also a lower concentration of ^{206}Pb with respect to ^{207}Pb than younger sources (e.g., Dickin, 1995). This is mainly because these rocks/ores became

physically and chemically separated from the crust long ago, giving rise to less radiogenic Pb (Doe, 1970; Shotyk et al., 2015). A prominent example is the use of Canadian and Australian Precambrian Pb ores for the manufacturing of leaded gasoline during the 20th century, which resulted in an overall atmospheric pollution with a less-radiogenic Pb signal ($^{206}Pb/^{207}Pb$=1.06-1.10, (Hansmann and Köppel, 2000). Other sources such as the Saharan dust (Grousset et al., 1994), coal (Farmer et al., 1999; Krause et al., 1993; Monna et al., 1997) display more radiogenic values ($^{206}Pb/^{207}Pb$>1.18, Bacon, 2002) than the majority of ore bodies. This enables discrimination between anthropogenic and natural Pb sources.

Lead has been shown to be immobile within Earth's surface archives, such as ombrotrophic peat bogs (in e.g., Belgium, Le Roux et al., 2004; Spain, Martínez Cortizas et al., 2002; Switzerland, Shotyk, 1996). This was also demonstrated by numerous workers based on Pb isotope compositions which correlate with historical inputs from known sources (e.g., Sweden, Brännvall et al., 1997; Scotland, Cloy et al., 2008; Farmer et al., 1997; Australia, Marx et al., 2010; Finland, Weiss et al., 2004). Altogether, the isotopic composition of Pb in peat archives implies that the system is not significantly affected by physio-chemical fractionation processes, neither during mineral extraction and purification, nor upon its deposition onto surficial archives.
Therefore Pb isotopes provide an efficient tool to determine sources and pathways of atmospheric pollution.

Table 2. Lead isotope composition of different anthropogenic and natural products

Origin	Material or product	$^{206}Pb/^{207}Pb$	$^{208}Pb/^{206}Pb$	Reference
NW Spain	peat bog (1)			Kylander et al (2010)
NW Spain	peat bog (2)			Kylander et al (2005)
Spain (pre pollution)	Aerosols	1.25		Kylander et al (2005)
	average ice records		1.21	Kylander et al (2010)
Spain	Penido Vello		1.26	Kylander et al (2010)
Switzerland	**Coal**		1.20	Chiaradia and Cupelin (2000)
Poland	Coal			DeVleeschouwer et al (2009)
UK	Coal	1.17		Sudgen et al (1993)
UK	Coal	1.18	2.47	Farmer et al (1999)
Portugal	Coal	1.18	2.47	Diaz-Somoano et al (2009)
Spain, New South	Coal	1.16	2.42	Diaz-Somoano et al (2009)
Wales, Australia	Broken Hill galena	1.04	2.31	Towsend et al (1998)
Australia	pre-Cambrian ore	1.03		Veron et al (1999)
Morocco	Pb ores	1.17		Veron et al (1999)
Sweden	Pb ores	1.02		Veron et al (1999)
UK	Pb ores	1.18		Sudgen et al (1993)
British Collumbia	Pb ores	1.16		Delves and Campbell (1993)

USA, S-Africa & Russia	Pb ores	1.15		Veron et al (1999)
average Europe	Pb ores	1.17		Regenberg et al (2002)
Switzerland	**leaded petrol**	1.08	2.12	Chiaradia and Cupelin (2000)
UK	1989-1991 leaded petrol	1.08		Sugden et al (1993)
South UK	1994 leaded petrol	1.06	2.33	Monna et al (1997)
Scotland	1989-1998 leaded petrol	1.08	2.36	Farmer et al (1999)
France	1980-1995 leaded petrol	1.08		Veron et al (1999)
France	1995 leaded petrol	1.06	2.35	Monna et al (1997)
Finland	gasoline	1.07		Keinonen (1992)
Israel	96 gasoline	1.22	2.15	Erel et al (1997)
Geneva, Switzerland	Aviation Petrol	1.09	2.35	Chiaradia and Cupelin (2000)
Geneva, Switzerland	Aviation Kerosene	1.08	2.36	Chiaradia and Cupelin (2000)
Switzerland	diesel 1997	1.08	2.15	Chiaradia and Cupelin (2000)
France	diesel 1997, Shell	1.11	2.38	Chiaradia and Cupelin (2000)
Taiwan	diesel 2012	1.11	2.12	Yao et al (2015)
Israel	**unleaded gasoline**	1.16	2.14	Erel et al (2001)
USA	unleaded gasoline 1997-1999	1.11		Hurst (2002)
Taiwan	unleaded gasoline 2012	1.19	2.10	Yao et al (2015)
Switzerland	1994-1995	1.14	2.42	Hansmann and Koppel (2000)
UK	1989	1.12	2.37	Veron et al (1999)
Uk	1989	1.10	2.43	Veron et al (1999)
UK	1997-1998	1.16	2.40	Bollhofer and Rosman (2002)
Switzerland	incinerator ashes	1.12	2.43	Hansmann and Koppel (2000)
France	1993-1996 incinerator shed	1.15	2.43	Mona et al (1997) Deboudt et al (1999)
		1.14	2.44	
France	1995 lead smelter	1.15	2.41	Deboudt et al (1999)
Switzerland	Incinerator ash	1.14	2.10	Chiaradia and Cupelin (2000)
Switzerland	Incinerator ash		2.10	Chiaradia and Cupelin (2000)
Switzerland	Heating oil	1.11	2.38	Chiaradia and Cupelin (2000)

Table 2. *(continued)*

4.3. Zinc isotope composition

The transition metal Zn is a building block in all six enzyme classes and regulatory proteins, demonstrating its important role in biological processes at the Earth's surface (Berg and Shi, 1996). Zinc is composed of five stable isotopes ^{64}Zn (48.63%), ^{66}Zn

(27.90%), ^{67}Zn (4.10%), ^{68}Zn (18.75%), and ^{70}Zn (0.62%), and the average atomic mass is 65.37777(22) (Ponzevera et al., 2006; Rosman and Taylor, 1998). In the natural environment, Zn has only one oxidation state of +2 and it is thus insensitive to isotope fractionation due to change in redox conditions.

Compared to Pb, Zn has received scientific interest during the last two decades, catalysed by advancements in analytical techniques and especially in the multicollector inductively coupled plasma mass spectrometry (MC-ICP-MS). Because of the small mass difference, and small isotopic variation of geological and biological materials at the Earth's surface (~2‰) the higher precision (<0.05‰ amu^{-1}, Maréchal et al. (1999) achieved with the MC-ICP-MS technique with respect to thermal ionization mass spectrometry (TIMS), (1-2‰ amu^{-1} Rosman, 1972) was an indispensable improvement towards resolvable discrimination between sources. The isotopic composition of Zn is expressed as the relative deviation from a standard reference, indicated as parts per 1000 (δ notation) and normalised to the most common isotope ^{64}Zn:

$$\delta^{66/64}Zn_{Sample} = \left[\frac{\left(^{66}Zn/^{64}Zn\right)_{Sample}}{\left(^{66}Zn/^{64}Zn\right)_{IRMM\text{-}3702}} - 1 \right] \times 1000$$

Where x corresponds to the masses 66, 67, 68, and 70.

Owing to the relatively high abundances of ^{64}Zn and ^{66}Zn, their analysis requires the highest analytical precision and data is presented as $\delta^{66/64}$Zn ratios in most studies. Pioneering studies have used the JMC Zn standard solution from the Lyon-CNRS laboratory (JMC_{Lyon}). However, as this standard solution is no longer available, recent Zn isotope ratio analyses are conducted relative to the monoelemental isotopic standard solution IRMM-3702 provided by the Institute for Reference Materials and Measurements (IRMM) (Cloquet et al., 2006). The $\delta^{66/64}$Zn composition of IRMM-3702 standard has been found to have an offset of -0.29±0.05‰ relative to the JMC_{Lyon} standard (Moeller et al., 2012) which allows a recalculation and thus consideration of previous studies in future discussions.

In order to correct for mass discrimination during the MC-ICP-MS analyses, and to correct for potential spectral and non-spectral isobaric interferences three different methods are applied: i) the standard sample bracketing technique, the ii) external normalisation, and the iii) the double spike technique (Cloquet et al., 2008). Several studies have addressed the advantages and disadvantages of the different techniques in more detail (e.g., Albarède, 2004; Archer and Vance, 2004; Bermin et al., 2006; Mason et al., 2004). Among these, the double-spike technique which is

defined by an addition of a respective amount of a solution enriched in two isotopes (usually ^{64}Zn-^{67}Zn) to the sample unknowns allows additional in-run correction for artificial fractionation caused by the chemical purification (Bermin et al., 2006). This correction method is based on either linear or exponential iterative solution (Compston and Oversby, 1969) and offers the lowest reported uncertainties (Moeller et al., 2012).

The main mechanisms considered to affect Zn isotope compositions at the Earth's surface are: the evaporation-condensation processes governed by Rayleigh dynamics, organic and inorganic adsorption, diffusion, and translocation (Cloquet et al., 2008). The magnitude of the isotope fractionation during the respective processes is illustrated in Figure 3.

Figure 3.

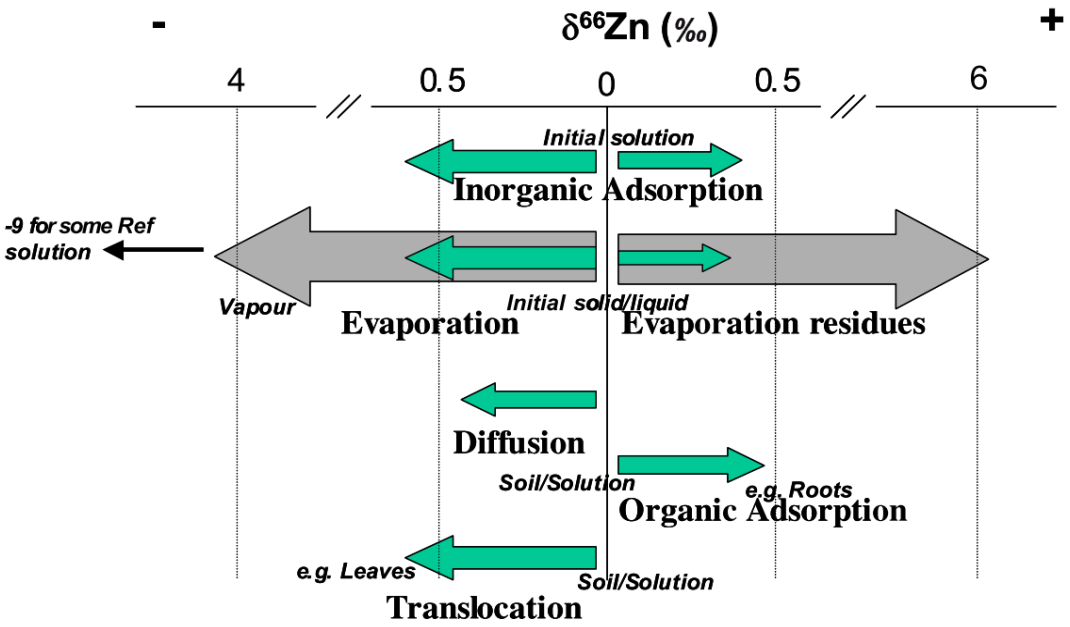


Fig. 3. The principal processes causing Zn isotope fractionation. The length of the arrows indicates the range of the observed δ^{66}Zn. The thin green arrows refer to fractionation caused by anthropogenic processes while the big gray arrows at evaporation are related to extraterrestrial materials. Figure from Cloquet et al. (2008)

In environmental studies, the application of Zn isotopes rests upon its status as one of the major pollutants in the atmosphere (Pacyna et al., 2007). Anthropogenic activities such mining, smelting, and fossil fuel combustion have been shown to significantly alter the concentration and isotope composition of Zn in the atmosphere (e.g., (Cloquet et al., 2006; Dolgopolova et al., 2006; Mattielli et al., 2009; Sivry et al., 2008; Sonke et al., 2008). Processes involving high temperature, and therefore evaporation-condensation, steps such as smelting, combustion, or electroplating produce the largest Zn isotope fractionation (Cloquet et al., 2008). Hereby, the lighter isotopes will

be preferentially volatilised into the gas and aerosol phase ($\delta^{66/64}$Zn<0‰) leaving the residues with an inherited heavy isotope signature ($\delta^{66/64}$Zn>0‰). Recent studies have demonstrated the possibility of distinguishing between different anthropogenic sources on the basis of Zn isotope composition of the emitted PM. Table 3 shows a compilation of the Zn isotope composition of different natural and anthropogenic sources relevant for this research investigation.

Table 3. Zinc isotope composition of different natural and anthropogenic sources

Type of material and origin	**$\delta^{66}Zn_{JMC}$** *(‰)*		**Reference**
	min	*max*	
Background peat	0.90		Weiss et al., 2007
Local dust	0.20		Weiss et al., 2007
Upper continental crust (UCC)	0.33		Little et al., 2014a
Worldwide average crustal rocks	0.20	0.50	Cloquet et al., 2008
Basalt	0.3	0.55	Archer and Vance 2004
Biotite-muscovite granite	-0.24	0.35	Dolgopolova et al 2006
Mineralised granite	-0.04	1.20	Dolgopolova et al 2006
Hornfels mineral	-0.39	0.26	Dolgopolova et al 2006
Loess from Western USA, China and	0.20	0.30	Othman et al., 2001
Jurassic rocks	0.60	0.90	Luck et al 1999
Manganese nodules	0.50	1.20	Marechal et al 2000
Marine carbonates and carbonated rocks	0.10	1.35	Pichat et al 2003
Black shales	1.10		Marechal et al 1999
Marine particles and deep surface	0.10	0.70	Marechal et al 1999
Black schist	0.85		Weiss et al 2007
Minerals (sphy, cpy, pyr)	0.10	0.50	Weiss et al 2007
Seawater	0.35		Taylor and McLennan
Ice accretions	-0.67	0.14	Voldrichova et al 2014
Lichens from a mining area (Russia)	0.40	1.40	Dolgopolova et al 2006
Soil from a larch forest Siberia	0.20		Viers et al., 2015
Mosses surface layers	0.14	0.20	Viers et al., 2015
Mosses bottom layers	0.50	0.70	Viers et al., 2015
Stem disc from a Larch, bark	0.73		Viers et al., 2015
Stem disc from a Larch, Sapwood	0.47		Viers et al., 2015
Stem disc from a Larch, bulk wood	0.36		Viers et al., 2015
Background (moss surface layers)	0.14	0.20	Viers et al., 2015
Peat bog sediment core early 20th century	0.30		Sonke et al 2008
Peat bog sediment core 1945-1950	0.14		Sonke et al 2008
Bus air filters and urban particulate matter	0.12		Cloquet et al 2006
Flue gases from city waste combustor	0.13		Cloquet et al 2006
Urbane waste incinerator & flue gases	0.07	0.19	Cloquet et al 2006
Lichens 2001 urban area France	-0.19	0.32	Cloquet et al 2006
Lichens 2003 urban area France	-0.15	0.50	Cloquet et al 2006
Automotive circulation	-0.20	-0.30	Cloquet et al 2006
Rainwater urban area France	-0.20	-0.10	Luck et al 1999
Rainwater rural area France	0.00	0.15	Luck et al 1999
Rainfall in French urban area (meteoric	0.18	0.20	Chen et al. 2008
Urban runoff France	-0.11	0.13	Chen et al. 2008
"common" anthropogenic aerosols	0.10	0.30	John et al 2007

Type of material and origin	$\delta^{66}Zn_{JMC}$ (‰)		Reference
	min	*max*	
Fly ash Czech Republic	0.16		Novak et al 2016
Atmospheric deposition Czech Republic	-0.40	0.29	Novak et al 2016
Tire wear France	0.04		Thapalia et al., 2010
Untreated wastewaters and sludge	0.28	0.33	Chen et al. 2008
Special high-grade Zn	0.14	0.31	John et al 2007
Zn metal dust purified by thermal distillation	0.09	0.19	John et al 2007
Zn metal shot purified electrochemically	0.22		John et al 2007
Galvanized steel	0.12	0.58	John et al 2007
Electroplated hardware	-0.56	-0.20	John et al 2007
Health products	0.09	0.24	John et al 2007
Leachate from Zn roofing	-0.10		Chen et al. 2008
Fly ash near base-metal smelter	-0.47		Novak et al 2016
Pb-Zn refinery (average)	-0.63	0.58	Mattielli et al 2009
Sphalerite from Navan ore body, Ireland	-0.32	0.23	Gagnevin et al., 2012
Basement whole samples Ireland	-0.05	0.20	Gagnevin et al., 2012
Lisheen, Irish midland ore field	-0.17	0.34	Wilkinson et al., 2005a
Late stage sphalerite sample Ireland	1.33		Wilkinson et al., 2005a
High temperature Zn ores	-0.44		Novak et al 2016
Low T ores (Mississippi valley Pb-Zn type)	0.16		Novak et al 2016
Coal Czech Rep.	-0.33		Novak et al 2016
Soft coal from Sokolov	-0.17		Novak et al 2016
Sphalerite from Olkusz (southern Poland)	0.02		Novak et al 2016
Primbram Sphalerite (central Czech Rep)	-0.23	-0.07	Novak et al 2016
Zinc ores from Slovakia	0.25		Novak et al 2016

Table 3 *(continued)*

5. General characteristics of peat as archive of atmospheric composition

5.1. The definition of peatlands

Peat is an actively growing, brownish-black organic deposit that forms under waterlogged conditions when the deposition rate of the organic matter is higher than the process of decomposition (e.g., Clymo, 2002). In its natural state, peat is made up of ca. 90% water and ca. 10% solid material (Kellner, 2003).

Today, almost 2% of the global landmass is covered by peat (Clymo, 1984). The development of peat was naturally initiated through the exposure of till after the retreat of the last ice sheets in the post-glacial period (10.000-8.000 years ago, Holocene, Hughes and Barber, 2003). A schematic illustration of the peat bog formation is provided in Figure 4. Peatlands are categorised into bogs, fens and marshes depending on factors such as topography, annual precipitation, botanical composition, nutrient status, erosion and humification rates (Purmalis and Klavins, 2012; Silamiķele et al., 2010; Steinmann and Shotyk, 1997). Fens and marshes are generally characterised as minerogenic (or topogenous), which means that they extract their nutrients via hydraulic systems such as rivers and/or ground water

horizons. These archives are usually nutrient rich, extending from acidic to alkaline, with pH values ranging from 4 to 9 (Clymo, 1983). Peat bogs, on the other hand, receive their nutrients solely via atmospheric depositions and are therefore classified as ombrotrophic (e.g., Shotyk, 1996). Thus, peat bogs are nutrient-poor acidic bodies with pH conditions ranging from 3.5 to 4.5 (Shotyk, 1988), but seasonal fluctuations are possible and have been linked to deviations from the pH norms. The general stratification of the peat bogs is comprised of the poorly decomposed upper layer, the *acrotelm* (0.2 to 0.8 m deep), and the heavily decomposed, and consolidated underlying layer, the *catotelm* (1 to 10 m deep). Due to its high porosity, the *acrotelm* has high hydraulic conductivity, and the decay of peat occurs via aerobic processes (Clymo, 1984). The *catotelm,* defined as bulk decomposed organic matter is permanently water saturated, and therefore has low hydraulic conductivity with anaerobic processes responsible for the biomass decay. The decay of plant matter expressed as a simple organic molecule (CH_2O) in the two peat segments as follows:

$$CH_2O + O_2 \rightarrow CO_2 + H_2O \qquad \text{(Aerobic)}$$

$$2CH_2O \rightarrow CH_4 + CO_2 \qquad \text{(Anaerobic)}$$

Both decomposition forms are accompanied by organic mass-loss in form of CO_2, which is released back to the atmosphere. The methane (CH_4) produced under anaerobic conditions within the *catotelm* represents the building block of amorphous humic acids, which are retained within the profile. The humic substances formed on decomposition have a great influence on the binding capacity of the metals within the peat profile (Livett, 1988). They are divided into different functional groups, with the principal ones being the phenolic-, carboxyl-, and alcoholic hydroxyl groups that serve as polyfunctional ligands. These complex and large humic molecules provide inner and outer positions for cation exchange and therefore sites for metal binding (Logan et al., 2008).

Figure 4.

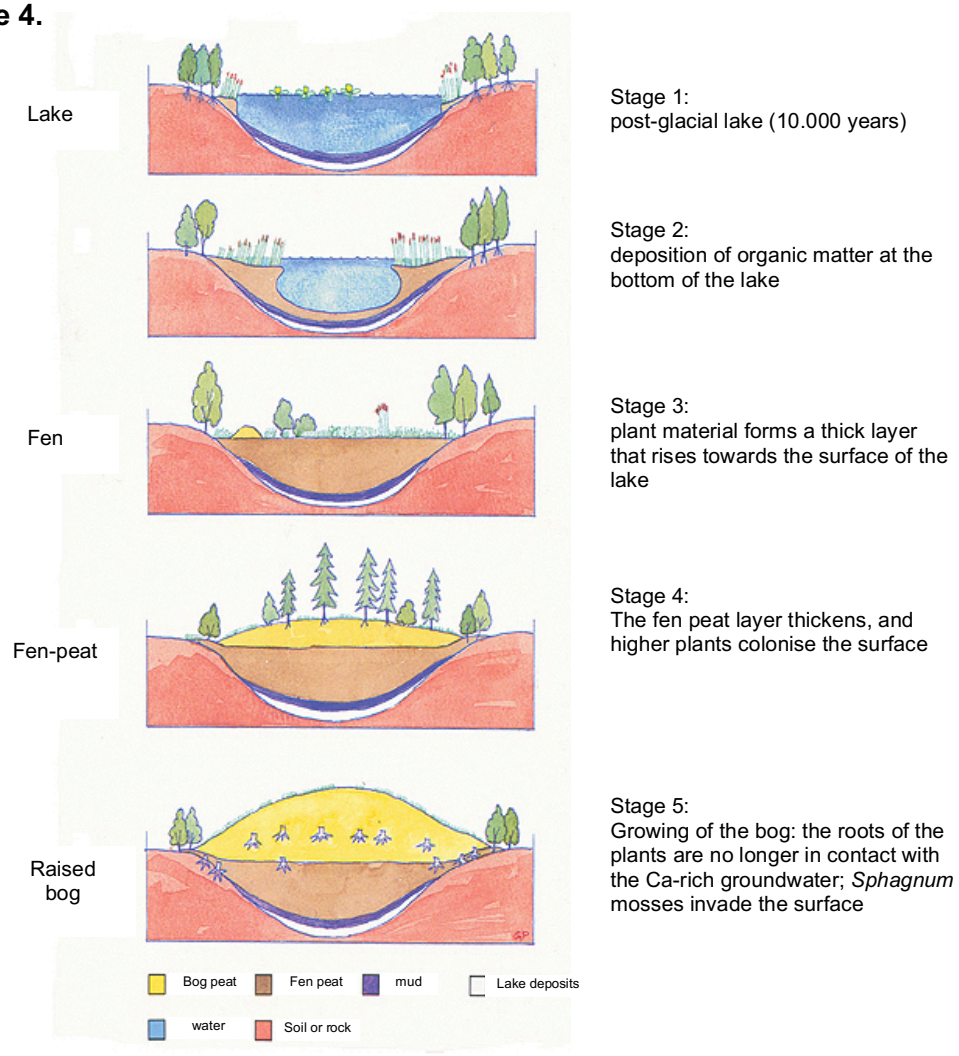


Fig. 4. Schematic illustration of raised peat bog development. Modified after a Figure from the website of the Irish peatland conservation council. (source: http://www.ipcc.ie/a-to-z-peatlands/raised-bogs/)

5.2. Mechanisms of metal retention in ombrotrophic peat bogs

The use of ombrotrophic peat bogs as archives of atmospheric deposition relies upon two important assumptions: i) a sole atmospheric input of elements and nutrients into the bog, and ii) immobile behaviour of elements and particles to enable a temporal reconstruction of the enrichment excursions (Hammond, 1978; Holynska et al., 1998; Shotyk, 1992, 1988; Zaccone et al., 2012). Because of the prevailing oxic conditions in the *acrotelm*, metal depositions occur in an environment of high redox potential. This means that metals will be present mainly as dissolved cations (e.g., Cu^{2+}, Pb^{2+}, Cd^{2+}, Zn^{2+}), which increases their availability for the uptake by the living *Sphagnum* moss. Although cations are potentially mobile in this form, the high abundance of dissolved organic matter has been shown to hinder elemental mobility in peat (Shotyk, 1988).

In the process of peat growth by accretion, the metals are gradually incorporated into the anaerobic *catotelm* - an area of low redox potential (Clymo, 1983). Here, the available metals form stable complexes with the humic substances. The resulting molecules are very large, hindering their mobility within the peat column. The binding strength between metals and humic acids depends on factors such as temperature, ionic strength, pH, as well as the concentration of the competing metals to a particular molecule site (Garcia-Mina, 2006). In his pioneering study, Clymo (1963) has shown that the strong metal binding capacities of mosses, and especially *Sphagnum* moss can be ascribed to their high amounts of ion exchange sites in the form of humic acids. Zechmeister et al. (2003) suggested that the metal retention onto moss follows the efficiency sequence Pb>Co,Cr>Cu,Cd,Ni,V>Zn>As. In examining the binding capacity of Cd, Cu, Pb, and Zn in organic matter Krosshavn et al. (1993) found out that Cu and Pb are absorbed at all pH levels (3-8), whereas Cd (II) and Zn (II) can sometimes compete with H^+ for the outer molecule sites, potentially resulting in 75-85% binding efficiency of the latter. Experiments conducted by Gao et al. (1999) also demonstrate a higher affinity of humic acids for Pb^{2+} with respect to Zn^{2+} and Cu^{2+}. However, as shown by Shotyk (1997) the retention of elements within a peat bog column is site specific and adequate examinations of the physical parameters are always necessary. Due to anoxic conditions within the lower parts of the *catotelm* the metals are expected to precipitate as sulphides, such as ZnS, CuS, PbS, CdS (e.g., Benoit et al., 1998). These precipitates are immobile and will likely stay at the depth of their coagulation within the peat archive. This altogether indicates that several chemo-physical factors, and possibly an interplay of these, are responsible for metal retention/mobilisation onto/from biological materials, and that additional information, such as chronology, and co-enrichment need to be evaluated when interpreting patterns of metal enrichment.

5.2. Dating techniques applied for peat bogs

Chronological constrains are necessary for the interpretation of peat bogs as archives of atmospheric deposition. The most common techniques applied for dating of geologically young, organic rich samples are: ^{14}C, ^{210}Pb-^{241}Am, and tephrochronology.

Carbon-14 is produced naturally in the atmosphere from the reaction of ^{14}N with neutrons produced by cosmic rays. Incorporated into CO_2 molecules, ^{14}C is taken up by plants through photosynthesis along with the stable isotopes ^{12}C and ^{13}C (Livett, 1988). The main advantages of the radiocarbon ^{14}C dating is its half-life of 5,730 ± 40 years which means that it can be used to date back as far as 50,000 years.

Lead-210 is a decay product of the inert ^{222}Rn gas, which is itself a by-product of the ^{238}U decay series. Due to its very short half-life: $T_{1/2}$= 22.5 yrs age information is often used to complement radiocarbon dating for the most recent period, i.e., last 100-150 to maximum 200 years in organic-rich archives (e.g., Oldfield et al., 1995, 1978). Several studies of cores from ombrotrophic peat bogs have shown good agreements between the chronology of naturally occurring ^{210}Pb and the calculated temporal variations (e.g., MacKenzie et al., 1997; Marx et al., 2010 and references therein), suggesting ^{210}Pb as promissing technique to date ombrotrophic bogs.

Americium-241 ($T_{1/2}$ = 432.2 yrs) is a radioactive isotope synthetically produced as a result of ^{239}Pu decay in nuclear weapon teststing from 1954, with peak fallout in 1963-4 as well as fallouts from the Tschernobyl reactor accident in 1986 (Appleby, 1998). Americium is accepted to be the least mobile in surficial deposits amongst the man-made radionuclides (e.g., Oldfield et al., 1995). It is also strongly particle-associated and highly immobile under low-pH conditions which prevail in the upper parts of ombrotrophic peat bogs (max. pH at the top of LHB=5). Combined with ^{210}Pb, it offers robust chronology of recent cumulates.

Volcanic eruptions are often accompanied by tephra emissions which can travel short (few hundred m) to very long distances (thousands of km) prior their deposition onto the surface. Once deposited, tephra layers provide isochronous markers in stratigraphic records, offering the possibility to date geological, palaeoclimatic or archaeological sequences (Froese et al., 2008; Lowe, 2011). The method of tephrochronology relies upon four critical factors: i) the stratigraphic “law of superposition” in order to permit a correlation between deposits at different sites, ii) an immobile behaviour of tephra shards within the peat profile (Langdon and Barber, 2004), iii) it requires that tephra layers can be geochemically characterised in order to be used as “fingerprints” of a particular event (Hall and Pilcher, 2002), and that iv) tephra layers from different volcanic sources (e.g., North Atlantic province) can be distinguished geochemically (Pilcher and Hall, 1992). Once identified, volcanic tephra layers offer the most robust chronological information, i.e., lowest uncertainty from all techniques (Lowe, 2011).

6. Peat bogs in Ireland

Ireland has the second-highest proportion of peat cover in the EU (~1,200,000 hectares), after Finland, and represents one of the few countries where a range of peatlands still exist in natural state (Hammond, 1978). Within this, three basic peat formations are recognized: *i)* raised bogs of the central plain, *ii)* blanket bogs dominating the western seaboard and the upland areas, and *iii)* fen peats (Hammond,

1981). In the following, we focus on the raised and blanket bogs as these two sub-categories have proved adequate for the reconstruction of atmospheric composition. To a large extent, the characteristics described below are also representative for peat bogs all around the world. A simplified distribution map of peat bog areas in Ireland is shown in Figure 5.

Raised bogs are characterised by a domed morphology which is raised above all surrounding soil and water areas. They started to form at the bottom of water-filled basins of glacial clays left behind after the retreat of the last glacial moraines, 15k-10k years ago. With continuing biomass accumulation, the water-filled basins were overgrown by vegetation, resulting in the gradual transformation of the bog from minerogenic to ombrotrophic in upward direction (e.g., Hammond, 1978). The majority of raised bogs in Ireland occur on land below 130 m a.s.l. and in a climatic zone where the rainfall is between 800 and 900 mm yr^{-1}. Their vegetation is composed of mosses, sedges, and heathers, which are adapted to acidic, nutrient poor, and waterlogged conditions (*source: Irish peatland conservation council*).

Blanket bogs cover large flat areas at the west coast of Ireland and upland areas, such as the Wicklow mountains in the east. This type of bog forms on top of minerals soil as a result of extensive erosion and leaching of surface layers through heavy and constant rain fall. In Ireland, the initiation of blanket bogs is ascribed to extensive deforestation by the first humans habiting the island (ca. 9.000 years ago) and therefore is an indirect effect of anthropogenic landscape modification. Most of the Irish blanket bogs are around 6000-8000 years old, with an average accumulation rate of ca. 0.6 mm yr^{-1}. (range: 0.1-1.2, Hammond, 1981). These accumulation rates are comparable with those of peatlands from other sites within the northern hemisphere which accumulate slowly at about 1 mm per year (Keddy, 2010): Scotland (0.7 - 1.1 mm yr^{-1}, Farmer et al., 1997; Küttner et al., 2014), but are somewhat lower than those established for Finish bogs (0.8 - 3.2 mm yr^{-1} Rausch et al., 2005). In general, accumulation rates are higher in the upper part of the peatland which is due to the minimum compression of the slowly decomposing acrotelm. Although blanket bogs are generally considered ombrotrophic, their occurrences in shallower regions means that they can occasionally receive terrigenous and lithogenic influx from the surrounding geology and soil.

A generalised stratigraphy of the Irish peat bogs includes an upper layer of actively growing *Sphagnum* moss, followed by a layer of poorly to variably humified *Sphagnum* peat, the acrotelm, with *Calluna* remains and *Eriophorum* fibres which overlie a basal layer of woody and fen plant remains, the *catotelm* (Hammond, 1981). The additional floristic gradient can vary between blanket and raised bogs, between montane blanket bogs on the west compared to the east coast, and between highland

and lowland blanket bogs. Although human impact over the last few centuries lead to a dramatic landscape alteration (extensive deforestation), including peat surfaces, numerous Irish peat sites still exist in natural state (Mitchell et al. 1998) and are under protection.

Due to its proximity to Iceland with its active volcanoes, several cryptotephra deposits from distinctive eruptions throughout the Holocene have been found in Irish peat (e.g., Hall and Pilcher, 2002; Pilcher et al., 1995; Pilcher and Hall, 1992; Plunkett et al., 2004; Rea et al., 2012). Tephra layers are valuable chronostratigraphic markers in palynological (e.g., Cole and Mitchell, 2003) and archaeological (Lomas-Clarke and Barber, 2007, 2004) studies and to establish chronologies between sites across the island (e.g., Reilly and Mitchell, 2015).

Figure 5.

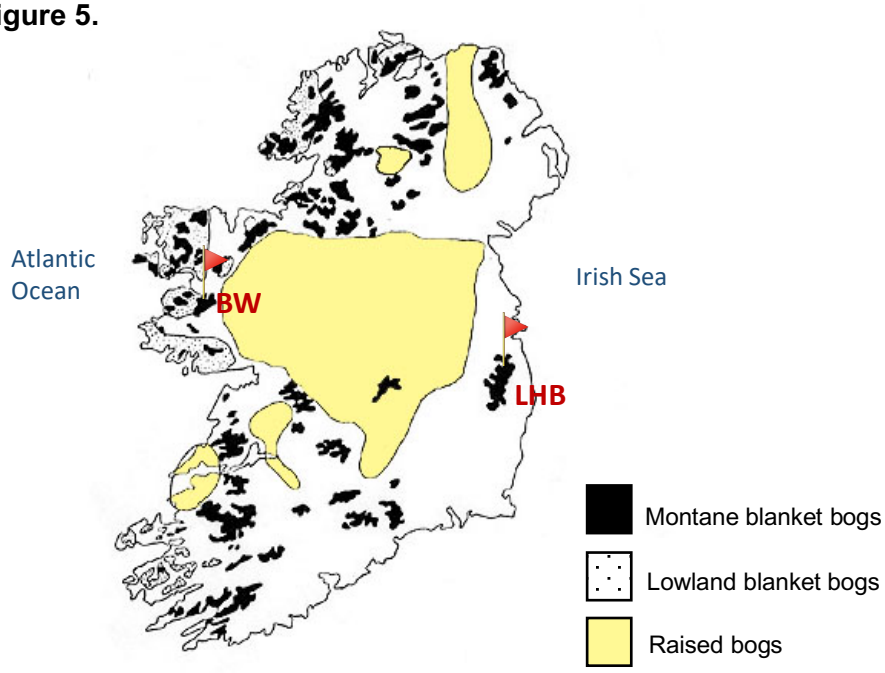


Fig. 5. Distribution of montane blanket bogs (black areas), lowland blanket bogs (dotted areas), and main concentration of the raised bogs (yellow are) in Ireland. Source: Irish peatland conservation council (http://www.ipcc.ie/a-to-z-peatlands/raised-bogs/). The two red flags represent the location of the two bogs investigated in this study: Liffey Head bog (Co. Wicklow, east coast) and Brackloon wood (Co. Mayo, west coast).

7. Mechanisms of metal retention using biomaterials

Developing mechanisms for metal extraction is important especially at sites known as "focal zones" for atmospheric and environment pollution with heavy metals. Such areas are, for example, main motorways and industrial districts - often associated with potential harm to wildlife and aquatic environment. A plethora of studies have focused on metal pollution, its consequences, and mitigation technologies during the past 30 years.

Convetional methods applied for metal sequestration and mitigation from aqueous solutions include filtration, membrane technologies, ion exchange, chemical precipitation or oxidation, and electrochemical treatment (e.g., Zhang and Banks, 2005). These methods can be, however, ineffective or expensive in certain circumstances (e.g., exceeding concentrations), and therefore techniques deploying living plants and/or biosorbents have developed significantly during the past 20 years. The experimental setup is based on the abilities of plant species to accumulate all or selective heavy metals through foliar absorption or root uptake, and/or passive metal binding to decomposed plant biomass (carboxyl-molecules) from aqueous solution (e.g., road runoff, Davis et al., 2003).

Investigations of heavy metal adsorption in soil close to a major highway in France conducted by Pagotto et al. (2001) have shown that Cd was the most easily exchangeable element with respect to physical and chemical conditions, but the quantities involved (efficiency) remained small. Lead and Cu were the least mobile elements, while Zn and Cd extraction from the soil was most efficient using acids with pH 2-4. Because surficial soil pH is usually >4, these authors concluded that Zn and Cd will usually remain adsorbed onto the soil and only events such as acid rains and accidental chemical spillage can lead to significant mobilization of these two metals.

The long-term performance (6 and 9 years) of a constructed wetland treating system along a motorway in Ireland has been investigated by Gill et al. (2014) and Gill et al. (2017). In these studies, a metal mass balance throughout the "*inlet - wetland - outlet*" system was performed. The authors found out that Cu, Pb and Zn showed much higher deposition at front of system, and that this method achieved an apparent removal efficiency of 5% for Cd, 60% for Cu, 31% for Pb, and 86% for Zn. The later was explained to emerge through the bio-essential role of Zn to plants and organisms in general, and through Zn absorption onto Fe-Mn hydroxides at root surface.

Although ombrotrophic peatlands receive their nutrients solely from atmospheric sources, meaning that some of the abovementioned post-depositional processes do not apply (e.g., runoff), these experimental studies offer some useful insights into the behavior of some metals in general and will be considered later on in the discussion.

References

Albarède, F., 2004. The Stable Isotope Geochemistry of Copper and Zinc. Rev. Mineral. Geochemistry 55, 409–427. https://doi.org/http://dx.doi.org/10.2138/gsrmg.55.1.409

Appleby, P.G., 1998. Dating recent sediments by 210Pb: Problems and Solutions. Stuk a-145,7-24.

Archer, C., Vance, D., 2004a. Mass discrimination correction in multiple-collector plasma source mass spectrometry: an example using Cu and Zn isotopes. J. Anal. At. Spectrom. 19, 656. https://doi.org/10.1039/b315853e

Archer, C., Vance, D., 2004b. Mass discrimination correction in multiple-collector plasma source mass spectrometry: an example using Cu and Zn isotopes. J. Anal. At. Spectrom. 19, 656. https://doi.org/10.1039/b315853e

Arimoto, R., Duce, R.A., Ray, B.J., Tomza, U., 2003. Dry deposition of trace elements to the western North Atlantic. Global Biogeochem. Cycles 17. https://doi.org/10.1029/2001GB001406

Bacon, J.R., 2002. Isotopic characterisation of lead deposited 1989-2001 at two upland Scottish locations. J. Environ. Monit. 4, 291–299. https://doi.org/10.1039/B109731H

Baker, J., Peate, D., Waight, T., Meyzen, C., 2004. Pb isotopic analysis of standards and samples using a 207Pb-204Pb double spike and thallium to correct for mass bias with a double-focusing MC-ICP-MS. Chem. Geol. 211, 275–303. https://doi.org/10.1016/j.chemgeo.2004.06.030

Barrie, L.A., 1986. Arctic air pollution: An overview of current knowledge. Atmos. Environ. 20, 643–663. https://doi.org/10.1016/0004-6981(86)90180-0

Benoit, J.M., Fitzgerald, W.F., Damman, A.W.H., 1998. The biogeochemistry of an ombrotrophic Bog: Evaluation of use as an archive of atmospheric mercury deposition. Environ. Res. 78, 118–133. https://doi.org/10.1006/enrs.1998.3850

Berg, J.M., Shi, Y., 1996. The Galvanization of Biology: A Growing Appreciation for the Roles of Zinc. Science (80-.). 271, 1081–1085. https://doi.org/10.1126/science.271.5252.1081

Bermin, J., Vance, D., Archer, C., Statham, P.J., 2006. The determination of the isotopic composition of Cu and Zn in seawater. Chem. Geol. 226, 280–297. https://doi.org/10.1016/j.chemgeo.2005.09.025

Bollhöfer, A., Rosman, K.J.R., 2001. Isotopic source signatures for atmospheric lead: The Northern Hemisphere. Geochim. Cosmochim. Acta 65, 1727–1740. https://doi.org/10.1016/S0016-7037(00)00630-X

Boutron, C.F., 1995. Historical reconstruction of the earth's past atmospheric environment from Greenland and Antarctic snow and ice cores. Environ. Rev. 3, 1–28. https://doi.org/10.1139/a95-001

Brännvall, M.-L., Bindler, R., Emteryd, O., Nilsson, M., Renberg, I., 1997. Braennvall et al. (1997) Water, Air and Soil Pollution, 100-3-4.pdf. Water. Air. Soil Pollut.

Callender, E., Rice, K.C., 2000. The urban environmental gradient: Anthropogenic influences on the spatial and temporal distributions of lead and zinc in sediments. Environ. Sci. Technol. 34, 232–238. https://doi.org/10.1021/es990380s

Candelone, J.-P., Hong, S., Pellone, C., Boutron, C.F., 1995. Post-Industrial Revolution changes in large-scale atmospheric pollution of the northern hemisphere by heavy metals as documented in central Greenland snow and ice. J. Geophys. Res. 100, 16605. https://doi.org/10.1029/95JD00989

Chen, J., Gaillardet, J., Louvat, P., 2008. Zinc isotopes in the Seine River waters, France: A probe of anthropogenic contamination. Environ. Sci. Technol. 42, 6494–6501. https://doi.org/10.1021/es800725z

Chiaradia, M., Cupelin, F., 2000. Behaviour of airborne lead and temporal variations of its source effects in Geneva (Switzerland): Comparison of anthropogenic versus natural processes. Atmos. Environ. 34, 959–971. https://doi.org/10.1016/S1352-2310(99)00213-7

Cloquet, C., Carignan, J., Lehmann, M.F., Vanhaecke, F., 2008. Variation in the isotopic composition of zinc in the natural environment and the use of zinc isotopes in biogeosciences: A review. Anal. Bioanal. Chem. 390, 451–463. https://doi.org/10.1007/s00216-007-1635-y

Cloquet, C., Carignan, J., Libourel, G., 2006. Isotopic Composition of Zn and Pb Atmospheric Depositions in an Urban / Periurban Area of Northeastern France. Environ. Sci. Technol. 40, 6594–6600.

Cloy, J.M., 2006. Chemical Records of Environmental Pollution in Ombrotrophic Peat Bogs. PhD Thesis The University of Edinburgh.

Cloy, J.M., Farmer, J.G., Graham, M.C., MacKenzie, A.B., Cook, G.T., 2008. Historical records of atmospheric Pb deposition in four Scottish ombrotrophic peat bogs: An isotopic comparison with other records from western Europe and Greenland. Global Biogeochem. Cycles 22, 1–16. https://doi.org/10.1029/2007GB003059

Clymo, R.S., 1963. Ion exchange in Sphagnum and its relation to bog ecology, *Annals of Botany, 21,* 309-324.

Clymo, R.S., 1983. Peat. Mines swamp, bog, fen moor. Gen. Stud. Vol.A. 159–224.

Clymo, R.S., 1984. The Limits to Peat Bog Growth. Philos. Trans. R. Soc. B Biol. Sci. 303, 605–654. https://doi.org/10.1098/rstb.1984.0002

Clymo R.S., Oldfield F., Appleby P.G., Pearson G.W., Ratnesar P. and Richardson N., 1990, The record of atmospheric deposition on a rainwater-dependent peatland, Philosophical Transactions of the Royal Society of London, B327, 331-338.

Cole, E.E., Mitchell, F.J.G., 2003. Human impact on the Irish landscape during the late Holocene inferred from palynological studies at three peatland sites. Holocene 13, 507–515. https://doi.org/10.1191/0959683603hl616rp

Collerson, K.D., Kamber, B.S., Schoenberg, R., 2002. Applications of accurate, high-precision Pb isotope ratio measurement by multi-collector ICP-MS. Chem. Geol. 188, 65–83. https://doi.org/10.1016/S0009-2541(02)00059-1

Compston, W., Oversby, V.M., 1969. Lead Isotopic Analysis Using a Double Spike. J. Geophys. Res. 74, 4338–4348. https://doi.org/10.1029/JB074i017p04338

Councell, T.B., Duckenfield, K.U., Landa, E.R., Callender, E., 2004. Tire-wear particles as a source of zinc to the environment. Environ. Sci. Technol. 38, 4206–4214. https://doi.org/10.1021/es034631f

Davis, T.A., Volesky, B.,Mucci, A., 2003. A review of the biochemistry of heavy metal biosorption by brown algae. *Water Res.*, **37**, 4311-4330.

De VleeSchouwer, F., Le Roux, G., Shotyk, W., 2010. Peat as an archive of atmospheric pollution and environmental change: A case study of lead in Europe. PAGES Mag. 18, 20–22.

Deboudt, K., Flament, P., Weis, D., Mennessier, J.P., Maquinghen, P., 1999. Assessment of pollution aerosols sources above the Straits of Dover using lead isotope geochemistry. Sci. Total Environ. 236, 57–74. https://doi.org/10.1016/S0048-9697(99)00286-7

Delves, H.T., Campbell, M.J., 1993. Identification and apportionment of sources of lead in human tissue. Environ. Geochem. Health 15, 75–84. https://doi.org/10.1007/BF02627825

Díaz-Somoano, M., Kylander, M.E., López-Antón, M.A., Suárez - Ruiz, I., Martínez-Tarazona, M.R., Ferrat, M., Kober, B., Weiss, D.J., 2009. Stable lead isotope compositions in selected coals from around the world and implications for present day aerosol source tracing. Environ. Sci. Technol. 43, 1078–1085. https://doi.org/10.1021/es801818r

Dolgopolova, A., Weiss, D.J., Seltmann, R., Kober, B., Mason, T.F.D., Coles, B., Stanley, C.J., 2006. Use of isotope ratios to assess sources of Pb and Zn dispersed in the environment during mining and ore processing within the Orlovka-Spokoinoe mining site (Russia). Appl. Geochemistry 21, 563–579. https://doi.org/10.1016/j.apgeochem.2005.12.014

Duong, T.T.T., Lee, B.K., 2011. Determining contamination level of heavy metals in road dust from busy traffic areas with different characteristics. J. Environ. Manage. 92, 554–562. https://doi.org/10.1016/j.jenvman.2010.09.010

Environmental Protection Agency, 2011. Particulate Matter Emissions.

Erel, Y., Emmanuel, S., Teutsch, N., Halicz, L., Veron, A., 2001. Partitioning of anthropogenic and natural lead in soils. Prepr. Ext. Abstr. Present. ACS Natl. Meet. Am. Chem. Soc. Div. Environ. Chem. 41, 992–996.

Espi, E., Boutron, C.F., Hong, S., Pourchet, M., Ferrari, C., Shotyk, W., Charlet, L., 1997. Changing concentrations of Cu, Zn, Cd and Pb in a high altitude peat bog from Bolivia during the past three centuries. Water. Air. Soil Pollut. https://doi.org/10.1023/A:1018364208168

Falahi-Ardakani, A., 1984. Contamination of environment with heavy metals emitted from automotives. Ecotoxicol. Environ. Saf. 8, 152–161. https://doi.org/10.1016/0147-6513(84)90057-5

Farmer, J.G., Mackenzie, A.B., Sugden, C.L., Edgar, P.J., Eades, L.J., 1997. A comparison of the historical lead pollution records in peat and freshwater lake sediments from central Scotland. Water. Air. Soil Pollut. https://doi.org/10.1023/A:1018320425006

Farmer, J.G., Eades, L.J., Graham, M.C., 1999. The lead content and isotopic composition of British coals and their implications for past and present releases of lead to the UK environment. Environ. Geochem. Health 21, 257–272. https://doi.org/10.1023/A:1006688515919

Fiacco, R.J., Thordarson, T., Germani, M.S., Self, S., Palais, J.M., Whitlow, S., Grootes, P.M., 1994. Atmospheric aerosol loading and transport due to the 1783-84 Laki Eruption in Iceland, interpreted from ash particles and acidity in the GISP2 ice core. Quat. Res. 42,

231–240. https://doi.org/10.1006/qres.1994.1074

Formenti, P., Andreae, M.O., Lange, L., Roberts, G., Cafmeyer, J., Rajta, I., Maenhaut, W., Holben, B.N., Artaxo, P., Lelieveld, J., 2001. Saharan dust in Brazil and Suriname during the Large-Scale Biosphere-Atmosphere Experiment in Amazonia (LBA) - Cooperative LBA Regional Experiment (CLAIRE) in March 1998. J. Geophys. Res. Atmos. 106, 14919–14934. https://doi.org/10.1029/2000JD900827

Froese, D.G., Lowe, D.J., Knott, J.R., Slate, J.L., 2008. Global tephra studies: John Westgate and Andrei Sarna-Wojcicki commemorative volume. Quat. Int. 178, 1–3. https://doi.org/10.1016/j.quaint.2007.12.005

Gagnevin, D., Boyce, A.J., Barrie, C.D., Menuge, J.F., Blakeman, R.J., 2012. Zn, Fe and S isotope fractionation in a large hydrothermal system. Geochim. Cosmochim. Acta 88, 183–198. https://doi.org/10.1016/j.gca.2012.04.031

Galer, S.J.G., 1999. Optimal double and triple spiking for high precision lead isotopic measurement. Chem. Geol. 157, 255–274. https://doi.org/10.1016/S0009-2541(98)00203-4

Gao, K., Pearce, J., Jones, J., Taylor, C., 1999. Interaction between peat, humic acid and aqueous metal ions. Environ. Geochem. Health 21, 13–26. https://doi.org/10.1023/A:1006592627852

Garcia-Mina, J.M., 2006. Stability, solubility and maximum metal binding capacity in metal-humic complexes involving humic substances extracted from peat and organic compost. Org. Geochem. 37, 1960–1972. https://doi.org/10.1016/j.orggeochem.2006.07.027

Gill, L.W., Ring, P., Higgins N., Johnston P.M., 2014. Accumulation of heavy metals in a constructed wetland treating road runoff, *Ecological Engineering*, 70, 133 - 139.

Gill, L.W., Ring, P., Casey, B., Higgins, N., Johnston, P.M., 2017. Long term heavy metal removal by a constructed wetland treating rainfall runoff from a motorway, *Science of the Total Environment*, 601-602, 32-44.

Gonzalez, R.O., Strekopytov, S., Amato, F., Querol, X., Reche, C., Weiss, D., 2016. New Insights from Zinc and Copper Isotopic Compositions into the Sources of Atmospheric Particulate Matter from Two Major European Cities. Environ. Sci. Technol. 50, 9816–9824. https://doi.org/10.1021/acs.est.6b00863

Grattan, J.P., Pyatt, F.B., 1994. Acid damage to vegetation following the Laki fissure eruption in 1783 - an historical review. Sci. Total Environ. 151, 241–247. https://doi.org/10.1016/0048-9697(94)90473-1

Grousset, F.E., Quetel, C.R., Thomas, B., Buatmenard, P., Donard, O.F.X., Bucher, A., 1994. Transient Pb Isotopic Signatures in the Western-European Atmosphere. Environ. Sci. Technol. 28, 1605–1608.

Guieu, C., Bozec, Y., Blain, S., Ridame, C., Sarthou, G., Leblond, N., 2002. Impact of high Saharan dust inputs on dissolved iron concentrations in the Mediterranean Sea. Geophys. Res. Lett. 29, 17-1-17–4. https://doi.org/10.1029/2001GL014454

Hall, V.A., Pilcher, J.R., 2002. Late-Quaternary Icelandic tephras in Ireland and Great Britain: Detection, characterization and usefulness. Holocene 12, 223–230. https://doi.org/10.1191/0959683602h1538rr

Hammond, R.F., 1978. The Peatlands of Ireland. Soil Surv. Bull. No. 35 1–63.

Hansmann, W., Köppel, V., 2000. Lead-istopes as tracers of pollutants in soils. Chem. Geol. 171, 123–144. https://doi.org/10.1016/S0009-2541(00)00230-8

Hinds, W.C., 1999. Aerosol Technology (2nd ed.). New York: John Wiley & Sons

Holynska, B., Ostachowicz, B., Ostachowicz, J., Samek, L., Wachniew, P., Obidowicz, A., Wobrauschek, P., Streli, C., Halmetschlager, G., 1998. Characterisation of210Pb dated peat core by various X-ray fluorescence techniques. Sci. Total Environ. 218, 239–248. https://doi.org/10.1016/S0048-9697(98)00211-3

Hong, S., Candelone, J.-P., Boutron, C.F., 1996. Deposition of atmospheric heavy metals to the Greenland ice sheet from the 1783–1784 volcanic eruption of Laki, Iceland. Earth Planet. Sci. Lett. 144, 605–610. https://doi.org/10.1016/S0012-821X(96)00171-9

Hughes, P.D.M., Barber, K.E., 2003. Mire development across the fen-bog transition on the Teifi floodplain at Tregaron Bog, Ceredigion, Wales, and a comparison with 13 other raised bogs. J. Ecol. 91, 253–264. https://doi.org/10.1046/j.1365-2745.2003.00762.x

Hurst, R.W., 2002. Lead Isotopes as Age-Sensitive , Genetic Markers Unleaded Gasoline. Enviromental Geosci. 9, 1–7.

John, S.G., Genevieve Park, J., Zhang, Z., Boyle, E.A., 2007. The isotopic composition of some common forms of anthropogenic zinc. Chem. Geol. 245, 61–69. https://doi.org/10.1016/j.chemgeo.2007.07.024

Johnson, D.W., Hils, J.E., 2013. Phosphate Esters, Thiophosphate Esters and Metal Thiophosphates as Lubricant Additives 132–148. https://doi.org/10.3390/lubricants1040132

Keddy, P.A., 2010. Wetland Ecology: Principles and Conservation (2nd edition). Cambridge University Press, UK. Cambridge. 497 p. Chapter 7.

Kellner E., 2003, Wetlands - Different types, their Properties and Functions, Department of Earth Sctences/Hydrology, Uppsala University, Technical Report TR- 04-08, SKB.

Keinonen, M., 1992. The isotopic composition of lead in man and the environment in Finland 1966-1987: isotope ratios of lead as indicators of pollutant source. Sci. Total Environ. 113, 251–268. https://doi.org/10.1016/0048-9697(92)90004-C

Kempter, H., Görres, M., Frenzel, B., 1997. Ti and Pb Concentrations in rainwater-fed bogs in Europe as indicators of past anthropogenic activities. Water. Air. Soil Pollut. https://doi.org/10.1023/A:1018376509985

Komárek, M., Ettler, V., Chrastný, V., Mihaljevič, M., 2008. Lead isotopes in environmental sciences: A review. Environ. Int. 34, 562–577. https://doi.org/10.1016/j.envint.2007.10.005

Krause, P., Kriews, M., Dannecker, W., Garbe-Schönberg, C.D., Kersten, M., 1993. Determination of $^{206/207}$Pb isotope ratios by ICP-MS in particulate matter from the North Sea environment. Fresenius. J. Anal. Chem. 347, 324–329. https://doi.org/10.1007/BF00323815

Krosshavn, M., Steinnes, E., Varskog, P., 1993. Binding of Cd, Cu, Pb, and Zn in soil organic matter with different vegetationsl background 185–193.

Kylander, M.E., Klaminder, J., Bindler, R., Weiss, D.J., 2010. Natural lead isotope variations in the atmosphere. Earth Planet. Sci. Lett. 290, 44–53. https://doi.org/10.1016/j.epsl.2009.11.055

Kylander, M.E., Weiss, D.J., Martínez Cortízas, A., Spiro, B., Garcia-Sanchez, R., Coles, B.J.,

2005. Refining the pre-industrial atmospheric Pb isotope evolution curve in Europe using an 8000 year old peat core from NW Spain. Earth Planet. Sci. Lett. 240, 467–485. https://doi.org/10.1016/j.epsl.2005.09.024

Küttner, A., Mighall, T.M., De Vleeschouwer, F., Mauquoy, D., Martínez Cortizas, A., Foster, I.D.L., Krupp, E., 2014. A 3300-year atmospheric metal contamination record from Raeburn Flow raised bog, south west Scotland. J. Archaeol. Sci. 44, 1–11. https://doi.org/10.1016/j.jas.2014.01.011

Langdon, P.G., Barber, K.E., 2004. Snapshots in time: Precise correlations of peat-based proxy climate records in Scotland using mid-Holocene tephras. Holocene. https://doi.org/10.1191/0959683604hl686rp

Le Roux, G., Weiss, D., Grattan, J., Givelet, N., Krachler, M., Cheburkin, A., Rausch, N., Kober, B., Shotyk, W., 2004. Identifying the sources and timing of ancient and medieval atmospheric lead pollution in England using a peat profile from Lindow bog, Manchester. J. Environ. Monit. 6, 502–510. https://doi.org/10.1039/B401500B

Legret, M., Pagotto, C., 1999. Evaluation of pollutant loadings in the runoff waters from a major rural highway. Sci. Total Environ. 235, 143–150. https://doi.org/10.1016/S0048-9697(99)00207-7

Little, S.H., Vance, D., Walker-Brown, C., Landing, W.M., 2014. The oceanic mass balance of copper and zinc isotopes, investigated by analysis of their inputs, and outputs to ferromanganese oxide sediments. Geochim. Cosmochim. Acta 125, 673–693. https://doi.org/10.1016/j.gca.2013.07.046

Livett, E.A., 1988. Geochemical Monitoring of Atmospheric Heavy Metal Pollution: Theory and Applications. Adv. Ecol. Res. 18, 65–177. https://doi.org/10.1016/S0065-2504(08)60180-4

Logan, E.M., Pulford, I.D., Cook, G.T., Mackenzie, A.B., 2008. Complexation of Cu2+ and Pb2+ by peat and humic acid. Eur. J. Soil Sci. 48, 685–696. https://doi.org/10.1111/j.1365-2389.1997.tb00568.x

Lomas-Clarke, S.H., Barber, K.E., 2007. Human impact signals from peat bogs - A combined palynological and geochemical approach. Veg. Hist. Archaeobot. 16, 419–429. https://doi.org/10.1007/s00334-006-0085-3

Lomas-Clarke, S.H., Barber, K.E., 2004. Palaeoecology of human impact during the historic period: Palynology and geochemistry of a peat deposit at Abbeyknockmoy, Co. Galway, Ireland. Holocene 14, 721–731. https://doi.org/10.1191/0959683604hl750rp

Lowe, D.J., 2011. Tephrochronology and its application: A review. Quat. Geochronol. https://doi.org/10.1016/j.quageo.2010.08.003

Luck JM; Othman DB; Albarède F; Telouk P, 1999. Pb, Zn and Cu isotopic variations and trace elements in rain, in: GEOCHEMISTRY OF THE EARTH'S SURFACE. pp. 199–202.

MacKenzie, A.B., Farmer, J.G., Sugden, C.L., 1997. Isotopic evidence of the relative retention and mobility of lead and radiocaesium in Scottish ombrotrophic peats. Sci. Total Environ. 203, 115–127. https://doi.org/10.1016/S0048-9697(97)00139-3

Maréchal, C.N., Nicolas, E., Douchet, C., Albarède, F., 2000. Abundance of zinc isotopes as a marine biogeochemical tracer. Geochemistry, Geophys. Geosystems 1, n/a-n/a. https://doi.org/10.1029/1999GC000029

Maréchal, C.N., Télouk, P., Albarède, F., 1999. Precise analysis of copper and zinc isotopic compositions by plasma-source mass spectrometry. Chem. Geol. 156, 251–273. https://doi.org/10.1016/S0009-2541(98)00191-0

Martínez-Cortizas, A., Pontevedra-Pombal, X., Nóvoa Muñoz, J.C., García-Rodeja, E., 1997. Four thousand years of atmospheric Pb, Cd and Zn deposition recorded by the ombrotrophic peat bog of Penido Vello (Northwestern Spain). Water. Air. Soil Pollut. https://doi.org/10.1023/A:1018312223189

Martínez Cortizas, A., García-Rodeja Gayoso, E., Weiss, D., 2002. Peat bog archives of atmospheric metal deposition. Sci. Total Environ. 292, 1–5. https://doi.org/10.1016/S0048-9697(02)00024-4

Marx, S.K., Kamber, B.S., McGowan, H.A., Zawadzki, A., 2010. Atmospheric pollutants in alpine peat bogs record a detailed chronology of industrial and agricultural development on the Australian continent. Environ. Pollut. 158, 1615–1628. https://doi.org/10.1016/j.envpol.2009.12.009

Mason, T.F.D., Weiss, D.J., Horstwood, M., Parrish, R.R., Russell, S.S., Coles, B.J., 2004. High-precision Cu and Zn isotope analysis by plasma source mass spectrometry Part 2 . Correcting for mass discrimination effects. Nat. Hist. 19, 218–226. https://doi.org/10.1039/B306953B\r10.1039/b306953b

Mather, T. a., Pyle, D.M.M., Oppenheimer, C., 2003. Tropospheric volcanic aerosol. Volcanism Earth's … 189–212. https://doi.org/10.1029/139GM12

Mattielli, N., Petit, J.C.J., Deboudt, K., Flament, P., Perdrix, E., Taillez, A., Rimetz-Planchon, J., Weis, D., 2009. Zn isotope study of atmospheric emissions and dry depositions within a 5 km radius of a Pb-Zn refinery. Atmos. Environ. 43, 1265–1272. https://doi.org/10.1016/j.atmosenv.2008.11.030

McConnell, J.R., Edwards, R., 2008. Coal burning leaves toxic heavy metal legacy in the Arctic. Proc. Natl. Acad. Sci. 105, 12140–12144. https://doi.org/10.1073/pnas.0803564105

McLennan, S.M., 2001. Relationships between the trace element composition of sedimentary rocks and upper continental crust. Geochemistry, Geophys. Geosystems 2. https://doi.org/10.1029/2000GC000109

Millot, R., Allègre, C.J., Gaillardet, J., Roy, S., 2004. Lead isotopic systematics of major river sediments: A new estimate of the Pb isotopic composition of the Upper Continental Crust. Chem. Geol. 203, 75–90. https://doi.org/10.1016/j.chemgeo.2003.09.002

Mitchell, F.J.G., Von Engelbrechten, S,E., Dwyer, R. and Cole, E., 1998. Investigation of the within site spatial variation of peat humification, Irish Association for Quaternary Studies Newsletter, 20, 8 - 9

Moeller, K., Schoenberg, R., Pedersen, R.B., Weiss, D., Dong, S., 2012. Calibration of the New Certified Reference Materials ERM-AE633 and ERM-AE647 for Copper and IRMM-3702 for Zinc Isotope Amount Ratio Determinations. Geostand. Geoanalytical Res. 36, 177–199. https://doi.org/10.1111/j.1751-908X.2011.00153.x

Monna, F., Lancelot, J., Croudace, I.W., Cundy, A.B., Lewis, J.T., 1997. Pb isotopic composition of airborne particulate material from France and the Southern United Kingdom: Implications for Pb pollution sources in urban areas. Environ. Sci. Technol. 31, 2277–2286.

https://doi.org/10.1021/es960870+

Muhlfeld, C., Rothen-Rutishauser, B., Blank, F., Vanhecke, D., Ochs, M., Gehr, P., 2008. Interactions of nanoparticles with pulmonary structures and cellular responses. AJP Lung Cell. Mol. Physiol. 294, L817–L829. https://doi.org/10.1152/ajplung.00442.2007

Muschack, W., 1990. Pollution of street run-off by traffic and local conditions. Sci. Total Environ. 93, 419–431. https://doi.org/10.1016/0048-9697(90)90133-F

Ng, A., Patterson, C., 1981. Natural concentrations of lead in ancient Arctic and Antarctic ice. Geochim. Cosmochim. Acta 45, 2109–2121. https://doi.org/10.1016/0016-7037(81)90064-8

Novak, M., Sipkova, A., Chrastny, V., Stepanova, M., Voldrichova, P., Veselovsky, F., Prechova, E., Blaha, V., Curik, J., Farkas, J., Erbanova, L., Bohdalkova, L., Pasava, J., Mikova, J., Komarek, A., Krachler, M., 2016. Cu-Zn isotope constraints on the provenance of air pollution in Central Europe: Using soluble and insoluble particles in snow and rime. Environ. Pollut. 218, 1135–1146. https://doi.org/10.1016/j.envpol.2016.08.067

Nriagu, J.O., 1989. A global assessment of natural sources of atmospheric trace metals. Nature 338, 47–49. https://doi.org/10.1038/338047a0

Nriagu, J.O., 1989. A global assessment of natural sources of atmospheric trace metals. Nature. https://doi.org/doi:10.1038/338047a0

Nriagu, Pacyna, J.M., 1988. Quantitative Assessment of Worldwide contamination of Air, Water, and Soil by Trace Metals. Nature 336, 403–405. https://doi.org/10.1038/332141a0

Oldfield, F., Appleby, P.G., Battarbee, R.W., 1978. Alternative ^{210}Pb dating: results from the New Guinea Highlands and Lough Erne. Nature 271. https://doi.org/10.1038/271339a0

Oldfield, F., Richardson, N., Appleby, P.G., 1995. Radiometric dating (210Pb, 137Cs, 241Am) of recent ombrotrophic peat accumulation and evidence for changes in mass balance. The Holocene 5, 141–148. https://doi.org/10.1177/095968369500500202

Oppenheimer, C., 2003. Ice core and palaeoclimatic evidence for the timing and nature of the great mid-13th century volcanic eruption. Int. J. Climatol. 23, 417–426. https://doi.org/10.1002/joc.891

Pacyna, E.G., Pacyna, J.M., Fudala, J., Strzelecka-Jastrzab, E., Hlawiczka, S., Panasiuk, D., Nitter, S., Pregger, T., Pfeiffer, H., Friedrich, R., 2007. Current and future emissions of selected heavy metals to the atmosphere from anthropogenic sources in Europe. Atmos. Environ. 41, 8557–8566. https://doi.org/10.1016/j.atmosenv.2007.07.040

Pacyna, J.M., Pacyna, E.G., 2001. An assessment of global and regional emissions of trace metals to the atmosphere from anthropogenic sources worldwide. Environ. Rev. 9, 269–298. https://doi.org/10.1139/er-9-4-269

Pagotto, C., Rémy, N., Legret, M., Le Cloirec, P., 2001. Heavy Metal Pollution of Road Dust and Roadside Soil near a Major Rural Highway, Environmental Technology, 22:3, 307-319.

Pernigotti, D., Belis, C.A., Spanó, L., 2016. SPECIEUROPE: The European data base for PM source profiles. Atmos. Pollut. Res. 7, 307–314. https://doi.org/10.1016/j.apr.2015.10.007

Pichat, S., Douchet, C., Albarède, F., 2003. Zinc isotope variations in deep-sea carbonates from the eastern equatorial Pacific over the last 175 ka. Earth Planet. Sci. Lett. 210, 167–178. https://doi.org/10.1016/S0012-821X(03)00106-7

Pilcher, J.R., Hall, V.A., 1992. Towards a tephrochronology for the Holocene of the north of

Ireland. Holocene 2, 255–259. https://doi.org/10.1177/095968369200200307

Pilcher, J.R., Hall, V.A., McCormac, F.G., 1995. Dates of Holocene Icelandic volcanic eruptions from tephra layers in Irish peats. Holocene 5, 103–110. https://doi.org/10.1177/095968369500500111

Plunkett, G.M., Pilcher, J.R., Gerry McCormac, F., Hall, V.A., 2004. New dates for first millennium BC tephra isochrones in Ireland. Holocene 14, 780–786. https://doi.org/10.1191/0959683604hl757rr

Ponzevera, E., Quétel, C.R., Berglund, M., Taylor, P.D.P., Evans, P., Loss, R.D., Fortunato, G., 2006. Mass Discrimination During MC-ICPMS Isotopic Ratio Measurements: Investigation by Means of Synthetic Isotopic Mixtures (IRMM-007 Series) and Application to the Calibration of Natural-Like Zinc Materials (Including IRMM-3702 and IRMM-651). J. Am. Soc. Mass Spectrom. 17, 1412–1427. https://doi.org/10.1016/j.jasms.2006.06.001

Purmalis, O., Klavins, M., 2012. Formation and Changes of Humic Acid Properties during Peat Humification Process within Ombrotrophic Bogs. Open J. Soil Sci. 2, 100–110. https://doi.org/10.4236/ojss.2012.22015

Pyle, D.M., Mather, T.A., 2003. The importance of volcanic emissions for the global atmospheric mercury cycle. Atmos. Environ. 37, 5115–5124. https://doi.org/10.1016/j.atmosenv.2003.07.011

Rea, H.A., Swindles, G.T., Roe, H.M., 2012. The Hekla 1947 tephra in the north of Ireland: Regional distribution, concentration and geochemistry. J. Quat. Sci. 27, 425–431. https://doi.org/10.1002/jqs.1566

Rausch, N., Nieminen, T., Ukonmaanaho, L., Le Roux, G., Krachler, M., Cheburkin, A.K., Bonani, G. and Shotyk, W., 2005. Comparison of atmospheric deposition of Cu, Ni, Co, Zn and Cd recorded by Finnish peat cores with monitoring data and emission records, *Environmental Science & Technology,* 39, 5989-5998.

Reilly, E., Mitchell, F.J.G., 2015. Establishing chronologies for woodland small hollow and mor humus deposits using tephrochronology and radiocarbon dating. https://doi.org/10.1177/0959683614557571.

Reimann, C., De Caritat, P., 2005. Distinguishing between natural and anthropogenic sources for elements in the environment: Regional geochemical surveys versus enrichment factors. Sci. Total Environ. https://doi.org/10.1016/j.scitotenv.2004.06.011

Rizzolo, J.A., Barbosa, C.G.G., Borillo, G.C., Godoi, A.F.L., Souza, R.A.F., Andreoli, R. V., Manzi, A.O., Sá, M.O., Alves, E.G., Pöhlker, C., Angelis, I.H., Ditas, F., Saturno, J., Moran-Zuloaga, D., Rizzo, L. V., Rosário, N.E., Pauliquevis, T., Yamamoto, C.I., Andreae, M.O., Taylor, P.E., Godoi, R.H.M., 2016. Mineral nutrients in Saharan dust and their potential impact on Amazon rainforest ecology. Atmos. Chem. Phys. Discuss. 1–43. https://doi.org/10.5194/acp-2016-557

Rosman, K.J.R., 1972. A survey of the isotopic and elemental abundance of zinc. Geochim. Cosmochim. Acta 36, 801–819. https://doi.org/10.1016/0016-7037(72)90089-0

Rosman, K.J.R., Chisholm, W., Boutron, C.F., Candelone, J.P., Gorlach, U., 1993. Isotopic evidence for the source of lead in Greenland snows since the late 1960s. Nature 362, 333–335. https://doi.org/10.1038/362333a0

Rosman, K.J.R., Chisholm, W., Hong, S., Candelone, J.P., Boutron, C.F., 1997. Lead from Carthaginian and Roman Spanish mines isotopically identified in Greenland ice dated from 600 B.C. to 300 A.D. Environ. Sci. Technol. 31, 3413–3416. https://doi.org/10.1021/es970038k

Rosman, K.J.R., Taylor, P.D.P., 1998. COMMISSION ON ATOMIC WEIGHTS AND ISOTOPIC ABUNDANCES - Isotopic Compositions of the Elements 1997 (Technical Report). Pure Appl. Chern. 70, 217–235.

Rynne, C., 2015. Industrial Ireland - An Archaeology. The Collins Press (9. Juli 2015), Cork.

Schmidt, A., Leadbetter, S., Theys, N., Carboni, E., Witham, C.S., Stevenson, J.A., Birch, C.E., Thordarson, T., Turnock, S., Barsotti, S., Delaney, L., Feng, W., Grainger, R.G., Hort, M.C., Höskuldsson, Á., 2015. Satellite detection, long-range transport, and air quality impacts of volcanic sulfurdioxide from the 2014-2015 flood lava eruption at Bardarbunga (Iceland). J. Geophys. Res. Atmos. 120, 9739–9757. https://doi.org/10.1002/2015JD023638.Received

Schroeder W.H., 1987, The roles of the atmosphere in influencing the pathways and fate of heavy metals in the environment - an overview, in Lindberg S.E. and Hutchinson T.C. (editors), Proceedings from the International Conference on Heavy Metals in the Environment, CEP Publishers, Edinburgh.

Shotyk, W., 1992. Natural and anthropogenic enrichments of arsenic through three Canadian ombrotrophic Sphagnum bog profiles. Arsen. Environ. Part I Cycl. Charact. 20, 381–401. https://doi.org/10.1016/0166-5162(92)90004-G

Shotyk, W., 1996. Peat bog archives of atmospheric metal deposition: geochemical evaluation of peat profiles, natural variations in metal concentrations, and metal enrichment factors. Environ. Rev. 4, 149–183. https://doi.org/10.1139/a96-010

Shotyk, W., 1997. Atmospheric deposition and mass balance of major and trace elements in two oceanic peat bog profiles, northern Scotland and the Shetland Islands. Chem. Geol. 138, 55–72. https://doi.org/10.1016/S0009-2541(96)00172-6

Shotyk, W., 1988. Review of the inorganic geochemistry of peats and peatland waters. Earth Sci. Rev. 25, 95–176. https://doi.org/10.1016/0012-8252(88)90067-0

Shotyk, W., Kempter, H., Krachler, M., Zaccone, C., 2015. Stable (^{206}Pb, ^{207}Pb, ^{208}Pb) and radioactive (^{210}Pb) lead isotopes in 1year of growth of Sphagnum moss from four ombrotrophic bogs in southern Germany: Geochemical significance and environmental implications. Geochim. Cosmochim. Acta 163, 101–125. https://doi.org/10.1016/j.gca.2015.04.026

Sigl, M., Winstrup, M., McConnell, J.R., Welten, K.C., Plunkett, G., Ludlow, F., Büntgen, U., Caffee, M., Chellman, N., Dahl-Jensen, D., Fischer, H., Kipfstuhl, S., Kostick, C., Maselli, O.J., Mekhaldi, F., Mulvaney, R., Muscheler, R., Pasteris, D.R., Pilcher, J.R., Salzer, M., Schüpbach, S., Steffensen, J.P., Vinther, B.M., Woodruff, T.E., 2015. Timing and climate forcing of volcanic eruptions for the past 2,500 years. Nature 523, 543–549. https://doi.org/10.1038/nature14565

Silamiķele, I., Nikodemus, O., Kalniņa, L., Purmalis, O., Kļaviņš, M., 2010. Peat humification character in two ombrotrophic bogs depending on peat properties. Proc. Latv. Acad. Sci. Sect. B Nat. Exact, Appl. Sci. 64, 159–166. https://doi.org/10.2478/v10046-010-0022-9

Sivry, Y., Riotte, J., Sonke, J.E., Audry, S., Sch??fer, J., Viers, J., Blanc, G., Freydier, R., Dupr??, B., 2008. Zn isotopes as tracers of anthropogenic pollution from Zn-ore smelters The Riou Mort-Lot River system. Chem. Geol. 255, 295–304. https://doi.org/10.1016/j.chemgeo.2008.06.038

Sonke, J.E., Sivry, Y., Viers, J., Freydier, R., Dejonghe, L., André, L., Aggarwal, J.K., Fontan, F., Dupré, B., 2008. Historical variations in the isotopic composition of atmospheric zinc deposition from a zinc smelter. Chem. Geol. 252, 145–157. https://doi.org/10.1016/j.chemgeo.2008.02.006

Steinmann, P., Shotyk, W., 1997. Chemical composition, pH, and redox state of sulfur and iron in complete vertical porewater profiles from two Sphagnum peat bogs, Jura Mountains, Switzerland. Geochim. Cosmochim. Acta 61, 1143–1163. https://doi.org/10.1016/S0016-7037(96)00401-2

Sugden, C.L., Farmer, J.G., MacKenzie, A.B., 1993. Isotopic ratios of lead in contemporary environmental material from Scotland. Environ. Geochem. Health 15, 59–65. https://doi.org/10.1007/BF02627823

Thapalia, A., Borrok, D.M., Van Metre, P.C., Musgrove, M., Landa, E.R., 2010. Zn and Cu isotopes as tracers of anthropogenic contamination in a sediment core from an Urban Lake. Environ. Sci. Technol. 44, 1544–1550. https://doi.org/10.1021/es902933y

Thordarson, T., 2003. Atmospheric and environmental effects of the 1783–1784 Laki eruption: A review and reassessment. J. Geophys. Res. 108, 4011. https://doi.org/10.1029/2001JD002042

Townsend, A.T., Yu, Z., Mcgoldrick, P., Hutton, J.A., 1998. Precise lead isotope ratios in Australian galena samples by high resolution inductively coupled plasma mass spectrometry. J. Anal. At. Spectrom. 13, 809–813. https://doi.org/10.1039/a801397g

Véron, A., Flament, P., Bertho, M.L., Alleman, L., Flegal, R., Hamelin, B., 1999. Isotopic evidence of pollutant lead sources in northwestern France. Atmos. Environ. 33, 3377–3388. https://doi.org/10.1016/S1352-2310(98)00376-8

Viers, J., Prokushkin, A.S., Pokrovsky, O.S., Kirdyanov, A. V, Zouiten, C., Chmeleff, J., Meheut, M., Chabaux, F., Oliva, P., Dupré, B., 2015. Zn isotope fractionation in a pristine larch forest on permafrost-dominated soils in Central Siberia. Geochem. Trans. 16, 3. https://doi.org/10.1186/s12932-015-0018-0

Voldrichova, P., Chrastny, V., Sipkova, A., Farkas, J., Novak, M., Stepanova, M., Krachler, M., Veselovsky, F., Blaha, V., Prechova, E., Komarek, A., Bohdalkova, L., Curik, J., Mikova, J., Erbanova, L., Pacherova, P., 2014. Zinc isotope systematics in snow and ice accretions in Central European mountains. Chem. Geol. 388, 130–141. https://doi.org/10.1016/j.chemgeo.2014.09.008

Walraven, N., Vanos, B.J.H., Klaver, G.T., Baker, J.H., Vriend, S.P., 1997. Trace element concentrations and stable lead isotopes in soils as tracers of lead pollution in graft-derijp, the netherlands. J. Geochemical Explor. 59, 47–58. https://doi.org/10.1016/S0375-6742(96)00056-8

Weiss, D., Shotyk, W., Boyle, E.A., Kramers, J.D., Appleby, P.G., Cheburkin, A.K., 2002. Comparative study of the temporal evolution of atmospheric lead deposition in Scotland

and eastern Canada using blanket peat bogs. Sci. Total Environ. 292, 7–18. https://doi.org/10.1016/S0048-9697(02)00025-6

Weiss, D.J., Kober, B., Dolgopolova, A., Gallagher, K., Spiro, B., Le Roux, G., Mason, T.F.D., Kylander, M., Coles, B.J., 2004. Accurate and precise Pb isotope ratio measurements in environmental samples by MC-ICP-MS. Int. J. Mass Spectrom. 232, 205–215. https://doi.org/10.1016/j.ijms.2004.01.005

Weiss, D.J., Rausch, N., Mason, T.F.D., Coles, B.J., Wilkinson, J.J., Ukonmaanaho, L., Arnold, T., Nieminen, T.M., 2007. Atmospheric deposition and isotope biogeochemistry of zinc in ombrotrophic peat. Geochim. Cosmochim. Acta 71, 3498–3517. https://doi.org/10.1016/j.gca.2007.04.026

Wilkinson, J.J., Eyre, S.L., Boyce, A.J., 2005. Ore-forming processes in Irish-type carbonate-hosted Zn-Pb deposits: Evidence from mineralogy, chemistry, and isotopic composition of sulfides at the Lisheen Mine. Econ. Geol. 100, 63–86. https://doi.org/10.2113/100.1.0063

Woodhead, J.D., Hergt, J.M., 1997. Application of the `double spike' technique to Pb-isotope geochronology. Chem. Geol. 138, 311–321. https://doi.org/10.1016/S0009-2541(97)00013-2

Yao, P.H., Shyu, G.S., Chang, Y.F., Chou, Y.C., Shen, C.C., Chou, C.S., Chang, T.K., 2015. Lead isotope characterization of petroleum fuels in Taipei, Taiwan. Int. J. Environ. Res. Public Health 12, 4602–4616. https://doi.org/10.3390/ijerph120504602

Yu, H., Chin, M., Yuan, T., Bian, H., Remer, L.A., Prospero, J.M., Omar, A., Winker, D., Yang, Y., Zhang, Y., Zhang, Z., Zhao, C., 2015. The fertilizing role of African dust in the Amazon rainforest: A first multiyear assessment based on data from Cloud-Aerosol Lidar and Infrared Pathfinder Satellite Observations. Geophys. Res. Lett. 42, 1984–1991. https://doi.org/10.1002/2015GL063040

Zaccone, C., Miano, T.M., Shotyk, W., 2012. Interpreting the ash trend within ombrotrophic bog profiles: Atmospheric dust depositions vs. mineralization processes. The Etang de la Gruère case study. Plant Soil 353, 1–9. https://doi.org/10.1007/s11104-011-1055-9

Zechmeister, H.G., Hohenwallner, D., Riss, A., Hanus-Illnar, A., 2003. Variations in heavy metal concentrations in the moss species Abietinella abietina (Hedw.) Fleisch. according to sampling time, within site variability and increase in biomass. Sci. Total Environ. 301, 55–65. https://doi.org/10.1016/S0048-9697(02)00296-6

Zhang, Y., and Banks, C. 2005. Factors Affecting the Removal of Selected Heavy Metals using a Polymer Immobilised Sphagnum Moss as a Biosorbent, Environmental Technology, 26:7, 733-744, DOI: 10.1080/09593332608618515

CHAPTER 3

Sampling sites and physical properties of the extracted monoliths

1. Geographical location and environmental setting of the sampling sites

1.1. Liffey Head bog, Co. Wicklow

Liffey Head bog (LHB) is situated in the Wicklow Mountains National Park, ca. 25 km south west of Dublin city and approximately 15 km inland from the east coast of Ireland (Fig. 5. in Chapter 2, and Fig. 1 a-b). It is a montane-type blanket bog (Hammond, 1978) covering an area of 1700 ha (IPCC,1 992). The relatively flat bog land is composed of a series of pool complexes and lies between 490 m and 520 m above sea level. Annual precipitation in this area is relatively high with mean values between 1200 mm and 1600 mm, and mean daily temperatures ranging between 5.5°C (January) and 15°C (July) (*source*: Meteorological Service, 1980). The wind dominates from the west (i.e., over from the north American continent, McCarthy et al., 2005), south-west (Frank and Landberg, 1997) and occasionally from eastern directions. The later have been associated with pollution transport over from the UK and European mainland (Aherne et al., 2000; Bowman and McGettigan, 1994; Feeley et al., 2013; www.earth.nullschool.net). The high-altitude blanket bog contains no trees or shrubs. The vegetation is versatile and comprises bog cotton, bog mosses, bog asphrodel, bog rosemary, with bilberry and crowberry in places (source: www.askaboutireland.ie). Surface pH conditions are between 4 and 4.5 (Geological Survey Ireland, GSI). The bog overlies the Leinster calc-alkaline granite batholith which is Devonian in age (415-350 million years ago) and therefore attributable to the Caledonian orogeny. The granite is surrounded by older mica-schists and quartzite. The Wicklow Mountains, as we find them today, were entirely shaped by the Quaternary glaciation during the Pleistocene period (2.6 to 11.700 years ago). Owing to the movement of the basal ice moraines, the U-shaped glens (valleys), named as Glendalough, Glendassan, Glenmalure, and Glenmacnass were formed and several high-grade lead-zinc mineralization veins were exposed.

The 115 cm core investigated in this study was extracted at 53°09.639'N, 006°17.641'W, and 518 m elevation above sea level on the 12th of March 2015. The monolith was extracted from the highest possible elevation at the approximate centre of the bog, away from the edge, to minimize complications arising from marginal drainage (Barber et al., 1994). Further, the core was extracted from an area of actively growing *Sphagnum* moss, which is a robust indicator of recent accumulation.

Figure 1.

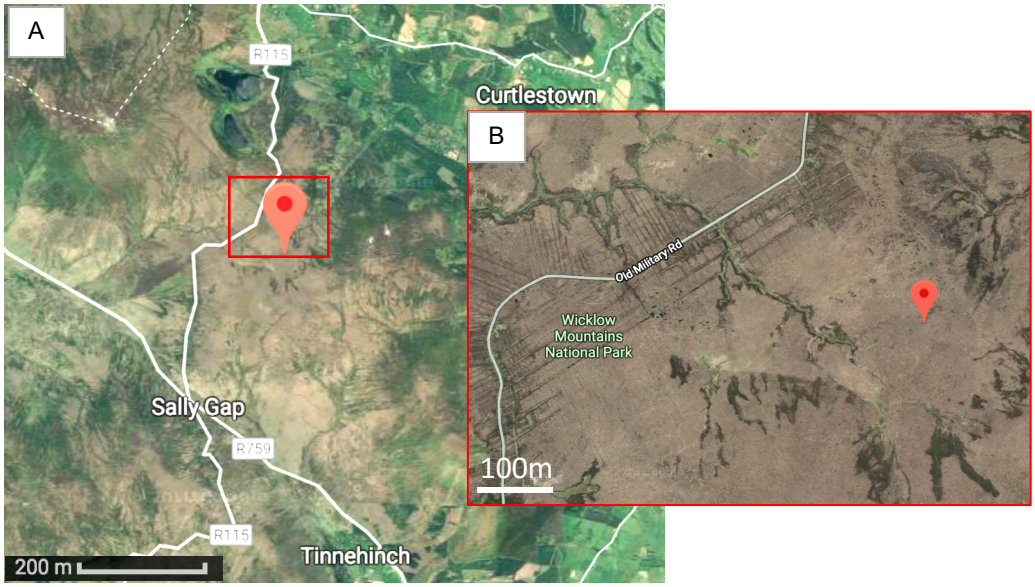


Fig. 1. a) geographical location of Liffey Head Bog, Co. Wicklow, east coast of Ireland; b) the site where the peat monolith was sampled for investigations.

1.2. Brackloon Wood, Co. Mayo

Brackloon Wood (BW), Co. Mayo is geographically located at the eastern slopes of Croagh Patrick, ca. 7 km south west of the Westport city at the west coast of Ireland (Fig. 5 in Chapter 2, and Fig. 2 a-b). In 1999, the area was designated the title: "Special Area of Conservation" by the European Habitat Directive.

Prevailing oceanic conditions are responsible for regular cloud cover and abundant rainfall in the area between 1600 mm and 2200 mm $year^{-1}$ (www.met.ie/climate/rainfall.asp). The area is influenced by the Gulf Stream and has a moderate climate with mean annual temperatures between 14°C and 16°C in July and between 4°C and 7°C in January. The wind at this site dominates from the south-west, with fluctuations from the west and north-west (e.g., Cooper et al., 2004 and references therein).

Brackloon Wood is a small remnant of Atlantic oak woodland (Cunnigham, 2005 and references therein) which covers approximately 74 hectares today. The dominant broadleaf tree species are birch, oak, elm, and ash, while the flora is composed of shade- and moisture tolerant bryophytes and fens (Cunningham, 2005). Regular rainfall facilitates the formation of soil, moor hummus, and *Sphagnum* moss dominated woodland peat. Surface pH conditions are between 3.5 and 4 (Geological Survey Ireland, GSI). The local geology is varied and is composed of both alkaline and acidic bedrocks, including Silurian sandstone, gneiss, and shale, Ordovician shale, sandstone, basalt, and rhyolite, and Carbonaceous limestone to the east.

The 62 cm core investigated in this study was extracted at 53°45'20.4984" N, 9°33'30.7908" W, and 52 m elevation above sea level on the 22nd of June 2015. Because Brackloon wood core was sampled in a forest environment, the following measures were taken to choose the right site: The (10 x 10 x 62 cm) peat monolith was taken from an elevated, *Sphagnum* moss dominated area in a forest glade with no tree cover within a radius of ca. 10-15 m to avoid potential disturbance by tree roots.

Figure 2.



Fig. 2. a) geographical location of the Brackloon wood, Co. Mayo, west coast of Ireland; b) the site where the peat monolith was sampled for investigations.

2. Sampling procedure

Both monoliths were extracted using a stainless steel Wardenaar corer (Wardenaar, 1987) and were wrapped in polyethylene film (Fig. 3a-b), as well as aluminium foil from the outside and brought to the laboratory. Prior investigations, the cores were stored in a wood box in a dark room at ca. 2°C.

2.1. Methods applied for physical properties determination

In laboratory, the monoliths were examined macroscopically for the presence of macrofossils (cm large wood pieces), thickness of *acrotelm* and *catotelm*, as well as the change in colour, which is representative of the degree of decomposition. The two peat cores were then carefully cut in 1 cm wide slices using a thin ceramic knife to avoid

contamination. All subsamples were placed in small polyethylene bags, labelled accordingly and stored in a dark room between experiments.

2.1.1. Moisture, ash content, loss on ignition, and bulk density

To determine the amount of water (moisture) and the dry mass of samples, between 3 and 6 g of homogenised, wet peat was dried in an oven at 105°C for 24 hours in ceramic crucibles. After re-weighing the samples, the moisture contents (given in %) were calculated as follows:

$$Moisture\ (\%) = \frac{[mass\ of\ wet\ peat\ (g) - mass\ of\ peat\ dried\ at\ 105°C\ (g)] * 100}{mass\ of\ wet\ peat\ (g)}$$

The ash contents (%) were determined by combusting the oven dried fraction of the peat subsamples (105°C) at 500°C in a muffle furnace for 6 hours. After cooling down to room temperature and re-weighing the uncombusted fraction, the ash content was calculated as follows:

$$Ash\ content\ (\%) = \left(\frac{mass\ of\ ashed\ peat\ (g)}{mass\ of\ peat\ dried\ at\ 105°C\ (g)}\right) * 100$$

Loss on ignition (LOI) was calculated by extracting the ash content after the combustion from the dry peat mass:

$$LOI\ (\%) = (g\ dry\ peat - g\ ash) * 100$$

Bulk peat density was determined for Liffey Head Bod core with the volumetric method. For this, a stainless-steel tube with the volume of 2 cm^3 was used for plugging the respective amount of peat material from the wet subsamples. Wet plugs were weighed, air dried at 50°C, and then re-weighed. Bulk densities, expressed as g cm^{-3} were calculated as follows:

$$Bulk\ density\ (g\ cm^{-3}) = \frac{mass\ of\ 50°C\ dried\ peat\ in\ plug\ (g)}{volume\ of\ peat\ (cm^3)}$$

Replicate analyses of at least one sample during the above listed procedures yield a good data reproducibility of <5%.

Figure 3.



Fig. 3. a) and b) peat extracting procedure using a stainless steel Wardenaar corer; c) A longitudinally cut fraction of LHB peat inside the ITRAX XRF core screener at the Geography department of the University College Dublin.

2.1.2. Core scanning via ITRAX XRF

The suitability of Liffey Head peat core as archive of historic anthropogenic pollution from the mining-smelting activities in the Wicklow uplands was preliminary tested with a non-destructive X-ray technique. For this, the core was subjected to elemental intensity investigations using a micro-Xray ITRAX core scanner at University College Dublin (Ireland) (Fig. 3c). This method was initially developed for sediment cores (Croudace et al., 2006) and requires virtually no sample preparation. A further advantage is the short operating time, usually between 10 and 18 hours, depending on the core length and resolution of the analyses. Because element intensities are obtained directly at the surface of the core, a fresh piece, cut lengthwise with a glass blade was prepared prior the analyses. The core fraction was carefully investigated for surficial irregularities which were then smoothed accordingly. These could affect the element

intensities during the experiment. In order to avoid desiccation during the measurement, the core was additionally covered with a 2 µm thin carbon film.

In this experiment, resolvable element intensities were measured for Ti, V, Cr, Fe, Ni, Cu, Zn, Ga, As, Rb, Sr, Y, Zr, Sn, Ba, Ta, W, and Pb. The X-ray radiograph image was performed at 45 kV and 30 mA with a dwell time of 200 ms, whereas XRF element intensities were obtained at 30 kV and 40 mA with an exposure time of 30 s at every 2 mm intervals along the profile. The results have been evaluated using the software ITRAXplot. A detailed description is given in Croudace et al. (2006) and Weltje and Tjallingii (2008).

3. Physical properties of the two monoliths – results

Both LHB and BW showed *Sphagnum* moss growth on top, indicating active peat accumulation. Several morphological and physical differences have been albeit identified between the two peat cores:

3.1. The decomposition status of the bogs

The 115 cm long LHB is composed of ca. 5 cm actively growing moss of fresh green colour. This layer overlies a denser segment of ca 18 cm of intermediately decomposed peat of bright brownish colour. The *acrotelm* transitions into *catotelm* between 25 and 30 cm from the surface. The *catotelm* is characterised by overall high water content which is however successfully retained into the peat monolith. The peat colour varies between bright brown and dark black at the base of the extracted core, where the decomposition process is most advanced. The *catotelm* has a fibrous texture indicative of decomposed grass species along with *Sphagnum* moss. Visibly, it shows a smooth surface and a relatively homogeneous density.

The 62 cm long BW monolith is characterised by a thin layer (4 cm) of actively growing *Sphagnum* moss of fresh green colour, followed by an area of partially decomposed peat of 14 cm thickness. In a relatively sharp transition zone at approximately 18 cm from the surface, the thin *acrotelm* transfers into the *catotelm*. The *catotelm* is composed of advanced decomposed organic matter with a high content of humins responsible for the uniform dark brown to black colour, as well as up to 3 cm large wood fragments. The catotelm has a dense texture with less water content compared to LHB, and no visible density gradient.

Figure 4.

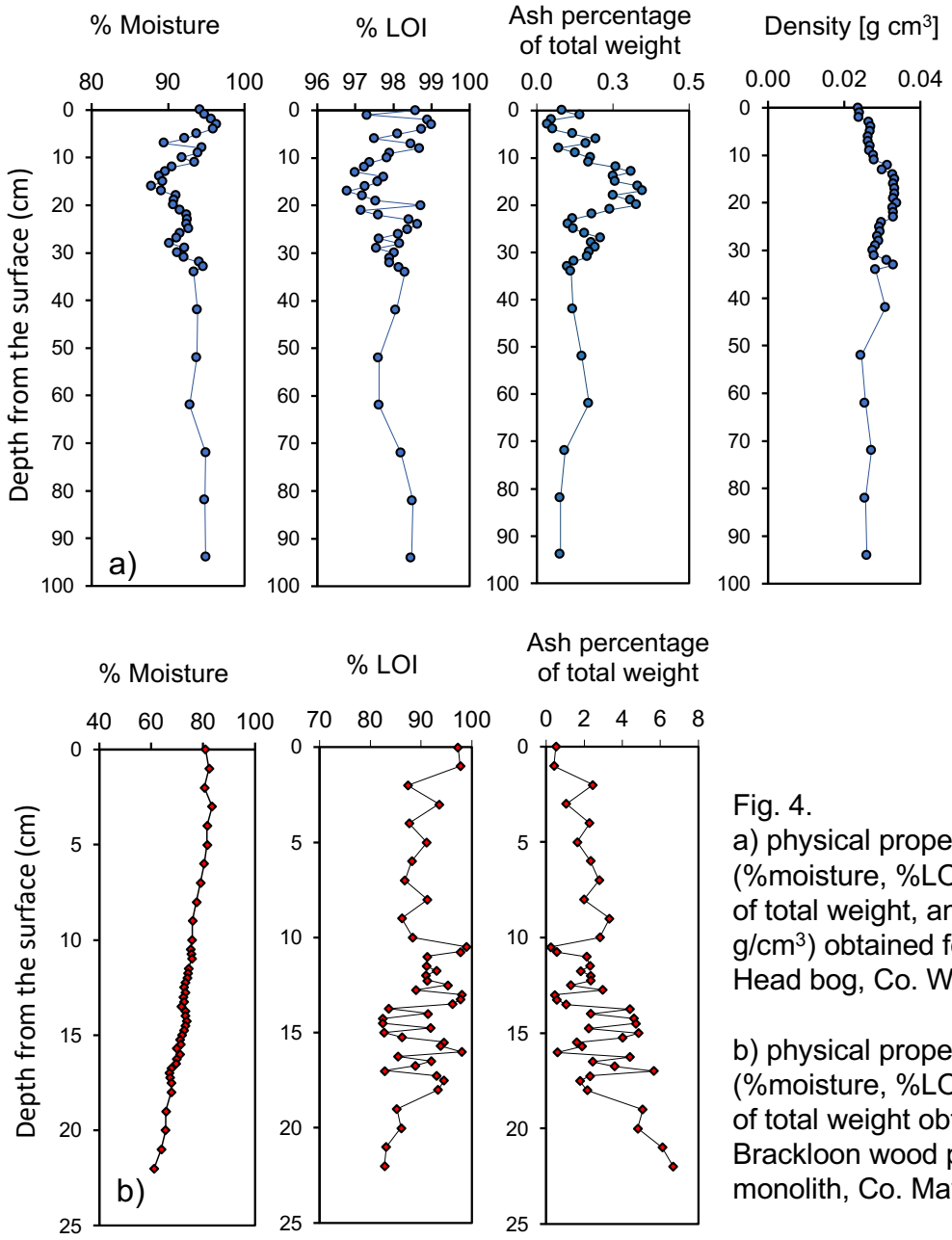


Fig. 4.
a) physical properties (%moisture, %LOI, ash % of total weight, and density g/cm^3) obtained for Liffey Head bog, Co. Wicklow.

b) physical properties (%moisture, %LOI, ash % of total weight obtained for Brackloon wood peat monolith, Co. Mayo.

Table 1. Physical properties, Liffey Head Bog, Co. Wicklow

Sample ID	Depth [cm]	Mass of wet sample [g]	Mass of 105°C dry sample [g]	Mass of ash [g]	Ash percentage of total weight [%]	Moisture [%]	Loss on ignition [%]	Density [g/cm3]
LHB 1.3	0-1	3.03	0.177	0.003	0.083	94.2	98.5	0.024
LHB 2.3	1-2	3.54	0.186	0.005	0.141	94.8	97.3	0.024
LHB 3.3	2-3	3.79	0.165	0.002	0.047	95.7	98.9	0.024
LHB 4.3	3-4	4.15	0.150	0.002	0.036	96.4	99.0	0.026
LHB 5.3	4-5	3.28	0.135	0.002	0.051	95.9	98.7	0.027
LHB 6.3	5-6	3.65	0.228	0.004	0.117	93.7	98.1	0.027
LHB 7.3	6-7	3.35	0.261	0.006	0.194	92.2	97.5	0.026
LHB 1.1	7-8	3.39	0.358	0.005	0.162	89.4	98.4	0.026
LHB 1.2	8-9	3.45	0.192	0.002	0.072	94.4	98.7	0.027
LHB 2.2	9-10	3.40	0.206	0.004	0.126	93.9	97.9	0.028
LHB 3.2	10-11	4.86	0.396	0.008	0.176	91.8	97.8	0.028
LHB 4.2	11-12	5.04	0.329	0.006	0.170	93.4	97.3	0.028
LHB 5.2	12-13	5.62	0.530	0.014	0.259	90.5	97.2	0.031
LHB 6.2	13-14	4.98	0.515	0.015	0.309	89.6	97.0	0.030
LHB 2.1	14-15	4.34	0.484	0.011	0.251	88.8	97.7	0.032
LHB 7.2	15-16	4.55	0.485	0.011	0.257	89.3	97.5	0.033
LHB 8.2	16-17	4.48	0.545	0.015	0.332	87.8	97.2	0.033
LHB 9.2	17-18	5.05	0.549	0.017	0.348	89.1	96.8	0.033
LHB 10.2	18-19	4.52	0.405	0.011	0.252	91.0	97.1	0.033
LHB 11.2	19-20	4.39	0.403	0.013	0.307	90.8	97.5	0.033
LHB 12.2	20-21	4.84	0.450	0.015	0.328	90.7	98.7	0.033
LHB 13.2	21-22	5.22	0.439	0.012	0.239	91.8	97.1	0.032
LHB 3.1	22-23	4.07	0.309	0.007	0.181	92.4	97.6	0.033
LHB 14.2	23-24	4.47	0.334	0.005	0.118	92.5	98.4	0.033
LHB 15.2	24-25	5.07	0.385	0.005	0.102	92.4	98.6	0.029
LHB 16.2	25-26	3.84	0.282	0.004	0.119	92.6	98.3	0.029
LHB 17.2	26-27	4.85	0.408	0.007	0.156	91.5	98.1	0.029
LHB 18.2	27-28	4.09	0.362	0.008	0.209	91.1	97.6	0.028
LHB 19.2	28-29	5.12	0.503	0.009	0.179	90.1	98.1	0.029
LHB 20.2	29-30	3.65	0.287	0.007	0.191	92.1	97.5	0.028
LHB 21.2	30-31	3.69	0.324	0.006	0.173	91.2	98.0	0.027
LHB 22.2	31-32	3.79	0.301	0.006	0.166	92.0	97.9	0.027
LHB 4.1	32-33	5.96	0.350	0.007	0.122	94.1	97.9	0.031
LHB 23.2	33-34	4.80	0.260	0.004	0.099	94.5	98.1	0.031
LHB 24.2	34-35	3.02	0.200	0.003	0.112	93.3	98.3	0.028
LHB 5.1	42-43	4.30	0.264	0.005	0.118	93.8	98.7	0.030
LHB 6.1	52-53	3.44	0.214	0.005	0.148	93.7	97.6	0.024
LHB 7.1	62-63	5.46	0.391	0.009	0.170	92.8	97.6	0.025
LHB 8.1	72-73	5.09	0.257	0.004	0.092	94.9	98.2	0.027
LHB 9.1	82-83	4.37	0.227	0.003	0.077	94.8	98.5	0.025
LHB 10.1	94-95	3.49	0.177	0.003	0.077	94.9	98.5	0.026

Table 2. Physical properties Brackloon wood, Co. May

Sample ID	Sample depth (cm)	Mass of wet sample [g]	Mass of 105°C dry sample [g]	Mass of ash [g]	Ash percentage of total weight [%]	Moisture [%]	Loss on ignition [%]
BW 2.1	0-1	6.03	1.15	0.032	0.52	80.9	97.2
BW 2.2	1-2	6.48	1.15	0.027	0.41	82.2	97.7
BW 2.3	2-3	6.64	1.29	0.163	2.46	80.4	87.4
BW 2.4	3-4	6.37	1.05	0.068	1.07	83.4	93.5
BW 2.5	4-5	6.39	1.17	0.146	2.28	81.5	87.6
BW 2.6	5-6	6.27	1.15	0.103	1.64	81.5	91.1
BW 2.7	6-7	6.31	1.24	0.147	2.33	80.3	88.1
BW 2.8	7-8	6.76	1.42	0.188	2.78	78.9	86.8
BW 2.9	8-9	6.63	1.50	0.132	1.98	77.3	91.2
BW 2.10	9-10	6.27	1.51	0.209	3.33	75.8	86.2
BW 2.11	10-10.5	6.08	1.47	0.172	2.83	75.7	88.3
BW 2.12	10.5-10.75	4.44	1.10	0.011	0.26	75.1	98.6
BW 2.13	10.75-11	4.78	1.17	0.027	0.56	75.4	97.7
BW 2.14	11-11.25	4.58	1.11	0.097	2.13	75.6	91.2
BW 2.15	11.25-11.50	5.00	1.28	0.115	2.31	74.3	91.0
BW 2.16	11.50-11.75	4.76	1.22	0.086	1.81	74.2	92.9
BW 2.17	11.75-12	4.92	1.28	0.116	2.35	73.9	90.9
BW 2.18	12-12.25	4.60	1.23	0.108	2.35	73.1	91.2
BW 2.19	12.25-12.50	4.21	1.15	0.054	1.28	72.7	95.3
BW 2.20	12.50-12.75	2.82	0.75	0.084	2.98	73.1	88.9
BW 2.21	12.75-13	3.26	0.90	0.015	0.47	72.4	98.0
BW 2.22	13-13.25	3.30	0.90	0.018	0.54	72.5	97.7
BW 2.23	13.25-13.50	3.23	0.91	0.035	1.06	71.6	96.1
BW 2.24	13.50-13.75	5.15	1.38	0.227	4.39	73.1	83.6
BW 2.25	13.75-14	2.89	0.78	0.068	2.34	73.0	91.3
BW 2.26	14-14.25	3.65	0.95	0.169	4.62	73.6	82.5
BW 2.27	14.25-14.50	3.63	0.97	0.171	4.72	73.1	82.4
BW 2.28	14.50-14.75	4.33	1.18	0.097	2.23	72.6	91.8
BW 2.29	14.75-15	3.24	0.91	0.157	4.85	71.9	82.7
BW 2.30	15-15.25	4.29	1.24	0.172	4.01	70.9	86.1
BW 2.31	15.25-15.50	3.75	1.07	0.060	1.59	71.3	94.4
BW 2.32	15.50-15.75	3.44	1.03	0.064	1.87	69.8	93.7
BW 2.33	15.75-16	3.52	1.01	0.020	0.58	71.1	97.9
BW 2.34	16-16.25	4.06	1.22	0.178	4.39	69.7	85.4
BW 2.35	16.25-16.50	3.55	1.08	0.080	2.44	69.6	91.9
BW 2.36	16.50-16.75	2.59	0.83	0.094	3.59	67.7	88.8
BW 2.37	16.75-17	3.76	1.24	0.213	5.64	67.0	82.8
BW 2.38	17-17.25	2.31	0.75	0.053	2.29	67.2	93.0
BW 2.39	17.25-17.50	3.16	1.02	0.056	1.76	67.7	94.5
BW 2.40	17.50-18	3.15	1.02	0.068	2.15	67.6	93.3
BW 2.41	18-19	4.37	1.50	0.221	5.06	65.6	85.2
BW 2.42	19-20	4.79	1.65	0.230	4.80	65.5	86.0
BW 2.43	20-21	4.76	1.72	0.291	6.09	63.8	83.1
BW 2.44	21-22	5.11	1.98	0.342	6.68	61.1	82.8

3.2. Moisture, ash content, and bulk density of the LHB and BW peat monoliths

The results of these investigations are presented in Figures 4 a-b and Tables 1 and 2. In general, LHB displays values of a typical ombrotrophic peat bog with low densities (0.024-0.034 g cm^{-3}), high moisture and water content (87-97 %) and high loss on ignition (LOI, 97-99 %).

The BW LOI is very heterogeneous down the core, with values fluctuating between 83 and 97 %, which are however within the values established for peat bogs. Moisture varies between 61 and 84 %. The high proportion of ash in some BW samples (0.26 – 6.7%), and especially in the lower part of the core are indicative of enhanced aeolian transport of sediment/soil particles at this site by either natural events or anthropogenic influence. The dense structure of the peat, the thin *acrotelm* layer, together with lower moisture contents are indicative of a slower peat accumulation rate at this BW site relative to LHB.

3.3. ITRAX-XRF element intensities in LHB

Element intensities and a radiograph image obtained with the X-ray method for the LHB peat core are presented in Figure 5. The analyses show well defined high intensity peaks for the elements Pb and Zn which emerge at similar depths between 10 and 20 cm from the surface. The enrichments of these elements remain, also if plotted against lithogenic element such as Si, Zr, or Sr. This is indicative of the presence of an anthropogenic source besides the natural dust/soil influx. Similarly, correlations between Fe and Ca (not shown) suggest a common lithogenic source for these two elements.

In order to better understand the information obtained by the ITRAX XRF method, element intensities (Pb, Zn, Ni, Cu, Cr, V, Sr, Zr, and Ta) at respective depths are plotted against the element concentration obtained with the solution analyses via Qs-ICP-MS (Fig. 6). Detailed description of this technique is given in the next Chapters 4-6.

The relatively good agreement (R^2=0.71) observed between the Pb intensities of the ITRAX XRF core scanning analyses and the accurate Pb concentrations obtained with the Qs-ICP-MS method reveals a high potential of the non-destructive core scanning for the investigation of Pb in peat archives. However, the relatively bad correlations obtained for other metals (Zn, Ni, Cr, Cu, V) as well as lithogenic elements (Sr, Zr, Ta), discloses significant limitations in applying ITRAX core screening technique to peat material. This has been intensively discussed in the work of (Weltje and Tjallingii, 2008) which concluded that fluctuations in the parameters: water content, particle size and distribution, density, material heterogeneity, and morphology along the core will produce a noisy background and ultimately affect the element intensities. Often, these parameters cannot be investigated at the same high resolution at which the element intensities are collected (2 mm), leading to an over- or underestimation of the signals. In addition, the ITRAX technique is not sensitive enough, as enrichment excursions in

other elements such as Mo, U, Th, Sn, Sb, Ag, and rare earth elements (REE) identified with the solution experiment (Chapters 4 and 5) were not detected with the ITRAX XRF.

It is worth reiterating that this preliminary investigation was conducted in order to select a suitable core for further study aiming at exploring potential metal enrichment related to the Pb mining in the Wicklow uplands. The element intensities obtained with the ITRAX XRF method are qualitative and were therefore not calibrated against the quantitative data obtained later with the Qs-ICP-MS. Notwithstanding, noted enrichments in Pb revealed the value of this core for further investigation and thus fulfilling the purpose of the investigation.

Figure 5.

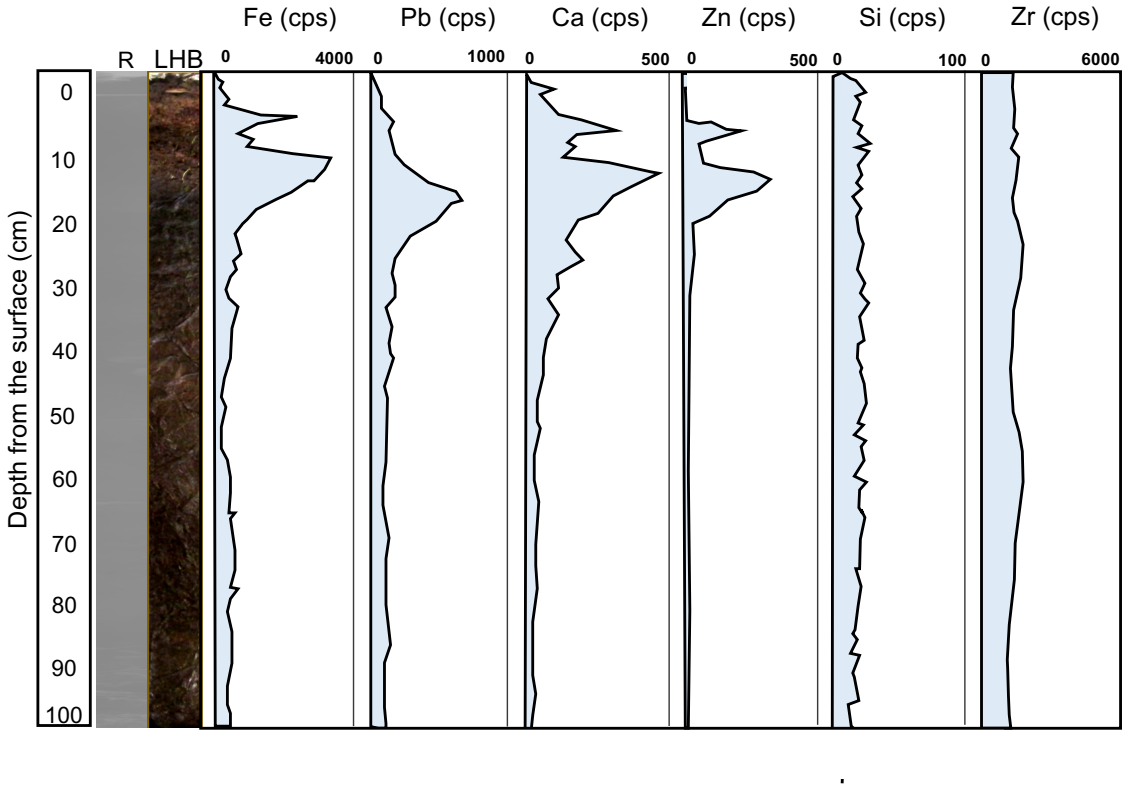


Fig. 5: Element intensities along the extracted LHB peat profile obtained with the ITRAX XRF core screening technique at UCD. Shown are counts per second for Fe, Pb, Ca, Zn, Si, and Zr, as well as a radiograph image (R).

Figure 6.

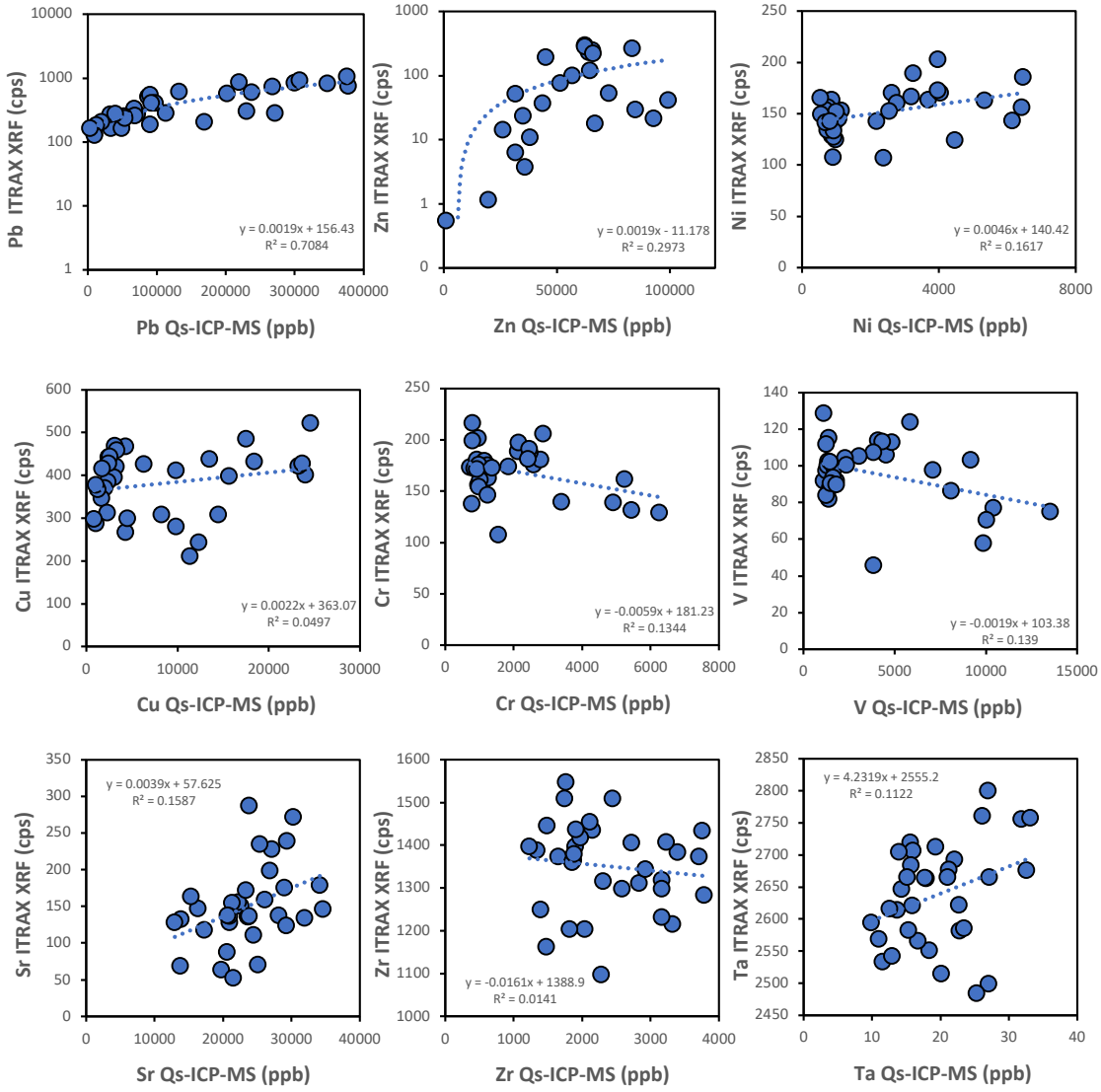


Fig. 6: Element intensities along the extracted LHB peat profile obtained with the ITRAX XRF core screening technique at UCD. Shown are counts per second for Fe, Pb, Ca, Zn, Si, and Zr, as well as a radiograph image (R).

4. Previous works and their findings on these sites

4.1. Liffey Head bog, Co. Wicklow

A 1 m long peat core extracted from the LHB has been previously subjected to an environmental investigation by (Cole and Mitchell, 2003) with the title “Human impact on the Irish landscape during the late Holocene inferred from palynological studies at three peat lands”. Deploying palynological methods, these authors found out that the area experienced continuous woodland reduction over the past 1200 years. At the same time, rise in grasses species suggest an expansion of open pasture between 1390 and 1800 AD (43-14 cm), while Cereal-type pollen support agricultural activity. From ca 1800

AD until present, the woodland cover is again increasing, which is among others seen in the appearance of non-native trees such as *Tilia* (linden tree), *Fagus* (beech tree), and *Picea* (spruce tree) surrounding the peat bog. The intensification of the tree pollen abundance during the first half of the 19th century is attributed to the Coronation Plantation of 500 acres of wood to celebrate the coronation of William IV (Joyce, 1971) in 1831. A recent intensification of the agricultural activity is seen in an increase of Cereal-type pollen at the top of the profile, which can be linked to increasing aerial fertiliser addition during the past 20 years.

In addition, investigations of Cole and Mitchell (2003) revealed the presence of two volcanic cryptotephra layers within the extracted 1 m long core. Based on major oxide composition and correlations with ^{14}C, the tephra was attributed to the volcanic eruptions of Hekla in 1510 (33-34cm) and 1947 (4-5cm). Therefore, a core from LHB seemed a promising study site giving the cryptotephra presence, significant human influence on the landscape, combined with metallurgical activity over the past two to three centuries.

The peat core extracted by Cole and Mitchell (2003) displayed typical ombrotrophic features with high LOI ranging between 95 and 99 %, high water content ~90 % with minor or insignificant fluctuations down the core.

4.2. Brackloon wood, Co. Mayo

Since 1991, Brackloon wood has been the focus of long-term monitoring activity by the University College Dublin based Forest Ecology Research group. Therefore, numerous paleoecological studies were performed on the wood ecosystem during the past ~25 years (von Engelbrechten et al., 2000). Recently, Brackloon forest was subjected to a study by (Reilly and Mitchell, 2015) entitled “Establishing chronologies for woodland small hollow mor humus deposits using tephrochronology and radiocarbon dating”. One of the main findings of this research were the identification of the Laki 1783-4 volcanic tephra embedded in a small hollow peat deposit at 12-14 cm from the surface. This is the first time this tephra layer was ever found in Irish surficial deposits. In addition to this, the studies of Cunningham (2005), and van Engelbrechten et al. (2000) give significant background information about the site, which is of eventual importance for understanding the element enrichments: The presence of spherical charcoal (SCP) fragments were noted between 8 and 14 cm from the surface. Because SCPs are usually formed at high temperature, their origin is most likely industrial, and were probably transported from the ironworks at Knappagh (ca. 2km NE) operating in the late-seventeenth century and early eighteenth century (Cunningham, 2005; and references therein). However, charcoal production was also carried within the forest,

which is visible from the presence of charcoal stands throughout the woodland (Cunningham, 2005). During the 1830s, numerous wool, bleach, flour, and corn mills operated in the surrounding area of the forest, which demonstrates small-scale industrial activity (Cunningham, 2005). Agricultural activity is also evident: “Bogs Commissioners’ report of the area around Westport (1813/14) that thousands of acres that were now reclaimed and cultivated using lime to improve the soil” (Reilly and Mitchell, 2015). The wood was acquired by the Land Commissioners in 1940s, then later transferred to the Forest and Wildlife service and subsequently to Coillte (The Irish Forestry Board).

Physical properties of the peat monolith collected in a small hollow of the forest by Reilly and Mitchell (2015): “The bottom (24 cm) consists of moderately well humified wood peat with frequent *Sphagnum* moss inclusions. There is a gradual change to wood-dominated to *Sphagnum*-dominated peat after this point. Loss on ignition values are around 90%. Noticed fluctuations reflect in part the change from wood-dominated to *Sphagnum*-dominated peat”

References

Aherne, J., de Kluizenaar, Y., van den Beuken, R., Farrell, E.P. Atmospheric chemical climate. In: Aherne J, Farrell EP, editors. Critical loads and levels. Dublin: Environmental Protection Agency; 2000. p. 37–76.

Barber, K.E., Chambers, F.M., Maddy, D., Stoneman, R., Brew, J.S., 1994. A sensitive high-resolution record of late Holocene climatic change from a raised bog in northern England. The Holocene 4, 198–205. https://doi.org/10.1177/095968369400400209

Bowman, J.J. and McGettigan, M., 1994. Atmospheric deposition in acid sensitive areas of Ireland - the influence of wind direction and a new coal burning electricity generation station on precipitation quality. Water Air Soil Pollut. 75, 159–75.

Cole, E.E., Mitchell, F.J.G., 2003. Human impact on the Irish landscape during the late Holocene inferred from palynological studies at three peatland sites. Holocene 13, 507–515. https://doi.org/10.1191/0959683603hl616rp

Cooper, J.A.G., Jackson, D.W.T., Navas, F., McKenna, J., Malvarez, G., 2004. Identifying storm impacts on an embayed, high-energy coastline: examples from western Ireland, Marine Geology, 210,1–4,261-280.

Croudace, I.W., Rindby, A., Rothwell, R.G., 2006. ITRAX: description and evaluation of a new multi-function X-ray core scanner. Geol. Soc. London, Spec. Publ. 267, 51–63. https://doi.org/10.1144/GSL.SP.2006.267.01.04

Cunnigham, D., 2005. Brackloon: The Story of an Irish Oak Wood.

Feeley, B., Bruen, M., Blacklocke, S., Kelly-Quinn, M., 2013. A regional examination of episodic acidification response to reduced acidic deposition and the influence of plantation forests in Irish headwater streams, Science of The Total Environment, 443, 173-183.

Frank, H.P., and Landberg, L., 1997. Modelling the Wind Climate of Ireland. Boundary-Layer Meteorology, 85(3), 359–377. doi:10.1023/a:1000552601288

Hammond, R.F., 1978. The Peatlands of Ireland. Soil Surv. Bull. No. 35 1–63.

Joyce, W.S.J. 1971: The neighbourhood of Dublin. Wake? eld: S.R. Publishers.

McCarthy, G.D., Gleeson, E., Walsh, S., 2015. The influence of the Ocean on the Climate of Ireland. Weather. 70, 8, 242–245

Reilly, E., Mitchell, F.J., 2015. Establishing chronologies for woodland small hollow and mor humus deposits using tephrochronology and radiocarbon dating. Holocene 25, 241–252. https://doi.org/10.1177/0959683614557571

von Engelbrechten, S., McGee, E., Little, D.J., Mitchell, F.J.G. 2000. A palaeoecological study of Brackloon Wood, Co Mayo; Vegetation dynamics and human impact throughout the Holocene period (c. 10,000-year BP – Present). Forest Ecosystem Research Group Report Number 42. Department of Botany, Trinity College Dublin.

Wardenaar, E.C.P., 1987. A new hand tool for cutting peat profiles. Can. J. Bot. 65, 1772–1773. https://doi.org/10.1139/b87-243

Weltje, G.J., Tjallingii, R., 2008. Calibration of XRF core scanners for quantitative geochemical logging of sediment cores: Theory and application. Earth Planet. Sci.

Lett. 274, 423–438. https://doi.org/10.1016/j.epsl.2008.07.054

Mean annual temperatures and precipitation values obtained from:

www.met.ie, and www.met.ie/climate/rainfall.asp

Information of peat bog flora from www.askaboutireland.ie

Soil pH values: Geological Survey Ireland: https://www.gsi.ie/en-ie/programmes-and-projects/tellus/activities/ground-survey/Pages/default.aspx

Real-time wind directions: https://earth.nullschool.net/#current/wind/surface/level/orthographic=-10.06,56.13,288 (real-time wind directions).

Chapter 4

Trace element and Pb isotope fingerprinting of atmospheric pollution sources: A case study from the east coast of Ireland †

Carolina Rosca[1*], Emma L Tomlinson[1], Walter Geibert[2], Cora A McKenna[1], Michael G Babechuk[1, 3] and Balz S Kamber[1]

[1]Department of Geology, School of Natural Sciences, Trinity College Dublin, Ireland

[2]Alfred-Wegner-Institut Helmholtz-Zentrum für Polar- und Meeresforschung, Bremerhaven, Germany

[3]*present address*: Department of Earth Sciences, Faculty of Science, Memorial University of Newfoundland, Canada

*corresponding author: roscaca@tcd.ie

† *a version of this chapter has been published as a research paper in the Journal "Applied Geochemistry", volume 96 (2018), 302-326*

Abstract

Unravelling inputs of multiple air pollution sources and reconstructing their historic contribution can be a difficult task. Here, trace metal concentrations and Pb isotopes were measured in an ombrotrophic peat core from the Liffey Head bog (LHB) in eastern Ireland in order to reconstruct how different sources contributed to the atmospheric pollution over the past century. Asynchronous peak enrichments occur in the heavy metals Pb, Cu, Ag, Zn, Cd, Sn, and Sb, suggesting involvement of several pollution sources. Pollution episodes were dated with the radionuclide (^{210}Pb-^{241}Am) technique and occur in the peat that accumulated between early 20th and 21st century. The Pb isotope composition of the peat (^{206}Pb/^{204}Pb: 18.351±0.013; ^{206}Pb/^{207}Pb: 1.174±0.012) demonstrates significant aerial influx of heavy metals from local mining and smelting activities during the 19th century until ca. 1957. A dramatic compositional shift defined by elevated Cr, Ni, Mo, Sn, Zn, and V concentrations and a sharp transition towards much less radiogenic ^{206}Pb values (^{206}Pb/^{204}Pb: 18.271±0.013 - 17.678±0.006; ^{206}Pb/^{207}Pb: 1.170±0.012 - 1.135±0.007) is documented from the 1940's until 2000. These are attributed to the hemispheric impact of lead petrol additives and modelled to have contributed between 6 and 78% to the total Pb pollution at this site. The subsequent turn to a more radiogenic Pb isotope signature since 2000 (^{206}Pb/^{204}Pb: 17.930±0.006; ^{206}Pb/^{207}Pb: 1.148±0.007) reflects the abolishment of leaded petrol in Ireland and Europe. However, there remains a persisting and even increasing pollution in Ni, Mo, Cu, rare earth elements, and especially Zn, collectively originating from countrywide peat, coal, oil combustion, aerosols released from unleaded vehicle fuels, with potential contributions from agricultural activities. This illustrates the continued environmental stress on important natural archives such as peat bogs despite the phase-out of leaded petrol.

Key words: anthropogenic pollution, heavy metals, Pb isotopes, ombrotrophic peat, Ireland

1. Introduction

Anthropogenic activities are responsible for significant perturbations of the heavy metal cycles at the Earth's surface. Ombrotrophic (rain-fed) peat is considered an excellent archive of historic atmospheric composition due to two key characteristics: i) the hydrological isolation from ground water and surface runoff ensures that the growing peat is exclusively fed by atmospheric inputs (i.e., dust, rain, snow, fog); and, ii) the inherently high abundance of complex-forming organic acids enables the preservation of metal-bearing aerosols (e.g., Shotyk and Le Roux, 2005). There is an increasing body of publications on historic atmospheric trace metal depositions, especially of Pb, Zn, Cu, Hg, As, Cd inferred from study of peat bogs from around the world, including Canada (e.g., Boyle, 1977; Pratte et al., 2013; Shotyk, 1992), Europe (e.g., Martínez Cortizas et al., 2012; Shotyk et al., 2002), Australia (e.g., Marx et al., 2010; Stromsoe et al., 2015), China (e.g., Ferrat et al., 2012), and South America (De Vleeschouwer et al., 2014). These studies report temporal variations in natural depositions (e.g. from dust), but also document significant changes in the atmospheric metal pollution load throughout the periods of modern industrialisation.

Radiogenic Pb isotope analyses are a robust tool to distinguish between natural and anthropogenic Pb inputs due to conservative behaviour in bogs, including very low mobility and insignificant post-depositional isotope fractionation (Shotyk et al., 2005 and references therein). The isotopic signature of Pb, which shows a broad compositional variability within the lithogenic units found at the Earth's surface, is determined by the geological age and respective U-Th-Pb concentrations of the parent rock. For example, Precambrian Pb ores from the Brocken Hill deposit at Mt. Isa, Australia display an unradiogenic $^{206}Pb/^{207}Pb$ of 1.04 (Townsend and Snape, 2002), whereas the Mississippi type Pb deposits in the USA carry a radiogenic $^{206}Pb/^{207}Pb$ signature ranging between 1.28 and 1.33 (Doe, 1970). Products manufactured using these ores will inherit their respective isotope signature. The pre-polluted $^{206}Pb/^{207}Pb$ values of Greenlandic ice (Rosman et al., 1997) and peat bogs from Spain (Kylander et al., 2005), Switzerland (Shotyk et al., 2001), and Sweden (Klaminder et al., 2003) range between 1.19 and 1.25. The temporal and geographic evolution of the Pb pollution fingerprint has helped to discriminate between the impact of mining-smelting and leaded gasoline around the northern hemisphere including Scotland (e.g., Cloy et al., 2008; Kylander et al., 2009), UK (e.g., Le Roux et al., 2004), Sweden (e.g., Bindler et al., 2004, Bränvall et al., 1997), NW Spain (Kylander et al., 2005; Martinez-Cortizas et al., 2012), Switzerland and Germany (e.g., Le Roux et al., 2005; Shotyk et al., 2002), and Canada (e.g., Kylander et al., 2009 and references there in). While often deployed separately, the information obtained from combining trace elements and (Pb) isotopic compositions is more powerful in differentiating between complex multiple sources. To date, there is not a

single study reporting Pb isotope chronologies in Irish peat bogs, and only two studies which investigated atmospheric depositions of Pb, Cd, and Hg: Kippure bog, Clara bog, Bellacorick bog (Schell et al., 1997), Knockroe bog, and Letterfrack bog (Coggins et al., 2006), which, compared to other European areas is rather scarce. There is thus a strong necessity to geochemically explore the Irish archives in more detail, especially in view of the rich metallurgical history of the island and Ireland's potential subjection to trans-Atlantic metal transport.

In this study, we investigate the elemental pollution history in an ombrotrophic peat bog from the Wicklow mountains in eastern Ireland with a particular focus on the last century. This archive is selected because of its proximity to the influence from various anthropogenic sources with overlapping or simultaneous occurrence. By combining the information gained from trace element and Pb isotope compositions, our aim is to deconvolute multiple input sources that have variably been emitted over the last century. Lead isotope data are used to produce a first temporal and geographical comparison with the isotope patterns established in other peat archives from northern Europe (UK), Canada, and the eastern US.

2. Background and methods

2.1. Study area and sample collection

In the Republic of Ireland, where ca. 1/6th (~1,200,000 hectares) of landmass is covered by peat, three basic peat formations are recognised: 1) raised bogs of the Central Plain, 2) blanket bogs dominating the western seaboard and the upland areas, and 3) fen peats (Hammond, 1978). Most of the Irish blanket and montane bogs are around 6000-8000 years old with average accumulation rates of 0.1-1.2 cm year^{-1} (Hammond, 1978). The site investigated here, Liffey Head bog (LHB) in Co. Wicklow (grid ref. O142 134; 06º 17'W, 53º 09'N) is an ombrotrophic, montane-type blanket bog situated 25 km southwest of Dublin city and approximately 15 km from the east coast of Ireland (Fig. 1). LHB occurs as a relatively flat bog land with a series of pool complexes and lies between 490 and 520 m above sea level. The annual precipitation in this part of the Wicklow Mountains is high, with means between 1600 and 2400 mm a^{-1} (*source: Meteorological Survey*). These conditions sustain a near-continuous deposition of atmospheric particulates onto the bog's surface. The upland area experiences aerosol transport mainly from south-westerly and westerly Atlantic winds, potentially carrying pollutants from mines in the Irish midlands. Occasional, but not periodic injections on easterly and south-easterly air masses have also been monitored in the Wicklows and interpreted to direct pollutants over from the UK and Europe (e.g., Bowman and McGettigan, 1994; Feeley et al., 2013).

The ombrotrophic bog is underlain by the Leinster batholith, a Caledonian age granitic intrusion with a strong I-type, calc-alkaline affinity (e.g., Oliver et al., 2002).

A vertical monolith of 1 m in length (10 x 10 x 115 cm) was extracted from the LHB in March 2015 from an area with living *Sphagnum* moss growth on top using a stainless steel Wardenaar corer. The core was sampled close to the centre of the bog at its highest elevation. On site, the core was wrapped in cling film and aluminium foil, placed in a wooden box, brought directly to the laboratory and stored in a dark room at ca. +2ºC. Using a thin ceramic knife, the core was cut into 100 one cm slices, each apportioned for individual analyses as described in detail below.

Figure 1.

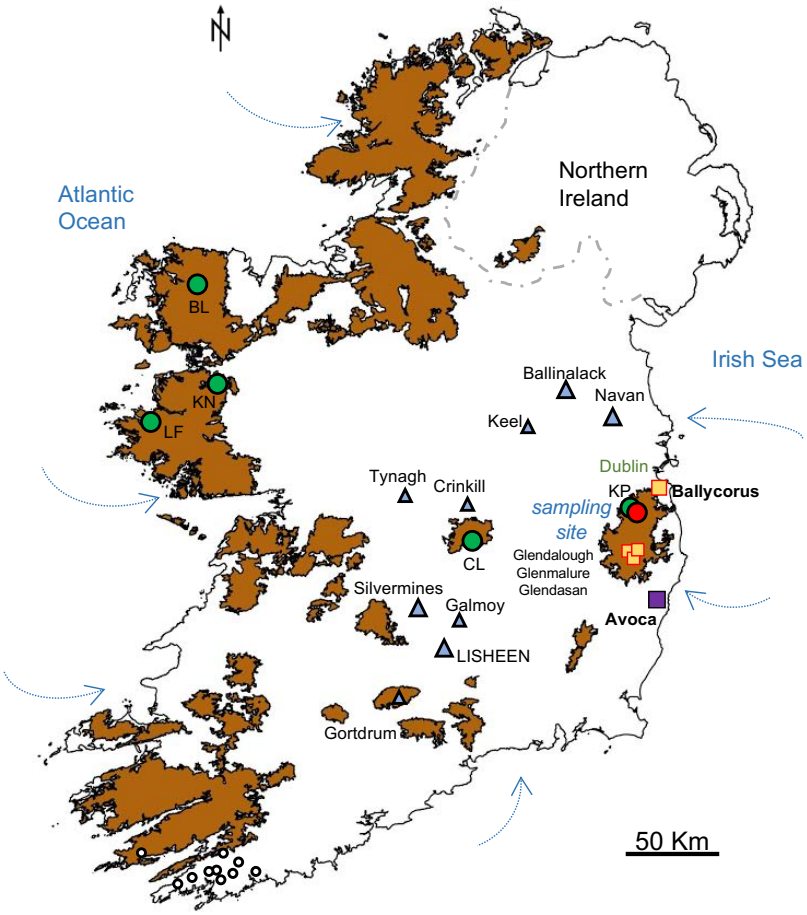


Fig. 1. Map of Ireland showing the geographic distribution of peat bogs (brown areas), compiled using data from GSI-Ireland (www.gsi.ie), the sampling site LHB (red dot) along with the historic Pb-Zn mining and smelting sites in the Wicklow mountains (yellow squares) and the historic Pb, Cu, S mines at Avoca (purple square). Peat bog sites discussed in the studies of Coggins et al (2006): Letterfrack (LF) and Knockroe (KN), and Schell et al. (1997): Bellacorick (BL), Clara (CL), and Kippure (KP) are indicated as green circles. The main Pb-Zn ore deposits hosted within the Lower Carboniferous of the Midland basin are indicated by blue triangles. Blue arrows represent the wind directions.

2.2. Analytical methods

2.2.1. Radiometric data and analysis

Lead-210 ($T_{1/2}$ = 22.3 yrs) derived chronologies were originally developed to date ice (Goldberg, 1963) and lake sediment deposits (Krishnaswami et al., 1971), and were later extended to peat archives (e.g., Appleby et al., 1997). Lead-210 chronologies are often used to complement radiocarbon dating to improve resolution for the most recent period, i.e., last 100-150 years in organic-rich archives (e.g., Appleby and Oldfield, 1992; Clymo et al., 1990). The anthropogenically produced ^{241}Am ($T_{1/2}$ = 432.2 yrs) is the least mobile among the man-made radionuclides in surficial deposits (e.g., Appleby et al., 1991; Oldfield et al, 1995) and is considered an important chronostratigraphic marker. Americium-241 is strongly particle-associated and highly immobile under low-pH conditions, which prevail in the upper parts of ombrotrophic peat bogs. Chronologies obtained from activities of anthropogenically originated ^{137}Cs ($T_{1/2}$ = 30.2 yrs) have been intensively discussed since the work of Oldfield et al. (1979). In organic-rich media like peat bogs, ^{137}Cs profiles may be difficult to interpret because of active participation of this element in biological processes which could induce vertical mobility (e.g., Appleby et al., 1991; Kudelsky et al., 1996).

The radioisotopes ^{210}Pb, ^{137}Cs, and ^{241}Am were analysed via gamma-spectrometry on a sub-set of samples to derive a chronology for the top section of the core. All analyses were performed on a planar HPGe gamma detector (Canberra) at the Alfred Wegener Institute for Polar and Marine Research in Bremerhaven, Germany. Peat samples were weighed and sealed with hot glue in gas-tight petri dishes to prevent loss of ingrowing ^{222}Rn. Subsequently, samples were stored for >3 weeks to allow the relevant daughters of ^{226}Ra to grow into secular equilibrium. Lead-210 was measured at 46 keV, ^{241}Am at 59 keV, and ^{137}Cs at 661 keV. The presence of ^{226}Ra was monitored at lines 186 keV, 295 keV, 351 keV, and 609 keV. Detectable ^{226}Ra was found in fewer than 50% of the samples, but its activity was less than 1% of the total ^{210}Pb. Consequently, no correction for supported ^{210}Pb was performed to avoid introducing unnecessary inconsistencies through the profile. Lead-210 is not reported as excess ^{210}Pb ($^{210}Pb_{ex}$) while noting that nearly all ^{210}Pb will be unsupported. Samples were counted until 1000 net counts of ^{210}Pb were reached, or for maximum of $6*10^5$ seconds if 1000 counts were not reached within this time period. Variable sample masses were expected to affect the detector efficiencies via self-absorption, especially at the low energy range. This was addressed by determining mass-dependent efficiencies using IAEA-385 Irish Sea reference material for ^{210}Pb and ^{241}Am. The uncertainty on these efficiencies was assumed to be 10%. For ^{137}Cs, an uncertainty of 5% was expected, considering the inevitably variable geometry of the unprocessed peat samples.

Counting errors were typically small compared to the uncertainty in the efficiencies. Therefore, we applied an error calculation based on the error propagation from detector efficiencies and counting statistics, without including the nominal uncertainty in the background determination. The reported uncertainties represent 1 sigma.

2.2.2. Moisture, density, and combustible matter content

Moisture contents were determined by drying a 2 cm^3 subsample (2 x 1 x 1 each cm piece of peat) at 105ºC for 24 hours. The % combustible fraction was defined via the loss on ignition (LOI) by combusting the dried aliquot at 550ºC for 4 hours in inert quartz glass crucibles. In the following, we refer to LOI and combustible matter content as synonyms. Bulk density (g cm^{-3}) was analysed at 5 cm resolution for the deepest part (40-100 cm) and at 3 cm resolution for the section between 0 and 40 cm following the method of Dean (1974).

2.2.3. Trace element and Pb isotope analyses

Trace element concentrations in dry (at 80ºC) peat, expressed as ng g^{-1} on 41 subsamples are presented in *Appendix A.1*. Data were acquired at Trinity College Dublin, Ireland via solution quadrupole ICP-MS (SQ-ICP-MS) using a Thermo Scientific iCAP-Qc. A new ash fraction was prepared for this purpose by combusting a peat aliquot for 6 hours at 450ºC. Between 10 and 50 mg of resulting ash was transferred into 15 ml Teflon beakers into which 0.8 ml of a triple sub-boiling distilled conc. HF and 0.2 ml conc. HNO_3 (4:1) was added. The capped beakers were placed into a digestion block at 150ºC for 72 hrs and agitated at least once every 24 hrs. After cool-down, drops were carefully collected before beakers were opened, and the solution was evaporated at 110ºC. The residues were then dissolved with 1 ml of ~6 M HCl to reduce any remaining organic components, and fluorides were converted by attacking with 2x0.5 ml conc. HNO_3 with evaporation to dryness between each step. Finally, the converted residue was dissolved in 3 ml of 2.5 M HNO_3 and subsequently topped up with additional Milli-Q water to produce 30 ml of 0.3 M HNO_3 solutions. Two blanks were prepared along with the samples throughout all ashing and digestion steps to account for potential contamination.

The ICP-MS analyses followed those of Eggins et al. (1997) with modifications described by Marx et al. (2010). For analyses, 2 ml solutions containing a small aliquot of each stock solution was diluted with 2% HNO_3 and spiked with an internal standard containing a mixture of ^{6}Li, Rh, Re, Bi and ^{235}U, which covers the full mass range of ionisation potentials and analysed elements. In some cases, the sample contained so

much Bi that this affected the signal from the internal standard, which was then excluded for drift correction. Following Eggins et al. (1997), an additional external drift monitor was employed. Oxide/hydroxide and dimer interferences were corrected according to Ulrich et al. (2010).

Multiple digestions of the USGS W-2a reference material were used for calibration, and six digests of the USGS rock standards BCR-2 (n=3) and BHVO-2 (n=3) were used as the quality control standards (Jochum et al. 2016; GeoReM). Relative standard deviations (RSDs) calculated from the multiple measurements of the respective standards were typically <2% for 38 out of 45 elements for both BHVO-2 and BCR-2 and the concentrations were comparable to the GeoReM preferred values demonstrating very good accuracy of this dataset (*Appendix A.2*). The remaining elements with inferior reproducibility are known to be heterogeneous in these standards (e.g. Kamber and Gladu, 2009; Weis et al., 2006).

Lead isotope ratios of all peat samples analysed for trace element composition (n=41) were measured on the same quadrupole ICP-MS at Trinity College Dublin (Table 1). Because trace element analyses consumed only a small fraction of the digest (<1%), the remaining stock solution was used for Pb purification on anion exchange resin (AGX-1x, 200-400 mesh) applying the HBr-HCl method described in Kamber and Gladu (2009). Total Pb yield was between 85-90% for all samples. Procedural blanks were negligible with amounts less than 0.1% of the total Pb. The quadrupole ICP-MS Pb analysis technique used followed Ulrich et al. (2010). Accuracy and precision of the Pb isotope ratios were determined from multiple analyses of SRM-NBS 982. Accuracy values were 95 ppm for $^{206}Pb/^{204}Pb$, 44 ppm $^{208}Pb/^{206}Pb$, and 25 ppm for $^{207}Pb/^{206}Pb$, relative to the values of Baker et al. (2004). Lead isotope ratios of the rock-reference materials BHVO-2 (n=2) and BCR-2 (n=2), presented in Table 1 are close to or within the values reported by Woodhead and Hergt (2000) and Baker et al. (2004). The observed heterogeneity in Pb isotope composition of second-generation USGS rock standards BHVO-2 and BCR-2 was caused during milling and has been widely discussed elsewhere (e.g., Weis et al., 2006).

3. Results

3.1. Peat properties

Density (Fig. 2c), LOI (Fig. 2d), and moisture contents are relatively constant throughout the core with values ranging between 0.023-0.034 g cm^{-3}, 96-99%, and 88-96% (by wt.), respectively. Evenly distributed moisture and density contents (especially in the uppermost 25 cm) indicate minor down-core compaction, favouring element retention at depth of deposition. High LOI values evidence negligible sediment input, validating the

ombrotrophic nature on the bog. The limited LOI fluctuations are strongly anti-correlated with lithophile elements Ti (R^2= *0.69)*, Sr (R^2= *0.74)*, Sc (R^2= *0.75)*, and Zr (R^2= *0.79)*, supporting that mineral dust is the dominant component of the residual incombustible ash (e.g., Shotyk et al., 2002). Within this core, the best combustible matter anti-correlation (R^2= *0.95*) is found with the Ta content (*Appendix B.1*). The amplitudes of moisture, and density variations are most pronounced in the youngest quarter of the core, i.e., the dated segment.

Table 1: Lead isotope compositions of peat sub-samples along the Liffey Head bog core together with published values for quality control standards.

Sample ID	*Depth (cm)*	$^{207}Pb/^{206}Pb$	*±2SD*	$^{208}Pb/^{206}Pb$	*±2SD*	$^{206}Pb/^{204}Pb$	*±2SD*
LHB1.3	*0 to 1*	0.8708	*0.0003*	2.1075	*0.0007*	17.930	*0.007*
LHB2.3	*1 to 2*	0.8745	*0.0003*	2.1156	*0.0007*	17.841	*0.007*
LHB3.3	*2 to 3*	0.8756	*0.0003*	2.1200	*0.0007*	17.795	*0.007*
LHB4.3	*3 to 4*	0.8765	*0.0003*	2.1188	*0.0007*	17.776	*0.007*
LHB5.3	*4 to 5*	0.8792	*0.0003*	2.1234	*0.0007*	17.746	*0.007*
LHB6.3	*5 to 6*	0.8818	*0.0003*	2.1239	*0.0007*	17.678	*0.007*
LHB7.3	*6 to 7*	0.8823	*0.0003*	2.1271	*0.0007*	17.657	*0.007*
LHB1.1	*7 to 8*	0.8820	*0.0004*	2.1282	*0.0005*	17.659	*0.012*
LHB1.2	*8 to 9*	0.8785	*0.0004*	2.1228	*0.0008*	17.719	*0.013*
LHB2.2	*9 to 10*	0.8787	*0.0004*	2.1215	*0.0008*	17.717	*0.013*
LHB3.2	*10 to 11*	0.8793	*0.0004*	2.1202	*0.0008*	17.712	*0.013*
LHB4.2	*11 to 12*	0.8774	*0.0004*	2.1216	*0.0008*	17.752	*0.013*
LHB5.2	*12 to 13*	0.8714	*0.0004*	2.1150	*0.0008*	17.872	*0.013*
LHB6.2	*13 to 14*	0.8715	*0.0004*	2.1156	*0.0008*	17.900	*0.013*
LHB2.1	*14 to 15*	0.8644	*0.0004*	2.1047	*0.0008*	18.028	*0.013*
LHB7.2	*15 to 16*	0.8613	*0.0004*	2.1042	*0.0008*	18.123	*0.013*
LHB8.2	*16 to 17*	0.8575	*0.0004*	2.0990	*0.0008*	18.195	*0.013*
LHB9.2	*17 to 18*	0.8544	*0.0004*	2.0953	*0.0008*	18.271	*0.013*
LHB10.2	*18 to 19*	0.8530	*0.0004*	2.0945	*0.0008*	18.314	*0.013*
LHB11.2	*19 to 20*	0.8529	*0.0004*	2.0951	*0.0008*	18.318	*0.013*
LHB12.2	*20 to 21*	0.8518	*0.0004*	2.0918	*0.0008*	18.351	*0.013*
LHB13.2	*21 to 22*	0.8520	*0.0004*	2.0928	*0.0008*	18.335	*0.013*
LHB3.1	*22 to 23*	0.8518	*0.0004*	2.0918	*0.0008*	18.350	*0.013*
LHB14.2	*23 to 24*	0.8511	*0.0004*	2.0903	*0.0008*	18.341	*0.013*
LHB15.2	*24 to 25*	0.8507	*0.0004*	2.0896	*0.0008*	18.379	*0.013*
LHB16.2	*25 to 26*	0.8496	*0.0004*	2.0878	*0.0008*	18.377	*0.013*
LHB17.2	*26 to 27*	0.8504	*0.0003*	2.0898	*0.0005*	18.366	*0.012*
LHB18.2	*27 to 28*	0.8505	*0.0003*	2.0916	*0.0005*	18.354	*0.012*
LHB19.2	*28 to 29*	0.8494	*0.0003*	2.0905	*0.0005*	18.384	*0.012*
LHB20.2	*29 to 30*	0.8502	*0.0004*	2.0895	*0.0008*	18.351	*0.013*
LHB21.2	*30 to 31*	0.8499	*0.0003*	2.0892	*0.0005*	18.383	*0.012*
LHB22.2	*31 to 32*	0.8505	*0.0003*	2.0914	*0.0005*	18.364	*0.012*
LHB4.1	*32 to 33*	0.8496	*0.0003*	2.0886	*0.0005*	18.367	*0.012*
LHB23.2	*33 to 34*	0.8509	*0.0003*	2.0888	*0.0005*	18.366	*0.012*
LHB24.2	*34 to 35*	0.8498	*0.0004*	2.0876	*0.0008*	18.361	*0.013*
LHB5.1	*42 to 43*	0.8487	*0.0003*	2.0862	*0.0005*	18.385	*0.012*
LHB6.1	*52 to 53*	0.8492	*0.0003*	2.0880	*0.0005*	18.385	*0.012*
LHB7.1	*62 to 63*	0.8482	*0.0003*	2.0864	*0.0005*	18.429	*0.012*
LHB8.1	*72 to 63*	0.8496	*0.0003*	2.0843	*0.0005*	18.400	*0.012*
LHB9.1	*82 to 83*	0.8505	*0.0003*	2.0887	*0.0005*	18.378	*0.012*
LHB10.1	*94 to 95*	0.8517	*0.0003*	2.0899	*0.0005*	18.346	*0.012*
NBS 982 (av) this study		0.4671	*0.0002*	1.0001	*0.0004*	36.740	*0.026*
	Baker et at (2004)	0.4671	*0.0000*	1.0002	*0.0000*	*36.743*	*0.002*
BCR-2 (av) this study		0.8351	*0.0004*	2.0663	*0.0008*	18.736	*0.013*
	Baker et at (2004)	0.8326	*0.0011*	2.0651	*0.0005*	18.765	*0.011*
	Woodhead and Hergt (2000)	0.833	*0.0009*	2.0644	*0.0006*	18.754	*0.012*
	Collerson et al (2000)	0.8329	*0.0007*	2.0644	*0.0011*	18.757	*0.012*
BHVO-2 (av) this study		0.8358	*0.0013*	2.0563	*0.0015*	18.618	*0.012*
	Baker et at (2004)	0.8333	*0.0008*	2.0509	*0.0009*	18.649	*0.019*
	Woodhead and Hergt (2000)	0.8337	*0.0011*	2.0514	*0.0012*	18.645	*0.039*

Figure 2.

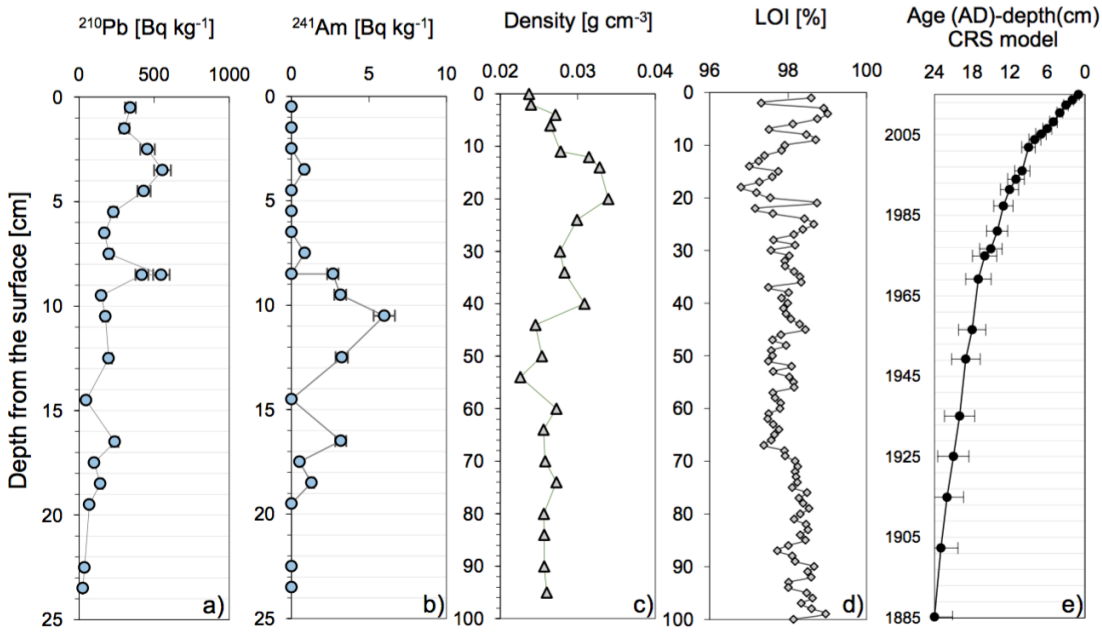


Fig. 2 **a)** and **b):** Radionuclide (210-Pb and 241-Am) activity distribution within the LHB peat core with errors at 1σ. Two additional samples investigated at 72 cm and 95 cm depth displayed no 210-Pb--241Am activity and are not plotted here. Radioactive equilibrium was reached at 24 cm from the surface. **c)** Density-, and **d)** Percent organic matter content along the LHB peat core. **e)** Age-depth relationship as received from the 210-Pb CRS model. The 1 sigma uncertainty in 210-Pb values including error propagation from calibrations is 10-12% (error bars). A combination of the 241-Am maximum and the 210-Pb inventory was used for the calculation of the final core chronology as detailed in the text.

3.2. Radionuclide chronology reconstruction

The detection limit of ^{210}Pb is located at 23-24 cm from the surface, indicating that almost the entire ^{210}Pb inventory is captured within this peat segment. The ^{210}Pb profile (Fig. 2a) is relatively complex and does not show a monotonous decrease with depth thus impeding the use of a constant initial concentration (CIC) approach. We therefore used constraints based on isotope specific properties in order to derive age information. Assuming that ^{210}Pb is not mobile, the complete inventory reflecting 4-5 half-lives is found in the top 24 cm of the peat profile. This implies a limit of 88-110 years at 24 cm, translating into an average accumulation rate of 0.22-0.27 cm yr^{-1}. Slower accumulation rates are expected if ^{210}Pb were somewhat mobile, but still within the calculated upper limit of 0.27 cm yr^{-1}. The sudden increase in ^{210}Pb activity at 8.5 cm cannot be due to a change in supply rate, but more likely represents a sudden collapse in the growth rate. Americium-241 (Fig. 2b) was found to be the least mobile among the investigated radionuclides, in agreement with findings of other studies (Gallagher et al. 2016). Americium-241 was present at much lower activities and it was detectable only in few samples. The broad ^{241}Am peak at 10-11 cm likely reflects the atmospheric release from nuclear tests in 1963-1964 (e.g., Gallagher et al., 2005). This would translate to a record of 50 years with an average accumulation rate of 0.21 cm yr^{-1} for the uppermost 11 cm.

However, this is a minimum value as ^{241}Am is also found at about half this activity in the sample below (at 12-13 cm), leaving the possibility that the actual ^{241}Am peak can be extended down to 12 cm depth. Two additional samples investigated at depths of 70-71 cm and 94-95 cm from the surface yielded no ^{210}Pb and ^{241}Am activity, but a small signal of ^{137}Cs (4.4 Bq kg^{-1}, Fig. 2c) was found at 70-71 cm. This observation suggests significant down core Cs mobility at our site (see *Appendix B.2*), meaning that ^{137}Cs is of little value in providing precise chronological information. Caesium mobility has been demonstrated in several studies of organic, clay-rich, low pH atmospheric and terrestrial archives, limiting its application as a chronologic tool (e.g., Appleby et al., 1991; Kudelsky et al., 1996). Consequently, ^{137}Cs activity was excluded from the chronology reconstruction of the LHB peat profile.

Combined, the activity profiles obtained from ^{210}Pb (S<0.27 cm yr^{-1}) and ^{241}Am (S >0.21 cm yr^{-1}, with a depth trend) yield an average accumulation of 0.24 ±0.03 cm yr^{-1} for the uppermost 24 cm of the LHB peat core, whereas slightly lower accumulation is expected for the uppermost 5 cm. This result is in agreement with the average values calculated for other Irish peat bogs (Hammond, 1978). The ^{210}Pb-^{241}Am age-depth relationship for the uppermost 24 cm was calculated based on the above information, and the results expressed as ages AD are presented along with element enrichment profiles in Figures 3 - 4.

3.3. Trace element data treatment

3.3.1. Principal component analysis (PCA)

A principal component analysis (PCA) has been suggested as a strategy to minimize the amount of factors governing enrichment in multi-element datasets such as the one presented here (e.g., Küttner et al., 2014; Martínez Cortizas et al., 2013; Muller et al., 2008). The main advantage of a factor analysis is that it allows the elements to be source-grouped according to their distribution patterns and loadings. We applied such PCA model for our dataset using the statistical software package PAST3 (Hammer et al., 2001). The results and interpretations are shown in *Appendix C*. In brief, three main components are able to explain 99.75% of the total variance. Factor 1 (PC1) accounts for the largest proportion of the variation (92.7%) with the other two factors, PC2 and PC 3, accounting to 4.4% and 2.7% respectively. PC1 includes the elements Pb, In, Sn, Sb, Ga, Cd, Cu, Zn, Ag, Ti, with Pb showing the highest association of 97%. PC2 groups the elements Ti, Zr, Ta, Ba, Li, As, Tl, Sr, and Rare Earth elements (REE) together, and PC3: Zn, W, Mo, Ni, Ti, Sr, Cr, and Fe. While 77% of Zn is shared with PC3, almost 15% of it is also shared with PC1, pointing to multiple sources controlling Zn enrichment in the LHB peat. Based on their element assemblages, the three element groups can be very carefully attributed to dust contributions from the historical Pb-Zn mining and

smelting, natural geogenic dust input, and emissions from fossil fuel combustion, respectively (*Appendix C*). The latter is yet to be characterised in more detail. We find that for the LHB dataset, the PCA approach offers a first insight into the major pollutant groups contributing to the element enrichment during the past century. However, in light of complex element apportioning to the respective components from co-occurring pollutants, the information obtained by the PCA is combined with other geochemical tools (e.g., enrichment factors) to better fingerprint sources contributing to metal enrichment in LHB.

3.3.2. Enrichment factors (EF)

When investigating anthropogenic pollution, upper crustal values (UCC) are sometimes used as a reference to extract the natural dust contributions. In doing so, metal enrichments are discussed relative to geogenic element backgrounds with a poorly soluble lithophile element, such as Ti, Sc, Sr, Zr, Al, Si, Y, Ta, or REE as a normalizer (e.g., Espi et al., 1997; Kempter et al., 1997; Marx et al., 2010; Shotyk, 1996). The use of the estimated UCC values as a measure for geogenic input has been, however, intensively debated in several studies (e.g., Martínez Cortizas et al., 2002; Reimann and De Caritat, 2000). The main criticism is that the calculated UCC values represent an average composition that is not necessarily representative of the local lithological background. This can ultimately result in an under- or overestimation of the natural geogenic budget transported into an archive. To overcome this issue, the interpretation of the element EF's relative to a local "baseline" or "background", representative for the area of interest has been proposed (e.g., Martínez Cortizas et al., 2002). This strategy is preferred for this study due to the versatile Irish geology, and trace element patterns are presented as enrichment factors (EF) with respect to the average of the least polluted and compositionally most consistent part of the core (62 and 100 cm from the surface). This bog "background" is used to calculate element EF's at shallower depths, as described in [1].

[1] $$EF = [(metal/Ta)_{sample} / (metal/Ta)_{background}]$$

The EF were calculated using the element concentrations in dried peat (at 105°C). Although Ti shows the highest loading (80%) within PC2 (geogenic dust), its partial association with PC1 (16% mining-smelting of local ores) and PC3 (*Appendix C*) restricts its application as natural dust indicator. We observe that, within this core, the best correlation with the residual ash (i.e., geogenic dust content) is built with Ta (R^2= *0.95, Appendix B.1*). This is (again) a strong argument that Ta is the best candidate to

extract dust depositions in our core. Tantalum has been shown to be an excellent proxy for geogenic input (e.g., Babechuk et al., 2015; Marx et al., 2010), but its successful analysis requires an acid-digest with HF of high purity, as employed here.

Trace element patterns show well-defined excursions of enrichments along the extracted LHB peat profile. In Figure 3 we show a representative selection of the results. Lead, Cu, and Zn depositions increase jointly from 62 cm depth and peak at different stages during the 20th century (Pb and Cu) until recently (Zn). Enhanced deposition is observed in a number of other metals which asynchronously reach their maxima between 1940 and 1960 (Ag and Sb), 1960 and 1970 (Ni), 1950's and recently (Mo). Rare earth elements (REE) are highest between 10 and 20 cm, i.e., first half of the 20th century, to then decrease again significantly in recently growing *Sphagnum* moss. A rapid decline in their enrichments is also observed for a number of other elements (e.g., Ag, Pb, Sn, Sb, In, Cd, U; not shown) between 1970 - present, whereas enrichments of Ni and Cu do not quite return to pre-anthropogenic levels and show diminished present-day atmospheric fallout (Fig. 3 and 5). Enrichment factors of Mo and Zn increase more rapidly from ca 1940 and reach highest values of 5 and 39, respectively in the sub-surface level of LHB.

3.4. Lead isotope compositions

Lead isotope ratios are presented together with EF_{backgr} of Cu, Zn, and Pb (Table 1 and Fig. 4). The Pb isotope composition is homogenous from the base of the core until ca. 18 cm ($^{206}Pb/^{204}Pb$: 18.271-18.429, $^{206}Pb/^{207}Pb$: 1.171-1.179). This turning point is coincident with major EF peaks observed for Cu and Pb. A dramatic change towards unradiogenic Pb signature is seen between 18 cm and 9 cm, where a small plateau is reached ($^{206}Pb/^{204}Pb$: 17.712-18.123, $^{206}Pb/^{207}Pb$: 1.138-1.161). The least radiogenic values ($^{206}Pb/^{204}Pb$: 17.657-17.678, $^{206}Pb/^{207}Pb$:1.135-1.136) are recorded at the depth interval between 8 and 4 cm from the surface. This period is followed by a reversal towards more radiogenic Pb isotope signature that extends up to the top of the bog. In detail, however, the modern isotope signature ($^{206}Pb/^{204}Pb$: 17.746-17.929, $^{206}Pb/^{207}Pb$: 1.137-1.148) does not quite return to the values below 18 cm.

Figure 3.

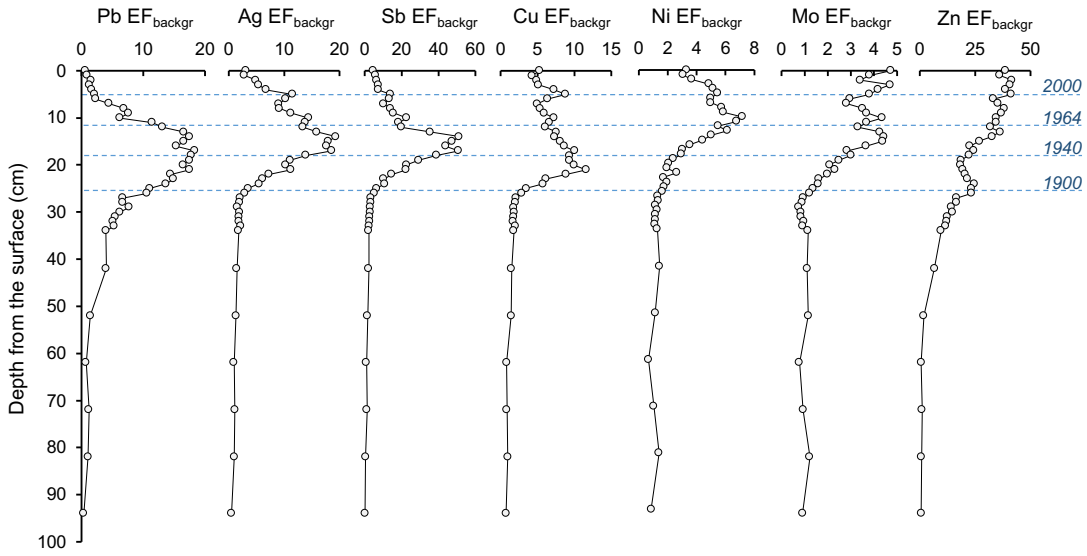


Fig. 3: Metal enrichment factors along the LHB peat core (grey circles) displayed relative to the background (EF_{backgr}) defined with the lowermost 4 samples (62-100cm). The chronology (AD) obtained from the ^{210}Pb-^{241}Am activity profiles is indicated in blue.

Figure 4.

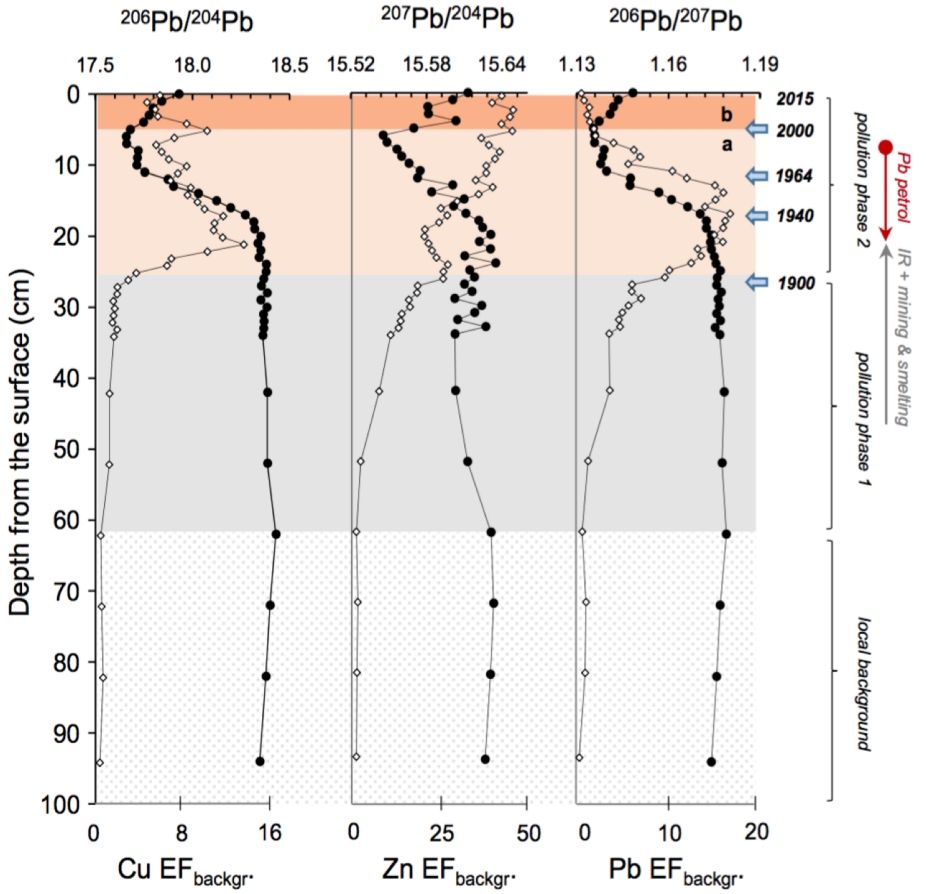


Fig. 4: Pb isotope ratios (black solid circles) together with EF_{backgr} of Cu, Zn and Pb (open diamonds) along the LHB peat core. Depth ranges distinguished by colours represent changes in either Pb isotopic composition, metal concentrations, or both. Radionuclide derived chronology and contemporaneous historical anthropogenic activities are also indicated.

4. Discussion

4.1. Temporal patterns in metal enrichments and implications for element mobility within Liffey Head bog

Conservative behaviour of at least some elements within ombrotrophic peatbogs is a prerequisite for their interpretation of atmospheric pollution histories. Lead, which is the element of primary interest in this study, has been shown to have no biological function (i.e., plant uptake) which can result in isotope fractionation (e.g., Shotyk, 1988). This is evidenced in several studies where the isotope excursions reflect chronological changes in the atmospheric Pb isotope composition. The large size of the (Pb^{2+}) cation results in its strong polarization to S-, P-, and N containing ligands which are main components in humic acids (Logan et al., 1997). Lead (as well as Cu) has been shown to be immobile over a broad range of pH conditions (3-8, Krosshaven et al., 1992). This is particularly important in the upper section of the bog, where a transition more acidic conditions occurs due to atmospheric exposure, and or in the area of water table fluctuation, which is considered the most important cause of remobilisation of some major elements and redox-sensitive metals (Clymo, 1983).

Acidic bog waters (pH = 3.5) have been associated with potential metal mobility, especially for Cd and Zn (Krosshaven et al., 1992). However, already at pH conditions of 4 - 5.5 (dominating in acrotelms) the mobility seems to strongly decrease (e.g., Pokrovsky et al., 2005). Consequently, experimental studies have shown that elements become less mobilised in basic environments, such as the catotelm. This is facilitated through the increasing amount of humic acids creating molecular sites for metal capture. To date, only few studies have investigated the behaviour of Sn, Sb, Co, Cr, Ni, V and In in ombrotrophic peat. For example, by investigating the trace metal enrichments in a peat bog from the Swiss Alps, Krachler et al. (2003) found out that V, Cr, and Ni followed trends of particulate depositions, with no significant accumulations at the surface of the bog. This was then interpreted as an immobile behaviour of these elements within the peat section. Nieminen et al. (2002) examined the metal accumulation in a peat bog from Finland and reported potential mobility of Zn, Ni, and As relative to Pb and Cu. It was suggested that further investigations are required for this archive to evaluate the magnitude of mobilisation, and potential interplay with other metal retaining mechanisms. Variable findings in different archives point at the necessity to examine and interpret metal excursions in each archive individually, as site-specific factors may play a significant role in metal remobilisation.

In the LHB, Cd, Ag, Sn, Sb, In, Co, Mo, Cr, and V are relatively well correlated with Pb (R^2=*0.71 to 0.88*) which is commonly accepted to be highly immobile in

ombrotrophic peat. Very strong correlations are observed between Ag-Sn-Sb-In (e.g., Ag/Sb: R^2=*0.93*), and Co-Mo-Cr-V-Zn (e.g., Co/V: R^2=*0.91*) dividing this wider group of elements into two suites, ultimately indicating the presence of at least two major pollution sources. The temporal deposition patterns of the Co-Mo-Cr-V group differ from those of Ag-Sn-Sb-In by displaying a continuing upward trajectory of their enrichment when other elements have shown improvement in their pollution load (Fig. 3). The onset of Zn enrichment is coincident with that of Pb. Both elements are well-correlated (R^2=*0.87*) from the bottom of the core until the second half of the 20th century, with maximum Pb $EF_{backgr.}$ and significant Zn enrichments observed for the period 1900s-1960 (Fig. 4). Chronologically, this corresponds to the contemporaneous Pb mining and smelting in the Wicklow uplands (Rynne, 2015). The divergence of Pb and Zn enrichment patterns towards the top of the core, i.e., over the last 50 years (R^2=*0.36,* Fig. 4) reflects either, i) the decreasing industrial use of the former and increased utility of the latter, or ii) post-depositional mobilisation of Zn (e.g., Weiss et al., 2007). The rapid decrease in the atmospheric Pb pollution load observed in the LHB from the 1960s onwards reflects the end of local mining and smelting. At the same time, significant correlations between Zn and other heavy metals such as Mo (R^2=*0.82*), or Ni (R^2=*0.80*) during the last decades likely hint at the emergence of a new pollution signal. In the following, the complex behaviour of element enrichments in LHB in the context of different pollution sources dominating the east coast of Ireland is discussed.

4.2. Sources of metal pollution deposited into the LHB

Next we evaluate the contributions from the various metal sources (lithogenic vs. anthropogenic) to the observed enrichment trends and Pb isotope composition in the LHB peat core in light of the known records of Irish industrial development. We would like emphasize, that while this study has the focus on reconstructing pollution sources over the past century, a thorough evaluation of the background and the period before 1900 is prerequisite for the interpretation of the element enrichments and peat Pb isotopy at shallower levels. We note that in environmental forensics, the most commonly used Pb isotope data presentation is the use of the following ratios: $^{206}Pb/^{207}Pb$ or $^{206}Pb/^{204}Pb$. While the former is justified by a better analytical precision, a normalisation to ^{204}Pb will result in the largest possible variability between reservoirs. Here, we assess the source apportionment with the conventional Pb diagram ($^{207}Pb/^{204}Pb$ vs. $^{206}Pb/^{204}Pb$) which offers better resolution. For ease of reference and comparison to previous studies, the calculated $^{206}Pb/^{207}Pb$ values are also included in the following discussion.

4.2.1. Local background composition (100-62 cm)

Lithophile element ratios in this peat segment (e.g., Y/Sc=1.5; Ba/Sc=39 to 43; Nb/Th=0.83 to 1.35) are comparable to typical upper continental crust (UCC) compositions (Y/Sc=1.6; Ba/Sc=41; Nb/Th=1.12, Mclennan, 2001), which are close or within the values reported for individual Wicklow granite units in the area (e.g., northern units Leinster batholith, Y/Sc=2.5 to 5; Ba/Sc=96 to 160; Nb/Th=0.9 to 7; Fritschele, 2016; Sweetman, 1987). This implies that the local bedrock and soils are the dominant source of elements at this depth, justifying our baseline selection. Lead isotope composition of the baseline, $^{206}Pb/^{204}Pb$= 18.387±0.012 and $^{207}Pb/^{204}Pb$= 15.626±0.010 ($^{206}Pb/^{207}Pb$=1.177±0.011) together with excess Pb concentrations [2] are used to calculate the natural, dust-free Pb isotopy of peat at shallower levels [3]. We note, that similar patterns are obtained by deploying the previously proposed Ti, Zr, or Sc (e.g., Shotyk, 2002) instead of Ta.

[2] $Pb_{excess} = Pb_{conc} - [(Pb/Ta)_{sample}/(Pb/Ta)_{background}]$

[3] $^{20x}Pb/^{204}Pb_{excess} = [(^{20x}Pb/^{204}Pb_{measured} * Pb_{conc}) - (^{20x}Pb/^{204}Pb_{backgr.} * Pb_{backgr.})] / Pb_{excess}$

where the Pb_{excess} and $^{20x}Pb/^{204}Pb_{excess}$ are the baseline corrected concentration and isotopic composition of Pb in the polluted samples, Pb_{conc} and $^{20x}Pb/^{204}Pb_{measured}$ are the analysed Pb concentration and isotopic compositions, Pb/Ta_{sample} is the ratio in the polluted part of the bog, $Pb/Ta_{backgr.}$ and $^{20x}Pb/^{204}Pb_{backgr.}$ represent the compositions of the background (100-62 cm), and $Pb_{backgr.}$ is the average Pb concentration in the unpolluted part of the bog. For further calculations, the subtracted local geogenic contribution was no longer considered.

4.2.2. Pollution phase 1 (62-25 cm, pre-1900 AD)

Enrichment factors of Cu, Zn, and Pb increase at this depth, which covers a time period before the 20th century. This peat segment is considered to have been impacted by anthropogenic activity. The very strong correlation between $EF_{backgr.}$ Pb and Zn (R^2=*0.96*) suggests a common source of these metals to the bog. Importantly, Pb isotope values do not change substantially from the composition of the local background (segment 62-100 cm, Fig. 4) and are comparable to the published values of the granitic Leinster batholith (Fig. 5a., e.g., Kennan et al., 1987), which is the host rock of local Pb-Zn-Ag mineralisation. The increasing heavy-metal input is thus interpreted to reflect Pb-Ag extractions from very high-grade but low-tonnage local galena-rich veins exposed in the Wicklow uplands (Rynne, 2015). This mining activity occurred between 1824 and

1890 AD (Schwartz and Critchley, 1997). Smelting of these and other Irish ores was conducted ~15 km NE from LHB (and ~35 NE km from the mining site) at Ballycorus (e.g., Callaghan, 2014; Shepard, 1981), which may have additionally contributed to the overall pollution load. Whereas Pb was the metal of interest of these extractions, concurrent atmospheric release of Zn is evident from the correlation with Pb. The synchronous onset of Zn and Pb enrichment is most probably the result of Zn co-occurring in most Pb ore bodies. An important known example of accidental initial Zn pollution from Pb mining was the giant Broken Hill deposit in south-central Australia, where the relative timing of Pb+Ag vs. Zn extraction is accurately reflected in a mire peat core ca. 1,000 km downwind from the mine (Marx et al., 2010). In the LHB, Pb isotope signal argues against a contribution of Pb, and by analogy of Zn, from the clearly distinguishable fingerprint of sphalerite-galena mineralisation hosted in the Lower Carboniferous strata of the Midland basin (e.g., Wilkinson and Eyre, 2005, Fig. 5a), subjected to small scale extractions during the same time period (Rynne, 2015).

Figure 5.

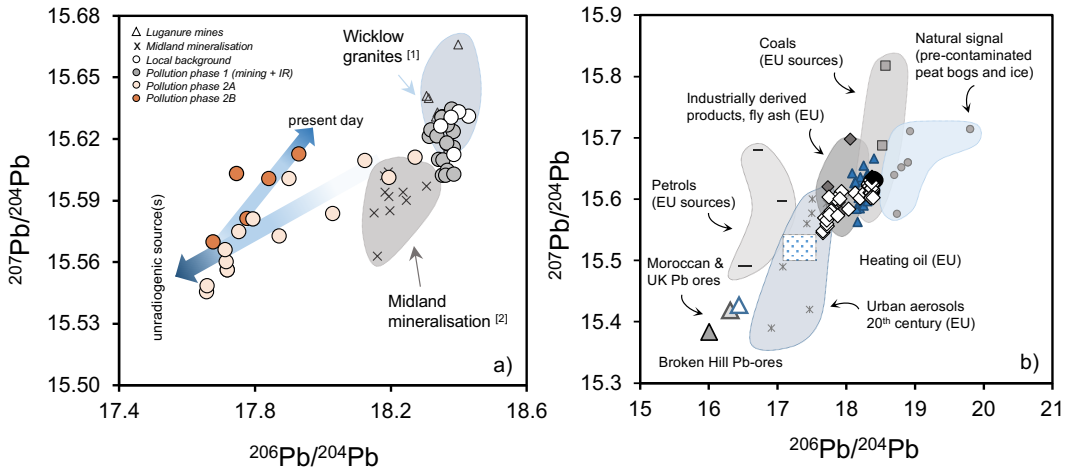


Fig. 5. a) Common Pb ($^{207}Pb/^{204}Pb$ vs. $^{206}Pb/^{204}Pb$) plot of LHB peat subsamples and literature values of local mineralisation: [1] Wicklow granites, Kennan et al. (1986), and the Midlands mineralisation [2] Hitzman et al. (1992), and Wilkinson et al. (2005). A sharp change in the Pb isotopic composition is observed from ca. 1940; b) Zoomed out common Pb diagram with pre-polluted peat samples (black solid circles) and all polluted LHB samples (white diamonds) together with the values of the local mineralisation. Also shown are Pb isotope ratios of pre-pollution at other sites (Kylander et al., 2005; 2010; Monna et al., 2010; Rosman et al., 1997) and for different anthropogenically derived pollutants compiled from Chiaradia and Cupelin, 2000; De Vleeschouwer et al., 2009; Hansmann and Koppel, 2000; Monna et al., 1997; Sudgen et al., 1993; Towsend et al., 1998; Veron et al., 1999; Walraven et al., 1997). Error bars for all LHB Pb isotope values are smaller than the symbols.

4.2.3. Pollution phase 2a (25-5 cm, ~1900-2000 AD)

Between 1900 and 1960's, concentrations of Cu, Ag, Pb, Sb, and Sn in dry peat exceed their values in UCC by 12x, 22x, 3x, and 6x, respectively, exposing a previously

underappreciated magnitude of industrial pollution in the Wicklow uplands. While remaining sub-parallel, REE enrichments are the highest during the early 1900s, suggestive of an enhanced fallout of atmospheric dust from local mining activities and Industrial Revolution. Silver, Cu, and Sb pollution coincide with early 20th century mining for coinage at Silvermines, Co. Tipperary and Luganure mines, and extraction of stibnite (Sb_2S_3) and pyrite (FeS_2) at Avoca (Fig. 1).

The enhanced atmospheric supply of redox sensitive elements such as V, Cr, Mo, Cd, and other metals such as Zn, Sn, V, and Ni observed in the LHB during the first half of the 20th century can be attributed to the continuing atmospheric pollution resulting from the combustion of UK sourced coals (e.g., Danihelka et al., 2003), extensively used for domestic and industrial purposes in Ireland. However, due to the similar Pb isotopic compositions of these coals ($^{206}Pb/^{207}Pb$=1.181-1.184±0.018; Farmer et al., 1999) with respect to the mining-dominated Pb signature in LHB peat (e.g., $^{206}Pb/^{207}Pb$= 1.177±0.011) coal pollution can only be inferred from the ensemble of observed trace metal enrichments.

A notable change in the geochemistry of the pollutant, specifically, a decrease in Pb and Ag and an increase in Zn, Mo, and Ni is evident from ca 1940 (Fig. 6a-d). Most important, this period documents the decoupling of Zn from Pb, as local mining pollution is gradually replaced by one or more modern sources of heavy metal pollution (e.g., *1920 AD*: Pb/Zn=0.4-0.6; *1970 AD*: Pb/Zn=0.1-0.05). This prominent change is also observed in Pb isotope composition. From ca 1940 onwards Pb isotopes reflect the transition from mining originated Pb to pollution from the hemispheric introduction of leaded gasoline known to have introduced a ^{206}Pb depleted signature to the atmosphere. Quantifying the potential contribution of vehicle exhaust emissions before 1940's is again, complicated by the continuing Pb pollution from the local mining until ca. 1957. We therefore attempted to disentangle the two contributions with a binary mixing calculation (Fig. 7b., and described in *Appendix D*) between the following end-members: **A**, pollutant 1 ($^{206}Pb/^{204}Pb$ =18.30, $^{207}Pb/^{204}Pb$ =15.62, $^{206}Pb/^{207}Pb$=1.174] mining/industrial signal of the early 20th century), and **B**: pollutant 2 ($^{206}Pb/^{204}Pb$= 17.20, $^{207}Pb/^{204}Pb$ =15.54, $^{206}Pb/^{207}Pb$=1.109] average European-Australian leaded gasoline). The modelled curves were calculated using different Pb concentrations of the respective end-member pollutants (10-200 μg g^{-1}).

Mixing calculations expose the increasing influence of leaded gasoline over the course of 20th century, becoming progressively more accentuated only after the decline of the local mining and smelting activity (post 1940, 18 cm). The least radiogenic $^{206}Pb/^{207}Pb$ values of 1.138±0.011 recorded in peat from the 1970-80s represent the peak Pb contribution from leaded petrol (Fig. 7a). However, because there is also notable variation in the Pb isotope composition of the ores used for the additives

($^{206}Pb/^{207}Pb$=1.06-1.12, Towsend et al., 1998; Veron et al., 1999), there is large uncertainty of 6 to 78% in the calculated contributions (Fig. 7b). Similar findings were made in studies of peat bogs and freshwater lake sediments from central Scotland (e.g., Farmer et al., 1997). Importantly, it is noted that during the main period of leaded gasoline use, 1950-1980 AD, Pb experienced a decrease in its pollution load (Fig. 3) in the LHB, which, by international comparison is unusual. The least radiogenic Pb isotopic signal measured in the peat that accumulated at the end of 20th century is most probably related to a higher proportion of Australian Pb ores in gasoline products (e.g., Farmer et al., 1999).

Figure 6.

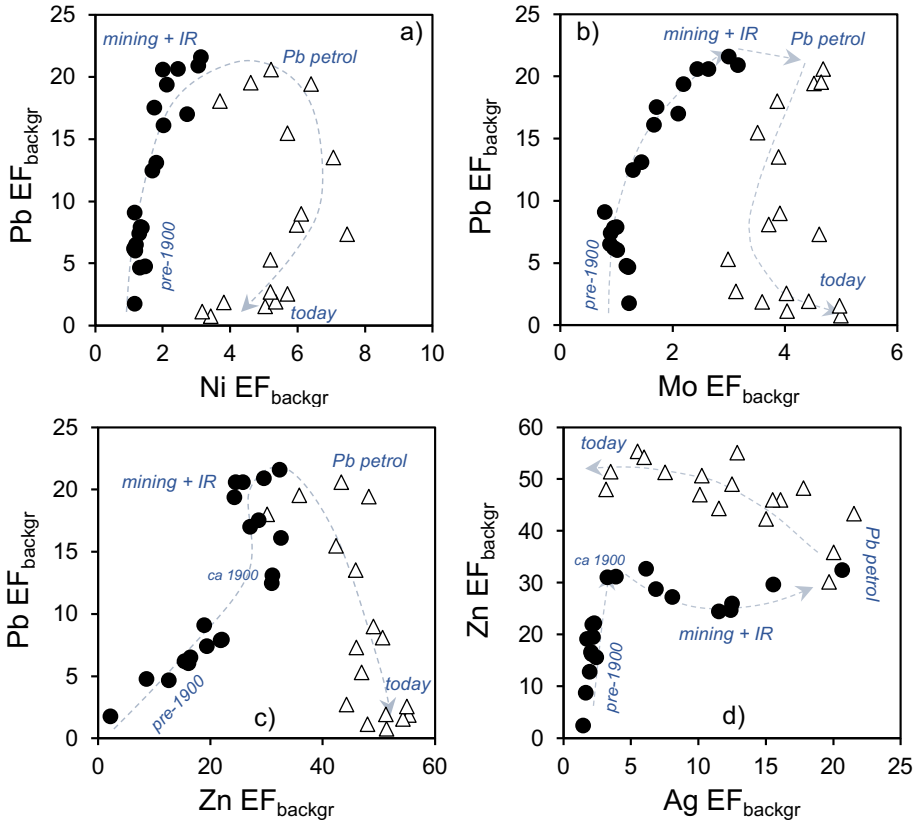


Fig. 6. Bivariate plots of selected metal EF_{backgr} of peat from the LHB core. Samples from the lower part of the core (prior the introduction of the Pb gasoline from 1940) are shown as solid black circles. Peat deposited from the 1940s until present day are shown as white open triangles. Grey arrows indicate upward direction from the base of the core to the top, i.e., from local background through the mining period, Industrial Revolution (IR), Pb gasoline to present day.

Despite continuing Pb-Zn (Tynagh, Navan, Silvermines, Galmoy, and Lisheen) and Cu-Ag-Hg (Ballynoe and Gortdrum) mining from the 1970's into the 21st century at different sites in Ireland, there is poor correspondence between the more recent enrichment peaks within LHB and the reported tonnage extractions, especially for Zn and Pb (see *Appendix B.3*). Potential explanations for this discordance could be that most ore is

extracted underground and that domestic smelting has ended, leading to historically lowest atmospheric pollution from recent Zn-Pb mining. In fact, absolute concentrations of Pb reach background levels of 5-20 µg g^{-1} within the uppermost 8 cm which demonstrates a general Pb depletion in all current atmospheric pollutants. In summary, in the LHB, the gasoline Pb signal was initially masked by high loads of local Pb contamination. Only when this subsided and overall Pb EF dropped, did gasoline become a significant contributor.

Figure 7.

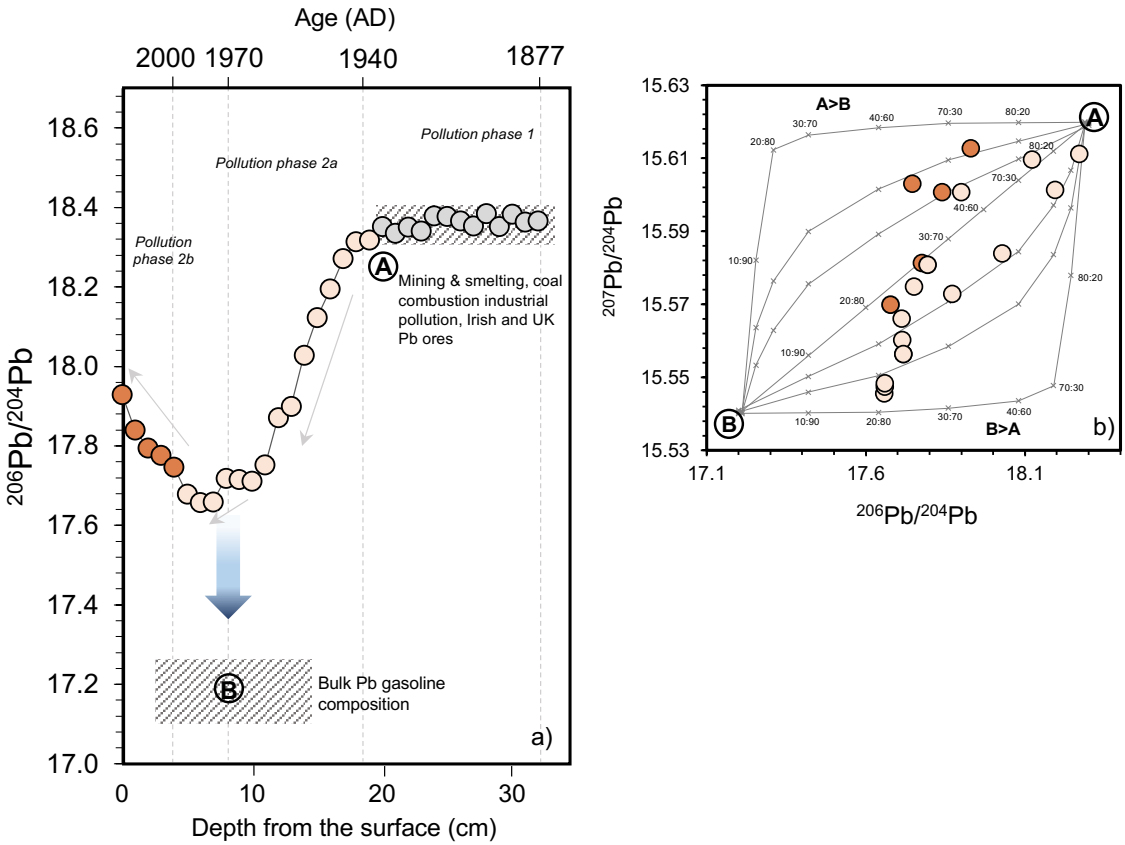


Fig. 7. a) Chronology-integrated $^{206}Pb/^{204}Pb$ isotope composition of the upper part of the LHB peat profile together with areas representative of the local mineralisation (Kennan et al., 1986) and potential anthropogenic pollution sources during the 19th to 21st century. b) Common Pb isotope binary mixing model using A: average Pb isotope values of local mineralisation ($^{206}Pb/^{204}Pb$=18.300; $^{207}Pb/^{204}Pb$=15.622, Kennan et al., 1986), and B: average compositions representative for aerosols associated with Pb enriched vehicle emissions ($^{206}Pb/^{204}Pb$=17.200; $^{207}Pb/^{204}Pb$=15.543, e.g., Chiaradia and Cupelin 2000; Monna et al., 1997; Veron et al., 1999). Lead concentrations range between 10 and 200 µg g^{-1}, corresponding to values measured along the LHB peat profile. For the calculation steps refer to the text and *Appendix C*. Error bars are smaller than the symbols.

4.2.4. Pollution phase 2b (4-0 cm, 2000-2015 AD)

With the abolition of leaded gasoline in 2000 AD in Ireland, Pb isotopic compositions progressively returned to more radiogenic values (Fig. 7a). However, these ratios ($^{206}Pb/^{204}Pb$=17.929±0.007; $^{207}Pb/^{204}Pb$=15.613±0.007; [$^{206}Pb/^{207}Pb$=1.148±0.007]) are

far from the unpolluted pre-industrial signal, implying either, i) a slow post-gasoline amelioration of atmospheric Pb pollution load, ii) recent pollution with partially ^{206}Pb depleted signature, iii) redistribution of some of the earlier Pb within the living part of the bog, or iv) a combination of these factors.

Similar to LHB, near-top pollution in REE, Zn, Cd, Ni, Mo, Cr, and Cu has also been observed at several other sites internationally and has variably been interpreted to result from the application of fertilisers and pesticides (e.g., Huang and Jin, 2008; Zhang and Shan, 2009). Because these metals are present in a variety of present-day pollutants, Marx et al. (2010) proposed a different approach to unravel pollution from agriculture by investigating the Y/Ho ratio. This ratio displays very little variability in terrestrial rocks (25-29 e.g., Kamber et al., 2005; Pack et al., 2007) but is consistently higher in seawater (40-70 e.g., Byrne and Lee, 1993; Nozaki et al., 1997). Marine sediments precipitated from seawater, including phosphates, which are widely used as fertilisers, inherit the hallmark feature of excess Y>Ho from seawater. The majority of fertilisers applied in Ireland from the second half of the 20th century contained pulverised phosphate from the Tethyan phosphorogenic province (Upper Cretaceous to Eocene strata of North Africa), shown to be enriched in the REE (e.g., Emsbo et al., 2015). In LHB peat, Y/Ho ratios remain relatively constant from the base of the core until ca. 2000 (26 to 28 ±1.31), followed by a rapid increase to 35±0.78 at the top (last 8 samples, *Appendix B.4*), coincident with increase in Zn and other trace metals (Fig. 3). The enrichments coincide with the start of the Irish forest fertilisation experiment in the 1980s, in which fertiliser was applied by air. The experiment aimed at restoring the woodlands in the Wicklow Mountains after their extensive exploitation during previous centuries. Although the necessity of investigating the geochemistry of this exact point source is recognised, we propose that near-surface metal and REE pollution in LHB peat was at least partially caused by accidental dispersion of fertiliser to nearby forests.

Recent enrichments of Cu and Ni cannot be directly associated with fertiliser application, and are more indicative of fossil fuel burning. Element ratios such as Pb/Ni and Cu/Pb in near-surface samples (3-6.7 and 0.4-1, respectively) are within the experimentally determined values of the aerosols and particulate matter (PM) resulting from combustion of peat (1.8-14.6 and 0.6-1, Othman and Latif, 2013). Peat is an important heating fuel in most rural areas of Ireland, and seasonal harvesting takes place also at the peripheries of LHB. In addition, there is an ongoing debate on the environmental impact of two major turf-fired electricity plants and several coal-burning stations continuing to operate in the Irish Midlands. Although peat and coal has been an important energy source throughout the last two centuries in Ireland, it is very likely that pollution from these sources became more accentuated only in recent years, after the elimination of the mining and leaded gasoline signal.

4.3. Timing of Pb pollution and synthesis of Pb isotope information from other relevant peat archives

Due to its location at the east coast of Ireland, LHB records processes that are part of broader regional and hemispheric pollution patterns. In order to facilitate a comparison between the Pb pollution history recorded by LHB and other Irish archives (Coggins et al., 2006; Schell et al.,1997), accumulation rates were calculated according to the method described in detail by Muller et al. (2008). In LHB, Pb deposition rates range between 0.45-1.8 μg cm^{-2} yr^{-1}, with values >1 μg cm^{-2} yr^{-1} observed at different stages throughout the 20th century (Fig. 8). Peak accumulation rates are detected between 1960's and 1980's, in excellent agreement with the Pb deposition rates in a peat archive situated ca 1-2 km away to the west, Kippure bog (Schell et al., 1997). Lead accumulation rates are higher in the LHB peat deposited during the early 20th century mining period, which is likely due to its relative proximity to the mining and smelting sites. Enhanced Pb deposition during the 1980's can be attributed to the leaded gasoline peak, as it can also be seen from the Pb isotope composition of LHB. In the Midlands (Clara bog), Pb deposition rates were up to 3 times lower than at the eastern seaboard (Fig. 8), yet still higher than at all sites investigated so far along the west coast (Knockroe, Co. Mayo 0.1-0.3 μg cm^{-2} yr^{-1}, Letterfrack, Co. Galway 0.4-0.5 μg cm^{-2} yr^{-1}, Coggins et al., 2006; and Bellacorick, Co. Mayo, 0.05-0.4 μg cm^{-2} yr^{-1} Schell et al., 1997). It appears that historical mining and smelting have not significantly influenced the archives on the west, although there is also the possibility that the clean Atlantic winds dominating here contribute to an overall dilution of atmospheric pollution. Peak Pb deposition at the west coast occurs slightly earlier during the 1960's and has been previously interpreted to render the long-range transport of polluting Pb from the American continent. We suggest that further investigations, such as the Pb isotopy of these westernmost archives are necessary before exact conclusions can be drawn. A trans-Atlantic Pb gasoline pollution during the 1960's would anticipate the isotope signal of the peat to be close to those of Canadian ($^{206}Pb/^{207}Pb$= 1.15-1.17, Bathurst) and USA ($^{206}Pb/^{207}Pb$= >1.28, e.g., Mississippi) ores.

In general, the timing of Pb isotopic excursions in LHB core coincide with those in bogs from Scotland (e.g., Farmer et al., 2002), Sweden (Bindler et al., 2004), or Spain (Martinez-Cortizas et al., 2012). All these archives commonly report a $^{206}Pb/^{207}Pb$ of 1.16-1.18 in the lower sections (i.e., geogenic influx, and/or mining), and a rapid change towards less radiogenic $^{206}Pb/^{207}Pb$ of 1.13-1.14 at peak Pb-gasoline pollution (1970 to 1980 AD). Because of the different chronology of recent atmospheric pollution in North America (e.g., Bindler et al., 2001; Pérez-Rodríguez et al., 2018; Weiss et al., 2002), it

is likely that the east coast of Ireland was, and currently is influenced by local pollution, as well as central- and north-European pollution circulation, rather than trans-Atlantic sources, as suggested from the dominant wind directions. The later could be, however, subjected to dilution considering the long travel distance.

Figure 8.

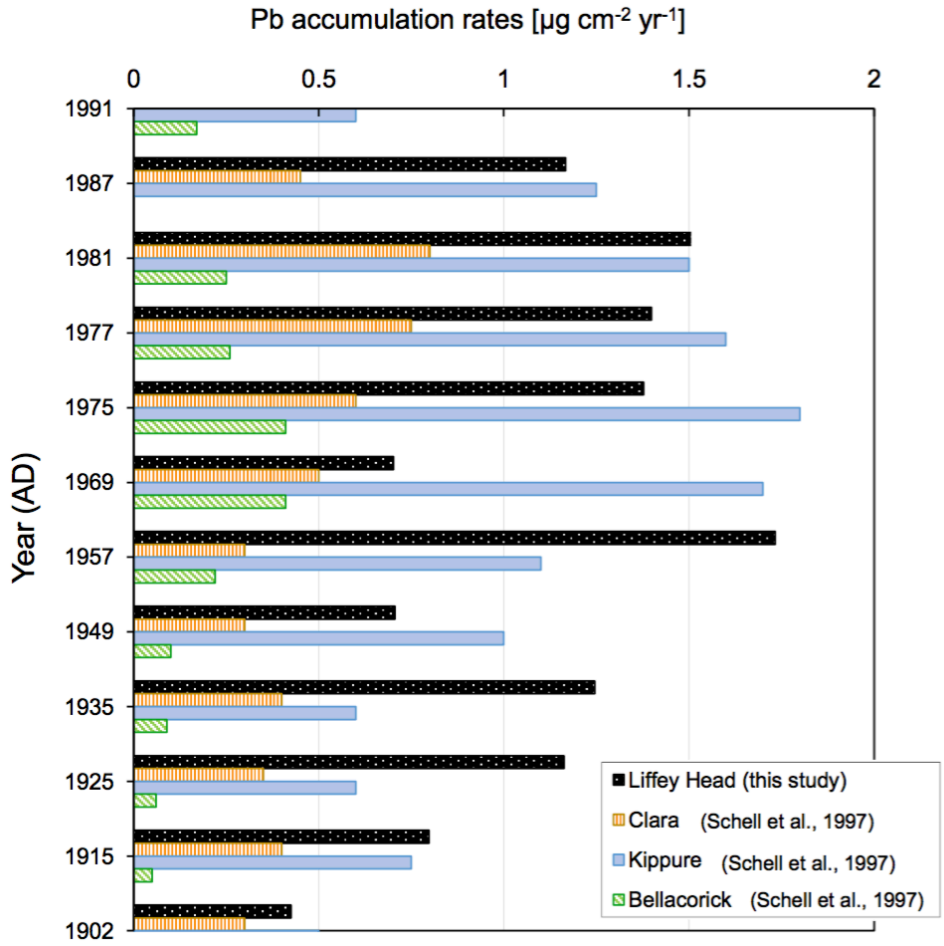


Fig. 8 Lead accumulation rates µg cm^{-2} yr^{-1} in the upper part of the LHB (this study). Shown are also accumulation rates calculated in other peat archives from Ireland (Schell et al., 1997).

5. Summary and conclusion

We investigated the atmospheric elemental and Pb isotope evolution resulting from local mining, industrial activities and leaded gasoline pollution in eastern Ireland over the last century from the geochemistry of a bog in the Wicklow Mountains. The elemental cycle associated with mining of local ores (e.g., Pb, Cu, Ag, Sn, Sb) was highly perturbed during the major period of mining and smelting in the Wicklow area (19^{th} to 20^{th} century), showing up to 20-fold, 15-fold, and 50-fold enrichments (Pb, Ag, and Sb, respectively)

with respect to the established baseline of the core. Element deposition associated with the combustion of fossil fuels (Zn, V, Ni, Cr and Mo) is detected throughout the polluted section of the core. This pollutant becomes increasingly more pronounced only after the abolition of the mining activity in the area (ca. 1940-recent). The Pb isotopes precisely document the shift towards less radiogenic $^{206}Pb/^{204}Pb$ values in response to the introduction of the Pb petrol additives from ca. 1940 (in this archive) until its complete elimination in 2000 in Ireland. In the most general sense, the observed isotopic shift ($^{206}Pb/^{207}Pb$=1.138±0.011 in 1970) is consistent with findings in other records of atmospheric Pb deposition around Europe (e.g., Sweden, Brännvall et al., 1997; Scotland, Farmer et al., 1997; Spain, Kylander et al., 2005; Switzerland, Weiss et al., 1999). However, unlike at most other sites, the introduction of leaded petrol is not associated with the highest atmospheric Pb pollution load at this site, which was instead caused by the historical Pb-Zn mining and smelting of local ores. Despite a notable decline in the leaded gasoline signal after 2000, the Pb isotopic composition has not quite returned to pre-industrial values, implying input from modern pollutant sources. Based on combined trace element and Pb isotope investigations, we suggest that coal, peat, and oil combustion, emissions from unleaded petrol, fertilizer application, as well as trans-regional industrial pollution (e.g., waste incinerators) potentially reaching Ireland on easterly airstreams are the sources contributing to aerial Pb pollution at this site today. The strong local control of the bog geochemistry demonstrated in this study emphasises the need to combine metal concentration and isotopic investigations for reconstructing historic pollution. Without having investigated the Pb isotopic patterns, the major Pb enrichment peak could have been erroneously attributed to an early Pb gasoline signal. The decline in most heavy metals (esp. Pb, Cu, Sb) in the present day *Sphagnum* moss is in line with observations made in bogs from elsewhere (e.g., Switzerland, Shotyk et al., 2001), and can be attributed to tougher air pollution prevention policies adopted in Europe over the last three decades.

Acknowledgements

The research leading to these results has received funding from the People Programme (Marie Currie Actions) IsoNose (www.isonose.eu) of the European Union's Sevenths Framework Programme FP7/2007-2013/under REA grant agreement no [608069].

References

Appleby, P.G., Richardson, N., Nolan, P.J., 1991. 241Am dating of lake sediments. Hydrobiologia 214, 35-42.

Appleby, P.G., Oldfield, F., 1992. Application of lead-210 to sedimentation studies. In: Ivanovich, I., Harmon, R.S. (Eds.), Uranium Series Disequilibria: Application to Earth, Marine an Environmental Science. Claredon, Oxford, UK, pp. 732-778.

Appleby, P.G., Shotyk, W., Fankhauser, A., 1997. Lead-210 age dating of three peat cores in the Jura Mountains, Switzerland. Water Air Soil Pollution 100, 223–231.

Babechuk, M.G., Kamber, B.S., Greig, A., Canil, D., Kodolányi, J., 2010. The behaviour of tungsten during mantle melting revisited with implications for planetary differentiation time scales. Geochimica et Cosmochimica Acta 74, 1448-1470

Babechuk, M.G., Widdowson, M., Murphy, M., Kamber, B.S., 2015. A combined Y/Ho, high field strength element (HFSE) and Nd isotope perspective on basalt weathering, Deccan Traps, India. Chemical Geology 396, 25-41. doi:10.1016/j.chemgeo.2014.12.017

Baker, J., Peate, D., Waight, T., Meysen, C., 2004. Pb isotopic analysis of standards and samples using a 207Pb-204Pb double spike and thallium to correct for mass bias with a double focusing MC-ICP-MS. Chemical Geology 211, 275-303

Boyle, R., 1977. Cupriferous bogs in Sackville area, new brunswick, Canada. Journal of Geochemical Exploration 495–527

Bowman, J.J., McGettigan, M., 1994. Atmospheric deposition in acid sensitive areas of Ireland-the influence of wind direction and a new coal burning electricity generation station on precipitation quality. Water Air Soil Pollution 75, 159-75

Bindler, R., Klarqvist, M., Klaminder, J., Forster, J., 2004. Does within-bog spatial variability of mercury and lead constrain reconstructions of absolute deposition rates from single peat records? The example of Store Mosse, Sweden, *Global Biogeochemical Cycles,* 18, GB3020.

Bränvall, M.L., Bindler, R., Emteryd, O., Nilsson, M., Renberg, I., 1997. Stable isotope and concentration records of atmospheric lead pollution in peat and lake sediments in Sweden. Water, Air Soil Pollution 100, 243-252

Byrne, R.H., Lee, J.H., 1993. Comparative yttrium and rare earth element chemistries in seawater. Marine Chemistry 44, 121-130

Callaghan, S., 2014. A comparison of the sedimentary record of the Upper Lake Glendalough, County Wicklow, with the historic lead mining of the area. The Journal of the Mining Heritage Trust of Ireland 14, 87-102

Carignan, J., Libourel, G., Cloquet, C., Le Forestier, L., 2005. Lead isotopic composition of fly ash and flue gas residues from municipal solid waste combustors in France: Implications for atmospheric lead source tracing. Environmental Science Technology 39, 2018–2024. doi:10.1021/es048693x

Chiaradia, M., Cupelin, F., 2000. Behaviour of airborne lead and temporal variations of its source effects in Geneva (Switzerland): comparison of anthropogenic versus natural processes. Atmospheric Environment 34, 959-71

Clymo, R.S., Oldfield, F., Appleby, P.G., Pearson, G.W., Ratnesar, P., Richardson, N., 1990. The record of atmospheric deposition on a rainwater dependent peatland. Philosophical Transactions of the Royal Society B 327, 105-112. doi:10.1098/rstb.1990.0070

Cloy, J.M., Farmer, J.G., Graham, M.C., MacKenzie, A.B., Cook, G.T., 2008. Historical records of atmospheric Pb deposition in four Scottish ombrotrophic peat bogs: An isotopic comparison with other records from western Europe and Greenland. Global Biogeochemical Cycles 22, 1–16. doi:10.1029/2007GB003059

Coggins, A.M., Jennings, S.G., Ebinghaus, R., 2006. Accumulation rates of the heavy metals lead, mercury and cadmium in ombrotrophic peatlands in the west of Ireland. Atmos. Environ. 40, 260–278. doi:10.1016/j.atmosenv.2005.09.049

Danihelka, P., Volna, Z., Jones, J.M., Williams, A., 2003. Emission of trace toxic metals during pulverized fuel combustion of Czech coals. Int. J. Energy Res. 27, 1181–1203. doi:10.1002/er.942

Dean, W.E.J., 1974. Determination of carbonate and organic matter in calcareous sediments and sedimentary rocks by loss on ignition: comparison with other methods. Journal of Sedimentary Petrology 44, 242–248

De Vleeschouwer, F., Fagel, N., Cheburkin, A., Pazdur, A., Sikorski, J., Mattielli, N., 2009. Anthropogenic impacts in North Poland over the last 1300 years - a record of Pb, Zn, Cu, Ni and S in an ombrotrophic peat bog. Science of the total Environment 407, 5674-84

De Vleeschouwer, F., Vanneste, H., Mauquoy, D., Piotrowska, N., Torrejón, F., Roland, T., Stein, A., Le Roux, G., 2014. Emissions from pre-Hispanic metallurgy in the South American atmosphere. PLoS One 9. doi:10.1371/journal.pone.0111315

Doe, R.B., 1970. Lead Isotopes. Berlin: Springer-Verlag; Eades.

Eggins, S.M., Woodhead, J.D., Kinsley, L.P.J., Mortimer, G.E., Slyvester, M.T., McCulloch, M.T., Hergt, J.M., Handler, M.R., 1997. A simple method for the precise determination of >40 trace elements in geological samples by ICPMS using enriched isotope internal standardisation. Chemical Geology 134, 311-326

Emsbo, P., McLaughlin, P.I., Breit, G.N., du Bray, E.A., Koenig, A.E., 2015. Rare earth elements in sedimentary phosphate deposits: solution to the global REE crisis? Gondwana Research 27, 776-785

Erel, Y. Veron, A., Halicz, L., 1997. Tracing the transport of anthropogenic lead in the atmosphere and in soils using isotopic ratios. Geochim Cosmochim Acta 61:4495–4505

Espi, E., Boutron, C.F., Hong, S., Pourchet, M., Ferrari, C., Shotyk, W., Charlet L., 1997. Changing concentrations of Zn, Cd and Pb in a high altitude peat bog from Bolivia during the past three centuries, Water, Air and Soil Pollution, 100, 289-296.

Farmer, J.G., Eades, L.J., Mackenzie, A.B., Kirika, A., Bailey-Watts, T.E., 1996. Stable lead isotope record of lead pollution in Loch Lomond sediments since 1630 AD. Environmental Science and Technology 30, 3080–3083. doi:10.1021/es960162o

Farmer, J.G., Mackenzie, A.B., Sugden, C.L., Edgar, P.J., Eades, L.J., 1997. A comparison of the historical lead pollution records in peat and freshwater lake sediments from central Scotland. Water Air Soil Pollution doi:10.1023/A:1018320425006

Farmer, J.G., Eades, L.J., Graham, M.C., 1999. The lead content and isotopic composition of

British coals and their implications for past and present releases of lead to the UK environment. Environmental Geochemistry and Health 21, 257–272. doi:10.1023/A:1006688515919

Farmer, J.G., Graham, M.C., Bacon, J.R., Dunn, S.M., Vinogradoff, S.I., MacKenzie, A.B., 2005. Isotopic characterisation of the historical lead deposition record at Glensaugh, an organic-rich, upland catchment in rural N.E. Scotland. Science of the Total Environment 346, 121–137. doi:10.1016/j.scitotenv.2004.11.020

Feeley, H.B., Bruen, M., Blacklocke, S., and Kelly-Quinn, M., 2013. A regional examination of episodic acidification response to reduced acidic deposition and the influence of plantation forests in Irish headwater streams. Science of the Total Environment 443, 173-183

Ferrat, M., Weiss, D.J., Dong, S., Large, D.J., Spiro, B., Sun, Y., Gallagher, K., 2012. Lead atmospheric deposition rates and isotopic trends in Asian dust during the last 9.5kyr recorded in an ombrotrophic peat bog on the eastern Qinghai-Tibetan Plateau. Geochimica et Cosmochimica Acta 82, 4–22. doi:10.1016/j.gca.2010.10.031

Fritschele, T., 2016. Age and Origin of Late Caledonian Granites and Ordovician Arc Magmatic Rocks in Ireland and the Isle of Man. Ph.D. thesis, University College Dublin, Dublin, 357

Gallagher, D., Mcgee, E.J., Mitchell, P.I., Alfimov, V., Aldahan, A., Possnert, G., 2005. Retrospective search for evidence of the 1957 Windscale fire in NE Ireland using 129I and other long-lived nuclides. Environmental Science and Technology 39, 2927–2935. doi:10.1021/es049049l

Gallagher, D.E., McGee J., and Mitchell P.I., 2016. A Recent History of 14C, 137Cs, 210Pb, and 241Am Accumulation at Two Irish Peat Bog Sites: an East Versus West Coast Comparison. Radiocarbon 43: 517-525

Geological Survey of Ireland (GSI): https://www.gsi.ie/Publications+and+Data/

Goldberg, E.D., 1963. Geochronology with 210Pb in radioactive dating. IAEA, Vienna, pp. 121-131.

Hammer, Ø., Harper, D.A.T., and P. D. Ryan, 2001. PAST: Paleontological Statistics Software Package for Education and Data Analysis. Palaeontologia Electronica 4(1): 9pp.

Hammond, R.F., 1978. The Peatlands of Ireland. Soil Survey Bulletin, 35 1–63

Hansmann, W., Köppel, V., 2000. Lead-istopes as tracers of pollutants in soils. Chemical Geology 171, 123–144. doi:10.1016/S0009-2541(00)00230-8

Hitzman, M.W., O'Connor, P.G., Shearley, E., Schaffalitzky, C., Beatty, D.W., Allan, J.R., and Thompson, T., 1992, Discovery and geology of the Lisheen Zn-Pb-Ag prospect, Rathdowney trend, Ireland, *in* Bowden, A.A., Earls, G., O'Connor, P.G., and Pyne, J.F., eds., The Irish minerals industry 1980–1990: Dublin, Irish Association for Economic Geology, p. 227-246

Huang, S., Jin, J., 2008. Status of heavy metals in agricultural soils as affected by different patterns of land use. Environmental Monitoring and Assessment 139, 317-327

Hurst, R.W., 2002. Lead isotopes as age-sensitive, genetic markers in hydrocarbons: 2. Kerogens, crude oils, and unleaded gasoline. Environmental Geoscience 9, 1–7

Jochum, K.P., Weis, U., Schwager, B., Stoll, B., Wilson, S.A., Haug, G.H., Andreae, M.O., Enzweiler, J., 2016. Reference Values Following ISO Guidelines for Frequently

Requested Rock Reference Materials, Geostandards and Geoanalytical Research 40:3, 333-350

Kamber, B.S., Greig, A., and Collerson, K.D., 2005. A new estimate for the composition of weathered young upper continental crust from alluvial sediments, Queensland, Australia. Geochimica et Cosmochimica Acta, 69, 1041–1058

Kamber, B.S., Gladu, A.H., 2009. Comparison of Pb purification by anion-exchange resin methods and assessment of long-term reproducibility of Th/U/Pb ratio measurement by quadrupole ICP-MS. Geostandards and Geoanalytical Research 33, 169-182

Kennan, P.S., McArdle, P., Gallagher, V., Morris, J.H., O'Connor, P.J., O'Keeffe, W.G., Reynolds, N.A., and Steed, G.M., 1987. A review of recent isotope research on mineralization in Ireland. Geological Survey of Ireland Bulletins 4, 1-10

Kempter, H., Gorres, M., Frenzel B., 1997. Ti and Pb concentrations in rainwater fed bogs in Europe as indicators of past anthropogenic activities, Water, Air and Soil Pollution, 100, 367-377.

Klaminder J., Renberg I. and Bindler R., 2003. Isotopic trends and background fluxes of atmospheric lead in northern Europe: Analyses of three ombrotrophic bogs from south Sweden, Global Biogeochemical Cycles, 17, art. no. 1019.

Krachler, M., Mohl, C., Emons, H., Shotyk W., 2003. Atmospheric deposition of V, Cr and Ni since the late glacial: Effects of climatic cycles, human impacts and companson with crustal abundances, Environmental Science & Technology, 37, 2658-2667.

Krishnasmami, S., Lal, D., Martin, J.M., Meybeck, M., 1971. Geochronology of lake sediments. Earth and Planetary Science Letters 11, 407-414.

Krosshaven, M., Steinnes, E., Varskog, P., 1992. Binding of Cd, Cu, Pb and Zn in soil organic matter with different vegetational background, Water, Air and Soil Pollution, 71, 185-193.

Kudelsky, A.V, Smith, J.T., Ovsiannikova, S.V, Hiltonb, J., 1996. Mobility of Chernobyl-derived 137Cs in a peatbog system within the catchment of the Pripyat River, Belarus 9697

Kylander, M.E., Weiss, D.J., Martínez Cortízas, A., Spiro, B., Garcia-Sanchez, R., Coles, B.J., 2005. Refining the pre-industrial atmospheric Pb isotope evolution curve in Europe using an 8000 year old peat core from NW Spain. Earth Planet. Sci. Lett. 240, 467–485. doi:10.1016/j.epsl.2005.09.024

Kylander, M.E., Weiss, D.J., Kober, B., 2009. Two high resolution terrestrial records of atmospheric Pb deposition from New Brunswick, Canada, and Loch Laxford, Scotland. Science of the Total Environment 407, 1644–1657. doi:10.1016/j.scitotenv.2008.10.036

Kylander, M.E., Klaminder, J., Bindler, R., Weiss, D.J., 2010. Natural lead isotope variations in the atmosphere. Earth and Planetary Science Letters 290, 44-53

Küttner, A., Mighall, T.M., De Vleeschouwer, F., Mauquoy, D., Martínez Cortizas, A., Foster, I.D.L., Krupp, E., 2014. A 3300-year atmospheric metal contamination record from Raeburn Flow raised bog, south west Scotland. J. Archaeol. Sci. 44, 1–11. https://doi.org/10.1016/j.jas.2014.01.011

Le Roux, G., Weiss, D., Grattan, J., Givelet, N., Krachler, M., Cheburkin, A., Rausch, N., Shotyk, W., 2004. Identifying the sources and timing of ancient and medieval atmospheric

lead pollution in England using a peat profile from Lindow bog, Manchester, Journal of Environmental Monitoring, 6, 502-510.

Le Roux, G., Aubert, D., Stille, P., Krachler, M., Kober, B., Cheburkin, A., Bonani, G., Shotyk, W., 2005. Recent atmospheric Pb deposition at a rural site in southern Germany assessed using a peat core and snowpack, and comparison with other archives. Atmospheric Environment 39, 6790–6801. doi:10.1016/j.atmosenv.2005.07.026

Logan, E.M., Pulford, I.D., Cook, G.T., MacKenzie, A.B., 1997. Complexation of Cu2+ and Pb2+ by peat and humic acid. European Journal of Soil Science, 48, 685–696.

Martinez-Cortizas, A., Garcia-Rodeja, E., Pontevedra Pombal, X., Novoa Munoz. J.C., Weiss, D., Cheburkin. A., 2002. Atmospheric Pb deposition in Spain during the past 4600 years recorded by two ombrotrophic peat bogs and implications for the use of peat as an archive. Sci. Total Environ. 292, 33-44.

Martínez Cortizas, A., Peiteado Varela, E., Bindler, R., Biester, H., Cheburkin, A., 2012. Reconstructing historical Pb and Hg pollution in NW Spain using multiple cores from the Chao de Lamoso bog (Xistral Mountains). Geochimica et Cosmochimica Acta 82, 68–78. doi:10.1016/j.gca.2010.12.025

Martínez Cortizas, A., López-Merino, L., Bindler, R., Mighall, T., Kylander, M., 2016. Early atmospheric metal pollution provides evidence for Chalcolithic/Bronze Age mining and metallurgy in Southwestern Europe. The Science of the Total Environment, 545-546, 398-406

Marx, S.K., Kamber, B.S., McGowan, H.A., Zawadzki, A., 2010. Atmospheric pollutants in alpine peat bogs record a detailed chronology of industrial and agricultural development on the Australian continent. Environmental Pollution 158, 1615–1628. doi:10.1016/j.envpol.2009.12.009

McDonough, W.F., and Sun, S.-S., 1995. Composition of the Earth. Chemical Geology 120, 223-253

Mclennan, S.M., 2001. Relationships between the trace element composition of sedimentary rocks and upper continental crust. Geochemistry, Geophysics, Geosystems 2. earthref.org/ERR/984/

Monna, F., Lancelot, J., Croudace, I.W., Cundy, A.B., Lewis, J.T., 1997. Pb isotopic composition of airborne particulate material from France and the Southern United Kingdom: Implications for Pb pollution sources in urban areas. Environmental Science and Technology 31, 2277–2286. doi:10.1021/es960870+

Mukai, H., Furuta, N., Fujii, T., Ambe, Y., Sakamoto, K., Hashimoto, Y., 1993. Characterization of sources of lead in the urban air of Asia using ratios of stable lead isotopes. Environmental Science and Technology 27, 1347–1356. doi:10.1021/es00044a009

Muller, J., Kylander. M., Martínez-Cortizas, A., Wüst, R.A.J., Weiss, D., Blake, K., 2008. The use of principle component analyses in characterising trace and major elemental distribution in a 55 kyr peat deposit in tropical Australia: implications to paleoclimate. Geochim Cosmochim Acta 72, 449–63.

Nozaki, Y., Zhang, Y.S., Amakawa, H., 1997. The fractionation between Y and Ho in the marine environment. Earth and Planetary Science Letters 148, 329-340

Nieminen, T.M., Ukonmaanaho, L., Shotyk, W., 2002. Enrichment of Cu, Ni, Zn, Pb and As in an ombrotrophic peat bog near a Cu-Ni smelter in Southwest Finland, Science of The Total Environment 292, 1–2.

Pages 81-89, Oldfield, F., Appleby, P. G., Cambray, R. S., Eakins, J. D., Barber, K. E., Battarbee, R. W., Pearson, G. R. and Williams, J. M., 1979. 210Pb, 137Cs and 239Pu profiles in ombrotrophic peat. - Oikos 33: 40-45.

Pokrovsky, O.S., Dupre, B., Schott J., 2005. Fe–Al–organic colloids control of trace elements in peat soil solutions: results of ultrafiltration and dialysis. Aquatic Geochemistry 11, 241-278

Oldfield, F., Richardson, N., Appleby, P.G., 1995. Radiometric dating (210Pb, 137Cs, 241Am) of recent ombrotrophic peat accumulation and evidence for changes in mass balance. The Holocene 5, 141-148.

Oliver, G.J.H., 2002. Chronology and terrane assembly, new and old controversies. In: Trewin, N.H. (Ed.), The Geology of Scotland. Geological Society, London, pp. 201–211

Othman, M., and Latif, M. T., 2013. Dust and gas emissions from small-scale peat combustion. Aerosol and Air Quality Research 13, 1045-4059

Pack, A., Russell, S.S., Shelley, J.M.G., van Zuilen, M., 2007. Geo- and Cosmochemistry of the twin elements yttrium and holmium. Geochimica et Cosmochimica Acta 71, 4592-4608

Pokrovsky, O.S., Dupre, B., Schott J., 2005. Fe–Al–organic colloids control of trace elements in peat soil solutions: results of ultrafiltration and dialysis. Aquatic Geochemistry 11, 241-278

Pratte, S., Mucci, A., Garneau, M., 2013. Historical records of atmospheric metal deposition along the St. Lawrence Valley (eastern Canada) based on peat bog cores. Atmospheric Environment 79, 831–840. doi:10.1016/j.atmosenv.2013.07.063

Reimann, C., de Caritat, P., 2005 Distinguishing between natural and anthropogenic sources for elements in the environment: regional geochemical surveys versus enrichment factors, Science of the Total Environment, 337, 91-107

Rosman K.J.R., Chisholm W., Hong S., Candelone J-P and Boutron C. F., I997. Lead from Carthaginian and roman Spanish mines isotopically identified in Greenland ice dated from 600 B.C. to 300 A.D., Environmental Science & Technology, 31, 34I3-34I6.

Rosman, K.J.R., Ly, C., Van De Velde, K., Boutron, C.F., 2000. A two century record of lead isotopes in high altitude Alpine snow and ice. Earth and Planetary Science Letters 176, 413–424. doi:10.1016/S0012-821X(00)00013-3

Rynne, Colin, 2015 Industrial Ireland, an Archaeology. The Collins press, Ireland

Schell, W.R., Tobin, M.J., Novak, M.J.V., Wieder, R.K, and Mitchell, P.I., 1997. Deposition history of trace metals and fallout radionuclides in wetland ecosystems using ^{210}Pb chronology. Water, Air, and Soil Pollution 100, 233-239.

Schwartz, S., P., and Critchley, M., F., 1996. The lead ore dressing floors at Glendalough and Glendasan, County Wicklow 1825-1923: A history, survey and interpretation of extant remains. Journal of Mining Heritage Trust of Ireland 12, 5-52.

Shepard, W.A., 1981. The host rock geology and geochemistry of the Aovca mines, Co. Wicklow, Ireland. Ph.D. Thesis. Trinity College Dublin

Shotyk, W., 1992. Natural and anthropogenic enrichments of arsenic through three Canadian ombrotrophic Sphagnum bog profiles. Arsen. Environ. Part I Cycl. Charact. 20, 381–401.

Shotyk, W., 1996. Peat bog archives of atmospheric metal deposition: geochemical evaluation of peat profiles, natural variations in metal concentrations and metal enrichment factors, Environmental Reviews, 4, 149-183.

Shotyk, W., Weiss, D., Kramers, J.D., Frei, R., Cheburkin, A.K., Gloor, M., Reese, S., 2001. Geochemistry of the peat bog at Etang de la Gruere, Jura Mountains, Switzerland, and its record of atmospheric Pb and lithogenic trace metals (Sc, Ti, Y, Zr, and REE) since 12,370 C yr BP. Geochimica et Cosmochimica Acta 65, 2337-2360

Shotyk, W., Krachler, M., Martinez-Cortizas, A., Cheburkin, A.K., Emons, H., 2002. A peat bog record of natural, pre-anthropogenic enrichments of trace elements in atmospheric aerosols since 12 370 14C yr BP, and their variation with Holocene climate change. Earth and Planetary Science Letters 199, 21–37. doi:10.1016/S0012-821X(02)00553

Shotyk, W., Le Roux, G., 2005. Biogeochemistry and Cycling of Lead. In: A. Sigel, H. Sigel and R.K.O. Sigel (Editors), Biogeochemical Cycles of the Elements. Metal Ions in Biological Systems. M. Dekker, New York, 240-275.

Smith, E.J., Rey-Castro, C., Longworth, H., Lofts, S., Lawlor, A.J., Tipping, E., 2004. Cation binding by acid-washed peat, interpreted with humic ion-binding model VI-FD. European Journal of Soil Science 55, 433-447

Stromsoe, N., Marx, S.K., McGowan, H.A., Callow, N., Heijnis, H., Zawadzki, A., 2015. A landscape-scale approach to examining the fate of atmospherically derived industrial metals in the surficial environment. Science of the Total Environment 505, 962–980. doi:10.1016/j.scitotenv.2014.10.072

Sugden, C.L., Farmer, J.G., MacKenzie, A.B., 1993. Isotopic ratios of lead in contemporary environmental material from Scotland. Environmental Geochemistry and Health 15, 59–65. doi:10.1007/BF02627823

Sweetman, T.M., 1987. "The geochemistry of the Blackstairs Unit of the Leinster Granite, Ireland." Journal of the Geological Society, London 144, 971-984

Thomas, A., and McArdle, P., 1998. Avoca: Our Mining Heritage. Geological Survey of Ireland, 17pp

Townsend, A.T., Snape, I., 2002. The use of Pb isotope ratios determined by magnetic sector ICP-MS for tracing Pb pollution in marine sediments near Casey Station, East Antarctica. Journal of Analytical Atomic Spectrometry 17, 922–928.

Towsend, A.T., Zongshou, Y., McGoldrick, P., Hutton, J.A., 1998. Precise lead isotope ratios in Australian galena samples by high resolution inductively coupled plasma mass spectrometry. Journal of Analytical Atomic Spectrometry 13, 809-13

Turney, C.S.M., 1998. Extraction of rhyolitic component of Vedde microtephra from minerogenic lake sediments. Journal of Palaeolimnology, 19, 199-206

Ulrich, T., Kamber, B.S., Woodhead, J.D., Spencer, L.A., 2010. Long-term observations of isotope ratio accuracy and reproducibility using quadrupole ICP mass spectrometry. Geostandards and Geoanalytical Research 34, 161-174

Véron, A., Flament, P., Bertho, M.L., Alleman, L., Flegal, R., Hamelin, B., 1999. Isotopic evidence of pollutant lead sources in Northwestern France. Atmospheric Environment 33, 3377-88

Walraven, N., van Os, B.J.H., Klaver, G.Th., Baker, J.H., Vriend, S.P., 1997. Trace element concentrations and stable lead isotopes in soils as tracers of lead pollution in Graft-De Rijp, the Netherlands. Journal of Geochemical Exploration 59, 47-58

Weis, D., et al., 2006. High-precision isotopic characterization of USGS reference materials by TIMS and MC-ICP-MS, Geochemistry, Geophysics, Geosystems 7, Q08006. doi:10.1029/2006GC001283

Weiss, D., Shotyk, W., Appleby, P.G., Kramers, J.D., Cheburkin, A.K., 1999. Atmospheric Pb deposition since the industrial revolution recorded by five Swiss peat profiles: Enrichment factors, fluxes, isotopic composition, and sources. Environmental Science and Technology 33, 1340–1352. doi:10.1021/es980882q

Weiss, D.J., Shotyk, W., Boyle, E.A., Kramers, J.D., Appleby, P.G., Cheburkin, A.K., 2002. Comparative study of the temporal evolution of atmospheric lead deposition in Scotland and eastern Canada using blanket peat bogs. Science of the Total Environment 292, 7–18. doi:10.1016/S0048-9697(02)00025-6

Weiss, D.J., Rausch, N., Mason, T.D.F., Coles, B.J., Wilkinson, J.J., Ukonmaanaho, L., Arnold, T., Nieminen, T.M., 2007. Atmospheric deposition and isotope biogeochemistry of zinc in ombrotrophic peat. Geochimica et Cosmochimica Acta 71. 3498-3517

Wilkinson, J.J., Eyre, S.L., 2005. Ore-forming processes in Irish-type carbonate-hosted Zn-Pb deposits: Evidence from mineralogy, chemistry, and isotopic composition of sulfides at the Lisheen mine. Economic geology 100, 63-86

Woodhead, J.D., and Hergt, J.M., 2000. Pb-isotope analysis of USGS reference materials, Geostandards Newsletter 24(1), 33-38

Zhang, H., Shan, B., 2009. Historical records of heavy metal accumulation in sediments and the relationship with agricultural intensification in the Yangtze–Huaihe region, China. The Science of the Total Environment 399, 113-120

https://www.met.ie/climate-ireland/climate-of-ireland.asp

Appendix A.1: Trace element concentrations (ppb) for peat subsamples along the Liffey Head bog peat monolith

Sample ID	LHB1.3	LHB2.3	LHB3.3	LHB4.3	LHB5.3	LHB6.3	LHB7.3	LHB1.1	LHB1.2	LHB2.2	LHB3.2	LHB4.2	LHB5.2	LHB6.2	LHB2.1	LHB7.2	LHB8.2	LHB9.2
depth (cm)	*0 - 1*	*1 - 2*	*2 - 3*	*3 - 4*	*4 - 5*	*5 - 6*	*6 - 7*	*7 - 8*	*8 - 9*	*9 - 10*	*10 - 11*	*11 - 12*	*12 - 13*	*13 - 14*	*14 - 15*	*15 - 16*	*16 - 17*	*17 - 18*
Li	371	806	352	298	459	740	885	341	256	428	579	688	689	710	543	504	578	540
Be	17.3	31.8	13.6	16.6	22.4	31.9	43.0	23.7	29.4	47.8	75.7	107	132	152	108	122	143	132
Sc	85.8	167	69.4	92.5	133	188	250	140	153	266	372	421	441	491	321	411	473	460
Ti	32120	59450	22870	31670	46970	55030	74480	52700	48350	80350	100300	114300	104300	111500	75580	96720	115600	101900
V	2087	4568	2015	2784	3752	4697	5644	3847	4535	8089	10420	9870	10040	13530	9175	7088	5852	4856
Cr	1352	2309	988	1214	1489	2161	3179	1556	2126	3401	5249	6269	4925	5450	2588	2799	2869	2478
Fe	212	243	258	380	280	337	294	336	355	286	263	293	426	435	304	270	277	540
Co	195	386	173	172	202	315	416	219	266	457	542	678	738	783	495	579	646	731
Ni	1494	2645	1243	1487	1922	3039	4092	2385	2620	4469	5332	6417	6152	6470	3700	4053	3972	3979
Cu	4350	6787	3024	2855	4939	8891	9458	4339	4494	8222	9818	11380	12360	14480	9844	13480	17510	24050
Zn	45550	81450	36630	32550	37480	59690	70920	43930	45270	72980	66860	84850	92870	99200	62470	64250	65870	83550
Ga	161	344	158	198	294	487	657	344	488	918	1400	1467	1741	2328	1932	2284	2388	2701
As	365	819	535	652	599	1179	2077	1170	1141	2128	3075	4133	6111	6153	5752	4778	5557	7696
Rb	1011	1703	726	718	771	1067	1307	832	724	1193	1261	1490	1461	1453	842	1120	1427	1433
Sr	19360	34860	14020	13600	15730	24470	34030	13800	13850	23780	21030	28190	31960	34650	23830	26130	26880	34190
Y	212	422	158	200	267	367	510	269	308	514	616	755	920	1033	771	1027	1039	1068
Zr	1242	2960	802	1110	1562	1817	2507	1481	1401	2316	2835	3325	3171	3399	1875	2729	3229	2927
Nb	112	202	75	110	165	196	265	165	171	281	363	419	395	420	241	345	421	366
Mo	550	849	295	370	401	541	621	347	412	722	830	891	955	1150	836	1031	1045	960
Ag	35.7	61.7	42.1	41.5	63.7	162	214	109	106	215	271	331	381	423	359	415	498	618
Cd	95.9	228	134	175	236	426	621	338	425	735	809	1007	1265	1555	1287	996	1033	1359
In	5.28	11.31	5.09	6.78	9.44	19.6	26.3	12.1	19.6	38.1	60.9	69.3	92.2	109	98.4	180	253	305
Sn	766	1544	542	703	935	1796	2592	1263	2140	4273	7768	9171	10330	12110	9769	16540	19810	17720
Sb	413	1018	442	460	543	1545	2175	960	1258	2333	3344	3416	4378	7331	7430	8559	9652	13210
Cs	66.4	136	63.5	71.1	86.1	117	143	82	72	121	136	166	170	168	91.2	118	148	152
Ba	9572	17780	7665	8466	10410	14420	18280	9847	9887	16610	16270	21320	23440	24710	16240	20110	21690	23670
La	325	655	259	312	407	548	772	412	457	755	864	1041	1200	1234	787	1140	1215	1230
Ce	464	1034	398	517	726	950	1309	750	877	1475	1754	2108	2461	2652	1824	2502	2643	2809
Pr	56.4	121	47.0	65.8	92.0	121	167	92.9	111	188	217	261	310	336	231	314	328	342
Nd	217	458	174	228	319	431	597	331	399	678	794	956	1148	1262	891	1208	1252	1315
Sm	40.3	84.8	32.5	42.4	58.6	80.3	110.6	60.8	75.2	127.2	151.8	181.4	222.9	246.4	183.6	251.0	262.6	281.1
Eu	9.11	16.9	6.92	9.09	12.4	17.3	23.6	12.0	14.9	25.4	30.5	36.6	46.5	51.6	40.0	55.0	59.8	65.7
Gd	35.2	69.2	28.3	37.0	51.0	69.2	94.5	50.7	65.1	110.0	130.6	157.7	192.6	213.1	158.6	220.2	223.4	237.2
Tb	5.45	10.5	4.48	5.78	7.93	10.7	14.6	7.50	9.14	15.5	18.6	22.7	27.6	30.9	23.2	31.7	33.1	34.8
Dy	31.6	59.4	25.8	33.4	45.9	61.1	85.0	45.3	54.2	90.4	110.6	133.8	162.0	181.3	133.7	184.1	192.4	198.4
Ho	6.48	12.2	5.31	6.87	9.45	12.6	17.3	9.21	11.0	18.5	22.4	27.3	32.6	36.4	26.5	36.4	37.7	38.5
Er	18.3	33.0	14.6	19.1	26.0	34.5	48.1	25.6	29.5	49.8	60.2	73.0	86.2	96.9	71.0	96.1	98.7	100.3
Tm	2.74	4.94	2.17	2.84	3.93	5.11	7.08	3.83	4.56	7.66	9.18	11.0	12.9	14.5	10.4	14.3	14.9	15.0
Yb	17.1	30.8	13.6	18.4	24.9	32.4	45.0	24.3	28.2	47.1	57.2	68.0	79.7	89.2	64.6	88.7	93.7	95.8
Lu	2.62	4.61	1.99	2.70	3.68	4.78	6.49	3.60	4.07	6.75	8.10	9.60	11.2	12.4	8.95	11.9	12.6	12.5
Hf	29.9	68.9	19.9	27.9	39.4	45.8	63.0	37.5	36.4	60.8	73.4	85.3	81.8	88.4	47.7	70.4	81.7	75.9
Ta	11.0	21.0	8.2	7.4	9.0	13.4	19.8	11.6	11.0	18.4	17.9	22.8	27.1	25.4	17.8	22.1	27.0	31.9
W	118	176	75.1	57.0	75.5	205	158	333	125	183	236	253	290	344	325	327	346	303
Tl	5.30	12.0	2.33	1.87	2.10	1.78	2.80	21.3	13.1	18.2	16.5	26.2	28.6	25.8	59.5	15.3	12.5	11.0
Pb	4552	12870	8330	6359	9572	18640	29450	33610	49100	90760	72190	169500	230700	271600	201900	237600	267600	377700
Th	49.2	107.6	40.7	57.6	87.1	114	150	89.6	98.0	165	220	254	270	278	168	244	263	244
U	30.1	57.4	27.0	31.7	43.7	66.6	89.2	48.3	54.1	94.6	127	149	163	185	122	162	181	186

Appendix A.1: *(continued)* Trace element concentrations (ppb) for peat subsamples along the Liffey Head bog peat monolith

Sample ID	LHB10.2	LHB11.2	LHB12.2	LHB13.2	LHB3.1	LHB14.2	LHB15.2	LHB16.2	LHB17.2	LHB18.2	LHB19.2	LHB20.2	LHB21.2	LHB22.2	LHB4.1	LHB23.2	LHB24.2	LHB5.1
depth (cm)	*18 - 19*	*19 - 20*	*20 - 21*	*21 - 22*	*22 - 23*	*23 - 24*	*24 - 25*	*25 - 26*	*26 - 27*	*27 - 28*	*28 - 29*	*29 - 30*	*30 - 31*	*31 - 32*	*32-33*	*33 - 34*	*34 - 35*	*42-43*
Li	544	697	706	502	481	264	212	243	258	380	280	337	294	336	355	286	263	293
Be	119	128	117	85.3	70.5	42.9	35.2	45.7	50.3	65.0	47.2	59.4	45.1	46.2	39.9	36.9	33.2	32.0
Sc	396	466	457	348	235	168	133	148	164	236	177	218	188	212	192	183	158	201
Ti	113000	142200	141600	95730	71300	48820	43140	53080	60030	88420	65530	82950	72870	83360	81910	69850	69870	79020
V	4075	4338	3838	3060	2274	1342	1108	1259	1364	1799	1330	1705	1446	1612	1468	1377	1241	1489
Cr	2146	2473	2431	1863	1233	916	727	851	965	1259	935	1146	1032	1246	989	996	783	935
Fe	544	697	652	212	243	258	380	280	337	294	336	355	286	263	293	426	435	304
Co	579	645	638	589	512	281	239	282	326	389	294	383	321	349	322	303	279	311
Ni	3189	3254	2774	2176	2553	966	804	916	978	1155	864	1070	875	932	766	736	688	918
Cu	18430	23230	24590	23680	15640	6339	4326	3306	3117	3316	2418	3036	2366	2594	2058	2456	1764	1715
Zn	62620	66140	64590	57030	51520	31910	26200	31730	36090	38220	27770	35090	26450	25940	21070	19930	13400	10910
Ga	1987	2086	1867	1557	1091	544	406	392	380	435	311	387	316	346	288	278	211	259
As	6926	9229	9740	9082	9153	4777	4694	6237	8137	10390	8370	10980	9527	9427	9507	7384	5278	7261
Rb	1470	1896	1973	1350	919	649	540	643	709	1039	758	907	789	871	754	745	529	615
Sr	27160	30330	29390	25460	22630	16410	15330	20650	25150	29030	22320	29310	23390	24540	21400	21000	20700	23690
Y	970	1014	974	742	542	373	329	396	436	551	393	495	409	436	357	361	341	387
Zr	3166	3789	3761	2589	2041	1346	1230	1494	1766	2452	1745	2151	1904	2117	1981	1914	1657	1857
Nb	395	493	487	334	213	177	151	189	216	311	227	284	248	282	241	234	203	229
Mo	833	878	721	667	496	237	167	184	186	216	151	182	151	171	164	154	158	183
Ag	382	386	353	318	177	88	57.0	46.1	44.1	46.1	31.6	37.2	34.3	37.2	31.8	36.0	24.0	23.7
Cd	1008	1170	1117	876	885	384	348	425	529	578	422	531	418	390	355	263	223	205
In	291	359	382	340	221	133	100	89.7	85.0	98.6	72.1	86.7	69.0	71.4	53.5	51.8	19.7	11.1
Sn	14550	16240	16450	12840	4909	3917	2872	2769	2749	3933	3038	3084	2503	2864	1828	2060	663	754
Sb	8287	7950	6082	4973	2814	1161	869	678	607	618	435	584	440	439	360	337	245	278
Cs	145	184	193	139	103	69.2	54.0	62.4	68.6	100	71.9	88.4	74.8	83.9	73.1	73.5	49.7	54.4
Ba	20290	22690	21260	15760	11390	8477	7065	8832	10190	12570	8955	11510	8942	9440	7777	7546	6936	7901
La	1143	1313	1256	927	624	486	382	469	522	703	515	663	549	616	523	517	485	554
Ce	2467	2757	2573	1927	1286	1013	795	965	1061	1400	1032	1334	1086	1222	1010	1002	1047	1166
Pr	300	331	309	232	156	123	96.3	119	130	168	124	161	130	144	119	118	111	136
Nd	1152	1255	1169	879	591	474	366	450	491	631	465	615	485	534	439	436	411	493
Sm	241.9	256.8	235.4	179.1	122.4	97.0	73.5	89.7	97.4	122.8	90.3	122.0	94.3	104.4	83.9	83.7	71.5	93.8
Eu	55.2	57.3	52.0	40.0	27.5	21.1	16.2	19.1	21.0	25.9	19.0	25.8	19.4	21.3	17.4	17.3	17.5	19.7
Gd	207.1	218.5	201.9	155.8	107.4	88.5	66.1	79.1	85.4	107.5	78.5	109.7	81.9	88.0	71.3	71.8	67.1	79.9
Tb	30.8	31.9	29.9	23.0	15.9	13.2	9.81	11.5	12.7	16.2	11.8	16.4	12.3	13.3	10.7	10.9	10.0	11.9
Dy	177.7	187.5	177.0	134.2	93.3	77.9	58.3	69.8	76.7	98.7	70.8	98.4	73.2	79.3	64.0	65.2	61.1	69.4
Ho	35.0	36.8	35.5	27.0	18.7	14.2	11.8	14.3	15.8	20.4	14.5	18.9	15.0	16.2	13.1	13.4	12.3	14.0
Er	92.4	98.5	95.0	71.9	50.6	42.5	32.2	39.2	43.2	56.1	39.7	56.6	41.2	44.9	36.6	37.2	34.0	37.9
Tm	13.9	15.0	14.6	10.8	7.51	6.37	4.72	5.80	6.35	8.44	5.96	8.51	6.20	6.75	5.47	5.61	5.09	5.57
Yb	90.2	96.8	92.8	68.8	47.3	40.6	29.8	36.6	40.2	52.7	37.1	53.7	38.7	42.6	34.3	35.2	31.5	34.5
Lu	11.9	13.2	12.8	9.44	6.63	5.71	4.25	5.13	5.72	7.58	5.34	7.75	5.59	6.07	5.15	5.15	4.56	5.10
Hf	82.2	100.3	99.7	70.6	59.5	45.3	34.0	42.3	49.5	68.6	48.2	69.0	52.3	58.2	53.6	52.0	48.8	49.4
Ta	26.1	33.2	32.7	27.2	23.5	13.8	9.9	12.6	14.4	21.3	15.7	22.8	16.8	19.3	16.1	15.9	13.0	15.4
W	229	237	209	184	171	78.2	97.6	56.0	51.4	61.2	44.2	62.4	44.4	52.5	61.4	53.2	47.9	67.6
Tl	9.90	13.5	15.8	104	84.4	37.8	23.9	36.8	53.3	66.8	52.2	74.4	49.1	50.2	52.6	39.0	34.1	38.7
Pb	300300	375600	347700	307200	219400	132500	87820	90520	98190	92270	67340	113600	67970	68960	52910	54070	33250	40010
Th	237	295	292	219	138	176	90.7	112	123	178	135	205	146	164	141	141	123	142
U	163	183	178	153	110	124	60.1	67.4	75.4	105	76.8	115	81.3	92.7	84.5	81.9	71.5	78.5

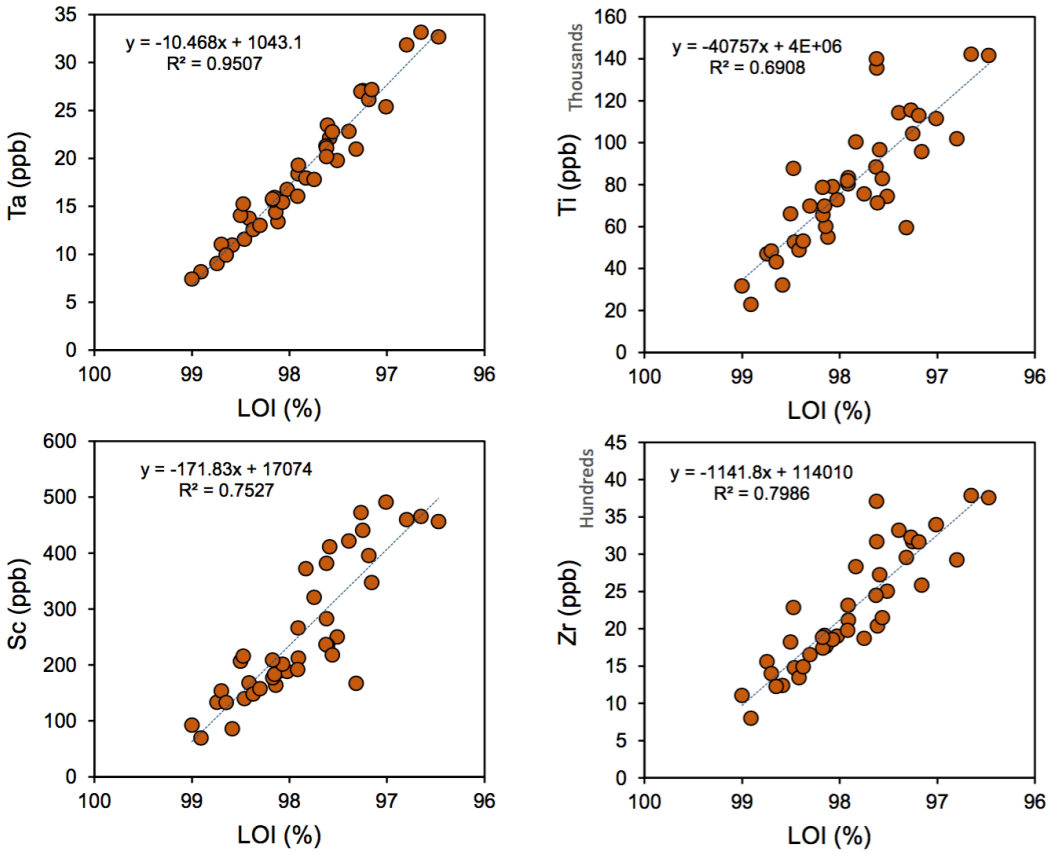
Appendix A.1: *(continued)* Trace element concentrations (ppb) for peat subsamples along the Liffey Head bog peat monolith

Sample ID	LHB6.1	LHB7.1	LHB8.1	LHB9.1	LHB10.1
depth (cm)	*52 - 53*	*62 - 63*	*72 - 73*	*82 - 83*	*94 - 95*
Li	426	435	304	270	277
Be	42.2	41.5	24.6	21.4	21.9
Sc	382	283	209	206	216
Ti	135600	140000	78770	66110	87760
V	2349	1799	1390	1238	1121
Cr	1381	1238	966	812	805
Fe	270	277	540	544	697
Co	273	184	221	163	128
Ni	991	561	680	814	539
Cu	2325	1234	1040	1040	852
Zn	4012	1411	1688	1195	987
Ga	337	312	250	204	195
As	6578	1609	1262	774	444
Rb	923	1032	671	518	567
Sr	23820	19830	21510	17300	12960
Y	599	582	368	320	316
Zr	3170	3713	1888	1824	2287
Nb	412	441	237	204	264
Mo	261	167	158	183	147
Ag	29.1	20.3	18.0	14.9	7.93
Cd	239	90.3	82.1	68.0	53.0
In	10.5	7.55	6.02	3.77	1.90
Sn	1719	1596	945	373	95
Sb	285	153	173	68	24
Cs	91.3	97.7	74.6	56.9	51.9
Ba	8991	7166	4596	4317	3929
La	843	853	540	530	515
Ce	1736	1621	1045	946	917
Pr	201	192	123	107	106
Nd	732	698	458	391	380
Sm	138.3	130.4	86.8	73.9	69.5
Eu	29.4	27.0	18.4	15.7	14.5
Gd	119.1	109.5	73.6	62.3	58.1
Tb	18.1	16.8	11.0	9.39	8.82
Dy	107.6	101.7	65.4	55.8	54.4
Ho	21.9	20.9	13.3	11.9	11.8
Er	59.9	58.4	36.8	31.2	32.0
Tm	8.85	8.84	5.45	4.61	4.89
Yb	54.6	55.5	34.0	28.8	31.0
Lu	8.10	8.23	5.05	4.28	4.62
Hf	83.1	96.6	49.2	46.5	58.5
Ta	21.1	20.2	15.8	14.0	15.2
W	89.8	64.5	48.4	43.2	41.5
Tl	28.4	10.0	4.36	2.07	3.35
Pb	19940	9952	12380	9812	3757
Th	211	209	141	123	129
U	131	108	91.0	90.3	85.4

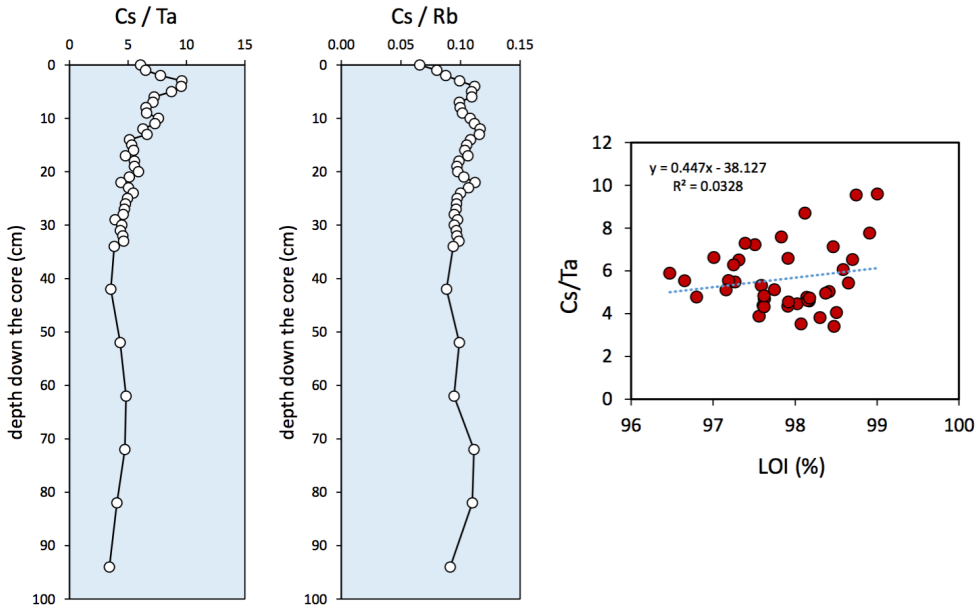
Appendix A.2: *Trace element concentrations for certified rock standard materials together with their preferred GeoReM values and RDS*

	BHVO-2							***BCR-2***						
	A-1	A-2	A-3	A-4	*Average*	*RSD*	*GeoReM*	*A-1*	A-2	A-3	A-4	*Average*	*RSD*	*GeoReM*
Li	4722	4784	4742	4826	*4769*	*0.97*	*4500*	*9535*	9408	9288	9274	*9376*	*1.30*	*9130*
Be	1009	997	981	1022	*1002*	*1.73*	*1076*	*2046*	2088	2051	2035	*2055*	*1.12*	*2170*
Sc	33230	33120	33180	33710	*33310*	*0.81*	*31830*	*34650*	34550	34450	33730	*34345*	*1.22*	*33530*
V	360200	355300	349300	345400	*352550*	*1.85*	*318200*	*414000*	409900	409400	415200	*412125*	*0.70*	*417600*
Cr	308500	306100	310500	317000	*310525*	*1.51*	*287200*	*16430*	16490	16410	16080	*16353*	*1.13*	*15850*
Co	45930	45520	44030	44650	*45033*	*1.90*	*44890*	*39410*	38260	38740	37750	*38540*	*1.83*	*37330*
Ni	119100	118700	121000	123600	*120600*	*1.84*	*119800*	*11830*	11980	11890	11860	*11890*	*0.56*	*12570*
Cu	127600	128800	124100	128990	*127373*	*0.79*	*129300*	*16850*	14420	16410	15500	*15795*	*6.82*	*19660*
Zn	99630	102000	98590	100500	*100180*	*1.45*	*103900*	*130000*	142400	135400	130400	*134550*	*4.30*	*129500*
Ga	21620	21610	21880	21950	*21765*	*0.81*	*21370*	*22340*	22120	22220	21500	*22045*	*1.70*	*22070*
As	952	1038	984	1042	*1004*	*4.35*	*700*	*659*	679	662	634	*658*	*2.78*	*860*
Rb	9375	9341	9540	9582	*9460*	*1.26*	*9261*	*48780*	48020	48330	47360	*48123*	*1.23*	*46020*
Sr	405300	404900	407500	412500	*407550*	*0.86*	*394100*	*346800*	346400	346400	335700	*343825*	*1.59*	*337400*
Y	24950	24950	25110	25520	*25133*	*1.06*	*25910*	*34430*	34320	34320	33020	*34023*	*1.98*	*36070*
Zr	177800	179100	177200	179700	*178450*	*0.64*	*171200*	*188900*	192200	190300	187900	*189825*	*1.00*	*186500*
Nb	18940	19060	19160	19470	*19158*	*1.19*	*18100*	*12490*	12310	12300	12360	*12365*	*0.70*	*12440*
Mo	3824	3236	4092	3337	*3622*	*11.18*	*4070*	*260400*	259500	253500	262700	*259025*	*1.52*	*250600*
Ag	120	113	100	111	*111*	*7.38*	*89*	*84*	95	90	104	*93*	*6.12*	*90*
Cd	122	114	105	123	*116*	*7.21*	*152*	*183*	193	174	213	*191*	*8.74*	*690*
In	92	92	92	91	*92*	*0.66*	*117*	*101*	99	98	100	*99*	*1.45*	*70*
Sn	2173	2202	1987	2001	*2091*	*5.38*	*1776*	*2549*	2699	2587	2454	*2572*	*3.94*	*2280*
Sb	89	98	80	88	*89*	*8.40*	*103*	*289*	306	317	279	*298*	*5.66*	*302*
Cs	97	96	96	102	*98*	*2.65*	*99.6*	*1178*	1144	1148	1133	*1151*	*1.67*	*1160*
Ba	133000	133100	135900	137600	*134900*	*1.66*	*130900*	*696200*	689700	681900	685700	*688375*	*0.89*	*683900*
La	15440	15400	15820	16040	*15675*	*1.97*	*15200*	*25460*	25270	25110	25410	*25313*	*0.63*	*25080*
Ce	38520	38390	39100	39930	*38985*	*1.79*	*37530*	*52290*	53150	53410	53320	*53043*	*0.97*	*53120*
Pr	5436	5423	5522	5654	*5509*	*1.93*	*5339*	*7077*	6905	6885	6956	*6956*	*1.24*	*6827*
Nd	24630	24580	24310	24780	*24575*	*0.80*	*24270*	*29870*	28780	28790	28670	*29028*	*1.94*	*28260*
Sm	6159	6161	6206	6365	*6223*	*1.57*	*6023*	*6769*	6619	6693	6585	*6667*	*1.23*	*6547*
Eu	2083	2081	2117	2151	*2108*	*1.56*	*2043*	*1983*	1933	1961	1974	*1963*	*1.11*	*1989*
Tb	6147	6178	6303	6313	*6235*	*1.79*	*6207*	*6966*	6711	6818	6769	*6816*	*0.80*	*1077*
Gd	942	942	954	978	*954*	*1.37*	*939*	*1080*	1062	1064	1075	*1070*	*1.60*	*6811*
Dy	5315	5335	5454	5491	*5399*	*1.61*	*5280*	*6572*	6527	6633	6741	*6618*	*1.40*	*6424*
Ho	1006	1007	1031	1046	*1023*	*1.89*	*989*	*1368*	1326	1357	1314	*1341*	*1.89*	*1313*
Er	2548	2553	2580	2640	*2580*	*1.64*	*2511*	*3738*	3680	3599	3623	*3660*	*1.69*	*3670*
Tm	343	343	348	355	*347*	*1.65*	*335*	*548*	543	529	534	*538*	*1.57*	*534*
Yb	1969	1965	2007	2016	*1989*	*1.30*	*1994*	*3486*	3377	3374	3365	*3401*	*1.69*	*3392*
Lu	276	277	282	283	*279*	*1.12*	*275*	*518*	508	496	507	*507*	*1.74*	*505*
Hf	4415	4412	4448	4531	*4452*	*1.25*	*4470*	*4973*	4913	4859	4833	*4895*	*1.27*	*4972*
Ta	1145	1133	1163	1135	*1144*	*1.20*	*1154*	*770*	764	762	766	*765*	*0.44*	*785*
W	200	200	199	207	*201*	*1.98*	*251*	*415*	418	411	429	*418*	*1.85*	*465*
Tl	21	20	21	21	*21*	*1.69*	*22*	*264*	260	255	254	*258*	*1.72*	*267*
Pb	1494	1486	1436	1460	*1469*	*1.81*	*1653*	*100100*	101100	98000	98670	*99468*	*1.39*	*10590*
Th	1184	1190	1200	1181	*1189*	*0.70*	*1224*	*5807*	5771	5761	5702	*5760*	*0.76*	*5828*
U	429	430	435	442	*434*	*1.39*	*412*	*1739*	1738	1688	1699	*1716*	*1.54*	*1683*
Fe	87270	87110	88100	87280	*87440*	*0.51*	*87500*	*98810*	97140	97940	97520	*97850*	*0.74*	*97700*
Ti	16680000	16620000	16460000	16750000	*16627500*	*0.73*	*16630000*	*13380000*	13550000	13650000	13760000	*13585000*	*1.17*	13685000

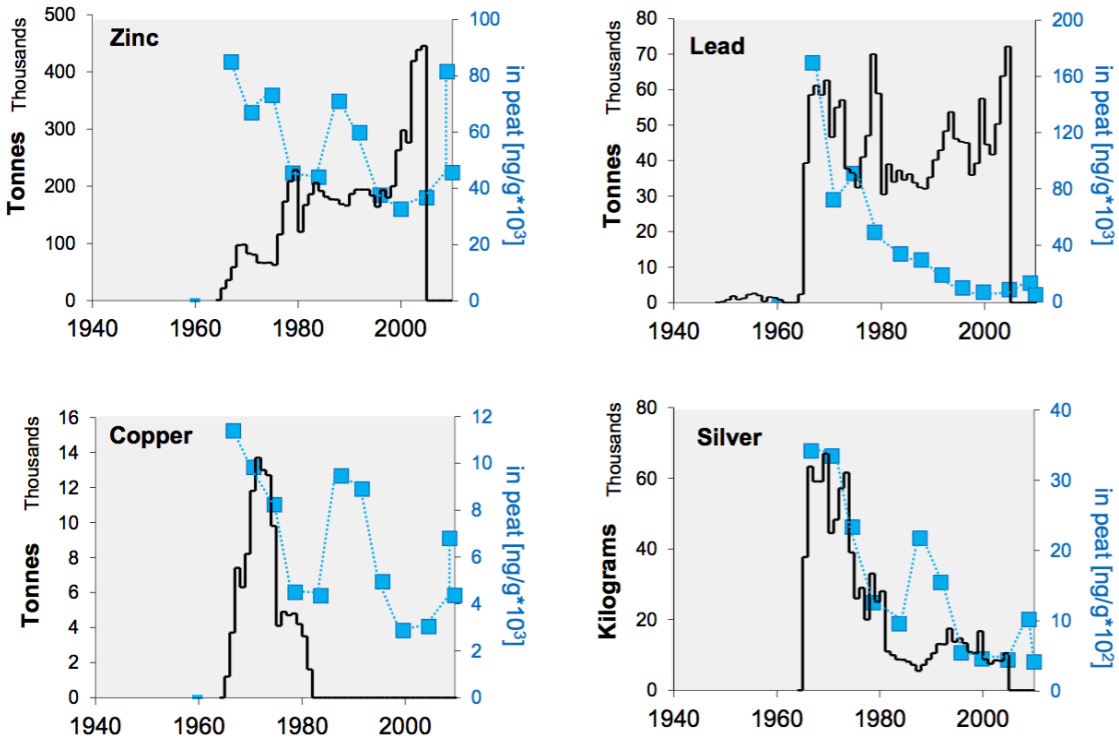
Appendix B.1: *Ta, Ti, Sc, and Zr (ppb) vs. LOI (%) along the uppermost 96 cm in the Liffey Head Bog*



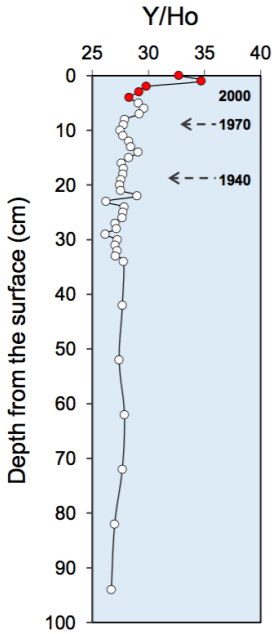
Appendix B.2: Cs/Ta and Cs/Rb patterns in the uppermost 96 cm of the Liffey Head bog. Shown is also the weak co-dependence of Cs/Ta vs. LOI (%)



Appendix B.3: Tonnage extractions of the elements Zn, Pb, Cu, and Ag in Ireland between 1960 and 2000 (black lines; source: http://www.mineralsireland.ie/mining+in+ireland/Current+Mining.htm, and Department of Communications, Energy and Natural Resources), together with the age-corresponding concentrations of these elements in LHB peat core (blue squares).



Appendix B.4: Background normalised Y/Ho (circles) along the LHB peat profile. The increasing ratios observed in the uppermost samples (from ca 2000) is interpreted as the addition of fertilisers being transported into the bog by air.



Appendix C: Principal Component Analysis (PCA) for LHB peat core

A principal component analysis (PCA) was conducted for the LHB dataset applying the statistical software package PAST3 developed by Hammer et al. (2001). Three components i.e. factors with eigenvalues >1 explain 99.75% of the total variance. Principal component (PC) 1 accounts for the largest variance (92.7%) and is strongly dominated by Pb, as well as other metals such as Sb, Sn, Cu, Ni, Ag, Cd (Fig. 1 a und b). The relative loadings suggest additional association of Zn (15%) and Ti (16%) with PC1 (Fig. 2a). The strong association of elements attributed to PC1 with Pb, as well as their occurrence as impurities in the Pb-Zn and Cu mineralisation of the Wicklow uplands point towards a common source, namely the mining and smelting activities in the area. This is supported by the highest abundance of PC1 observed in the peat segment accumulated during the mining period (first half of the 20th century, Fig. 3a).

Principal component 2 accounts for 4.4% of the total variance and its strongest association is seen with Ti (82%, Fig. 2b). Further elements which fall within this group are Zr, Th, Sc, Ta, Nb, Hf, Sr, As, and the REE's (Fig. 1a and b). Apart from As, which can have a i) bacterial, ii) mining dust, or iii) mobility as origin, all these immobile elements are associated with (different) mineralogical phases aerially transported onto the peat. They are thus good indicators of geogenic dust input. PC 2 is successfully detected in the peat accumulated before and after the major mining period (Fig. 3b). It is however highly possible that the strong mining signal present between (1900 and 1964 AD, Fig. 3a) has masked the lower-loaded component 2. The highest loading of Ti within PC2 would suggest that Ti the best dust indicator. However, the strong association of this element with both PC1 (local mining-smelting) and PC3 complicates the deconvolution of its origin. Therefore, a different approach must be followed to select a lithogenic element for the correction of the natural dust input onto the LHB peat.

Principal component 3 accounts for 2.7% of the total variance and includes the elements Mo, Ni, V, Cr as well as Rb, Sr, Ba, Fe, and Zn. Associated with 79% of its total load, Zn is the most dominant element of this group (Fig. 2c). It thus appears that the overall Zn load is shared between PC1 and PC3, with significantly stronger association with PC3. This is an interesting finding which suggests that Zn pollution in LHB peat core is not governed by the local mining and smelting of local Pb-Zn ores (PC1). The increasing load of PC3 in the upper part of the core, from 1940 AD (CR.2.1) towards present (Fig. 3c) indicates rising significance of a recent pollution source, enriched not only in Zn, but also in other transition metals listed above. The origin of PC3 is carefully attributed to emissions from fossil fuels, which are discussed in more detail in the manuscript (section 4.3 to 4.5) by deploying additional tools such as Pb isotopes and element enrichment factors (EF).

Figure 1: Principal component analysis (**PCA**)

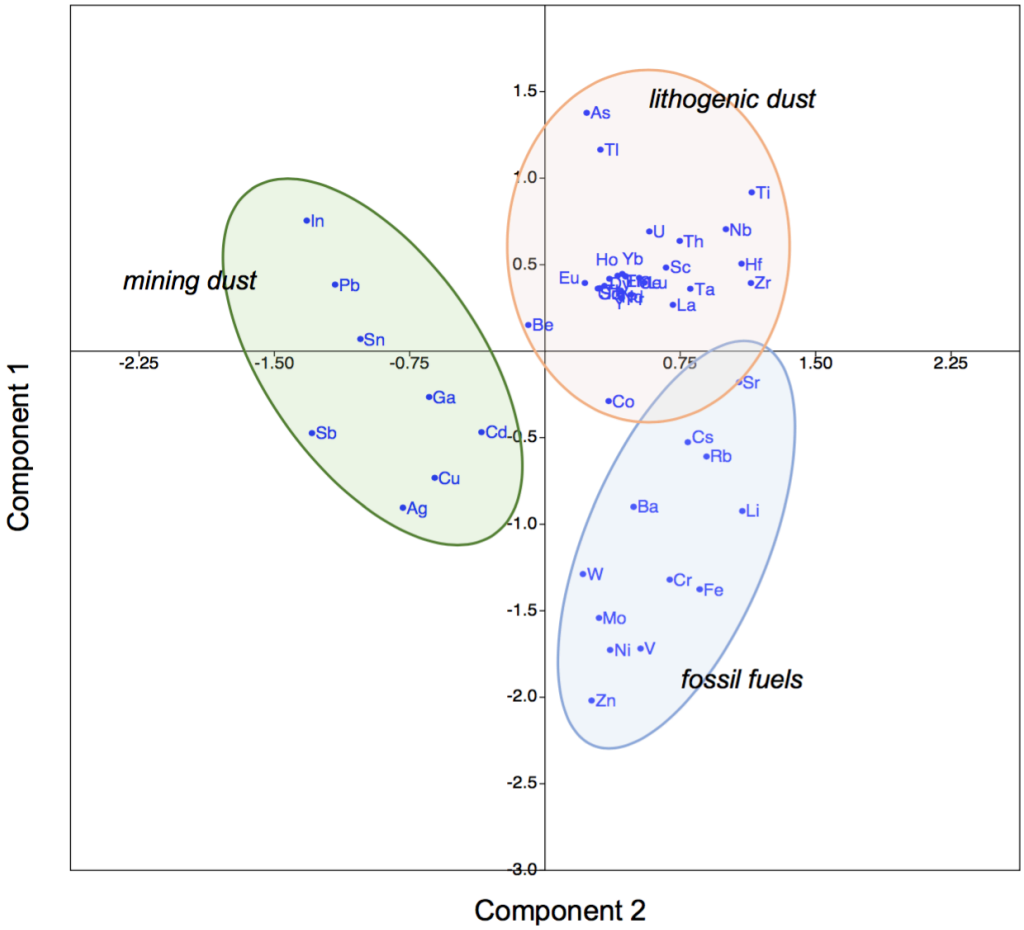


Figure 2: Dominant element loadings for each component

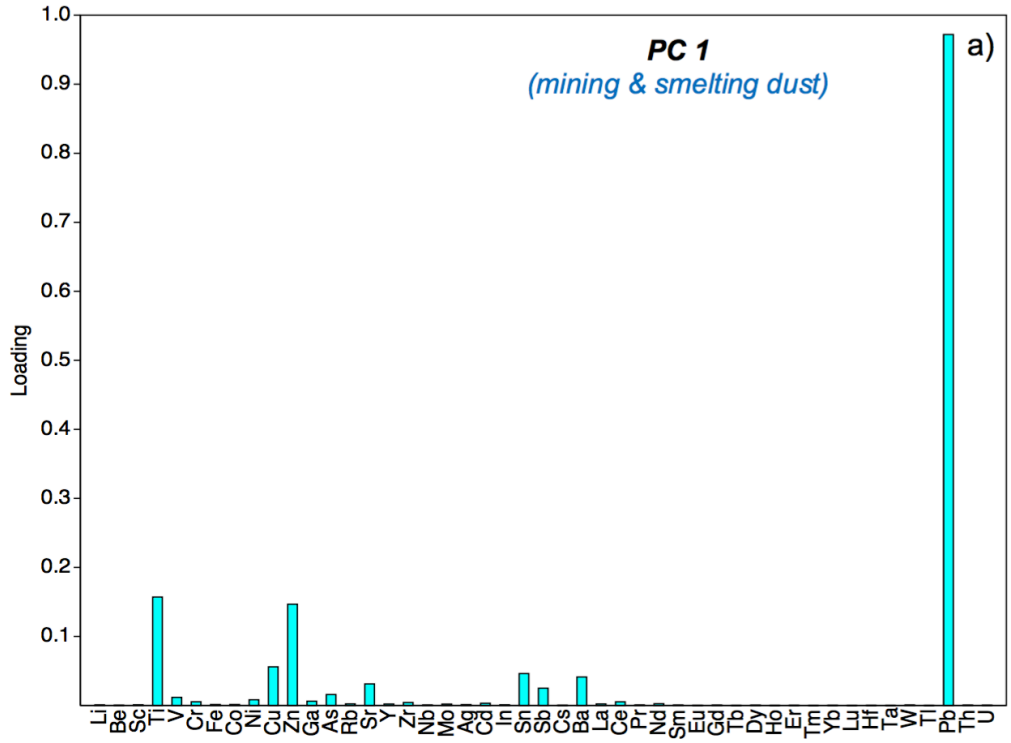
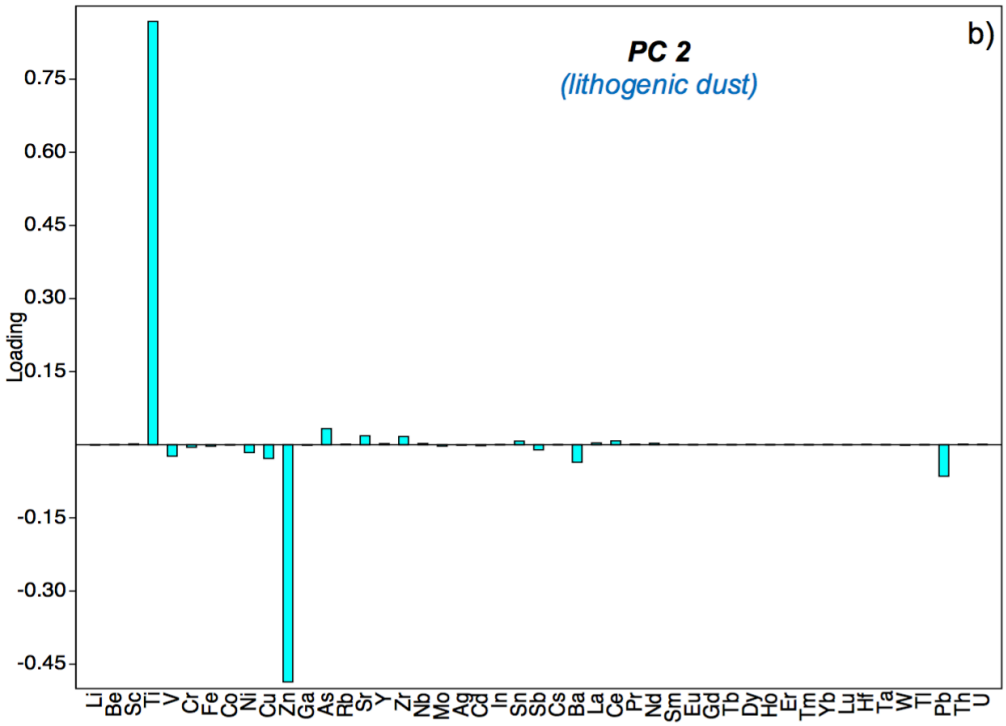


Figure 2: continued



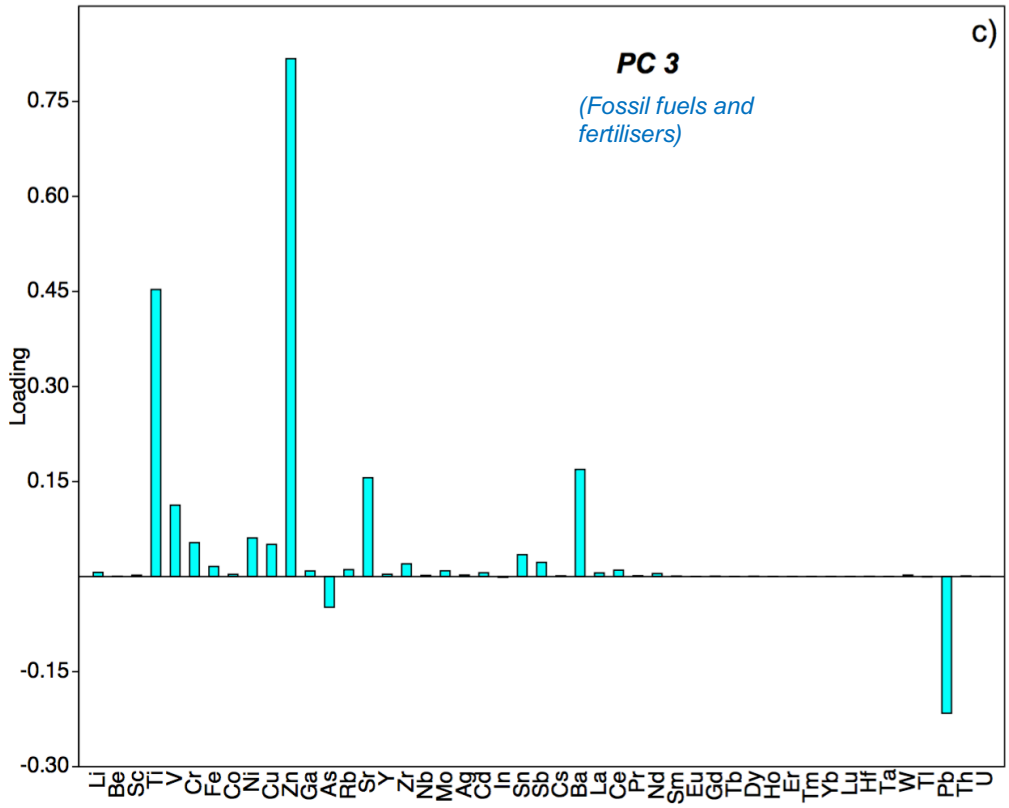
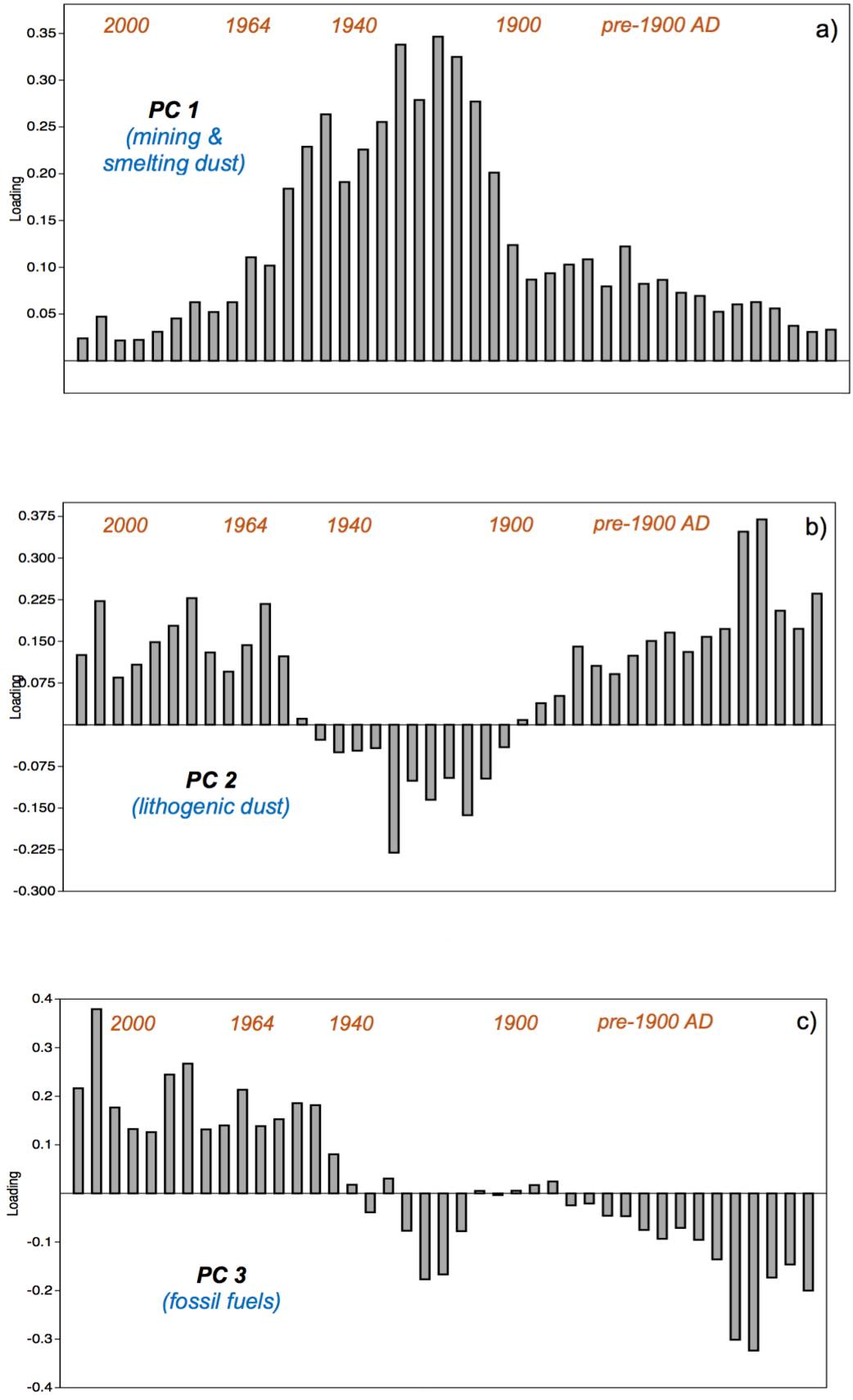


Figure 3: Loading of principal components: samples-ages (AD)



Appendix D: Continuation of the modelling in *section: 4.3 Sources of metal pollution in the LHB during the last four centuries:*

The different theoretical mixing curves (hyperbolas) between the two end-members were weighted by concentrations and calculated using following formulas:

[4] $(^{206}Pb/^{204}Pb)_{mix} = f_b[Pb_1]_b * (^{206}Pb/^{204}Pb)_b + (1-f_b)[Pb_2]_a * (^{206}Pb/^{204}Pb)_a / f_b[Pb_1]_b + (1-f_b)[Pb_2]_a$

[5] $(^{207}Pb/^{204}Pb)_{mix} = f_b[Pb_1]_b * (^{207}Pb/^{204}Pb)_b + (1-f_b)[Pb_2]_a * (^{207}Pb/^{204}Pb)_a / f_b[Pb_1]_b + (1-f_b)[Pb_2]_a$

where *[Pb₁]* or *[Pb₂]* are the concentrations ranging between 10 and 200 ppm, *a* and *b* are the Pb isotope values of the respective end-members: pollutant 1 – local mining ($^{206}Pb/^{204}Pb$ =18.30, $^{207}Pb/^{204}Pb$ =15.62, Kennan et al., 1987), and pollutant 2 – average values for leaded gasoline ($^{206}Pb/^{204}Pb$= 17.20, $^{207}Pb/^{204}Pb$ =15.54, estimated using values compiled by Komarek et al., 2008).
f_b represents the fraction of the end-members (pollutants) involved in the mixing, with $f_a+f_b=1$.

Eliminating f_b from the mixing equations gives:

[6] $\mathbf{A}(^{206}Pb/^{204}Pb)_{mix} + \mathbf{B}(^{206}Pb/^{204}Pb)_{mix} * (^{207}Pb/^{204}Pb)_{mix} + \mathbf{C}(^{207}Pb/^{204}Pb)_{mix} + \mathbf{D} = 0$ where,

[7] $\mathbf{A} = [Pb_1]_b * [Pb_2]_a * (^{207}Pb/^{204}Pb)_b - [Pb_1]_a * [Pb_2]_b * (^{207}Pb/^{204}Pb)_a$

[8] $\mathbf{B} = [Pb_1]_a * [Pb_2]_b - [Pb_1]_b * [Pb_2]_a$

[9] $\mathbf{C} = [Pb_1]_b * [Pb_2]_a * (^{206}Pb/^{204}Pb)_a * [Pb_1]_a * [Pb_2]_b * (^{207}Pb/^{204}Pb)_b$

[10] $\mathbf{D} = [Pb_1]_a * [Pb_2]_b - (^{207}Pb/^{204}Pb)_a * (^{206}Pb/^{204}Pb)_b - [Pb_1]_b * [Pb_2]_a * (^{207}Pb/^{204}Pb)_b * (^{206}Pb/^{204}Pb)_a$

$_a$ = respective composition of pollutant 1, and $_b$ = respective composition of pollutant 2

$[Pb_1]$ = concentration of the 1st pollutant, $[Pb_2]$ = concentrations of the 2nd pollutant

Term B gives the curvature index

Chapter 5

Combined zinc-lead isotope and trace-metal assessment of recent atmospheric pollution sources recorded in peat bogs from Ireland †

Carolina Rosca[1*], Ronny Schoenberg[2], Emma L Tomlinson[1], and Balz S Kamber[1]

[1]Geology Department, Trinity College Dublin, Ireland
[2]Geochemistry Department, Ebert-Hard University Tuebingen, Germany
*corresponding author: roscaca@tcd.ie

† *A version of this manuscript is currently under review in the journal "Science of the Total Environment"*

Abstract

Atmospherically-fed, nominally unpolluted Earth surface archives such as ombrotrophic peat bogs, lake sediments, and ice consistently show an upward increase in Zn concentrations of unclear origin. Here, we present a stable Zn-isotope dataset for a historically polluted, near-urban ombrotrophic peat bog (Liffey Head bog) from the east coast of Ireland and combine this with trace-element (Zn, Cd, Ni, Cu, Cr, V, Mo, Ta, Pb, Th, Ga) and radiogenic Pb-isotope data to understand sources of recent atmospheric pollution. The studied peat record has experienced mining-related metal input prior 1940 AD and is compared to a peat archive from a rural site at the west coast of Ireland (Brackloon wood). The latter site only experienced limited anthropogenic influence from charcoal production in the past. Trace-element concentrations of particulate matter (PM) collected from relevant sources (lithogenic dust, industrial fertiliser, coal, peat, wood, oil, diesel, and petrol) were additionally used to evaluate significant contributors to the present-day atmospheric pollution.

In both archives, we observed a clear near-surface increase in Zn deposition, accompanied by enrichments in Co, Ni. Mo, V, Cr, and Cd, suggesting a co-genetic origin of these elements. In detail however, differences in the metal ratios (e.g., Zn/Cd: 49-482, east, and 149-265, west) are attributed to a higher contribution from traffic emissions (diesel, petrol) and oil-burning in the near-urban site, and dominant atmospheric influence from solid fossil fuel (coal and wood) combustion at the rural site.

The Zn-isotope composition in the historically-polluted Liffey Head archive evolved from heavy (0.72‰±0.03) in the peat accumulated during the 19th century, to lighter (0.18‰±0.03) $\delta^{66}ZnJMC_{Lyon}$ values towards the top of the extracted monolith (i.e., recent); the most pronounced shift occurring from the beginning of the 20th century. Zinc-isotope ratios are positively correlated with $^{206}Pb/^{207}Pb$ and metal/Cd ratios, collectively fingerprinting the gradual change from a mining-dominated to a traffic-dominated atmospheric pollution at the east coast of Ireland over the past century. A prevalent input, interpreted to represent emissions from diesel engines, is observed for the most recent period (past 20 years). Our study shows that combined with trace elements and radiogenic Pb-isotopes, the change in the Zn-isotope composition represents a real pollution signal and, thus, an additional tool towards better characterising the Anthropocene. Finally, a comparison of the temporal trends found in the present study with records from pristine archives in many other northern hemisphere sites, strongly suggests that atmospheric pollution from combustion of fossil fuels is at its highest level today.

Key words: ombrotrophic peat, Zn-isotopes, Ireland, fossil fuel combustion, diesel

1. Introduction

Atmospheric heavy metal pollution is a global phenomenon (United Nations Environment Programme, 2017). Significant regulatory actions have been taken during the last decades to reduce anthropogenic emission levels of greenhouse gases (GHG) and toxic metals such as Pb, Hg, As (*WHO, annual reports 2015*). Despite these measures, concentrations of heavy metals (e.g., Cd, Co, V, Ni, Cu, Mo) and especially zinc (Zn) have remained elevated throughout the 20th century and in many places have not declined. This is evidenced from atmospheric depositions onto archives such as peat bogs and lake sediments (Fig. 1) located relatively close to historic mining and smelting centres (e.g., Belgium, Sonke et al., 2008; Scotland, Küttner et al., 2015; Finland Har., Rausch et al., 2015; Canada, Schindler and Kamber, 2013). However, increasing upward trends in Zn concentrations are also obvious in records widely considered pristine (Canada, Pratte et al., 2003; Finland Hj., Rausch et al., 2005), including in remote areas such as Greenland (Planchon et al., 2002a) and the Arctic (Lepane et al., 2007) (Fig. 1). These latter contaminations are indicative of long-range pollution transport. The earliest detectable elevated Zn concentrations in Greenland ice go back to the Industrial Revolution (Candelone et al., 1995), while cumulative Zn depositions from non-lithogenic sources in Antarctic snow (Planchon et al., 2002) have continuously increased since the second half of the 20th century. Simultaneous Zn increase is observed in ocean dry deposition near Bermuda (Arimoto et al., 2003). Thus, the global rise in surficial Zn concentration is archive- and site-independent and continues into recent times despite improvements in the pollution load of other heavy metals, such as Pb, over the last two decades (Gabrielli and Vallelonga, 2015).

Zinc has been used by humans for many purposes during the last three centuries. Its prodigious economic and infrastructural importance has, however, only been recognised during the last century, triggering a steady increase in worldwide exploitation of Zn to meet societal demand (Sverdrup and Ragnarsdóttir, 2014). The amount of Zn liberated to the environment has apparently increased proportionally to its industrial consumption but the detailed reasons for this relationship are not known on a hemispheric scale. Important anthropogenic Zn sources to the atmosphere are mines and smelters and pyrometallurgical plants producing and purifying Zn, including galvanisation of steel and other Fe products (Pierson and Brachaczek, 1974). Second-tier point sources include waste incineration, cement production, phosphate fertilisers, urbanisation, as well as stationary and vehicle fuel combustion (Hildemann et al., 1991). The increasing variety of emission sources combined with the lack of regulatory frameworks currently limits an accurate assessment of the magnitude of present-day Zn atmospheric pollution (Pacyna and Pacyna, 2001).

In environmental forensics, Zn pollution is assessed by comparing the isotopic signature of point sources such as waste incinerator fumes and residues (Cloquet et al., 2006), urban PM (PM= suspended particulate matter in the atmosphere composed of aerosols and particles, e.g., tire wear, Thapalia et al., 2010), as well as industrial products (e.g., electroplated hardware, John et al., 2007) with the composition of atmospheric aerosol. This is facilitated through direct measurements of Zn in precipitates (i.e., rain, snow, dry deposits e.g., Chen et al., 2008; Luck et al., 1999; Mattielli et al., 2009; Voldrichova et al., 2014). Information of past atmospheric Zn sources is obtained by investigating the Zn-isotope composition of atmospherically-fed archives such as peat bogs (e.g., Sonke et al., 2008; Weiss et al., 2007), lake sediments (Thapalia et al., 2010), as well as ice and snow accumulations (e.g., Voldrichova et al., 2014).

The aim of this study is to qualitatively assess recent anthropogenic emissions and source(s) of Zn and associated metals into the Irish atmosphere over the past ca. 150 years. This timespan comprises important socio-economic periods such as historical mining of local ores, the industrial revolution, the use of leaded gasoline, and urbanisation. It was hypothesised that these various events might have delivered unique Zn signals to the atmosphere and that they could ultimately be recorded in natural archives. The target sites were two Irish peat bogs: i) a site with a strong historic mining influence at the east coast, close to the major urban area of the country - Dublin, and ii) a rural forest region from the west coast. The peat from the historically pre-polluted, near-urban site was analysed comprehensively with trace element geochemistry as well as stable Zn- and radiogenic Pb-isotope ratios. The rural control site was investigated solely for its trace metal composition.

Figure 1.

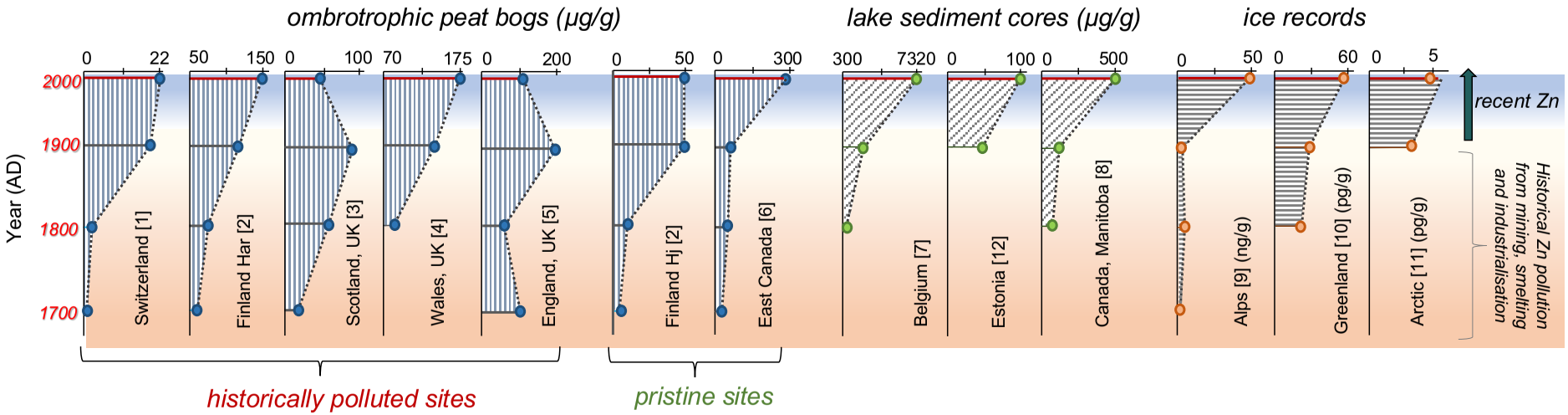


Fig. 1. Schematic illustration of Zn enrichments in different natural archives from the northern hemisphere since 1700 AD. Dara from [1] Shotyk et al 2002; [2] Rausch et al 2005; [3] Küttner et al. (2014); [4] Mighall et al. (2002); [5] Livett et al. (1979); [6] Pratte et al. (2013); [7] Sonke et al. (2008); [8] Outridge et al. (2011); [9] Barbante et al. (2004); [10] Candelone et al. (1995); [11] Planchon et al 2002a; [12] Lepane et al. (2007).

2. Background and site descriptions

The montane-type Liffey-Head bog (LHB) from the Wicklow mountains in eastern Ireland (53°9'32.3172"N, 6°17'18.7692"W) is a *Sphagnum* moss dominated ombrotrophic peat bog. The area experiences annual precipitation between 1600 and 2400 mm a^{-1}, which sustains near-continuous deposition of aerosols and particulate matter (here collectively referred to as PM). Predominant winds circulate from the south-west and west, potentially carrying pollutants from the currently active Zn-Pb mining districts of the Midland basin, and occasionally from the east, possibly carrying aerosols from the UK and northern continental Europe (*Meteorological Survey, 2015*). The peat bog formed on the Leinster granitic batholith which uplifted the Wicklow mountains during the Caledonian orogeny. The uplands are hosts to numerous historically significant Pb, Zn, Cu, and Ag mining and smelting sites which operated from the 18th century into the first half 20th century (Rynne, 2015).

Brackloon wood (BW) is situated in Co. Mayo along the west coast of Ireland (53°45'20.4984"N, 9°33'30.7908"W). It represents a small remnant of the once prolific Atlantic oak woodland (Cunningham, 2005). Oceanic conditions of frequent rain and cloud cover dominate at this site. The wood is located in a basin on the eastern slopes of the Croagh Patrick mountain. The surrounding geology is complex exposing acidic and alkali-rich rocks such as: Silurian sandstone, gneiss, and shale; Ordovician shale, sandstone, basalt, and rhyolite; and Carbonaceous limestone to the east. Extensive tree clearance during previous centuries has given rise to peat mires within the residual woodlands (Reilly and Mitchell, 2015b), with some being recently dominated by *Sphagnum* moss. The wood ecosystem experiences near-constant exposure to clean North Atlantic winds (west and south-west direction) and has only suffered limited anthropogenic activities such as charcoal production during the 1500's and 1600's (Cunningham, 2005). The wood was acquired by the Land Commissioners in 1940s, later transferred to the Forest and Wildlife service and subsequently to Coillte (The Irish Forestry Board). Since 1999, Brackloon wood holds the status of "Special Area of Conservation".

3. Methodology

3.1. Liffey Head bog (LHB) - near-urban site

A complete vertical monolith (10 x 10 x 115 cm) was extracted from the centre of LHB in June 2015 using a stainless-steel Wardenaar corer. The physical properties of the peat (moisture, ash content, and density) were determined according to the methods described in Chapter 3. The upper part of the core was dated using ^{210}Pb-^{241}Am activity

distribution and was subject to a pilot study of trace metal and Pb-pollution from mining and industrial activities. These results are found in Chapter 4. In the present study, the dataset was revisited and augmented with new Zn-isotope data. To our knowledge, these are the first Zn-isotope results for environmental samples from Ireland. The new Zn-isotope data were interpreted together with the Pb-isotope and metal ratio information to gain a better understanding of the Zn enrichment history, with particular focus on deposition during the past century.

Zinc-isotope analyses were conducted on samples taken at high spatial and temporal resolution from the uppermost 33 cm of the core, which represent a depositional record of the past ca. 148 years. Zinc purification and isotope analyses were performed at the Isotope Geochemistry Group, Eberhard Karls University of Tuebingen, Germany. Aliquots were taken from HNO_3 converted digests of combusted peat bog samples and rock reference materials BCR-2, BHVO-2, and BIR-1a. They all contained at least 1µg of Zn and were spiked with an appropriate amount of purified ^{64}Zn-^{67}Zn double-spike (DS) tracer solution (in 1 mol L^{-1} HNO_3) to achieve a DS proportion of 0.6 to the total amount of zinc in the mixture (Moeller et al., 2012). Equilibration of samples and double-spike zinc was achieved by heating the mixed aliquots in closed beakers at 120°C for 24 hours. The spiked digests were converted to chloride form (6M HCl) for chromatographic purification using in-house shrink Teflon columns loaded with 1.1 mL of BioRad DOWEX AG MP-1, 100-200 mesh anion resin. The double-spike technique allows the in-run correction of instrumental mass-bias effects, but also accounts for Zn isotope fractionation potentially caused by anion-exchange chemistry (Marechal, 1999). Procedural blanks were below 1 ng total Zn and therefore negligible compared to the total amount of processed zinc.

Zinc-isotope ratio measurements were performed on a ThermoFischer Scientific NeptunePlus MC-ICP-MS in low resolution mode using a Cetac ARIDUS II desolvating nebulizer system without N_2 purging to minimise potential polyatomic oxide and nitride interferences. Signals of $^{64}Zn^+$, $^{66}Zn^+$, $^{67}Zn^+$, $^{68}Zn^+$ and $^{70}Zn^+$ together with the interference monitors $^{62}Ni^+$ (for correction of $^{64}Ni^+$ on $^{64}Zn^+$) and $^{72}Ge^+$ (for correction of $^{70}Ge^+$ on $^{70}Zn^+$) were detected simultaneously. Small background signals (e.g., from the long-term memory of the uptake system, the Ni cones or sample carrier solution) were corrected with on-peak zero measurements of the sample carrier solution prior each measurement. A $10^{10}\Omega$ resistor was used to measure the signal of the highly abundant isotope ^{64}Zn (49.2% natural abundance plus ^{64}Zn enrichment from the double-spike), a $10^{12}\Omega$ resistor was used to measure the least abundant ^{70}Zn signal (0.61% natural abundance), with all other signals detected using $10^{11}\Omega$ resistors on the respective amplifiers.

Isotopic data of samples are reported as the ‰-difference of the $^{66}Zn/^{64}Zn$ isotope abundance ratio relative to that of the isotopically certified reference material IRMM-3702 in the δ-notation, according to equation [1]:

$$\delta^{66/64}Zn_{IRMM\text{-}3702} = \left[\frac{\left(^{66}Zn/^{64}Zn\right)_{Sample}}{\left(^{66}Zn/^{64}Zn\right)_{IRMM\text{-}3702}} - 1 \right] \times 1000 \qquad [1]$$

For ease of reference and comparison to other studies, the results are tabulated (Table 1) relative to the "JMC-Lyon" solution standard, which is no longer available, by applying an offset of +0.29±0.05‰ on $\delta^{66/64}Zn_{IRMM\text{-}3702}$ (Moeller et al., 2012). The external (2 SD) reproducibility for $\delta^{66}Zn$ on IRMM-3702 during the course of this study was better than 0.03‰. Accuracy was controlled by interleaved analyses of an in-house solution standard prepared from an "Alfa Aeser" Puratronic Zn wire yielding an average $\delta^{66}Zn$ of -10.295±0.026 (2SD, *n=8*), which is within the laboratory long-term reproducibility of -10.278±0.051 (*n=21*). The USGS standards BCR-2, BHVO-2, and BIR-1a yielded average $\delta^{66/64}Zn_{JMC\text{-}Lyon}$ values of 0.280±0.036‰ (*n=4*), 0.315±0.036‰ (*n=4*), and 0.236±0.028‰ (*n=6*), respectively, and lie within the range reported in the literature (Table 2), demonstrating the accuracy of this dataset.

Table 1. Zinc isotope ratios of certified rock reference materials expressed as $\delta^{66}Zn/^{64}Zn$ (‰) relative to the IRMM-3702 solution standard.

Rock Standard	$\delta^{66/64}Zn_{IRMM3702}$ *(‰)*	$\delta^{66/64}Zn_{JMC\text{-}L}$ *(‰)*	*±2 SD*	*Reference*
BCR-2	-0.05	0.25	*0.01*	Sossi et al. (2015)
	0.04	0.33	*0.13*	Moeller et al. (2012)
	-0.09		*0.08*	Bigalke et al. (2010)
		0.20	*0.09*	Archer and Vance (2004)
		0.29	*0.12*	Chapman et al. (2006)
		0.32	*0.13*	Cloquet et al. (2006)
		0.26	*0.04*	Toutain et al. (2008)
		0.25	*0.04*	Sonke et al. (2008)
		0.33	*0.09*	Herzog et al. (2009)
		0.32	*0.05*	Pons et al. (2016)
	0.01	0.30	*0.04*	***This study*** *(n=4)*
BHVO-2	0.19	0.48	*0.13*	Moeller et al. (2012)
		0.29	*0.09*	Herzog et al. (2009)
		0.21	*0.09*	Moynier et al. (2010)
		0.33	*0.04*	Chen et al. (2013)
		0.27	*0.06*	Sossi et al. (2015)
	0.06	0.35	*0.04*	***This study*** *(n=4)*
BIR-1a	-0.10	0.20	*0.03*	Sossi et al. (2015)
		0.26	*0.09*	Herzog et al. (2009)
		0.31	*0.04*	Chen et al. (2013)
	-0.05	0.24	*0.03*	***This study*** *(n=6)*

The values with respect to the no longer available JMC-Lyon solution standard were calculated by applying a correction factor of +0.29±0.05 (Moeller et al., 2018). Other literature values are also indicated for comparison.

Table 2. Excess Zn, Cd, Pb, V, Cr, Ni, and Cu metal concentrations (µg/g) along the a) Liffey Head bog (LHB), and b) Brackloon wood (BW) peat archive, together with Metal/Cd ratios calculated using the excess concentrations.

Sample-ID	[cm]	%moisture	%CM	Zn	Cd	Pb	V	Cr	Ni	Cu	Ta*	Zn/Cd	Cu/Cd	Cr/Cd	Ni/Cd	V/Cd	$^{206}Pb/^{207}Pb^{a)}$	±2SD	$\delta^{66/64}Zn_{IRMM-3702}$ (‰)	$\delta^{66/64}Zn_{JMC-L}$ (‰)	±2SD
LHB 1.3	0-1	94.2	98.6	45.5	0.096	4.55	2.09	1.35	1.49	3.85	0.011	482	40.7	14.3	15.8	22.1	*1.148*	*0.007*	-0.110	0.18	*0.03*
LHB 2.3	1-2	94.8	97.3	81.5	0.228	12.9	4.57	2.31	2.65	6.99	0.021	359	30.8	10.2	11.7	20.1	*1.144*	*0.007*	-0.051	0.24	*0.03*
LHB 3.3	2-3	95.7	98.9	36.6	0.134	8.33	2.01	1.11	1.34	3.02	0.008	278	22.9	8.40	10.2	15.3	*1.142*	*0.007*	-0.071	0.22	*0.03*
LHB 4.3	3-4	96.4	99.0	32.6	0.175	6.36	2.78	1.21	1.49	2.86	0.007	190	16.6	7.07	8.64	16.2	*1.141*	*0.007*	-0.018	0.27	*0.03*
LHB 5.3	4-5	95.9	98.7	37.5	0.236	9.57	3.75	1.49	1.92	4.94	0.009	162	21.3	6.41	8.27	16.2	*1.137*	*0.007*	-0.072	0.22	*0.03*
LHB 6.3	5-6	93.7	98.1	59.7	0.425	18.6	4.70	2.16	3.04	8.89	0.013	142	21.1	5.13	7.22	11.2	*1.135*	*0.007*	-0.032	0.26	*0.03*
LHB 7.3	6-7	92.2	97.5	70.9	0.621	29.5	5.64	3.18	4.09	9.46	0.020	115	15.4	5.16	6.64	9.16	*1.136*	*0.007*	0.053	0.34	*0.03*
LHB 1.1	7-8	89.4	98.5	43.9	0.338	33.6	3.85	1.56	2.39	4.34	0.012	132	13.0	4.66	7.13	11.5	*1.136*	*0.011*	-0.112	0.18	*0.03*
LHB 2.2	9-10	94.4	98.7	73.0	0.735	90.8	8.09	3.40	4.47	8.22	0.018	100	11.3	4.66	6.13	11.1	*1.139*	*0.012*	-0.028	0.26	*0.03*
LHB 5.2	12-13	90.6	97.3	92.9	1.26	231	10.0	4.93	6.15	12.4	0.027	73.8	9.8	3.91	4.89	7.98	*1.148*	*0.012*	0.046	0.34	*0.03*
LHB 2.1	14-15	88.7	97.8	62.5	1.29	202	9.17	2.59	3.70	9.84	0.018	49.0	7.71	2.03	2.90	7.19	*1.157*	*0.012*	0.110	0.40	*0.03*
LHB 8.2	16-17	87.9	97.3	65.9	1.03	268	5.85	2.87	3.97	17.5	0.027	64.1	17.0	2.79	3.87	5.70	*1.166*	*0.012*	0.157	0.45	*0.03*
LHB 9.2	17-18	89.1	96.8	83.6	1.36	378	4.86	2.48	3.98	24.1	0.032	61.8	17.8	1.83	2.94	3.59	*1.170*	*0.012*	0.199	0.49	*0.03*
LHB 11.2	19-20	90.8	97.6	66.1	1.17	376	4.34	2.47	3.25	23.2	0.033	56.8	19.9	2.12	2.79	3.72	*1.172*	*0.012*	0.241	0.53	*0.03*
LHB 13.2	21-22	91.6	97.2	57.0	0.875	307	3.06	1.86	2.18	23.7	0.027	65.5	27.2	2.14	2.50	3.51	*1.174*	*0.011*	0.180	0.47	*0.03*
LHB 14.2	23-24	92.5	98.4	31.9	0.384	133	1.34	0.916	0.97	6.34	0.014	84.0	16.7	2.41	2.54	3.53	*1.175*	*0.012*	0.263	0.55	*0.03*
LHB 18.2	27-28	91.2	97.6	38.2	0.578	92.3	1.80	1.26	1.16	3.32	0.021	66.6	5.77	2.19	2.01	3.13	*1.176*	*0.011*	0.371	0.66	*0.03*
LHB 21.2	30-31	91.2	98.0	26.4	0.418	68.0	1.45	1.03	0.874	2.37	0.017	63.9	5.71	2.49	2.11	3.49	*1.177*	*0.011*	0.401	0.69	*0.03*
LHB 23.2	33-34	94.6	98.2	19.9	0.363	54.1	1.38	1.00	0.736	2.46	0.016	55.4	6.82	2.77	2.04	3.83	*1.175*	*0.011*	0.426	0.72	*0.03*
LHB 10.1 (**B**)	94-95	94.9	98.5	0.987	0.053	3.76	1.12	0.805	0.539	0.852	0.015	18.6	16.1	15.20	10.17	21.18	*1.174*	*0.011*	0.184	0.47	*0.03*

a)

Sample-ID	[cm]	%moisture	%CM	Zn	Cd	Pb	V	Cr	Ni	Cu	Ta*	Zn/Cd	Cu/Cd	Cr/Cd	Ni/Cd	V/Cd
BW 2.1	0-1	80.9	97.3	79.3	0.539	34.3	52.1	69.8	21.8	18.5	0.615	149	34.6	131	40.9	97.6
BW 2.3	2-4	80.4	87.4	50.8	0.305	27.5	47.0	66.5	17.9	15.2	0.657	168	50.2	219	59.2	155
BW 2.5	4-5	81.6	87.6	49.3	0.317	36.8	52.5	69.0	21.0	17.9	0.677	157	57.2	220	67.0	167
BW 2.7	6-7	80.4	88.1	58.4	0.314	36.6	59.7	76.2	22.7	19.2	0.781	187	61.5	244	72.8	191
BW 2.9	7-8	78.8	86.8	44.0	0.170	33.2	50.9	67.9	18.9	15.4	0.660	261	91.2	402	112	301
BW 2.11	10-11	75.4	97.7	38.0	0.182	32.5	46.4	60.3	17.2	14.3	0.625	210	79.3	333	95.2	256
BW 2.15	11-12	74.0	90.9	35.0	0.154	32.8	43.7	62.7	17.3	13.9	0.583	229	91.0	410	113	286
BW 2.19	12-13	72.4	98.1	37.5	0.163	37.7	49.7	66.4	18.0	15.5	0.688	232	95.9	411	111	308
BW 2.24	13-14	73.0	91.3	30.5	0.146	39.2	44.5	65.1	16.0	13.3	0.604	210	92.1	449	111	308
BW 2.28	14-15	71.9	82.7	35.7	0.181	36.5	47.5	62.7	17.3	16.2	0.617	198	89.9	348	96.0	264
BW 2.31	15-16	71.2	98.0	37.9	0.148	32.1	51.6	67.2	20.8	15.4	0.679	259	105	459	142	352
BW 2.34	16-17	67.1	83.0	35.8	0.136	22.9	46.4	62.5	16.8	14.6	0.639	265	108	462	124	343
BW 2.42 (**B**)	19-20	65.5	86.1	26.9	0.091	14.4	38.0	50.3	13.6	12.2	0.542	295	134	551	149	416

b)

Lowermost samples from the two bogs (LHB10.1 (B) and BW2.42 (B), respectively) and Ta* concentrations were used for the background correction of all samples at shallower levels and applying the formula [2] as described in paragraph 4.2. Trace element and Pb isotope data for LHB, are from Chapter 4. All BW trace-element data, and Zn isotope composition (indicated relative to the JMC-Lyon standard) for the LHB samples were obtained in this study.

3.2. Brackloon wood (BW) - rural site

The BW peat monolith was taken from an elevated, *Sphagnum* moss dominated area in a forest glade with no tree cover within a radius of 15 m to avoid potential disturbance by tree roots. An intact block (10x 10 x 62 cm) was extracted with a stainless steel Wardenaar corer, wrapped in cling film and stored in a dark room at <2°C. In the laboratory, the monolith was sub-sampled into 1 cm slices, each further apportioned for moisture, ash content, LOI, and trace-element aliquots. Previous studies of moor-humus wood peat in the area (e.g., Reilly and Mitchell, 2015) have shown the presence of volcanic tephra embedded in the decomposed organic material. Because where available, tephra layers offer robust chronostratigraphic markers (e.g., Swindles et al., 2010), a search for tephra in this monolith was conducted following the density-separation method of Blockley et al. (2005).

Trace-element analyses of peat sub-samples were conducted at Trinity College Dublin, Ireland via solution quadrupole ICP-MS (Qs-ICP-MS) using a Thermo Scientific iCAP-Qc and following the protocol described in Chapter 4. In brief, a homogenised fraction (between 10 and 30 mg) of the combusted peat ash (6h at 450°C) was digested in three main steps with triple sub-boiled concentrated HCl, HNO_3, and HF-HNO_3 (4:1) mix until a clear and colourless sample solution was obtained. After evaporation, the residue was converted with HNO_3 and dissolved in 3 ml of 2.5 M HNO_3 and subsequently topped up with additional Milli-Q water to produce 30 ml of 0.3 M HNO_3 sample solutions. Procedural blanks were carried out along with the samples through all combusting and digestion steps to account for potential contamination.

Trace element measurements were conducted following the ICP-MS procedure of Eggins et al. (1997) with slight modifications after Marx et al. (2010). In brief, 2 ml solutions were prepared for analyses, containing: i) a small aliquot of each stock solution, ii) topped up with carrier acid (2% HNO_3), and iii) an internal standard containing a mixture of ^{6}Li, Rh, Re, Bi and ^{235}U, which covers the full mass range of analysed elements. Oxide/hydroxide and dimer interferences were corrected following Ulrich et al. (2010). The external drift monitor correction of Eggins et al. (1997) was employed. Five separate digestions of the USGS W-2a reference material were used for calibration, and two digests of the USGS rock reference materials AGV-2, BHVO-2, and BIR-1, each were deployed as quality control standards. The results are shown in the *Appendix A* together with accepted reference material values of Jochum et al. (2016), GeoReM database. Internal errors were all better than the external reproducibility, measured as the relative standard deviation (RSD) for multiple analyses of reference materials. For metals that are homogeneous in second-generation USGS

reference materials, the RSD was <3% (4 out of 11 elements investigated in this study) for metals that suffer from nugget-effect contamination (e.g. Weis et al., 2006; Kamber and Gladu, 2009), As, Ag, Sn, W, but also Be and Th, the reproducibility was inferior (RSD>10%). These elements are not the focus of this study. The entire element dataset obtained for BW peat samples in indicated in Table 3, Chapter 6.

4. Results

4.1. Morphological and physical properties of the peat profiles

The 115 cm long LHB is composed of ca. 5 cm actively growing moss which overlies a denser segment of ca. 18 cm of intermediately decomposed peat of bright brownish colour known as the *acrotelm*. The *acrotelm* transitions into the *catotelm* (advanced decomposed organic material) between 25 and 30 cm from the surface and displays a fibrous texture indicative of decomposed grass species along with *Sphagnum* moss. The uppermost 115 cm from the LHB shows physical properties typical of ombrotrophic peat, including low densities (0.024-0.034 g cm^{-3}), high moisture and water content (87-97%) and high loss on ignition (LOI, 97-99%, Table 2).

The 62 cm long BW monolith is characterised by a thin layer (4 cm) of actively growing *Sphagnum* moss of fresh green colour, followed the partially decomposed *acrotelm* of 14 cm thickness. In a visible zone at approximately 18 cm from the surface, the *acrotelm* transitions into the *catotelm*, which is composed of advanced decomposed organic matter with a high content of humins responsible for the uniformly dark brown to almost black colour. The LOI is high but notably heterogeneous down the core, fluctuating between 83 and 97% (Table 2). These are slightly lower values than is typical of ombrotrophic peat bogs and this is likely due to the nature of the peat: *Sphagnum* dominated wood peat. The ash percentage to total wet weight fluctuates between 0.26 and 6.7% and correlates with the decreasing moisture content (61-84%) along the investigated peat segment. All these parameters collectively indicate additional import of element/sediment/soil at this site either by natural events or through anthropogenic influence.

4.2. Chronological constraints on the peat records

LHB - near-urban site: Chronology for the uppermost 25 cm has been obtained with the radionuclide (^{210}Pb-^{241}Am) technique as described in Chapter 4. In brief, the peat accumulation rate was found to be constant at 0.25 and 0.24±0.03 cm $year^{-1}$ within the upper 25 cm from the surface (1900 AD – today). Moisture (88-96%) and peat density (0.023-0.034 g cm^{-3}) show little variability throughout the length of the core,

therefore the accumulation rate was extrapolated down to 33 cm, translating into the age 1877±5 AD. Hence, the peat segment comprising the first 33 cm from the surface corresponds to ca. 148 years of peat accumulation.

BW - rural site: A cryptotephra layer was found at 14 to 16 cm from the surface. It was identified as belonging to the ejecta of the Laki 1783-1784 AD volcanic eruption (as shown in detail in the next Chapter, 6). This implies that the uppermost ca. 15 cm represent a record of ca. 232±10 years. If peat deposition is assumed to have been constant since 1783-4 AD, this translates into an average accumulation rate of 0.07 cm $year^{-1}$. This is somewhat slower than peat accumulations in average Irish bogs (0.1-1.2 cm yr^{-1}, Hammond, 1978), possibly reflecting peat growth in a woodland environment. The exact chronology of peat accumulation at this control site is not important, as the aim of the analysis was to estimate potential long-range pollution for the most recent period (uppermost 10 cm, calculated to represent the past 154 years).

4.3. Geochemical characteristics of the peat profiles

To investigate the metal deposition onto the bogs originating from anthropogenic sources, it is first necessary to extract the metal inventory entering the bogs from natural sources. This is of high importance especially in the BW core where the lower LOI suggests a more enhanced extraneous flux compared to LHB. Because of the varied geology which underlies and surrounds the respective boglands, it is impossible to quantify elemental contributions from single, individual rock types. Measured element concentrations were therefore corrected against the local background (B) of the respective area using element/Ta ratios measured in samples representing the least enriched (i.e. oldest and most pristine) sections of the bog: i) BW 19-20 cm, pre-1783 AD and, ii) LHB 94-95 cm depth (Table 2). As explained earlier in Chapter 4, Ta was selected as the denominator in equation [2] as its origin is considered primarily lithogenic, and because of good correlations between Ta and residual ash content in both bogs. We note that similar results would be obtained if Ti, Zr, or Sc (Shotyk et al., 1996) were used for normalisation instead.

$$Metal_{excess} = Metal_{measured} - [(Metal/Ta_{measured})/(Metal/Ta_{backgr.})] \quad [2]$$

LHB - near-urban site: Excess Zn, Pb, Cd, and Cu (not shown) display similar patterns between 1877 and 1940 AD (Fig. 2a, b, e). These patterns reflect pollution associated with the major mining and smelting period of Pb-Zn-Ag and Cu in the Wicklow uplands (Chapter 4). Next follow episodes of enrichments in other elements (e.g., Ni, Cr, Mo, V) emerging from ca. 1900 AD, culminating at the same depths as Pb, Zn, and Cd. This

event is followed by a gradual decoupling of Pb-Cu-Ag from enrichments of Zn-Cd-Ni-Cr-Mo-V from the second half of the 20th century until the most recent time (Fig. 2a-e). The decoupling is mainly related to a significant decline in metal concentrations associated with metallurgical activities, and most strongly shown by decline in Pb concentration towards the top (Pb_{excess}= 5-13 µg g^{-1}) when other metals (Cu, Ni, Mo, Cr, V), especially Zn (Fig. 2a-e), continued to increase in concentration.

BW - rural site: Lead concentrations remain at background level throughout the entire monolith 30-33 µg g^{-1} (Fig. 2h). An increase in element concentrations, i.e. excess metal, only begins to emerge from ca. 10 cm from the surface (calculated 1861 AD). This is seen for Cd (0.3-0.5 µg g^{-1}), Mo (0.8-0.9 µg g^{-1}), Ni (18-23 µg g^{-1}), Co (7-10 µg g^{-1}), Cd, Zn (51-79.5 µg g^{-1}) (Fig. 2i-l.), V (52-60 µg g^{-1}), and Cr (70-76 µg g^{-1}) with the highest values detected in samples at the surface of the bog, i.e., the most recently grown peat.

Figure 2.

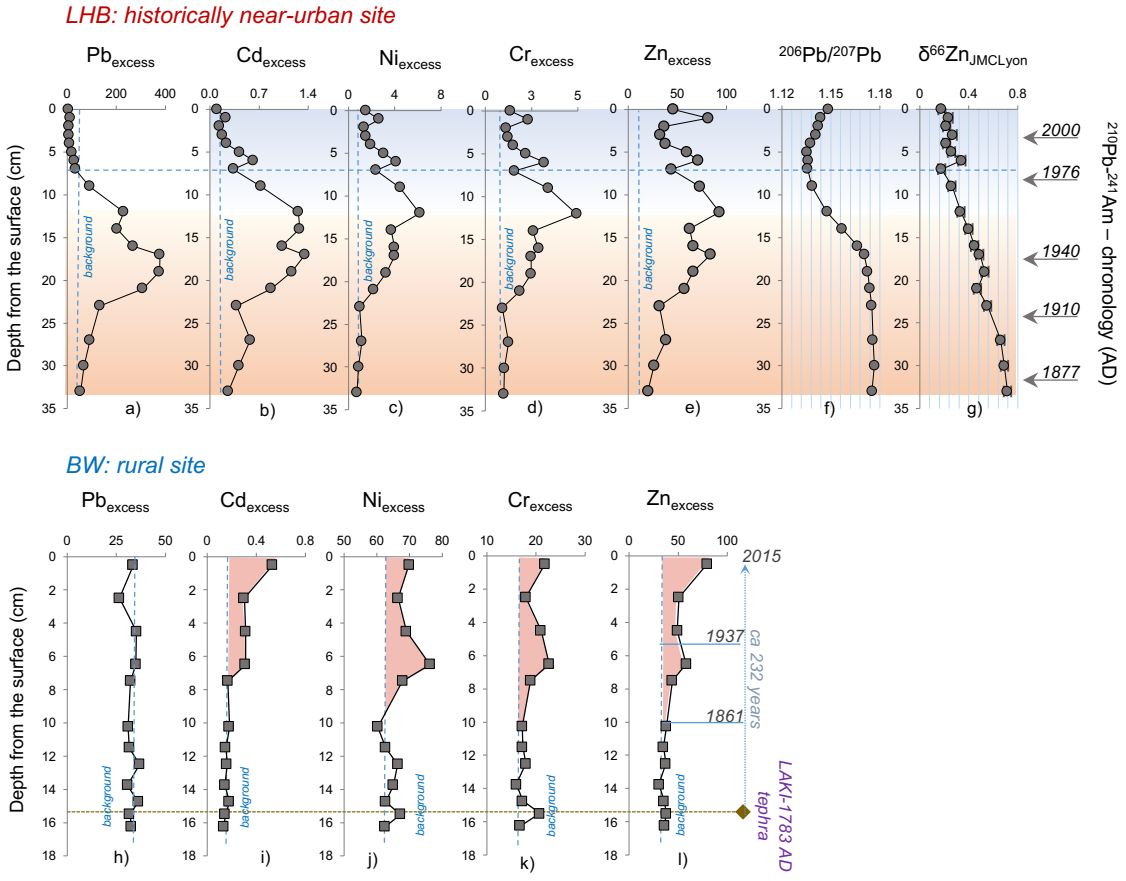


Fig. 2. Excess ppm enrichments of Pb, Cd, Ni, Cr, and Zn (calculated as described in paragraph 4.2) in the historically pre-polluted, near-urban Liffey head peat bog (LHB) from the east coast, and Brackloon wood peat core (BW) from a rural site at the west coast of Ireland. Lead isotope ratios along LHB are from Chapter 4. Zinc isotope analyses in LHB were obtained in this study. Age-model reconstructions were obtained with the radionuclide method for LHB core (Rosca et al., 2018), and extrapolated for BW using the identified LAKI 1783-4 tephra layer at 15 cm from the surface.

The element inventories of PM recently deposited into the two peat monoliths are compared using the background corrected percental values of the sample LHB3.3 at 3.5 cm from the surface in LHB and BW2.1 at 0.5 cm from the surface in BW. The reasoning behind this choice being the three-fold slower peat accumulation in BW archive compared to LHB. The results presented in Figure 3 show: i) relatively similar cumulative percental compositions of Pb, Cu, and Cd (Fig. 3) at these two sites, ii) higher concentrations of Zn and Mo in LHB compared to BW, and proportionally more Ni, Cr, and V deposited through PM onto the rural BW site. Background corrected metal ratios in the LHB sample LHB3.3 (e.g., Cr/Cd=8.5; V/Cd=15; Zn/Cd=278; Zn/Pb=4.5; Cr/Pb=0.1) are different than those in BW2.1 (Cr/Cd=131; V/Cd=98; Zn/Cd=149; Zn/Pb=2.5; Cr/Pb=2.1), and also collectively different than the composition of the upper continental crust (UCC, Cr/Cd=847; V/Cd=1092; Zn/Cd=725; Zn/Pb=4; Cr/Pb=5, McLennan et al., 2002). These modern-day enrichments are independent of the different peat accumulation rates of the two archives and are indicative of compositional differences in the nature of PM deposited onto the two peat bogs.

Figure 3.

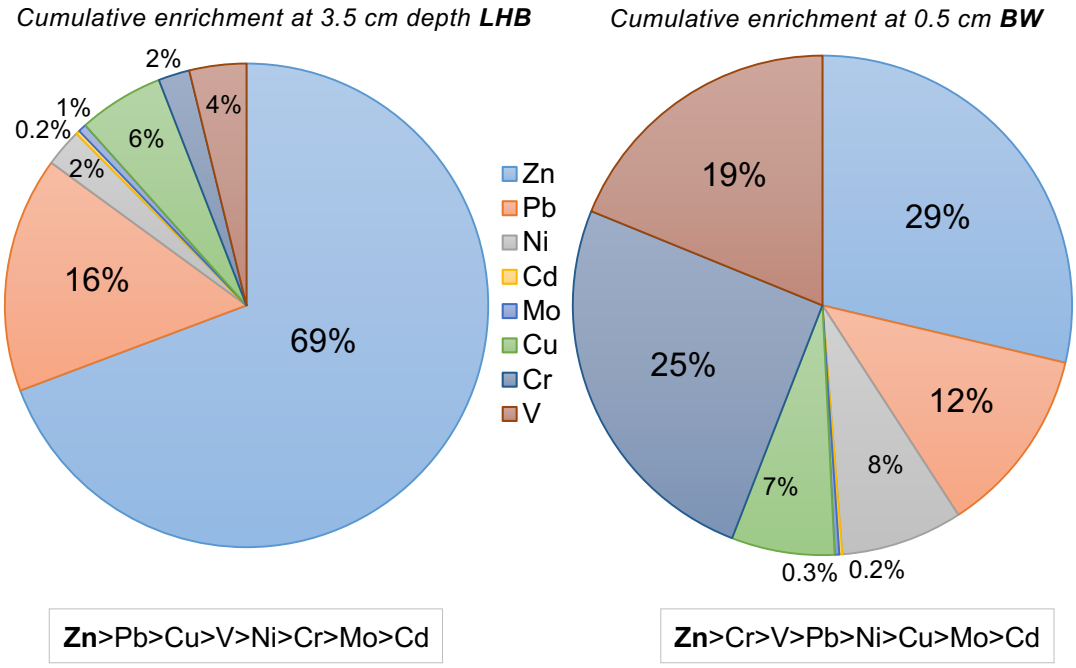


Fig. 3. Illustrative apportionment of selected elements (Zn, Pb, Ni, Cd, Mo, Cu, Cr, and V) in the uppermost 3 cm (living and poorly decomposed *Sphagnum* moss) of LHB and surface, 0 cm in BW peat cores from Ireland. To calculate these, the sum of the above listed elements was normalised to 100%. The enrichment sequences were built according to the respective percentages.

The Zn-isotope composition in LHB evolves from relatively heavy ($\delta^{66/64}$Zn= 0.47 ±0.03‰) at the base of the core (94-95 cm) to significantly lighter ($\delta^{66/64}$Zn= 0.18 ±0.03‰) towards the surface, i.e. recently grown *Sphagnum* moss (Fig. 2g). The heaviest $\delta^{66}Zn_{JMCLyon}$ values of 0.72 ±0.03‰ are detected at 33 cm from the surface, representative of 1877 AD. Recent Zn isotope fractionation by the *Sphagnum* moss (i.e. peat precursor) was assessed by investigating the isotope composition of Sphagnum roots ($\delta^{66/64}$Zn= 0.24 ±0.03‰) and branches with leaves ($\delta^{66/64}$Zn= 0.18 ±0.03‰), yielding a δ^{66}Zn difference of 0.06±0.03‰. Zinc isotopes are anti-correlated with Zn concentrations (expressed as Zn/Ta in Fig. 4a), and positively correlated with Pb isotopes and metal ratios (Fig. 4b).

Figure 4.

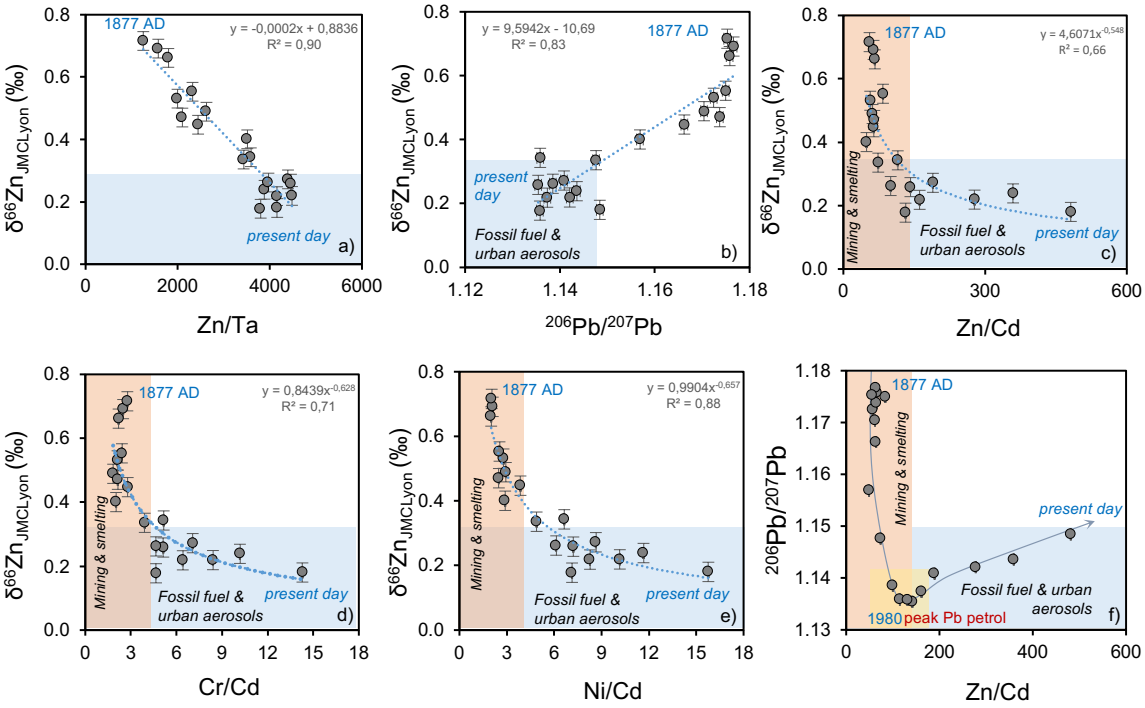


Fig.4. Zinc isotope ratios against excess (background corrected) a) Zn/Ta, b) $^{206}Pb/^{207}Pb$, c) Zn/Cd, d) Cr/Cd, and e) Ni/Cd, in the Liffey Head peat bog; Additionally, Pb isotope compositions are shown against excess Zn/Cd in plot f). Differently shaded areas represent PM compositions associated with the mining activity in the Wicklow uplands which ended in 1940 (orange), and isotopic values associated with recent anthropogenic activities (fossil fuels and urban aerosols) after Cloquet et al. (2006) and references therein, John et al. (2007) for Zn isotopes, and Chiaradia and Cupelin (2000), Hansmann and Koppel (2000), Veron et al. (1999) for Pb isotopes. The peak period of leaded gasoline identified to have emerged around 1980 AD is evident in the mixing curve between the mining and present-day pollution end-members (yellow square). For metal ratios, error bars are smaller than the symbols.

5. Discussion

Zinc concentrations are known to show an upwards increase in both pristine and historically polluted records (Fig. 1), but the cause of this increase has remained unresolved. Importantly, the Zn enrichment is independent of the type of environmental archive (peat, ice, snow, lake sediment), and accompanied by increased concentrations in other metals including Cd, Ni, Cu, V, Cr, etc. Unlike during the 18th to 19th centuries, the near-continuous modern increase cannot easily be related to regional metallurgical activities or enhanced lithogenic supply (e.g. erosion due to change in land use). These observations point towards an increasing atmospheric control through recent anthropogenic activities. However, due to the diffuse and ubiquitous nature of human Zn emissions to the surficial environment, exact apportioning of respective pollutants remains a difficult task. In the following sections, we first evaluate the possibility of upward Zn mobility in the two archives investigated in this study as an explanation for apparent increase in PM loading. After assessing this, we combine trace element and isotope systematics to identify major pollution end-members at these two contrasting sites over the past 100 years, with special focus on fingerprinting the most recent pollution sources.

5.1. Constraints on Zn mobility within the two archives

Before using Zn as a tracer of atmospheric deposition, we must first establish that it has remained relatively immobile within the matrix of the studied archives. As a building block in more than 300 enzymes and proteins, Zn is a bio-essential element to organisms and plants (e.g., Plum et al., 2010). Consequently, the continuing upward Zn enrichments in peat bogs, similar to those observed in LHB and BW, have been interpreted to emerge through element recycling by growing vegetation at the surface (e.g., Rausch et al., 2005). Although biological uptake is considered an important factor which can affect post-depositional redistribution of Zn, it remains unknown to what extent this relocation alters the fingerprint of initial atmospheric pollution signal. Similar to Pb, Zn is considered relatively immobile within the catotelm, whereas its behaviour within the acrotelm is still poorly understood. pH-pE diagrams suggest that Zn will be present as Zn^{2+} (similar to Cd^{2+}, Cu^{2+}, Pb^{2+}) in acidic (pH>3.5) bog waters (Drever, 1982) at the surface and therefore subjected to potential mobility. Schnitzer and Hansen (1970) concluded that the reason why less metal is bound at lower pH is because H^{+} and metal ions compete for the molecular sites, and because of poor dissociation of functional groups (particularly carboxyl) within the acrotelm, binding sites are limited. Complexes formed between Zn^{2+} and humic acids were found to be less stable than for

example between Pb^{2+} and humic acids (e.g., Gao et al., 1999). However, as Zn^{2+} will likely be bound to an organic phase, this complexation is expected to significantly retard its mobility within the peat column (Shotyk, 1988).

So far, the two main factors affecting the redistribution of Zn within peat bogs were considered i) bioaccumulation within the acrotelm, and ii) sulphide (ZnS) precipitation within the catotelm (pH <6). These two processes are extensively discussed by e.g., Cloy (2006) using three different ombrotrophic bogs from Scotland. Noteworthy, in this study all three bogs displayed different Zn enrichment patterns, which complicates the generalisation of the Zn excursions in peats. On the other hand, Jones and Hao (1993) suggested that enrichments of Zn, Cu, Cd, and Pb in a peat bog from northern England reflect their industrial use in the area. This is further supported by peatland investigations in Europe by Turetsky et al. (2004), who suggest that enrichment excursions of Cu, V, and Zn can be linked to their historical use.

The still enigmatic behaviour of Zn within peat bogs points at the necessity to investigate its behaviour in each archive individually. In the following assessment we interrogate the complete dataset, including the lower segments of the peat archives.

5.1.1. Liffey Head Bog

Within LHB, the 19th to 20th century Zn enrichments correlate well with enrichments in Cu and Pb. These can very plausibly be related to known metallurgical activities in the area (Chapter 4). Zinc concentrations are at a minimum in the lowermost analysed part of the core (53 cm) and increase upwards from the onset of local mining at 1794 AD until 1940 AD (Chapter 4). This observation indicates that downward mobility of Zn is insignificant at this site. This is in line with experimental studies which demonstrated that high contents of decomposed organic matter within the *catotelm* will facilitate complexation between metals and organic ligands, ultimately resulting in the capture and retention of divalent cations at the depth of their deposition (e.g., Baker and Senft, 1995). Further up in the profile, the Zn enrichment excursions identified in the *acrotelm* (from 18 cm towards the surface) are accompanied by well-defined enrichment peaks in other elements, including Ni, Cr, Cu, and V. Importantly, only V has been found to eventually beneficial to plants (Faure, 1998), questioning the notion that the increase in Zn concentration is an effect of sole upward bio-accumulation.

The enrichment in these metals (and Zn) is negatively correlated with the conservative elements Ta, Zr, and Sc (Chapter 4) which are immobile within peat bogs (Shotyk et al., 1996). Therefore, increased lithogenic input can be ruled out as the reason for enrichment. This is consistent with the finding that the maximum LOI values of 98% was measured at sub-surface levels. Owing to the contrasting geochemical

behaviour of the lithogenic tracers, the progressively more accentuated metal enrichment points towards the presence of a real pollution signal. This signal is unlikely to reflect mining, which can be identified confidently lower in the core.

In certain cases, Zn assimilation by plants has been shown to cause isotope fractionation via preferential incorporation of the lighter isotopes into the shoots- and leaves with respect to the roots (e.g., Viers et al., 2007; Weiss et al., 2005). To date, there are no experimental data for Zn fractionation by *Sphagnum* moss. Regardless, in a peat bog, any potential original inter-vegetal Zn isotope fractionation would be obliterated by progressive biomass decay, ultimately resulting in the preservation of the initial atmospheric signal. Zinc isotope fractionation by percolating fluids (e.g. Weiss et al., 2007) is not considered to be significant because of the undisturbed Pb-Zn-Ag-Cu co-enrichments within LHB core. Furthermore, kinetic isotope fractionation by percolating fluids is expected to lead to the sequestration of light isotopes and the concentration of heavy Zn isotopes at the base of the core. In contrast, in the LHB core, the deepest analysed sample is isotopically lighter ($\delta^{66/64}Zn_{JMCLyon}$= 0.47±0.03‰, LHB,10.1, 94-95cm) than the peat deposited during the mining activities of the 19th century ($\delta^{66/64}Zn_{JMCLyon}$=0.72 to 0.53±0.03‰). Most importantly, Zn isotopes are positively correlated with Pb isotopes (Fig. 4b) which, due to their restricted overall mobility in this kind of environment are commonly accepted as a robust tool to trace sources of atmospheric pollution (Shotyk et al., 2002; Weiss et al., 1999).

Collectively, these observations argue against Zn-isotope variability within the uppermost 33 cm of the LHB reflecting post-depositional fractionation. Instead, we propose that it reflects the progressively dominant deposition of Zn with PM.

5.1.2. Brackloon wood

An important feature of this peat monolith is that it does not show enrichments in the heavy metal Pb (Fig. 2h), which could be linked to historical mining, and/or influence from leaded gasoline during the 20th century. Similar to the LHB monolith, Zn concentration describes a trajectory of increasing enrichments upward the surface. The enrichment emerges from ca. 10 cm depth (calculated age ca. 1861 AD) and here too, it is accompanied by elevated concentration of further metals such as Cd, Ni, Cr (Fig. 2i-l), strongly suggesting a co-genetic origin of the metals. Again, Zn concentration is anti-correlated with Ta, which is considered a conservative and relatively immobile element within peat bogs. The pollution history of the BW bog is simple, consisting of only one main episode that therefore it is straightforward to assess element mobility. The concentrations of the potentially mobile elements of interest were investigated with respect to the conservative and fluid immobile elements Th and Ga. As shown in

Appendix B, many of the heavy metals of interest show reasonably strong correlations with Ga and Th (R^2=0.6-0.8), while a poorer correlation is observed with Zn (R^2=0.25-0.35). This is mainly caused by the much stronger Zn excess observed towards the surface of the monolith. Very string correlations between Zn and Mo (R^2=0.85), Zn and Cd (R^2=0.91), and Zn and Co (R^2=0.93) (not shown) are found and they suggest a parallel enrichment of these metals. We consider the co-enrichment between Zn and non-vital metals whose concentrations, in turn correlate with immobile elements, as string argument against significant upward mobility of Zn in this profile.

5.2. Defining sources of Zn and accompanying metals deposited onto the two bogs

Because there are many possible origins of atmospheric Zn pollution, we chose to investigate Zn together with changing metal ratios along the cores and in the context of ratios known from representative pollution sources. By examining metal ratios, geochemical variabilities in enrichment factors due to differences in peat accumulation rates of LHB and BW can be excluded. After permutation of all plausible heavy metal ratios, it emerged that plots of Zn/Cd vs. metal/Cd (Fig. 5) are the most diagnostic for discriminating between different sources impacting the two investigated archives. One reason for this is that Cd was released to the atmosphere as a by-product of historic Zn and Pb mining and smelting (up to 1940 AD), and a second that it continues to be a major constituent of most present-day pollutants (Gabrielli and Vallelonga, 2015; Marx et al., 2010). Combined, the metal-Zn-Cd systematics afford differentiation between past and present pollution sources.

Metal ratios of possible modern pollution sources are listed in Table 3 and include ratios of vehicle emissions and PM collected locally in Dublin city (exhaust emissions from diesel engines dating between 2003 to 2016 and petrol engines of 2006 and 2017 vintage; from Gallagher et al., 2018; and personal communication), European diesel, bio-diesel and lubricating oil combustion compositions (Dwivedi et al., 2006), as well as other fossil fuel emissions (heating oil, smokeless coal, peat briquettes, wood, mixed fuel; from Gallagher et al., 2018), Columbian coal (Tewalt et al., 2006), waste incinerator gases (UK and Europe in general), industrially produced fertilisers (as solids, Rauf et al., 2002) and recently mined Irish-ores (Wilkinson et al., 2005). Not available for comparison were data for other potential sources such as aviation fuel, heavy fuel oil (HFO), and low sulphur fuel oil (LSFO) powering cargo ships.

Table 3. Metal/Cd ratios in PM (with diameters of 2.5 and 10 microns) from relevant anthropogenic sources in Ireland

Source:	Locality	Cr/Cd	Ni/Cd	V/Cd	Cu/Cd	Zn/Cd	Reference
Diesel ($PM_{2.5}$)	Ireland	80.6	32.2	4.17	75.4	2386	Gallagher et al. (2018)
Petrol ($PM_{2.5}$)	Ireland	29.5	6.67	1.21	71.0	157	Gallagher et al. (2018)
Oil ($PM_{2.5}$)	Ireland	57.3	17.8	1.37	44.2	300	Gallagher et al. (2018)
Fuel oil ($PM_{2.5}$)	Turkey	18.1	1123	3666	3.56	261	Yatkin et al. (2008)
Coal burning ($PM_{2.5}$)	Turkey	174	127	216	81.2	214	Yatkin et al. (2008)
Smokeless Coal ($PM_{2.5}$)	Ireland	12.0	3.36	7.32	8.01	95.9	Gallagher et al. (2018)
Coal power plant ($PM_{2.5}$)	Turkey	14.9	17.7	35.7	5.87	53.5	Yatkin et al. (2008)
Coal power plant (gas)	Poland	1789	615	26.5	7.82	77.2	Larsen et al. (2008)
Columbian coal (raw)	USGS	84.0	123	-	188	167	Tewalt et al. (2006)
Peat Briquettes (PM)	Ireland	7.74	0.078	0.011	2.06	3.45	Gallagher et al. (2018)
Wood burning ($PM_{2.5}$)	Ireland	0.317	0.067	0.004	0.847	17.7	Gallagher et al. (2018)
Wood burning (PM_{10})	Turkey	19.7	0.303	-	1.04	15.7	Yatkin et al. (2008)
Mixed Fuel ($PM_{2.5}$)	Ireland	3.95	3.53	5.48	9.09	81.5	Gallagher et al. (2018)
Waste incinerator (PM) household	UK	0.475	0.031	-	0.431	13.75	Belevi and Moench (2000)
Waste incinerator (PM) mixed	UK	0.411	0.067	-	0.61	20.0	Belevi and Moench (2000)
Sea spray ($PM_{2.5}$)	Spain	6.54	0.002	0.080	0.082	-	Pey et al. (2013)
Aged sea spray ($PM_{2.5}$)	Spain	0.440	243	8730	2.7E-9	2.4E-9	Pey et al. (2013)
Industrial fertilisers	*average*	0.340	6.84	-	1.41	5.8	Rauf et al. (2002)
Midland mineralisation	Ireland	32.8	53.7	38.9	20.7	281	Kalveram (2018)
Wicklow granites	Ireland	2.77	1.50	3.9	6.8	45	estimated from Rosca et al. (2018)
Upper Continental Crust	*average*	847	449	1092	255	725	McLennan et al. (2001)

Table 3: Indicated are liquid and solid fossil fuel emission sources from Ireland (Gallagher et al., 2018) and other European countries (Larsen et al., 2008, Pey et al., 2013, Yatkin et al., 2008, data from SPECIEUROPE: http://source-apportionment.jrc.ec.europa.eu). Values for lithogenic sources are from Kalveram, 2018 (Midland mineralization, estimated from Rosca et al. 2018), and upper continental crust (UCC, McLennan et al., 2001).

5.2.1. Sources of metals onto LHB – near urban site

At the LHB site, peat deposited between 1877 and 1940 AD (33-18 cm) is characterised by a relatively radiogenic Pb-isotope signal ($^{206}Pb/^{204}Pb$= 18.429-18.314±0.013, $^{206}Pb/^{207}Pb$=0.172-0.176±0.012) and a heavy Zn-isotope signature ($\delta^{66/64}Zn_{JMCLyon}$= 0.53±0.03‰ to 0.72±0.03‰). These isotope systematics are accompanied by enrichment in Pb, Zn, and Cu (Zn/Cd= 56-84, Cu/Cd= 5.5-27, and Ni/Cd= 2-3). The Pb-isotope composition is similar to that of Wicklow granites and its mineralisation ($^{206}Pb/^{204}Pb$= 18.398-18.305, Kennan et al., 1987), supporting significant input from historic local mining. The strong correlation between the Pb and Zn isotopes at this depth (33-18 cm) indicates that the mining-related input had a heavy Zn isotope composition. A possible explanation for this signal would require a reconstruction of the historic ore processing steps. It is well documented that ore aggregates were physically processed at the extracting location and in neighbouring valleys (e.g., Glendassan valley, Rynne, 2015), which resulted in the formation of numerous tailings. Focused studies have shown that mine dumps and tailings are generally enriched in heavy Zn isotopes with respect to the aerosols emitted during smelting and the water used for washing ore (Mattielli et al., 2009, Sivry et al., 2008). Based on these generalised findings for Zn tailings, we suggest that the heavy Zn isotope signal recorded by the

peat bog during the mining period most likely reflects occasional aeolian transport of isotopically heavy tailing dust.

In order to identify sources of anthropogenic metal release to the atmosphere for the period between the mining (19th century until ca. 1940 AD) and present, conservative mixing models involving putative end-members of known composition and representative for Ireland (Table 3), were calculated. Binary mixing lines were constructed from a combination of end-members with equation [3]:

$$Metal/Cd_{SPL} = (f_a \times C_{W\text{-}min}) + (f_b \times C_{coal}) \quad [3]$$

In this example for binary mixing between lithogenic mineral dust and coal combustion aerosols, the parameters are as follows:

$Metal/Cd_{SPL}$ are the background corrected compositions of the samples;

$f_a = 1 - f_b$, yields the relative proportion of the end-members;

$C_{W\text{-}min}$ is the concentration of the elements in Wicklow granite;

C_{coal} is the concentration in either combusted coal, wood, petrol, oil, or diesel.

Elemental concentrations of other end-members (other than coal) plot along the upward trajectory defined by the peat the samples (Fig. 5) and include petrol, diesel, and oil. The calculated f_a and f_b were used for a quantitative approximation of the relative contributions. The results of the mixing calculations are shown in Figures 5a-d. It transpires that the composition of the peat deposited during the mining period until the first half of the 20th century records an influence from coal combustion (Ni/Cd= 6-18, and Zn/Cd= 157-300). This becomes evident from Figures 5a, c, and d, where a mere 5% of coal emission contribution to the mining signal (W-min) is sufficient to explain the recorded signal in the peat. This geochemical finding is strongly supported by historical records of Ireland's dependence on coal for smelting and for domestic use (Rynne, 2015) during the 19th and 20th century.

Further up in the profile, from the second half of 20th century until the end of it, Ni/Cd, Zn/Cd depart from the values of coal emissions. This geochemical signal (Ni/Cd= 4-6, Zn/Cd= 64-132, $^{206}Pb/^{204}Pb$= 18.195-17.678 ±0.013) also clearly differs from the composition of Pb-Zn mining in the Lower Carboniferous strata of the Midland basin (e.g., Ni/Cd= 54, Zn/Cd= 281, Kalveram et al., 2018; $^{206}Pb/^{204}Pb$= 18.15-18.3; Wilkinson et al., 2005). The Zn/Cd, Ni/Cd, and Cu/Cd values instead point towards the composition of PM from combustion of mineral oil (Zn/Cd= 300, Ni/Cd= 18, Cu/Cd= 44) and its derivative product petrol (Zn/Cd= 157, Ni/Cd= 7, Cu/Cd= 157; Table 3 and Fig. 5a-d). Mixing calculations between Wicklow mineralisation (W-min) and PM resulting from the

combustion of petrol and heating oil (Fig. 5a-d) reported by Gallagher et al. (2018) were performed. The trajectories of the mixing lines can explain the observed changes in the metal inventory of the samples through transition from coal towards oil-based fuels. This finding is consistent with the location of peak period leaded gasoline spike in the core established with Pb-isotopes (Chapter 4). To our knowledge, no Zn-isotope data for PM resulting from leaded gasoline exist. These would help to better constrain the significance in the shift towards much lighter Zn-isotope ratios higher up in the LHB peat. We suggest that the peat isotope signal ($\delta^{66/64}Zn_{JMCLyon}$= 0.34±0.03‰) at local peak Pb gasoline pollution time (1970-1980 AD) could be a first approximation.

Despite European-wide Pb-petrol phase-out at the end of 20th century (2000 in Ireland), the trace-element "flavour" of the PM deposited onto LHB peat shows persisting influence from combustion of oil-derived fuels (Fig. 5a, b, d). Unlike Pb, Zn was not added to fuels as an anti-knock agent and may not have been removed as a consequence of the Pb phase-out. We note that the Irish consumption statistics document a steady proportional increase contribution of crude oil towards combined total energy sources over the past 50 years, constituting 47% today (CSO statistics, 2015). Oil is used for residential heating in both urban and rural areas, in industry, and in the transport sector.

A striking feature in the LHB core is that the youngest four samples, deposited from the beginning of the 21st century, require a source that is even more Zn-rich to explain the Zn/Cd, V/Cd, and Cr/Cd exceeding those in PM from combustion of crude oil. This becomes most evident in the Zn/Cd vs. Cr/Cd plot (Fig. 5b) where the samples lie on a mixing line, different from that pointing to oil and petrol sources. Section 5.3 interrogates this youngest pollution source in more detail.

Figure 5.

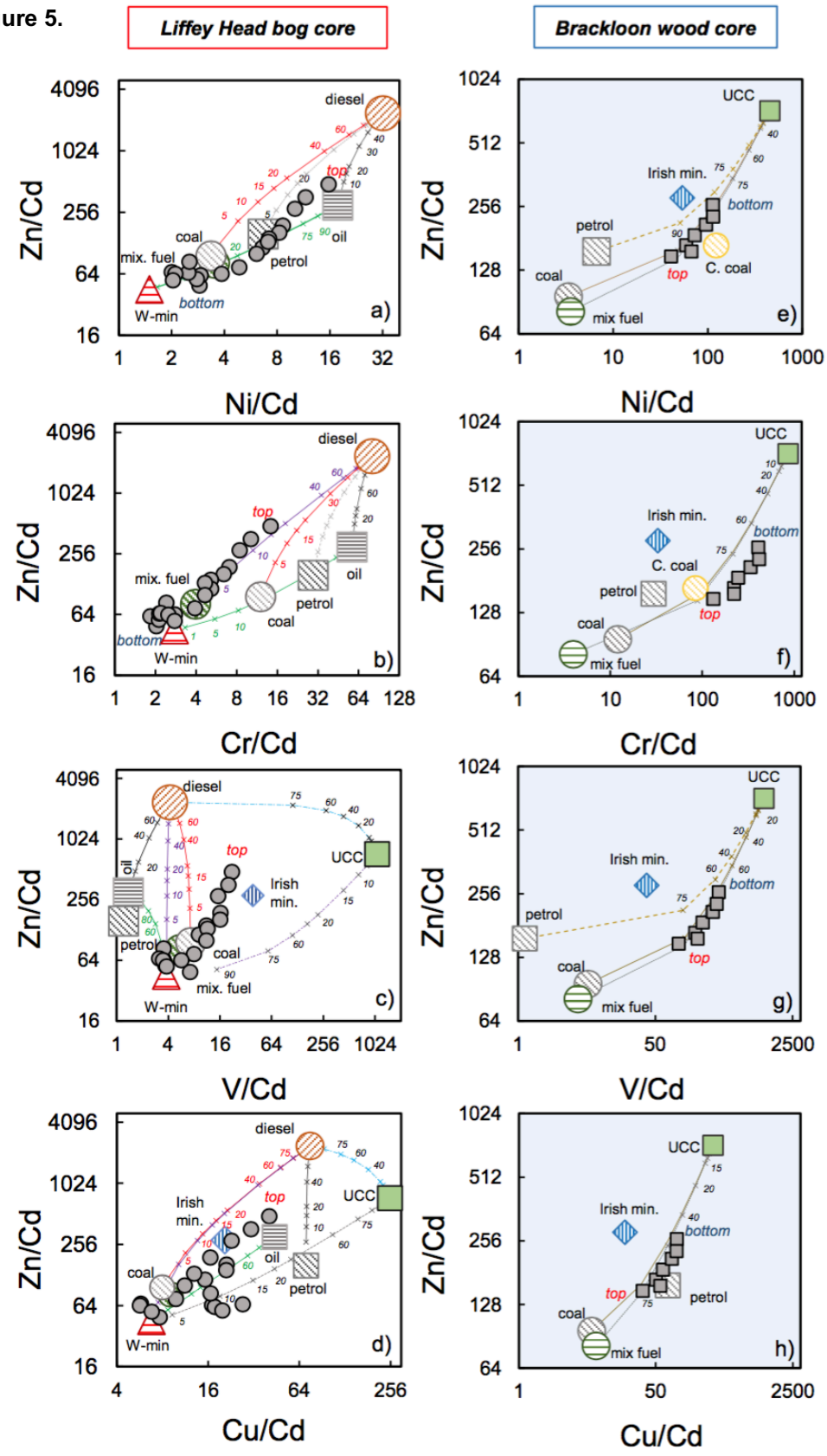


Fig. 5. Background corrected ratios of Zn/Cd vs Metal/Cd in the LHB a-d), spanning the period between1877 AD (bottom) until 2015 (top), and BW e-h) comprising the peat accumulated between 1783 AD (bottom) and 2015 (top). Shown are also the respective metal ratios for potential anthropogenic sources as listed in Table 3. Error bars are smaller than the symbols.

5.2.2. Sources of metals onto BW - rural site

The BW core shows continuous input of heavy metals such as Cd, Ni, Cr, V, and Zn for the past ca. 150 years (from ca. 10 cm from the surface) (Fig. 2h-l). Because this signal occurs within the uppermost 10 cm, the element enrichments cannot be attributed to compaction through advanced breakdown of organic matter, further supporting the presence of a real pollution signal. All samples deposited in the time-period 1861 AD until present evolve on a mixing path between a Cd-depleted end-member (Ni/Cd= 449, Zn/Cd= 725, Cr/Cd= 847) at 10 cm, and a source somewhat more enriched in Cd (yielding lower metal/Cd values) towards the top of the profile (Fig. 2h-l; Table 2). The "Cd depleted" signal which is higher at 10 cm is likely of local lithogenic origin. Several rock end-members (from rhyolite which builds up the Croagh Patrick, to river sand, shales, and carbonates) were considered to approximate the geology surrounding the Brackloon wood area. A median composition of these rocks was found to be close to the values of the upper continental crust (UCC, Cd=98ppb, McLennan et al., 2002), which is therefore considered a valid approximation to the local lithogenic signal (Fig. 5e-h). Calculated mixing curves between UCC and a range of fossil fuel sources (similar procedure as for LHB) showed that coal and mixed fuel (composed of coal-wood-peat) are the most plausible pollution end-members. The mixing lines traverse the composition of the samples and suggest increasing coal-mixed fuel component towards the surface of the profile. This is also consistent with the proportionally higher ash content at 10 cm (7-8 %) compared to the sub-surface section (4-0 cm, 2-4 %).

As detailed in Cunningham (2005), charcoal production at BW took place during the 1500s and 1600s, and aerially transported charcoal fragments were also found in the peat deposited during the 17th and 18th century; however, records of such activity for the last two centuries are not documented. From the mixing trajectories in Figures 5e-h, it is obvious that the coal signal resumes towards the surface of the bog, indicative of persisting influence from solid fossil fuels into recent times. Due to dense vegetation and relatively long time-period (ca. 200 years) since the completion of charcoal production in the direct surrounding of the forest, a resuspension of charcoal particles is unlikely. Current real-time analyses of atmospheric metal composition at the Atlantic-facing cities of Galway and Cork show that solid fuel burning is the dominant source of PM in background air in these regions of Ireland *(Aonghus McNabola, Dept. of Engineering, TCD, personal communication)*. In rural areas of Ireland, coal and peat continue to be extensively used for heating and due to cold average summer temperatures, are a year-round source of PM. We therefore propose that domestic heating is the major contributor to the relatively recent Zn contamination at the BW site, and by analogy also responsible for Cu, Cd, V, Cr, Ni pollution.

5.3. The impact of road transport on the increasing atmospheric Zn pollution in Ireland

As noted earlier, the elemental ratios of the uppermost four samples of the LHB core, representing peat accumulated since 2000 AD, depart slightly from the petrol contamination vector (Fig. 5a-d). Recently grown *Sphagnum* moss on top of LHB displays the metal enrichment sequence: Zn>Pb>Cu>V>Ni>Cr>Mo>Cd (Fig. 3). Interestingly, this relative order is analogous to those in snow (Zn>As>Cr>Pb>Cu>Ni>Cd) and lichens (Zn>Pb>Cr>As>Cu>Ni>Cd) at other European sites (e.g., Czech Republic, Francová et al., 2017). In their study, Francová et al. (2017) explained this elemental succession as stemming in part from traffic emissions, inviting a closer investigation of this source for our site. The characterisation of vehicle PM in Ireland, and especially Dublin city recently conducted by Gallagher et al. (2018) has shown that compositional variations can exist within individual classes of engine types (petrol vs. diesel, Euro Norm type of engine). Their results show that on the basis of element ratios, it is possible to discriminate between PM produced from vehicular combustion of diesel (Zn/Cd= 2386, Ni/Cd= 32, Cr/Cd= 80, V/Cd= 4.2) and PM from petrol engines/exhaust systems (Zn/Cd= 157, Ni/Cd= 7, Cr/Cd= 30, V/Cd= 1.2). When the PM deposited onto recently growing LHB *Sphagnum* moss (Fig. 5a-d) is analysed in this context, a possible influence from diesel emissions emerges. This possibility is supported by the Pb-isotope composition ($^{206}Pb/^{204}Pb$= 17.79-17.93) being close or within the reported values for diesel products ($^{206}Pb/^{204}Pb$= 17.29-17.83, Chiaradia and Cupelin, 2000; Yao et al., 2015). At the same time, the light Zn-isotope ratios of the *Sphagnum* moss ($\delta^{66/64}Zn_{JMCLyon}$= 0.18 to 0.23±0.03‰) is also in general agreement with the composition of PM in traffic dominated urban areas of e.g., north-eastern France ($\delta^{66/64}Zn_{JMCLyon}$= 0.12±0.21‰, Cloquet et al., 2006) and Barcelona ($\delta^{66/64}Zn_{JMCLyon}$= -0.25 to 0.23±0.05‰, Gonzalez et al., 2016, Fig. 6). Combined, all these tracers support recent atmospheric depositions from vehicular combustion of diesel, which are supported by Irish traffic statistics. Like many other EU countries (Cames and Helmers, 2013), Ireland has witnessed a sharp increase in the number diesel-powered vehicles. By 2013, approximately 73% of all new private cars, which made up 36% of the total fleet, as well as 99% of public coaches and busses were diesel fuelled (Alam et al., 2015). There are currently insufficient elemental and isotopic data available for whole fuel - engine - exhaust pipeline chain and emissions from diesel-powered vehicles to confidently attribute the elevated, isotopically light Zn in the topmost LHB to this source at this stage. It is, however, likely that the excess Zn could emerge from lubricant and anti-wear additives such as zinc-dialkyldithiophosphate (Johnson and Hils, 2013).

Altogether, our findings reveal that i) small-size PM (2.5), resulting from the incomplete combustion of liquid fuels in automobile engines have the potential to be

transported beyond the borders of urban areas, and that ii) fossil fuel-powered vehicles continue to represent a dominant source of metal pollution to the atmosphere despite the ban of leaded petrol.

Figure 6.

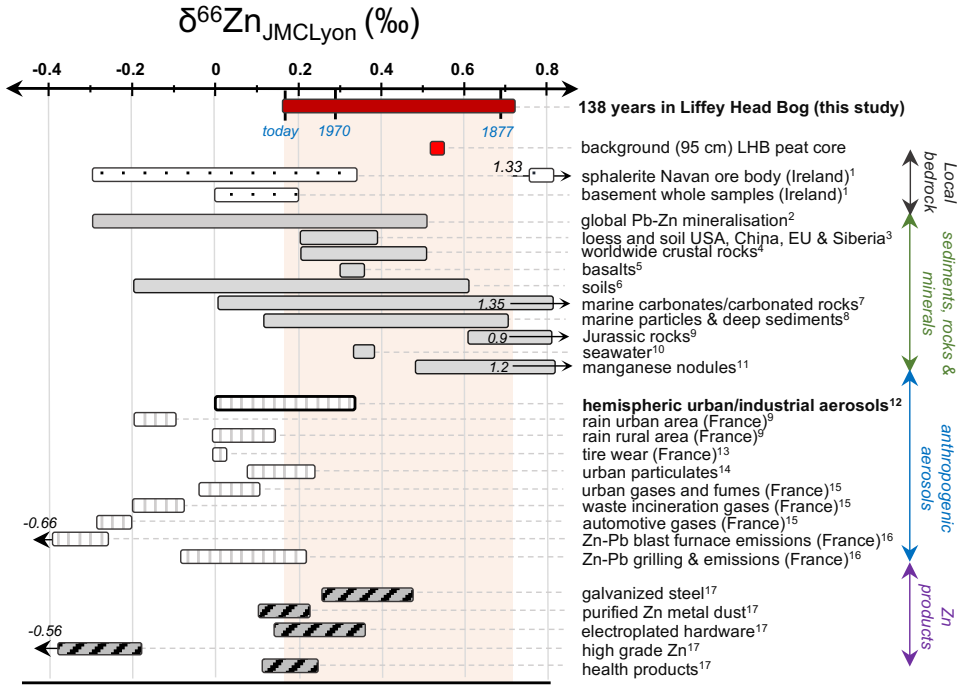


Fig. 6 Zinc isotope development in Liffey Head bog since 1877 AD until 2015, and the background sample from 94-95 cm depth together with Zn isotope data for different materials after: [1] Gagnevin et al. (2012) and Wilkinson et al. (2005a); [2] Marechal et al. (1999), Vance et al. (2016a); [3] Othman et al. (2001); [4] Cloquet et al. (2008); [5] Archer and Vance (2004), Marechal et al. (1999); [6] Viers et al (2007), Bigalke et al (2010a, 2011), Vance et al. (2016a); [7] Pichat et al. (2003); [8] Marechal et al. (1999), Viers et al. (2004); [9] Luck et al. (1999); [10] Taylor and Mclennan (1995); [11] Marechal et al. (2000); [12] Novak et al. (2016); [13] Thapalia et al. (2010); [14] Chen et al. (2008); [15] Cloquet et al. (2006), [16] Mattielli et al. (2009), [17] John et al. (2007).

5.4. Comparison to other archives of geographic relevance and identification of long-range pollution fingerprints

Recent enrichments in Zn have been identified at different pristine and historically polluted sited sites within the northern hemisphere (Fig. 1). At an interregional to hemispheric scale, defining sources of atmospheric Zn pollution from their PM deposition onto different natural archives is complicated by: i) variable histories of local metallurgical activities, which require adequate individual assessment; ii) the scarcity of other elements investigated along with the metals of interest (typically Cu, Cd, Zn, and Pb), and; iii) the analytical difficulty associated with determining Zn-isotope composition for pristine archives (e.g., Greenland, the Arctic). Owing to the restricted amount of

available data from different archives we attempt a first-order evaluation of the anthropogenic fingerprint only for the time-period 1900 AD - recent. We compiled and compared data from snow/ice from Greenland (Candelone et al., 1995); ombrotrophic peat from northern Spain (Gallego et al., 2013); montane peat from Switzerland (Shotyk et al., 2002); and "background"-peat bog from Finland - Hietajärvi (Rausch et al., 2005). In order to understand very recent enrichments, we deliberately considered sites that had not been affected by contamination from known point sources such as mining and smelting since the second half of the 20th century until present. In view of the compositional variability of traffic exhaust emissions (Gallagher et al., 2018), we opted to concentrate on a representative compositional range for PM resulting from traffic exhausts. The resulting diagrams (Fig. 7) suggest that even in purportedly pristine environments there is Zn pollution and that a Zn-rich end-member is required to explain the metal enrichment trends towards the surface.

Figure 7.

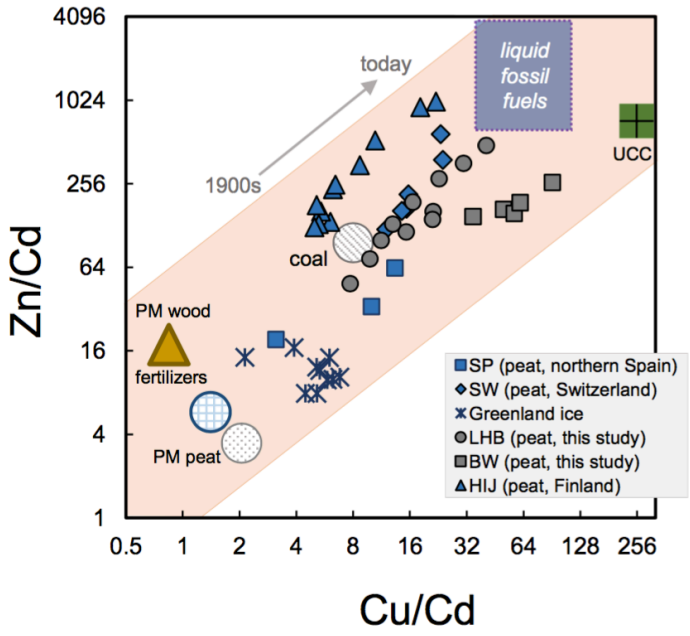


Fig. 7. Cadmium normalised Zn and Cu enrichments during the last century within LHB (filled circles) and BW (filled square) peat core along with enrichments in other peat archives from Finland (HIJ – considered pristine site, Rausch et al., 2005), Swiss Alps (Shotyk et al., 2002), and northern Spain (Gallago et al., 2013). Additional element ratios in surface ice layers from Greenland (Candelone et al., 1995) are indicated with the asterisk symbol. Metal ratios in PM from different anthropogenic sources as listed in Table 3 are shown with pattern-filled symbols. The area for liquid fossil fuel includes values for oil, petrol, and diesel from Gallagher et al. (2018). Error bars are smaller than the symbols.

Traffic fuel combustion input is most prominent in the peat bogs from Finland (Rausch et al., 2005), Switzerland (Shotyk et al., 2002), and eastern Ireland (this study). A Zn-rich end-member is it is also evident in Greenland ice (Candelone et al., 1995), peat from northern Spain (Gallego et al., 2013), and the BW peat from the west coast of Ireland (this study). Deposition of these contaminants likely occurs via long-range transport of emissions from combustion of solid fossil fuels.

6. Summary and concluding remarks

This study demonstrates that combining metal ratio data with Pb- and Zn-isotope ratios helps to identify sources of anthropogenic metal pollution onto two peat bogs. Both the near-urban Liffey Head bog (east coast) and rural Brackloon wood archive (west coast) show an upward increase in Zn enrichment accompanied by enrichment in other metals, including Cd, Cr, Ni, Cu, V, and Mo. Other studies (Cloquet et al., 2008; Pratte et al., 2013) have attributed the upward enrichment in the essential element Zn to bio-accumulation but this explanation is not supported by the correlations of Zn enrichment and isotope systematics of the LHB. Namely, within LHB, Zn-isotope ratios positively correlate with those of radiogenic isotope ratios of Pb (widely considered immobile) and with elemental metal ratios (e.g., Zn/Cd, Ni/Cd, Cr/Cd). This suggests limited overall mobility of Zn within the investigated upper section of the core. We also note that similar enrichment of Zn and associated metals is observed in snow packs and ice where bioaccumulation could not have been a factor.

We prefer to attribute the upward Zn enrichment with the lighter isotope signal ($\delta^{66/64}$Zn= 0.18 - 0.23 ±0.03‰) together with the gradual change in metal ratios, to pollution fossil fuel combustion, which has become a more dominant PM source in recent times. The upward increase in Zn depositions with a lighter Zn-isotope signature observed in other peat archives within the northern hemisphere, might therefore also reflect increasing recent pollution from fossil fuel combustion. We identified different pollution signatures that influence the respective sea borders: coal and mixed fuel combustion at the west coast of Ireland, and dominant emissions from coal, oil, petrol, and diesel in the archive at the east coast. This finding likely reflects the rural location of BW, exposed to prevailing North Atlantic winds, contrasting with and the proximity of the LHB to urban Dublin, a point source of highest population- and traffic density. This study shows that, combined with other geochemical tools, Zn enrichments and isotope compositions constitute a genuine modern pollution signal, characterising the Anthropocene.

References

Alam M. S., Duffy P., Hyde B., McNabola A. (2015) Estimation and back extrapolation of CO2 emissions from the road transport sector: Emissions in Ireland, 1990 to 2013. *WIT Trans. Ecol. Environ.* **198**, 63–75. https://doi.org/10.2495/AIR150061

Archer C. and Vance D. (2004) Mass discrimination correction in multiple-collector plasma source mass spectrometry: an example using Cu and Zn isotopes. *J. Anal. At. Spectrom*. **19**, 656. doi:10.1039/b315853e

Arimoto R., Duce R. A., Ray B. J., Tomza U. (2003) Dry deposition of trace elements to the western North Atlantic. *Global Biogeochem. Cycles* **17**. doi:10.1029/2001GB001406

Baker D. E., Senft J. P. (1995) Copper. In: Alloway BJ, editor. Heavy metals in soils. London: *Blackie Academic and Professional*, 11–37.

Barbante C., Schwikowski M., Döring T., Gaeggeler H., Schotterer U., Tobler L., van de Velde K., Ferrari C., Cozzi G., Turetta A., Rosman K., Bolshov M., Capodaglio G., Cescon P., Boutron C. (2004) Historical Record of European Emissions of Heavy Metals to the Atmosphere since the 1650s from Alpine Snow/Ice Cores Drilled near Monte Rosa. *Environmental science & technology* **38**, 4085-90. 10.1021/es049759r.

Belevi H. and Moench H. (2000) Factors determining the element behaviour in municipal solid waste incinerators. 1. Field studies, *Environ. Sci. Technol.*, **34**, 2501–2506.

Ben Othman D., Luck J. M., Grousset F., Rousseau D. D., Albarède F. (2001) Cu, Zn (and Pb) isotopes in Aerosols and Loesses. *EUG joint Assembly*, Strasbourg, France.

Bigalke M., Weyer S., Kobza J., Wilcke W. (2010) Stable Cu and Zn isotope ratios as tracers of sources and transport of Cu and Zn in contaminated soil. *Geochim. Cosmochim. Acta* **74**, 6801–6813.

Blockley S. P. E., Pyne-O'Donnell S. D. F., Lowe J. J., Matthews I. P., Stone A., Pollard A. M., Turney C. S. M., Molyneux E.G. (2005) A new and less destructive laboratory procedure for the physical separation of distal glass tephra shards from sediments. *Quat. Sci. Rev*. **24**, 1952–1960. https://doi.org/10.1016/j.quascirev.2004.12.008

Cames M. and Helmers E. (2013) Critical evaluation of the European diesel car boom - Global comparison, environmental effects and various national strategies. *Environ. Sci. Eur.* https://doi.org/10.1186/2190-4715-25-15

Candelone J-P., Hong S., Pellone C., Boutron C. F. (1995) Post-Industrial Revolution changes in large-scale atmospheric pollution of the northern hemisphere by heavy metals as documented in central Greenland snow and ice. *J. Geophys. Res.* **100**, 16605. https://doi.org/10.1029/95JD00989

Chapman J. B., Mason T. F., Weiss D. J., Coles B. J., Wilkinson, J. J. (2006), Chemical Separation and Isotopic Variations of Cu and Zn From Five Geological Reference Materials. *Geostandards and Geoanalytical Research* **30**, 5-16. doi:10.1111/j.1751-908X.2006.tb00907.x

Chen H., Savage P. S., Teng F-Z., Helz R.T., Moynier, F. (2013) Zinc isotope fractionation during magmatic differentiation and the isotopic composition of the bulk Earth. *Earth*

Planet. Sci. Lett. **369**–**370**, 34-42

Chen J., Gaillardet J., Louvat P. (2008) Zinc isotopes in the Seine river waters, France: a probe of anthropogenic contamination. *Environ. Sci. Technol*. **42**, 6494–6501. http://dx.doi.org/10.1021/es800725z.

Chiaradia M. and Cupelin F. (2000) Behaviour of airborne lead and temporal variations of its source effects in Geneva (Switzerland): Comparison of anthropogenic versus natural processes. *Atmos. Environ*. **34**, 959–971. https://doi.org/10.1016/S1352-2310(99)00213-7

Cloquet C., Carignan J., Libourel G. (2006) Isotopic Composition of Zn and Pb Atmospheric Depositions in an Urban / Periurban Area of Northeastern France. *Environ. Sci. Technol*. **40**, 6594–6600.

Cloquet C., Carignan J., Lehmann M. F., Vanhaecke F. (2008) Variation in the isotopic composition of zinc in the natural environment and the use of zinc isotopes in biogeosciences: A review. *Anal. Bioanal. Chem*. **390**, 451–463. https://doi.org/10.1007/s00216-007-1635-y.

Cloy, J.M. (2006) Chemical Records of Environmental Pollution in Ombrotrophic Peat Bogs, PhD thesis, University of Edinburgh.

Cunningham D. (2005) Brackloon: The Story of an Irish Oak Wood. COFORD; 1st edition, ISBN-10: 1902696395

Dong S., Ochoa Gonzalez R., Harrison R. M., Green D., North R., Fowler G., Weiss D. (2017) Isotopic signatures suggest important contributions from recycled gasoline, road dust and non-exhaust traffic sources for copper, zinc and lead in PM10in London, United Kingdom. *Atmos. Environ*. **165**, 88–98. https://doi.org/10.1016/j.atmosenv.2017.06.020

Drever, J.I. (1982) The Geochemistry of Natural Waters, *Surface and Groundwater Environments*, Prentice Hall Limited, New Jersey.

Dwivedi D., Agarwal A. K., Sharma M. (2006) Particulate emission characterization of a biodiesel vs diesel-fuelled compression ignition transport engine: A comparative study. *Atmos. Environ.* **40**, 5586–5595. doi:10.1016/j.atmosenv.2006.05.005.

Eggins S. M., Woodhead J. D., Kinsley L. P. J., Mortimer G. E., Sylvester P. J., McCulloch M. T., Hergt J. M., Handler M. R. (1997) Internal standardisation. *Chem. Geol*. **1**, 311–326. https://doi.org/http://dx.doi.org/10.1016/S0009-2541(96)00100-3

Francová A., Chrastný V., Šillerová H., Vítková M., Kocourková J., Komárek M. (2017) Evaluating the suitability of different environmental samples for tracing atmospheric pollution in industrial areas. *Environ. Pollut*. **220**, 286–297. https://doi.org/10.1016/j.envpol.2016.09.062

Gabrielli P. and Vallelonga P. (2015) Environmental Contaminants. https://doi.org/10.1007/978-94-017-9541-8

Gagnevin D., Boyce A. J., Barrie C. D., Menuge J. F., Blakeman R. J. (2012) Zn, Fe and S isotope fractionation in a large hydrothermal system. *Geochim. Cosmochim. Acta* **88**, 183–198. doi:10.1016/j.gca.2012.04.031

Gallagher M., Mcnabola A., Kamber B., Gill L., Ghosh B., Saniul Alam M. (2018) Chemical Fingerprints of the major sources of PM2.5 in Dublin, Ireland: A focus on Diesel Vehicle Emissions. *Int. J. Environ. Impacts* **1**, 13–24. https://doi.org/10.2495/EI-V1-N2-13-24

Gallego J. L. R., Ortiz J. E., Sierra C., Torres T., Llamas, J. F. (2013) Multivariate study of trace element distribution in the geological record of Roñanzas Peat Bog (Asturias, N. Spain). Paleoenvironmental evolution and human activities over the last 8000 cal yr BP. *Sci. Total Environ*. **454**, 16–29. https://doi.org/10.1016/j.scitotenv.2013.02.083

Gao, K., Pearce, J., Jones, J., Taylor, C. (1999) Interaction between peat humic acid and aqueous metal ions, *Environmental Geochemistry and Health* **21**, 13-26.

Hammond R. F. (1978) The Peatlands of Ireland. *Soil Survey Bulletin* **35**, 1–63.

Hansmann W. and Köppel V. (2000) Lead isotopes as tracers of pollutants in soils. *Chemical Geology* **171**, 123-144.

Herzog G. F., Moonier F., Albarede F., Berezhnoy A. A. (2009) Isotopic and elemental abundances of copper and zinc in lunar samples, Zagami, Pele's hairs, and a terrestrial basalt. *Geochim. Cosmochim. Acta* **73**, 5884-5904

Hildemann L. M., Markowski G. R., Cass G. R. (1991) Chemical Composition of Emissions from Urban Sources of Fine Organic Aerosol. *Environ. Sci. Technol*. **25**, 744–759. https://doi.org/10.1021/es00016a021

Hitzman M. W., O'Connor P. G., Shearley E., Schaffalitzky C., Beatty D. W., Allan J. R., Thompson T. (1992) Discovery and geology of the Lisheen Zn-Pb-Ag prospect, Rathdowney trend, Ireland, in Bowden, A.A., Earls, G., O'Connor, P.G., and Pyne, J.F., eds., The Irish minerals industry 1980–1990: Dublin, *Irish Association for Economic Geology*, 227–246.

John S. G., Genevieve Park J., Zhang Z., Boyle E. A. (2007) The isotopic composition of some common forms of anthropogenic zinc. *Chem. Geol.* **245**, 61–69. https://doi.org/10.1016/j.chemgeo.2007.07.024

Jones, J.M., Hao, J. (1993) Ombrotrophic peat as a medium for historical monitoring of heavy metal pollution, *Environmental Geochemistry and Health*, **15**, 67-74.

Johnson D. W., Hils J. E. (2013) Phosphate Esters, Thiophosphate Esters and Metal Thiophosphates as Lubricant Additives 132–148. Doi.org/10.3390/lubricants1040132`

Kalveram A-K. (2017) Characterising dispersed metal plumes in surficial soils and sediments in the Irish Midlands: Using isotope fingerprints to develop vectors in mineral exploration. PhD thesis, Trinity College Dublin, Ireland. http://www.tara.tcd.ie/handle/2262/82844?show=full

Kamber B. S. and Gladu A. H. (2009) Comparison of Pb purification by anion-exchange resin methods and assessment of long-term reproducibility of Th/U/Pb ratio measurements by quadrupole ICP-MS. *Geostand. Geoanalytical Res.* **33**, 169–181. doi:10.1111/j.1751-908X.2009.00911.x

Küttner A., Mighall T. M., De Vleeschouwer F., Mauquoy D., Martínez Cortizas A., Foster I. D. L., Krupp E. (2014) A 3300-year atmospheric metal contamination record from Raeburn Flow raised bog, south west Scotland. *J. Archaeol. Sci.* **44**, 1–11.

doi:10.1016/j.jas.2014.01.011

Larsen B. R., Juninnen H., Mønster J., Viana M., Tsakovski S., Duvall J. R., Norris G., Querol X. P. (2008) The Krakow Receptor Modeling Inter-Comparison Exercise; EUR 23621 EN; European Communities: Brussels.

Lepane V., Varvas M., Viitak A., Alliksaar T., Heinsalu A. (2007) Sedimentary record of heavy metals in Lake Rõuge Liinjärv, southern Estonia. *Est. J. Earth Sci.* **56**, 221–232. doi:10.3176/earth.2007.03

Livett E., Lee J., Tallis J. (1979) Lead, Zinc and Copper Analyses of British Blanket Peats. *Journal of Ecology,* **67**(3), 865-891. doi:10.2307/2259219

Luck J. M., Ben Othman D., Albarede F., Telouk P. (1999) Pb, Zn and Cu isotopic variation and trace elements in rain. In: Geochemistry of the Earth's Surface (ed. Armannsson). *Balkema*, 199–202.

Maréchal C. N., Telouk P., Albarede F. (1999) Precise analysis of copper and zinc isotopic compositions by plasma-source mass spectrometry. *Chem. Geol.* **156**, 251–273.

Maréchal C. N., Nicolas E., Douchet C., Albarède F. (2000) Abundance of zinc isotopes as a marine biogeochemical tracer. *Geochemistry, Geophys. Geosystems* 1, https://doi.org/10.1029/1999GC000029

Marx S. K., Kamber B. S., McGowan H. A., Zawadzki A. (2010) Atmospheric pollutants in alpine peat bogs record a detailed chronology of industrial and agricultural development on the Australian continent. *Environ. Pollut.* **158**, 1615–1628. https://doi.org/10.1016/j.envpol.2009.12.009

Mattielli N., Petit J. C. J., Deboudt K., Flament P., Perdrix E., Taillez A., Rimetz-Planchon J., Weis D. (2009) Zn isotope study of atmospheric emissions and dry depositions within a 5 km radius of a Pb-Zn refinery. *Atmos. Environ.* **43**, 1265–1272. https://doi.org/10.1016/j.atmosenv.2008.11.030

Mclennan S. M. (2001) Relationships between the trace element composition of sedimentary rocks and upper continental crust. *Geochemistry, Geophysics, Geosystems* 2.earthref.org/ERR/984/

Mighall T. M., Abrahams P. W., Grattan J. P., Hayes D., Timberlake S., Forsyth S. (2002) Geochemical evidence for atmospheric pollution derived from prehistoric copper mining at Copa Hill, Cwmystwyth, mid-Wales, UK. *Sci. Total Environ.* **292**, 69–80. doi:10.1016/S0048-9697(02)00027-X

Moeller K., Schoenberg R., Pedersen R. B., Weiss D., Dong S. (2012) Calibration of the New Certified Reference Materials ERM-AE633 and ERM-AE647 for Copper and IRMM-3702 for Zinc Isotope Amount Ratio Determinations. *Geostand. Geoanalytical Res.* **36**, 177–199. https://doi.org/10.1111/j.1751-908X.2011.00153.x

Moynier F., Yin Q. Z., Gillet P., Beck P., Ferroir T., Barrat J. A. and Albarède F. (2010) Volatilization induced by impacts recorded in Zn isotope composition of ureilites. *Chem. Geol.* doi:10.1016/j.chemgeo.2010.07.005.

Novak M., Sipkova A., Chrastny V., Stepanova M., Voldrichova P., Veselovsky F., Prechova E., Blaha V., Curik J., Farkas J., Erbanova L., Bohdalkova L., Pasava J., Mikova J., Komarek

A., Krachler M. (2016) Cu-Zn isotope constraints on the provenance of air pollution in Central Europe: Using soluble and insoluble particles in snow and rime. *Environ. Pollut*. **218**, 1135–1146. doi:10.1016/j.envpol.2016.08.067

Ochoa Gonzalez R., Strekopytov S., Amato F., Querol X., Reche C., Weiss D. (2016) New Insights from Zinc and Copper Isotopic Compositions into the Sources of Atmospheric Particulate Matter from Two Major European Cities. *Environ. Sci. Technol.* **50**, 9816–9824. https://doi.org/10.1021/acs.est.6b00863

Outridge P. M., Rausch N., Percival J. B., Shotyk W., McNeely, R. (2011) Comparison of mercury and zinc profiles in peat and lake sediment archives with historical changes in emissions from the Flin Flon metal smelter, Manitoba, Canada. *Sci. Total Environ.* **409**, 548–563. doi:10.1016/j.scitotenv.2010.10.041

Pacyna J. M., and Pacyna E. G. (2001) An assessment of global and regional emissions of trace metals to the atmosphere from anthropogenic sources worldwide*. Environ. Rev*. **9**, 269–298. https://doi.org/10.1139/er-9-4-269

Pey J., Querol X., Alastuey A., Forastiere F., Stafoggia M. (2013) African dust outbreaks over the Mediterranean Basin during 2001-2011: PM10 concentrations, phenomenology and trends, and its relation with synoptic and mesoscale meteorology. *Atmos. Chem. Phys*. https://doi.org/10.5194/acp-13-1395-2013

Pichat S., Douchet C., Albarede F. (2003) Zinc isotope variations in deep-sea carbonates from the eastern equatorial Pacific over the last 175 ka. *Earth Planet. Sci. Lett.* **210**, 167–178.

Pierson W. R. and Brachaczek W. W. (1974) Airborne Particulate Debris from Rubber Tires. 23, ACS Rubber Division Ecology Symposium, Toronto, Ontario, Canada (May, 1974). *Rubber Chem. Technol*. **47**, 1275

Planchon F. A. M., Boutron C. F., Barbante C., Cozzi G., Gaspari V., Wolff E. W., Ferrari CP., Cescon, P. (2002) Short-term variations in the occurrence of heavy metals in Antarctic snow from Coats Land since the 1920s. *Sci. Total Environ*. **300**, 129–142. doi:10.1016/S0048-9697(02)00277-2

Plum L. M., Rink L., Hajo H. (2010) The essential toxin: Impact of zinc on human health. *Int. J. Environ. Res. Public Health* **7**, 1342–1365. doi:10.3390/ijerph7041342

Pons M.-L., Debret B., Bouilhol P., Delacour A., Williams H. (2016) Zinc isotope evidence for sulfate-rich fluid transfer across subduction zones. *Nat. Commun*. **7**, 13794.

Pratte S., Mucci A., Garneau M. (2013) Historical records of atmospheric metal deposition along the St. Lawrence Valley (eastern Canada) based on peat bog cores. *Atmos. Environ*. **79**, 831–840. https://doi.org/10.1016/j.atmosenv.2013.07.063

Rauf M. A., Ikram M., Akhter N. (2002) Analysis of Trace Metals in Industrial Fertilizers. *J. Trace Microprobe Tech.* **20**, 79–89. https://doi.org/10.1081/TMA-120002462

Rausch N., Nieminen T., Ukonmaanaho L., Le Roux G., Krachler M., Cheburkin A. K., Bonani G., Shotyk W. (2005) Comparison of atmospheric deposition of copper, nickel, cobalt, zinc, and cadmium recorded by Finnish peat cores with monitoring data and emission records. *Environ. Sci. Technol.* **39**, 5989–5998. https://doi.org/10.1021/es050260m

Reilly E. and Mitchell F. J. (2015) Establishing chronologies for woodland small hollow and mor humus deposits using tephrochronology and radiocarbon dating. *Holocene* **25**, 241–252. https://doi.org/10.1177/0959683614557571

Rosca C., Tomlinson E. L., Geibert W., McKenna C. A., Babechuk M. G., Kamber B. S. (2018) Trace element and Pb isotope fingerprinting of atmospheric pollution sources: A case study from the east coast of Ireland, *Applied Geochemistry,* **96,** 302-326, doi: 10.1016/ j.apgeochem.2018.07.003.

Rynne C. (2015) Industrial Ireland - An Archaeology. *The Collins Press*, Cork.

Sen Gupta B., Curran M., Hasan S., Ghosh T. K. (2009) Adsorption characteristics of Cu and Ni on Irish peat moss. *J. Environ. Manage.* **90**, 954–960. doi:10.1016/j.jenvman.2008.02.012

Schindler M., Kamber B. S. (2013) High-resolution lake sediment reconstruction of industrial impact in a world-class mining and smelting center, Sudbury, Ontario, Canada. *Applied Geochemistry* **37**,102–116.

Schnitzer, M., Hansen, E.M. (1970) Organo-metallic interactions in soils: 8. An evaluation of methods for the determination of stability constants of metal-fulvic acid complexes, *Soil Science*, **109**, 333-340.

Shotyk, W. (1988) Review of the inorganic geochemistry of peats and peatland waters, *Earth-Science Reviews*, **25**, 95-176.

Shotyk W. (1996) Peat bog archives of atmospheric metal deposition: geochemical evaluation of peat profiles, natural variations in metal concentrations, and metal enrichment factors. *Environmental Rev.*, **4**, 149–183.

Shotyk W., Weiss D., Heisterkamp M., Cheburkin A. K., Appleby P. G., Adams F. C. (2002) New peat bog record of atmospheric lead pollution in Switzerland: Pb concentrations, enrichment factors, isotopic composition, and organolead species. *Environ. Sci. Technol.* **36**, 3893–3900. https://doi.org/10.1021/es010196i

Shotyk W., Krachler M., Martinez-Cortizas A., Cheburkin A. K., Emons H. (2002) A peat bog record of natural, pre-anthropogenic enrichments of trace elements in atmospheric aerosols since 12 370 14C yr BP, and their variation with Holocene climate change. *Earth Planet. Sci. Lett.* **199**, 21–37. doi:10.1016/S0012-821X(02)00553-8

Sivry Y., Riotte J., Sonke J. E., Audry S., Schafer J., Viers J., Blanc G., Freydier R., Dupre B. (2008) Zn isotopes as tracers of anthropogenic pollution from Zn-ore smelters The Riou Mort-Lot River system. *Chem. Geol.* **255**, 295–304. doi:10.1016/j.chemgeo.2008.06.038

Sonke J. E., Sivry Y., Viers J., Freydier R., Dejonghe L., André L., Aggarwal J. K., Fontan F., Dupré B. 2008. Historical variations in the isotopic composition of atmospheric zinc deposition from a zinc smelter. *Chem. Geol*. **252**, 145–157. https://doi.org/10.1016/j.chemgeo.2008.02.006

Sossi P. A., Halverson G. P., Nebel O., Eggins S.M. (2015) Combined separation of Cu, Fe and Zn from rock matrices and improved analytical protocols for stable isotope determination. *Geostand. Geoanal. Res*. **39**, 129-149

Sverdrup H. and Ragnarsdóttir K. V. (2014) Natural Resources in a Planetary Perspective.

Geochemical Perspect. **3**, 129–341. https://doi.org/10.7185/geochempersp.3.2

Swindles G., DeVleeschouwer F., Plunkett G. (2010) Dating peat profiles using tephra: stratigraphy, geochemistry and chronology. *Mires Peat* **7**, 1–9.

Tewalt S. J., Belkin H. E., SanFilipo J. R., Merrill M. D., Palmer C. A., Warwick P. D., Karlsen A. W., Finkelman R. B., Park A. J. (2010) Chemical analyses in the World Coal Quality Inventory, version 1: U.S. Geological Survey Open-File Report 2010-1196, 4 p. (http://pubs.usgs.gov/of/2010/1196/, accessed 16 May 2013).

Thapalia A., Borrok D. M., Van Metre P. C., Musgrove M., Landa E. R. (2010) Zn and Cu isotopes as tracers of anthropogenic contamination in a sediment core from an Urban Lake. *Environ. Sci. Technol.* **44**, 1544–1550. https://doi.org/10.1021/es902933y

Toutain J. P., Sonke J., Munoz M., Nonell A., Polve M., Viers J., Freydier R., Sortino F., Joron J. L., Sumarti S. (2008) Evidence for Zn isotopic fractionation at Merapi volcano, *Chem. Geol.*, **253**, 74-82

Ulrich T., Kamber B. S., Woodhead J. D., Spencer L. A. (2010) Long-Term Observations of Isotope Ratio Accuracy and Reproducibility Using Quadrupole ICP-MS. *Geostand. Geoanalytical Res*. **34**, 161–174. https://doi.org/10.1111/j.1751-908X.2010.00046.x

United Nations Environment Programme, 2017. Towards a Pollution-Free Planet 111. https://doi.org/10.1002/9780470670590.wbeog931

Vance D., Matthews A., Keech A., Archer C., Hudson G., Pett-Ridge J., Chadwick O.A. (2016) The behaviour of Cu and Zn isotopes during soil development: Controls on the dissolved load of rivers. *Chem. Geol.* **445**, 36–53. doi:10.1016/j.chemgeo.2016.06.002

Veron A., Flament P., Bertho M. L., Alleman L., Flegal R., Hamelin B. (1999) Isotopic evidence of pollutant lead sources in Northwestern France. *Atmos. Environ*. **33**, 3377-3388

Viers J., Oliva P., Nonell A., Gélabert A., Sonke J. E., Freydier R., Gainville R., Dupré B. (2007) Evidence of Zn isotopic fractionation in a soil-plant system of a pristine tropical watershed (Nsimi, Cameroon). *Chem. Geol.* **239**, 124–137. doi:10.1016/j.chemgeo.2007.01.005

Voldrichova P., Chrastny V., Sipkova A., Farkas J., Novak M., Stepanova M., Krachler M., Veselovsky F., Blaha V., Prechova E., Komarek A., Bohdalkova L., Curik J., Mikova J., Erbanova L., Pacherova P. (2014) Zinc isotope systematics in snow and ice accretions in Central European mountains. *Chem. Geol.* **388**, 130–141. https://doi.org/10.1016/j.chemgeo.2014.09.008

Weis D., Keiffer B., Maerschalk C., Barling J., de Jong J., Williams G. A., Hanano D., Pretorius W., Mattielli N., Scoates J. S., Goolaerts A., Friedman R. M., Mahoney J. B. (2006) High-precision isotopic characterization of USGS reference materials by TIMS and MC-ICP-MS. *Geochem. Geophys. Geosyst.* **7**, Q08006.

Weiss D., Shotyk W., Appleby P. G., Kramers J. D., Cheburkin A. K. (1999) Atmospheric Pb deposition since the industrial revolution recorded by five Swiss peat profiles: Enrichment factors, fluxes, isotopic composition, and sources. *Environ. Sci. Technol.* **33**, 1340–1352. https://doi.org/10.1021/es980882q

Weiss D. J., Rausch N., Mason T. F. D., Coles B. J., Wilkinson J. J., Ukonmaanaho L., Arnold T., Nieminen T. M. (2007) Atmospheric deposition and isotope biogeochemistry of zinc in

ombrotrophic peat. *Geochim. Cosmochim. Acta* **71**, 3498–3517. https://doi.org/10.1016/j.gca.2007.04.026

Weiss D. J., Mason T. F. D., Zhao F. J., Kirk G. J. D., Coles B. J., Horstwood M. S. A. (2005) Isotopic discrimination of zinc in higher plants. *New Phytol*. **165**, 703–710. doi:10.1111/j.1469-8137.2004.01307.x

Wilkinson J. J., Eyre S. L., Boyce A. J. (2005) Ore-forming processes in Irish-type carbonate-hosted Zn-Pb deposits: Evidence from mineralogy, chemistry, and isotopic composition of sulfides at the Lisheen Mine. *Econ. Geol*. **100**, 63–86. https://doi.org/10.2113/100.1.0063

Yao P. H., Shyu G. S., Chang Y. F., Chou Y. C., Shen C. C., Chou C. S., Chang T. K. (2015) Lead isotope characterization of petroleum fuels in Taipei, Taiwan. *Int. J. Environ. Res. Public Health* **12**, 4602–4616. https://doi.org/10.3390/ijerph120504602

Yatkin S. and Bayram A. (2008) Determination of major natural and anthropogenic source profiles for particulate matter and trace elements in Izmir, Turkey, *Chemosphere* **71**, 685-696

http://www.cso.ie/en/releasesandpublications/ep/p-eii/eii2016/energy/

http://www.met.ie

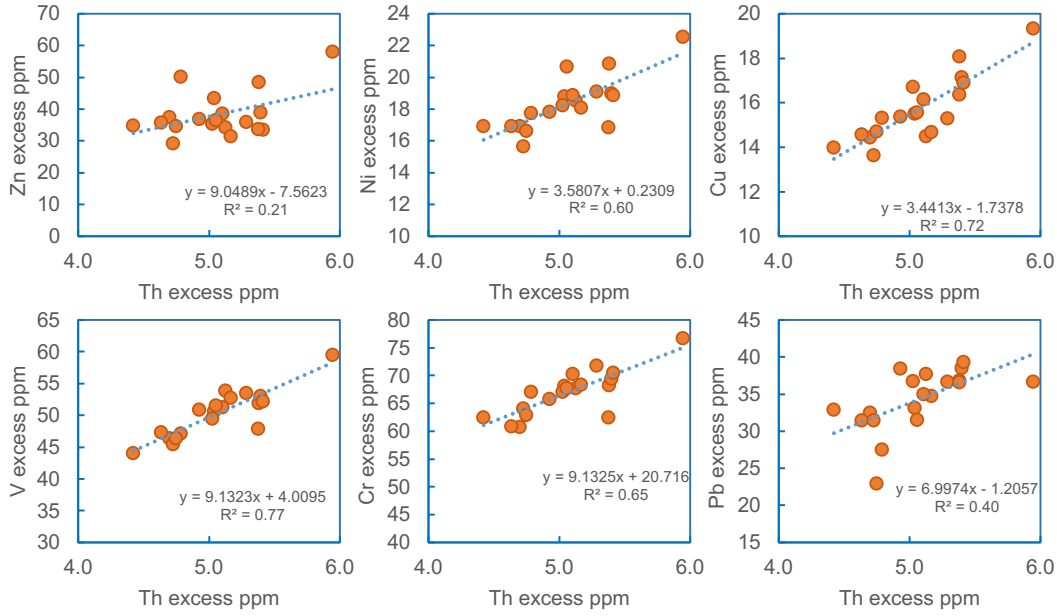
Appendix A

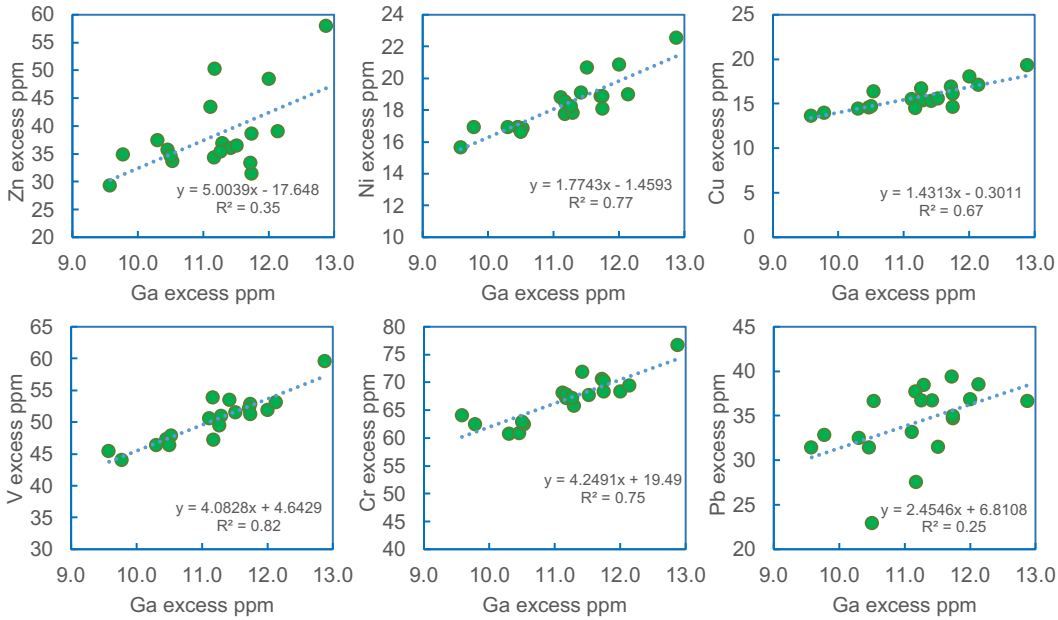
Trace element data of rock reference materials and calculated RDSs

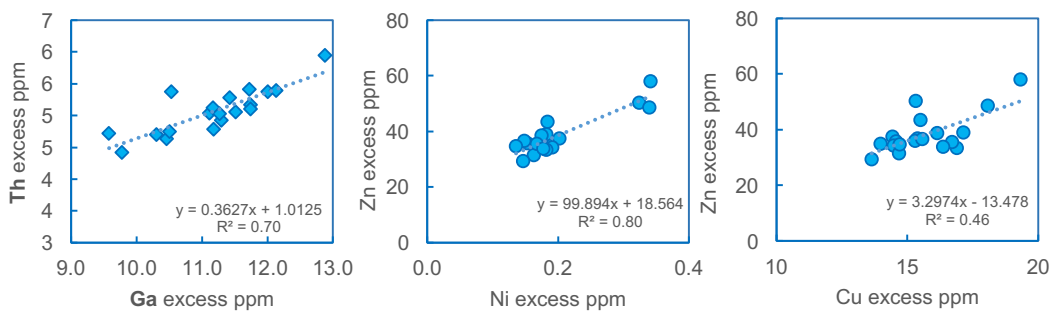
	BIR-1			BHVO-2			AGV-2		
	This expt.	*GeoRem*	*% dev*	This expt.	*GeoRem*	*% dev*	This expt.	*GeoRem*	*% dev*
Li	3141	*3206*	*2.01*	4502	*4500*	*0.03*	10723	*10800*	*0.71*
Be	89	*102*	*10.48*	982	*1076*	*8.74*	2117	*2209*	*4.15*
Sc	49874	*43210*	*13.42*	32520	*31830*	*2.17*	13261	*13110*	*1.15*
V	332601	*320600*	*3.74*	317682	*318200*	*0.16*	115908	*118500*	*2.19*
Cr	418052	*392900*	*6.40*	306538	*287200*	*6.73*	16170	*16220*	*0.31*
Co	53727	*52220*	*2.89*	45678	*44890*	*1.75*	15903	*15460*	*2.87*
Ni	169919	*168900*	*0.60*	118365	*119800*	*1.20*	18017	*18870*	*4.52*
Cu	122937	*120700*	*1.85*	130348	*129300*	*0.81*	49315	*51510*	*4.26*
Zn	65064	*70400*	*7.58*	102372	*103900*	*1.47*	81092	*86700*	*4.47*
Ga	15715	*15460*	*1.65*	21312	*21370*	*0.27*	20207	*20420*	*1.04*
As	101	*170*	*40.61*	1044	*700*	*49.21*	892	*670*	*33.15*
Rb	205	*210*	*2.47*	9157	*9261*	*1.13*	67858	*67790*	*0.10*
Sr	112910	*108600*	*3.97*	403608	*394100*	*2.41*	670724	*659500*	*1.70*
Y	15174	*15600*	*2.73*	24743	*25910*	*4.51*	18517	*19140*	*3.26*
Zr	15255	*14800*	*3.07*	174341	*171200*	*1.83*	238240	*232000*	*2.69*
Nb	561	*553*	*1.36*	18962	*18100*	*4.76*	14343	*14120*	*1.58*
Mo	43	*68*	*6.44*	7030	*4070*	*72.74*	1990	*2000*	*0.49*
Ag	36	*41*	*11.83*	125	*89*	*40.40*	129	*90*	*42.80*
Cd	53	*77*	*6.72*	129	*152*	*6.16*	130	*184*	*6.31*
In	56	*57*	*1.81*	92	*117*	*21.27*	48	*47*	*2.65*
Sn	834	*701*	*18.98*	1939	*1776*	*9.20*	2090	*1830*	*14.23*
Sb	481	*462*	*4.09*	119	*103*	*15.44*	410	*458*	*10.58*
Cs	6	*6*	*0.95*	99	*100*	*0.32*	1180	*1173*	*0.59*
Ba	6635	*6750*	*1.70*	133203	*130900*	*1.76*	1157353	*1134000*	*2.06*
La	631	*627*	*0.58*	15415	*15200*	*1.41*	38427	*38210*	*0.57*
Ce	1994	*1920*	*3.84*	38169	*37530*	*1.70*	70470	*69430*	*1.50*
Pr	395	*372*	*6.31*	5501	*5339*	*3.04*	8310	*8156*	*1.89*
Nd	2499	*2397*	*4.24*	24870	*24270*	*2.47*	30875	*30490*	*1.26*
Sm	1136	*1113*	*2.04*	6119	*6023*	*1.60*	5578	*5509*	*1.26*
Eu	531	*520*	*2.19*	2072	*2043*	*1.44*	1516	*1553*	*2.41*
Tb	376	*362*	*3.82*	946	*939*	*0.73*	638	*651*	*2.05*
Gd	1932	*1809*	*6.81*	6166	*6207*	*0.66*	4505	*4678*	*3.70*
Dy	2633	*2544*	*3.51*	5228	*5280*	*0.98*	3400	*3549*	*4.19*
Ho	600	*572*	*3.89*	1026	*989*	*3.78*	690	*682*	*1.21*
Er	1777	*1680*	*5.78*	2551	*2511*	*1.59*	1823	*1825*	*0.10*
Tm	263	*256*	*2.76*	331	*335*	*1.24*	260	*262*	*0.84*
Yb	1708	*1631*	*4.75*	1975	*1994*	*0.95*	1633	*1653*	*1.24*
Lu	255	*248*	*2.82*	280	*275*	*1.72*	246	*251*	*1.86*
Hf	609	*582*	*4.58*	4371	*4470*	*2.22*	5140	*5137*	*0.06*
Ta	39	*41*	*3.93*	1168	*1154*	*1.23*	849	*865*	*1.86*
W	7	*27*	*74.27*	194	*251*	*22.51*	455	*553*	*17.75*
Tl	1	*2*	*27.71*	21	*22*	*5.05*	275	*275*	*0.01*
Pb	2938	*3037*	*3.3*	1518.2	*1653.0*	*8.2*	12404	*13140*	*5.60*
Th	35	*32*	*8.7*	1179.6	*1224.0*	*3.6*	5959	*6174*	*3.49*
U	10	*10*	*1.8*	423.6	*412.0*	*2.8*	1863	*1885*	*1.16*

Appendix B

Binary plots of selected metals against either Th or Ga for Brackloon wood peat core from Co. Mayo. Correlations between Th and Ga, Zn vs. Ni, and Zn vs. Cu are also shown.







CHAPTER 6

Deposition of atmospheric heavy metals to the Irish peat following the Icelandic Laki 1783-1784 volcanic eruption

manuscript draft

Abstract

In this study, we examine the aerosol heavy metal composition from the perspective of the Icelandic Laki 1783-4 volcanic deposits in the Brackloon wood peat archive at the west coast of Ireland. Density based tephra separation conducted at high resolution (1 cm) throughout the uppermost 20 cm from the extracted monolith (10 x 10 x 62 cm) reveal the presence of brown and vesicular cryptotephra shards (25-80 µm) at 13-15 cm from the surface. Based on major- and trace element investigations, these cryptotephra were identified as the products of the Laki volcanic eruption. Additionally conducted trace element analyses of bulk peat from the tephra-bearing peat layer as well as above (11-12 cm) and below (16-17 cm) were used to assess whether bulk peat element enrichments occurred as a result of tephra and/or aerosol deposition. Our results show that minor excess concentrations in Ti, Fe, and V observed in the tephra-bearing peat cannot unequivocally be attributed to an addition of basaltic tephra. Moreover, a striking volcanic sulphur peak as previously reported in ice archives from Greenland and elsewhere is missing in this core. If examined in more detail, however, subtle S enrichments above background concentrations can still be identified in the tephra bearing layer and could be partially explained by contributions from volcanic aerosol deposition. Subtle enrichments in Cu, Pb, Cd, Zn in the tephra-bearing layer and particularly their ratios Cu/Cd, Pb/Cd, Pb/Zn, Cu/Zn show very good correlations with the composition of these elements deposited onto Greenland ice, suggesting a common “flavour” of the deposited metals, probably from the same Laki aerosol source. Altogether, this pioneering study shows the potential of peat-hosted trace element systematics as a new perspective in Quaternary Geology to identify aerosol heavy metal depositions following significant volcanic eruptions such as the Laki event. The potential increases by investigating peat archives with more pristine background trace element concentrations and volcanic deposits from even more recent eruptions.

1. Introduction

Given recent concerns regarding the atmospheric heavy metal pollution, it is extremely important to assess enrichments resulting from human activities in the context of contributions from natural sources. For example, it has been estimated that the amount of sulphur released to the atmosphere during a dormant volcanic period is insignificant compared to the amount of sulphur release from anthropogenic activities (Mather et al., 2003). On the other hand, the total sulphur content released to the atmosphere during a volcanic eruption surpasses anthropogenic emissions by far (Schmidt et al., 2015). In addition to sulphur contents, episodic emissions from volcanoes have been also associated with significant atmospheric release of heavy metals (Hg, Zn, Cd, Cu, Pb; Nriagu, 1989). Owing to the episodic nature of these events, the elemental diversity of volcanic plumes, as well as the globally heterogeneous distribution of volcanoes, the short- and long-term impact of emitted metals are still poorly understood.

The inventory of heavy metals released to the atmosphere from historically significant volcanic eruptions is usually investigated from their depositions in snow and ice cumulates from e.g., Greenland and the Antarctic (e.g., Fiacco et al., 1994). However, such ice core investigations are restricted to polar regions and refined climate models need to include lower latitude archives. To date however, the impact of aerosol deposition on natural archives other than snow remain largely unconstrained. Peat bogs may represent such an alternative archive.

In this study, I explore the heavy metal flavour of the aerosols transported into the Irish atmosphere following the violent Lakagígar (Laki) 1783-1784 volcanic eruption and deposited onto an actively growing woodland peat archive from the west coast (Brackloon Wood, Co. Mayo). The volcanic event is known to have severely impacted the atmosphere, inducing a significant climate change that lasted up two years after the eruption (e.g., Highwood and Stevenson, 2003; Jacoby et al., 1999; Thordarson, 2003; Witham and Oppenheimer, 2004). A drop in annual temperatures of up to 4°C resulted in crop failure and elevated mortality rates in major parts of the northern hemisphere (e.g., Grattan et al., 2003; Jacoby et al., 1999). During the course of 8 months of eruption (Sigmarsson et al., 1991), a total of 122 Tg SO_2 were emitted to the atmosphere, with estimated 60% of this released over the first six weeks of activity (Thordarson, 2003; Thordarson and Self, 1993). Along with the high amount of S, further element enrichments (e.g., Cd, Tl, Bi, Zn, Pb, Cu) have been identified in the Greenland ice segment containing the Laki tephra (e.g., Hong et al., 1996; McConnell and Edwards, 2008), which demonstrates the significant release of other trace elements as well.

The principal focus of this study is to use a peat bog archive to qualitatively assess the heavy metal composition of the aerosols introduced into the Irish atmosphere following the Laki 1783-4 volcanic eruption. The approach taken here is to identify the tephra horizon in a peat core, to separate and analyse the tephra and to undertake bulk analysis on the tephra bearing peat horizon and bracketing peat layers. In detail, the principal research questions of this pioneering investigation are:

1) Can the geochemical signature of volcanic tephra be identified in bulk peat?
2) Is a sulphur peak related to this eruption visible in the bulk peat archive?
3) Can, around the horizon of tephra occurrence, an additional geochemical signature of aerosol deposition be identified? For instance, do trace metals such as Zn, Cd, Cu, and Pb show aerosol-related enrichments in bulk peat?
4) What is the magnitude of metal contribution from this volcanic event onto the Irish landscape compared to other natural and anthropogenic sources?

2. Brackloon wood – area of investigation

A *Sphagnum* moss dominated woodland peat monolith, with the dimensions 10x10x62 cm, was extracted from the Brackloon wood which is small remnant of Atlantic oak woodland (Cunningham, 2005) located the west coast of Ireland (Co. Mayo), on the eastern slopes of Croagh Patrick. The peat core was extracted from an elevated area in a forest glade with no tree cover within a radius of 10-15 m to minimize potential disturbance by the roots. The wood area is dominated by prevailing oceanic conditions with constantly high moisture contents and precipitation, enabling continuous depositions of airborne particulates onto the surface of the recently accumulating peat and moor humus (Reilly and Mitchell, 2015). Local geology is versatile and includes both alkaline and acidic bedrocks such as Silurian sandstone, gneiss, and shale, Ordovician shale, sandstone, basalt, and rhyolite, and Carbonaceous limestone to the east.

This site was selected for this investigation due to i) prevailing clean north Atlantic winds which are responsible for volcanic tephra and aerosol transport from the active volcanoes of Iceland, and ii) a previous identification of volcanic tephra corresponding to the Laki 1783-4 eruption by Reilly and Mitchell (2015).

3. Anthropogenic activity in the area relevant for this study

From the 16th to the 18th centuries, the area around and inside Brackloon wood was known for charcoal production necessary for iron smelting at Knappagh, not far away

from the forest (Cunningham, 2005). This is evidenced today from charcoal fragments present in soil near the charcoal production site at Brackloon, and also reported by (Reilly and Mitchell, 2015). Charcoal production ceased at the end of the 18th century, as it did the iron smelting activity situated in close vicinity to the forest.

It is also reported that: "Until the middle of the last century, lime was burned by most farmers and was applied to the land to improve the soil and used for whitewashing buildings. The abundance of limekilns is evident from the first Ordnance Survey of 1839" (Cunningham, 2005, based on The Bogs Commissioners' report of the area (1813/14) states). It remains however unclarified whether only the surrounding bogs (e.g., Lough Greney bog to the east) were subjected to this type of fertilization, or also the area inside Brackloon wood.

Elements which might be added to the bog as a result of these volcanic activities are heavy metals: Pb, Cu, Ni, Mo, Zn, V - associated with coal production, as well as Ca, Sr, Mg - associated with the lime application to fertilize the soil and peat.

4. Methodology

4.1. Tephra separation

In order to determine whether tephra is present in the extracted monolith, and to identify the tephra bearing horizon in this core, a separation from the peat matrix and mineralogical components is required. Glass shards were extracted from the peat using the heavy liquid flotation method of Blockley et al. (2005). This method was selected to avoid any possible chemical alteration that may arise from the alternative acid digestion technique (Blockley et al., 2005). This is especially important for cryptotephra (small shards between 25 and 80 µm diameter) which display a high surface to volume ratio (Blockley et al., 2005; Dugmore and Newton, 1992). Extracted shards for electron probe, energy dispersive X-ray spectroscopy, and LA-ICP-MS microanalyses were mounted on 1-inch epoxy resin pucks and exposed at the surface by careful polishing.

4.2. Major element investigation via EDS-SEM and WDS-EMPA

Major and minor element chemistry of individual tephra shards was determined using two different techniques: a wavelength-dispersive electron microprobe (WDS-EMPA) and an energy dispersive spectrometer coupled with a scanning electron microscope (SEM-EDS). WDS-EMPA is typically the preferred method due to its lower detection limits, but not always possible due to large beam diameter (>10 µm). EDS is thus a complementary method (ca. 0.02 and 0.2 respectively). Details of the two individual methods are given below:

4.2.1. In-situ major oxide analysis via WDS-EMPA

Major oxide and minor element chemistry of individual volcanic shards was determined in January 2016 using a wavelength-dispersive JEOL 8600 electron microprobe at the RLAHA laboratory, University of Oxford, UK. A beam accelerating voltage of 15 kV was applied with a 6 nA current and a beam diameter of 10 μm. Prior measurements, the instrument was calibrated with a suite of appropriate mineral standards, Smithsonian glasses (Jarosewich, 2002): microcline (Si), augite (Mg), pyrope (Ca, Fe and Mn), anorthoclase (Al, Na and K), apatite (P), rutile (Ti) and synthetic Cr_2O_3 and NiO oxides (Cr and Ni, respectively). Peak count times were 30 s for most elements and 10s for Na. To account for accuracy, synthetic glass standards (MPI-DING suite; Jochum et al., 2006) from the Max Plank institute we analysed as unknowns interleaved between the tephras. These included mafic (GOR128-G - komatiite), through intermediate (StHs6/80-G - andesite) to felsic (ATHO-G - rhyolite) glasses. Obtained glass data was not normalised to 100%, but lower totals up to 97% were accepted due to the high volatile content of the tephras. Errors were typically < ± 0.7% RSD for Si; and ~ ±3% for other major elements.

4.2.2. In-situ major element analysis via FE-SEM-EDS

Major element analyses and backscattered electron images of tephra separates were obtained in June 2016 at the iCRAG labs at Trinity College Dublin. We used a Field Emission Scanning Electron Microscope (FE-SEM) Tescan MIRA XMU instrument equipped with an Oxford X-Max 80 mm^2 Energy Dispersive Spectrometer (EDS) detector running Oxford INCA X-ray microanalysis software. Analyses were performed on carbon-coated resin mounts under high vacuum conditions using an accelerating voltage of 20 kV. Operating conditions were 370-485 pA beam current and 18.5 mm working distance; X-rays were acquired for 30 s per spot, reaching >500,000 counts. Beam current drift was controlled by frequent analysis of cobalt and matrix correction was made using an Oxford-PP (ZAF-type; Z: atomic number, A: absorption, F: fluorescence) procedure. Prior analyses, calibration was finely optimised for glass analysis with Smithsonian microbeam standards (Jarosewich, 2002) as describes above. Precision and accuracy were monitored at the beginning of each analytical session and with sample exchanges, by analysing Smithsonian microbeam standard basaltic and rhyolitic glasses (Jarosewich, 2002) as well as MPI-DING reference glasses from the Max-Planck Institute (Jochum et al., 2006). Relative standard deviation was better than 2% for SiO_2, MgO, Al_2O_3, FeOT, CaO, and Na_2O; and accuracy was better than 5% for elements compared to the published Laki 1783-1784 basaltic tephra values of Thordarson et al. (1996). Major oxide trace element data is presented on Table 1.

4.3. Trace element investigation of tephra via LA-ICP-MS

The analytical set-up comprised a Teledyne Photon Machines Analyte G2 193 nm Excimer laser ablation system equipped with a HelEx II 2-volume cell, coupled to a Thermo Scientific iCAP Qc ICP-MS. Samples were ablated using a frequency of 10 Hz, a laser energy of 2.75 J cm^{-2} and square spots of 5 and 10 µm. The follow isotopes were measured with dwell times of 20 ms except where indicated in parentheses: ^{29}Si, ^{27}Al, ^{44}Ca, ^{48}Ti, ^{51}V, ^{66}Zn, ^{85}Rb, ^{88}Sr, ^{89}Y (40), ^{90}Zr, ^{93}Nb, ^{133}Cs (30), ^{138}Ba, ^{139}La, ^{140}Ce, 141Pr, ^{146}Nd (30), ^{147}Sm (30), ^{153}Eu (40), ^{157}Gd (40), ^{163}Dy (40), ^{166}Er (40), ^{172}Yb (40), ^{178}Hf (30), ^{181}Ta (40), ^{207}Pb, ^{232}Th (30), ^{238}U. Only samples that yielded >5 seconds of signal were considered. Instrument tuning was carried out by rastering NIST612 using an 85 µm square spot, 10 Hz repetition rate, 40 $\mu m s^{-1}$ scan speed and 2.75 J cm^{-2} laser energy. The intensities were optimized at ^{7}Li, ^{43}Ca, ^{140}Ce, ^{232}U, ^{238}Th, and intensities for ThO were minimised to <0.1%. Data were processed using iolite software (Paton et al., 2011). Calibration was carried out using NIST612 (Jochum et al., 2011) and the data reduction scheme 'X_Trace_Elements_IS' with ^{29}Si as the internal standard. The MPI-DING glasses StHs6/80-G, KL2, GOR132-G and KL2-G (Jochum et al., 2006) were analysed as secondary reference standards to monitor accuracy and precision. Relative standard deviations were <5% for all elements. In general, a lower accuracy was obtained for the major elements Ti, Fe, and the trace element Pb with this technique (>20%). Therefore, the concentrations for Ti and Fe were calculated from the major oxide data obtained with WDS-EMPA and SEM-EDS. Trace element concentrations were within the reported values of Jochum et al. (2006), with external reproducibility ranging between 2 and 8%, demonstrating the good quality of this dataset.

Table 1. Major oxide composition (wt. %) of basaltic shards recovered from the Brackloon wood peat core analysed with FE-SEM-EDS and WDS-EMPA

	Na_2O	MgO	Al_2O_3	SiO_2	P_2O_5	K_2O	CaO	TiO_2	Cr_2O_3	MnO	FeOT	NiO	*Total*	*Comments*
Laki/1	2.8	5.4	13.9	50.4	0.39	0.45	9.4	2.5	0.02	0.2	13.8	0.02	*99.4*	*FE-SEM-EDS*
Laki/2	2.7	5.3	13.8	50.1	0.36	0.46	9.2	2.6	0.01	0.2	13.9	0.01	*99.1*	*FE-SEM-EDS*
Laki/3	2.8	5.4	14.0	50.5	0.37	0.45	9.4	2.6	0.04	0.2	14.2	0.02	*98.8*	*FE-SEM-EDS*
Laki/4	2.8	5.5	13.8	50.3	0.35	0.50	9.4	2.6	0.01	0.2	14.2	0.03	*99.6*	*FE-SEM-EDS*
Laki/5	2.7	5.3	13.9	50.2	0.38	0.44	9.3	2.6	0.03	0.2	13.7	0.04	*99.1*	*FE-SEM-EDS*
Laki/6	2.8	5.4	13.2	50.6	0.37	0.43	9.6	3.1	0.02	0.2	13.8	0.04	*98.7*	*FE-SEM-EDS*
Laki/7	2.7	5.3	13.0	50.2	0.37	0.45	9.5	3.0	0.03	0.2	13.7	0.04	*99.3*	*FE-SEM-EDS*
Laki/8	2.4	5.2	12.9	50.2	0.36	0.42	9.4	3.0	0.04	0.2	13.8	0.03	*99.6*	*FE-SEM-EDS*
Laki/9	2.8	6.9	13.0	50.3	0.38	0.43	9.6	3.1	0.03	0.3	14.0	0.03	*99.7*	*FE-SEM-EDS*
Laki/6-b	2.89	5.33	13.05	49.74	0.32	0.43	9.85	2.89	n.a.	0.20	13.39	n.a.	*98.1*	*WDS-EMPA*
minimum	2.4	5.2	12.9	49.9	0.2	0.42	9.2	2.5	0.0	0.2	12.2	0.01		
maximum	2.9	6.9	14.0	50.7	0.4	0.50	9.7	3.1	0.0	0.3	14.2	0.04		
average	***2.75***	***5.42***	***13.41***	***50.34***	***0.35***	***0.44***	***9.60***	***2.83***	***0.02***	***0.22***	***13.8***	***0.03***		***this study***
average	2.77	5.40	13.20	49.94	0.32	0.45	9.90	3.05		0.22	14.2	2.77	*99.5*	*Thordarson et al. (1996)*
average	2.26	5.29	12.72	49.81	0.35	0.50	9.63	2.95		0.22	13.5	2.26	*97.2*	*Reilly and Mitchell (2015)*

n.a. means below detection limit

Table 2. LA-ICP-MS trace element data (ppm) obtained for individual shards extracted from the Brackloon wood peat monolith

	Al	*2SE*	*LOD*	**Ca**	*2SE*	*LOD*	**Ti**	*2SE*	*LOD*	**V**	*2SE*	*LOD*	**Zn**	*2SE*	*LOD*	**Rb**	*2SE*	*LOD*
Laki/1	**68200**	*6500*	*4.5*	**69600**	*5600*	*340*	**2290**	*250*	*0.073*	**491**	*79*	*0.53*	**203**	*47*	*10*	**10.9**	*2*	*0.11*
Laki/3	**75100**	*4300*	*6.3*	**75100**	*5200*	*450*	**2410**	*160*	*0.11*	**472**	*45*	*0.66*	**111**	*49*	*16*	**9.9**	*1.5*	*0.13*
Laki/7	**70500**	*5000*	*5.5*	**70300**	*7900*	*480*	**2300**	*360*	*0.13*	**466**	*66*	*0.61*	**125**	*30*	*15*	**9.1**	*1.3*	*0.21*
Laki/8	**54400**	*9600*	*4.2*	**49100**	*3600*	*410*	**1610**	*100*	*0.08*	**319**	*18*	*0.68*	**91**	*44*	*12*	**8.5**	*2.5*	*0.12*
Laki/9	**67500**	*4700*	*4.5*	**63910**	*970*	*300*	**2130**	*290*	*0.074*	**437**	*81*	*0.53*	**167**	*62*	*11*	**8.8**	*1.8*	*2.1*
	Sr	*2SE*	*LOD*	**Y**	*2SE*	*LOD*	**Zr**	*2SE*	*LOD*	**Nb**	*2SE*	*LOD*	**Cs**	*2SE*	*LOD*	**Ba**	*2SE*	*LOD*
Laki/1	**240**	*45*	*0.036*	**42**	*12*	*0.034*	**198**	*35*	*0.095*	**20.9**	*3.6*	*0.044*	**0.124**	*0.068*	*0.042*	**101**	*14*	*0.061*
Laki/3	**246**	*26*	*0.062*	**40.8**	*4.7*	*0.047*	**210**	*24*	*0.071*	**21.4**	*2.6*	*0.062*	**0.169**	*0.087*	*0.068*	**100.2**	*5.9*	*0.1*
Laki/7	**228**	*24*	*0.066*	**38**	*4.2*	*0.038*	**175**	*15*	*0.15*	**19.4**	*1.9*		**0.106**	*0.099*	*0.089*	**92**	*16*	*0.091*
Laki/8	**178**	*10*	*0.079*	**31.9**	*2.3*	*0.037*	**137**	*15*	*0.12*	**14**	*1.3*	*0.059*	**0.093**	*0.055*	*0.042*	**68**	*12*	*0.062*
Laki/9	**205**	*13*	*0.036*	**35.4**	*5.8*	*0.03*	**180**	*23*	*0.078*	**16.8**	*2.8*	*0.035*	**0.076**	*0.092*	*0.031*	**85**	*10*	
	La	*2SE*	*LOD*	**Ce**	*2SE*	*LOD*	**Pr**	*2SE*	*LOD*	**Nd**	*2SE*	*LOD*	**Sm**	*2SE*	*LOD*	**Eu**	*2SE*	*LOD*
Laki/1	**16.2**	*2.2*	*0.037*	**39.7**	*4.4*	*0.044*	**5.7**	*0.87*	*0.045*	**25.3**	*5.9*	*0.12*	**7.3**	*1.5*	*0.19*	**2.19**	*0.44*	*0.064*
Laki/3	**14.54**	*0.69*	*0.11*	**39.2**	*4.4*	*0.058*	**5.09**	*0.79*	*0.024*	**27.2**	*3.2*	*0.22*	**6.2**	*1.6*	*0.2*	**2.48**	*0.37*	*0.074*
Laki/7	**13.2**	*2.1*	*0.07*	**37.1**	*9.3*	*0.068*	**5.3**	*1.4*	*0.043*	**24.1**	*5.4*	*0.17*	**6.3**	*1.7*	*0.33*	**1.98**	*0.55*	*0.051*
Laki/8	**11.4**	*2.1*	*0.059*	**24.1**	*1.4*	*0.051*	**3.66**	*0.37*	*0.043*	**19.2**	*2.3*	*0.17*	**5.6**	*1.5*	*0.24*	**1.83**	*0.6*	*0.061*
Laki/9	**14.3**	*1.7*	*0.059*	**36.6**	*3.3*	*0.024*	**4.14**	*0.38*	*0.041*	**21.7**	*1.9*	*0.18*	**5.09**	*0.87*	*0.12*	**1.95**	*0.27*	*0.039*
	Gd	*2SE*	*LOD*	**Dy**	*2SE*	*LOD*	**Er**	*2SE*	*LOD*	**Yb**	*2SE*	*LOD*	**Hf**	*2SE*	*LOD*	**Ta**	*2SE*	*LOD*
Laki/1	**8.8**	*2*	*0.17*	**8.1**	*2.1*	*0.088*	**4.21**	*0.67*	*0.054*	**4.19**	*0.84*	*0.13*	**4.71**	*0.56*	*0.061*	**1.03**	*0.13*	*0.028*
Laki/3	**8.9**	*1.6*	*0.15*	**8.29**	*0.94*	*0.19*	**4.28**	*0.97*	*0.092*	**4.1**	*0.92*	*0.17*	**4.32**	*0.95*	*0.13*	**1.138**	*0.067*	*0.028*
Laki/7	**6.1**	*1.7*	*0.26*	**6.5**	*1.7*	*0.1*	**3.4**	*0.92*	*0.097*	**2.9**	*1*	*0.13*	**4.6**	*1.5*	*0.14*	**1.15**	*0.41*	*0.022*
Laki/8	**4.45**	*0.88*	*0.19*	**5.13**	*0.75*	*0.12*	**2.24**	*0.6*	*0.073*	**1.98**	*0.69*	*0.1*	**3.58**	*0.17*	*0.076*	**0.893**	*0.045*	*0.032*
Laki/9	**7.1**	*1*	*0.16*	**7.1**	*2.4*	*0.095*	**3.07**	*0.47*	*0.042*	**3.51**	*0.64*	*0.099*	**3.91**	*0.95*	*0.08*	**1.21**	*0.32*	*0.014*
	Pb	*2SE*	*LOD*	**Th**	*2SE*	*LOD*	**U**	*2SE*	*LOD*									
Laki/1	**1.31**	*0.6*	*0.27*	**1.16**	*0.21*	*0.026*	**0.49**	*0.18*	*0.035*									
Laki/3	**1.48**	*0.54*	*0.36*	**1.34**	*0.42*	*0.04*	**0.32**	*0.15*	*0.051*									
Laki/7	**1.52**	*0.72*	*0.32*	**1.1**	*0.43*	*0.032*	**0.31**	*0.13*	*0.05*									
Laki/8	**0.55**	*0.29*	*0.4*	**0.9**	*0.13*	*0.036*	**0.212**	*0.045*	*0.053*									
Laki/9	**0.71**	*0.19*	*0.28*	**1.12**	*0.28*	*0.04*	**0.353**	*0.067*	*0.033*									

4.4. Trace element investigation of peat via Qs-ICP-MS

Trace element data on bulk peat subsamples along the core was performed at Trinity College Dublin, Ireland, via solution quadrupole ICP-MS (Qs-ICP-MS) measurement using a Thermo Scientific iCAP-Qs. In preparation for trace element investigations, ca. 10 g of wet peat sample from selected depths was dried at 105ºC overnight. The dried samples were then combusted in inert glass crucibles for 8 hours at 450ºC in a muffle furnace to destroy organic molecules. A homogenised fraction of the combusted peat sub-sample (between 10 and 30 mg) was transferred into 15 ml Teflon beakers into which 1 ml of a HF-HNO_3 (4:1) mixture was added. The beakers were left to digest on the hotplate at 150ºC for 72 h and agitated at least once every 24 h. After the evaporation at 110ºC the residue was converted with 1 ml of 50% HCl to reduce the organic components, and resulting fluorides were further eliminated by treatment with 2x1 ml conc. HNO_3 with evaporation to dryness between each step. Finally, the converted residue was taken up in 3 ml of 20% HNO_3 and diluted to a 30 ml stock solution, with dilution factors ranging between 200 and 1800, depending on the initial mass of sample weighed. The ICP-MS analyses followed the experimental design of Eggins et al. (1997) with modifications described in Kamber et al. (2003). For analyses, 2 ml centrifuge tubes were prepared containing a respective aliquot from each sample (depending on the dilution factor of the stock solution) which was gravimetrically diluted with 2% HNO_3. To each solution, 0.2 g of internal standard containing a mixture of 10.6 ppb ^{6}Li, 4.4 ppb each ^{103}Rh, ^{187}Re, and ^{209}Bi and 1.5 ppb ^{235}U was added to cover the full mass range of analysed elements and ionization potentials. In general, the addition of the internal standard mix serves for the correction of matrix-related signal suppression and instrumental drift during the measurement session. Oxide interferences were corrected according to Ulrich et al. (2010), while the W-2 standard was used for calibration. The USGS rock standards AGV-2, BIR-1, and BHVO-2 were used to monitor external accuracy of the trace element data. These were treated in the same way as the peat samples during digestion and were analysed interleaved as unknowns with the batch of samples. Internal errors were all better than the external reproducibility, measured as the relative standard deviation (RSD) for multiple analyses of reference materials. For metals that are homogeneous in second-generation USGS reference materials, the RSD was <3%, for metals that suffer from nugget-effect contamination (e.g. Weis et al., 2006; Kamber and Gladu, 2009) the reproducibility was inferior (>10%). This was observed for Be, As, Ag, W, Tl, Sn, during this experiment. These elements are not discussed in this study. All element concentrations (expressed as ng/g) are shown in Table 3.

Table 3. Trace element concentrations (ng/g), C-N-S concentrations (%) and physical parameters for peat sub-samples from the Brackloon wood peat monolith

sample ID	BW2.1	BW2.3	BW2.5	BW2.7	BW2.9	BW2.11	BW2.15	BW2.18	BW2.19	BW2.20	BW2.21	BW2.22	BW2.23	BW2.24	BW2.25	BW2.26	BW2.27	BW2.28	BW2.31	BW2.34	BW2.42
depth [cm]	0.5	2.5	4.5	6.5	7.5	10.25	11.5	12.25	12.5	12.75	13	13.25	13.5	13.75	14	14.25	14.5	14.75	15.5	16.25	19.5
moisture (%)	80.91	80.44	81.57	80.36	77.39	75.72	74.34	73.16	72.73	73.1	72.4	72.5	71.62	73.12	73.01	73.61	73.12	72.62	71.32	69.74	65.51
loss on ignition (%)	97.26	87.41	87.61	88.14	91.23	88.35	91.01	91.22	95.3	88.93	98.05	97.78	96.14	83.63	91.3	82.5	82.45	91.83	94.43	85.48	86.07
N (%)	1.8649					1.624		1.328			1.295		1.4844	1.4806		1.4408	1.3994	1.4265	1.2451	1.3591	1.2594
C (%)	34.015					24.377		20.832			20.247		21.884	21.39		20.722	20.405	20.042	18.97	19.536	18.688
S (%)	0.33					0.386		0.371			0.372		0.391	0.392		0.389	0.391	0.386	0.379	0.39	0.4
Li	19287	17491	17940	20674	18322	16842	15753	16757	17341	18975	18525	18547	17813	15605	18079	18032	17207	16255	18601	16053	13402
Be	1635	1357	1481	1765	1607	1463	1397	1471	1523	1668	1683	1675	1479	1354	1541	1508	1615	1586	1577	1557	1231
Sc	9929	9269	9710	10533	9407	8474	8177	8644	9166	9912	9657	9685	9569	8165	9459	9650	9311	8882	9364	8755	7092
V	53150	47182	51899	59553	50597	46376	44042	47302	50936	53089	53883	53480	52801	45416	52219	51295	49485	47888	51507	46383	38320
Cr	70695	67131	68312	76693	68172	60728	62516	60887	65830	69472	67770	71837	68338	64059	70556	70273	67136	62436	67739	62881	50573
Co	10015	7845	7882	7380	5437	4776	4388	4585	4560	4904	4790	4871	4919	4206	4879	4964	4620	4448	5900	4516	3835
Ni	21696	17757	20854	22535	18810	16928	16931	16917	17833	18990	18558	19104	18100	15646	18889	18885	18233	16838	20665	16634	13453
Cu	18888	15325	18088	19330	15505	14439	13988	14579	15380	17147	14488	15294	14679	13639	16895	16143	16710	16365	15564	14720	12575
Zn	80147	50247	48475	58028	43465	37406	34895	35717	36873	39007	34290	36016	31430	29295	33425	38597	35442	33737	36474	34609	26075
Ga	11891	11180	12008	12882	11118	10304	9781	10462	11296	12142	11174	11424	11747	9582	11726	11748	11268	10535	11519	10506	8684
As	1299	1127	1304	1408	1140	1071	1053	1034	1139	1244	1193	1215	1168	998	1232	1140	1185	1154	1115	1053	810
Rb	76983	76000	76997	84068	69339	63345	60956	64730	68620	72749	69224	69828	70914	58129	68057	66147	65925	59856	61317	60240	50405
Sr	160431	139791	177093	172559	123302	106877	101859	100210	108426	116096	108054	112365	117969	96577	111855	107716	108155	102223	105380	102291	83532
Y	45111	42532	47459	50816	46774	41046	40940	41833	47745	50315	49253	51096	50881	44949	52837	49229	52580	49375	49314	49112	39944
Zr	95414	99512	102922	120134	92750	83408	83291	88163	94205	97815	97447	102209	104635	84356	96677	89122	94502	88193	100419	98324	79589
Nb	10544	10419	10945	12023	10311	9536	9270	9399	10689	10890	10399	10715	10694	9420	10975	10771	10322	9617	10628	10117	8382
Mo	836	739	838	878	543	450	409	399	448	447	432	452	435	385	459	433	421	409	391	349	230
Ag	679	651	802	876	586	524	531	569	661	621	599	690	642	615	838	659	670	684	724	469	323
Cd	553	325	341	342	185	203	174	154	181	183	192	175	164	148	183	176	168	179	149	136	92
In	60	54	56	55	55	42	46	46	64	64	46	47	57	52	51	47	57	57	47	43	49
Sn	5786	4887	4665	3303	5749	2166	3060	3433	8233	7047	1923	2010	5425	5092	2442	7120	2519	6390	1877	1601	7685
Sb	486	395	486	514	414	410	400	425	496	508	491	484	429	417	456	423	458	461	380	368	283
Cs	6346	6354	6800	7334	5692	5187	4796	4884	5530	5433	5497	5500	5631	4760	5410	5673	5235	4939	4974	4873	4653
Ba	428224	400589	419386	461880	392954	362635	344881	367358	400057	410074	398354	399380	408640	337410	405046	385844	396906	354895	389272	363761	282764
La	60215	53229	60274	66820	58400	52189	51115	52070	58648	62321	63346	63986	62525	60654	63048	63163	61671	60191	59213	58424	47989
Ce	80265	71678	79771	84327	74215	65704	64538	67378	74430	84564	135631	111841	111401	97816	90218	78414	80682	71931	71910	72246	53846
Pr	13322	12921	13609	15249	13131	11999	11722	12063	13378	13899	13351	14865	13804	12306	15035	13641	14578	13518	14327	13571	10314
Nd	53058	46483	51450	55955	50398	44990	44761	45310	49668	52684	52608	53695	55318	48840	55122	54825	52315	51789	50469	49974	40660
Sm	9260	8693	9690	10173	9311	8291	8143	8258	9069	9649	9589	9747	9575	8415	9965	9602	9494	8978	9161	8821	7160
Eu	1997	1826	2024	2121	1956	1728	1709	1722	1877	1998	2064	2040	2115	1877	2125	2022	2068	1912	1952	1859	1514
Tb	1217	1121	1185	1286	1187	1045	1029	1047	1134	1195	1232	1216	1229	1081	1249	1245	1227	1185	1192	1159	927
Gd	8626	7633	8501	9123	8089	7627	7195	7353	8565	8814	8889	8588	8694	7754	8892	8733	8874	8077	8362	8035	6187
Dy	7050	6576	6887	7399	6863	6172	5914	6105	6787	7228	7151	7386	7269	6463	7399	6928	7206	6827	7208	6758	5447
Ho	1445	1326	1473	1572	1397	1285	1215	1293	1410	1485	1524	1470	1542	1283	1545	1537	1511	1419	1453	1395	1085
Er	3817	3724	3985	4372	3767	3459	3333	3527	3815	4009	4157	4139	4286	3790	4393	4307	4374	4004	4151	3925	3227
Tm	582	541	591	630	556	519	488	528	572	593	617	615	620	536	617	596	622	593	611	577	475
Yb	3488	3348	3637	4095	3598	3286	3138	3289	3574	3719	3879	3750	3876	3361	3819	3725	3772	3603	3801	3449	2803
Lu	548	478	540	598	515	469	461	486	532	547	566	541	558	477	580	565	554	533	528	526	438
Hf	2500	2732	2678	3118	2494	2241	2196	2475	2508	2480	2583	2725	2708	2273	2553	2412	2659	2375	2760	2558	2184
Ta	731	672	692	798	675	639	596	633	704	718	729	706	719	618	707	695	683	631	678	653	555
W	857	744	752	848	721	675	643	670	723	741	734	737	741	683	751	749	697	658	730	698	543
Tl	687	636	714	771	657	604	581	585	642	677	658	659	658	552	664	648	624	594	623	548	439
Pb	34277	27526	36821	36646	33188	32525	32871	31433	38468	38511	37701	36687	34717	31453	39369	34987	36732	36625	31528	22939	14537
Th	5518	4788	5383	5946	5040	4700	4423	4636	4929	5398	5128	5288	5169	4727	5414	5106	5027	5380	5057	4749	3812
U	10333	9119	10172	11581	10007	9318	9021	9442	10663	11830	11063	11453	11050	10428	11987	10612	11463	11530	11074	10272	8189

4.5. Carbon-Nitrogen-Sulphur analyses

Carbon-Nitrogen-Sulphur concentration were analysed in the peat samples containing the tephra, as well as above and below the tephra layer, on 31st January, 2018. Analyses were performed with a TRUMAC LECO instrument, which consists of a high temperature [>1000°C] ceramic horizontal furnace combined with a C-N-S determinator, at Alltech laboratories, Ireland. Prior investigations, the samples were oven-dried at 95°C for 24 hours, and the instrument was calibrated with a dilution series of synthetic organic standards. Between 0.35 and 0.75 g of dried samples were used for analysis, yielding signals within the calibrated range of concentrations. Quality was controlled with repeat analyses of international soil standards, which yielded absolute external reproducibilities of 0.25% (C), 0.11%(N) and 0.01% (S).

5. Results and Discussion

5.1. Element mobility along the peat profile

Potential element mobility in this core was discussed in detail in Chapter 5. In brief, fair to very good correlations (R^2=0.7-0.9) between conservative lithophile elements Ti, Sc, Sr, Zr, as well as LOI and heavy metals (Ni, Cr, Zn, Pb, Cu, Mo) suggest that element concentrations are governed by the residual sediment content. Likewise, co-variations (R^2=0.6-0.9) between fluid immobile elements Th and Ga and excess (background corrected) heavy metal concentrations (*Appendix B* in Chapter 5) suggest restricted mobility of heavy metals within this profile. Due to the versatile composition of geogenic, air-deposited materials with different Th/Ga ratios, some deviations from perfect correlations are expected. Overall, this monolith was considered adequate regarding its preservation potential to study the chronologic enrichment of heavy metals deposited onto the bog from natural and anthropogenic sources (Chapter 5).

Sulphur is a carbon-loving element and is usually bound onto the humic-compounds in decomposing peat bogs. Due to this strong relationship, peat bogs are often seen as natural sinks for S (e.g., Mikutta and Rothwell, 2016). Being a strongly redox-dependent element, excess sulphur concentrations can be subjected to mobilisation through the depth-related changes in the reducing-oxidizing conditions along a peat column (Novak, 1994). In strongly reducing conditions, S precipitates as sulphide minerals, often leading to an enrichment in other metals such as As and Hg at the precipitation depth as well (e.g., Mikutta and Rothwell, 2016). Because in this study only the uppermost 17 cm of the peat monolith are investigated (*acrotelm* only), significant oxygen gradients, and/or element accumulations are not observed, suggesting that S

mobility must be very minor, i.e. negligible. The peat segment was therefore considered representative of atmospheric S composition.

5.2. Location and geochemical composition of the investigated tephra

Volcanic cryptotephra ranging between 25-80 µm in size was found in the peat at 13 to 15 cm depth from the surface. Within this depth range, the highest abundance of shards was observed at 14-15 cm depth (24 shards in $2cm^3$, compared to a total of 6 in the segment above). An Olympus BX 40 binocular microscope was used to investigate the tephra fraction prior mounting on resin pucks for further analyses. Due to an enhanced lithological influx at this site, which is also seen in the relatively low LOI throughout the core (±90%), the separated fraction contained also equally sized minerals from local rocks, mostly quartz and carbonate. The volcanic tephra could be distinguished from other mineral fractions by its brown colour, platy habit with sharp edges, as well as the presence of large vesicles identified through concave shapes in the shards (Fig. 1). In general, the tephra seems intact with a clear, semi-transparent colour, no indication of devitrification, leaching, or breakdown as indication of element leaching into the peat.

Figure 1.

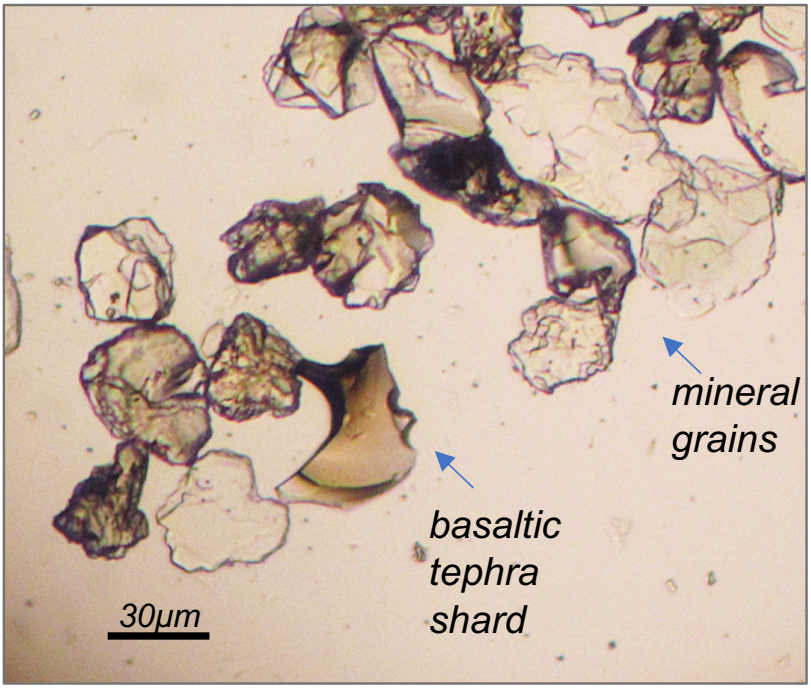


Fig. 1: Microscope image of a brown shard recovered from bulk peat at 13-15 cm depth in Brackloon wood monolith, as well as other minerals (quartz and carbonates) present in the tephra fraction

Figure 2.

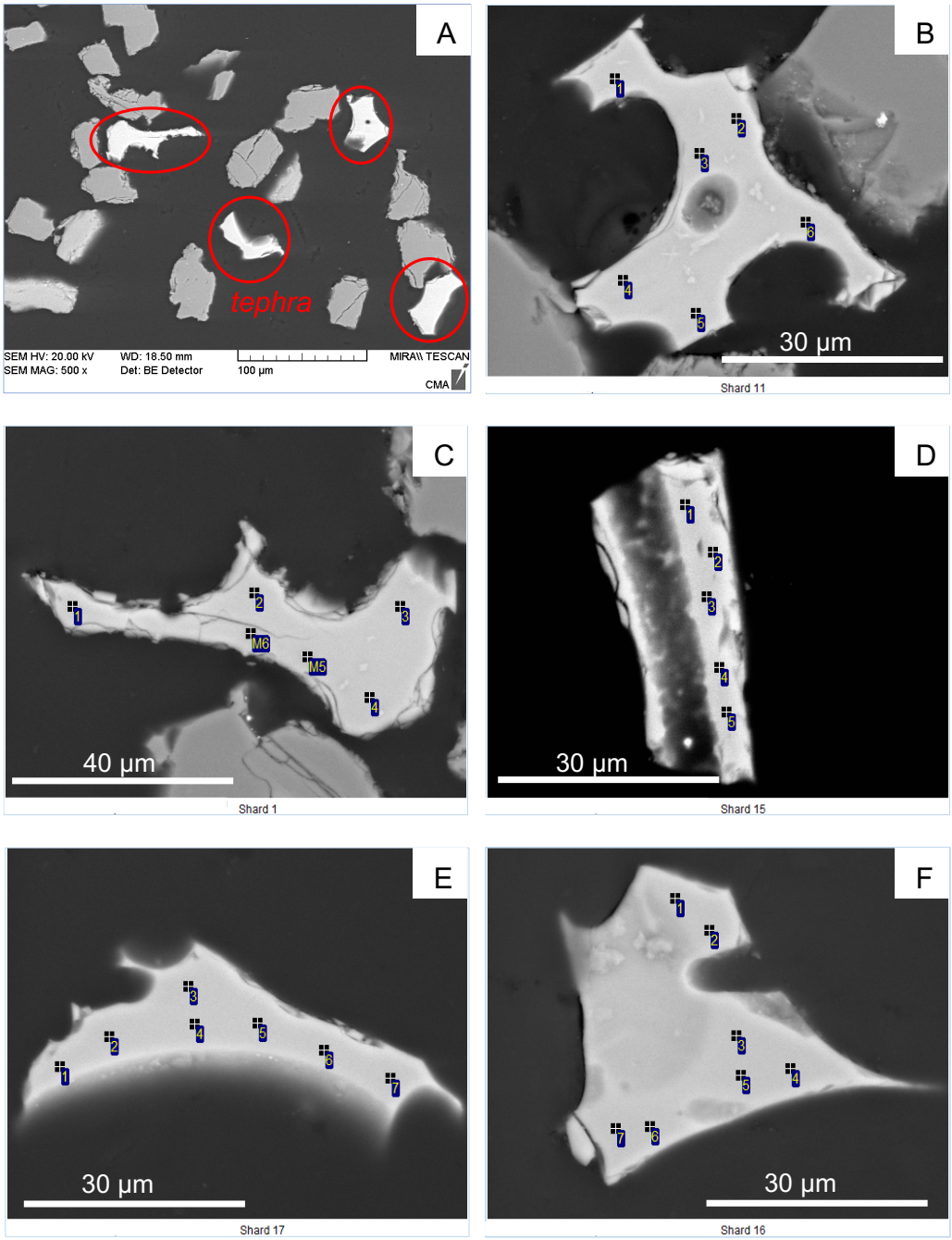


Fig. 2: Scanning electron microscope tephra images and points analysed within the tephra shards.

Due to the small size of the volcanic shards (25-45 µm), results of WDS-EMPA investigation are restricted to two analyses. Further analyses of major oxide compositions were therefore performed via X-ray spectrometer technique, which facilitates the use of a smaller beam diameter. A total of nine shards were successfully analysed with this technique; the results are presented in Table 1. In order to account for potential compositional heterogeneity within the shards, individual tephra specimens were subject

to multiple analyses covering the entire surface (Fig. 2). The tephra shows a narrow compositional range with homogeneous element distribution between central area and rim: SiO_2 =49.9-50.7%, FeOT= 12.2-14.2%, CaO =9.2-11.7%, MgO= 5-6.9%, Na_2O= 2.4-2.9%, TiO_2 =1.8-3-1%, K_2O= 0.2-0.5%, and P_2O_5= 0.4% (Fig. 3). These compositions are comparable to previously obtained values (Reilly and Mitchell, 2015; Thordarson et al., 1996). A comparison between the data obtained with the two techniques shows that more reliable total abundances are obtained for TiO_2, MgO, and Al_2O_3 with the EDS technique (Fig. 3).

The total alkali vs. silica diagram (Fig. 4), after Le Bas et al. (1986) allows a classification of the shards as basaltic, with tendency to basaltic andesitic. This is in line with the findings of Reilly and Mitchell (2015) at the same location in Ireland.

Figure 3.

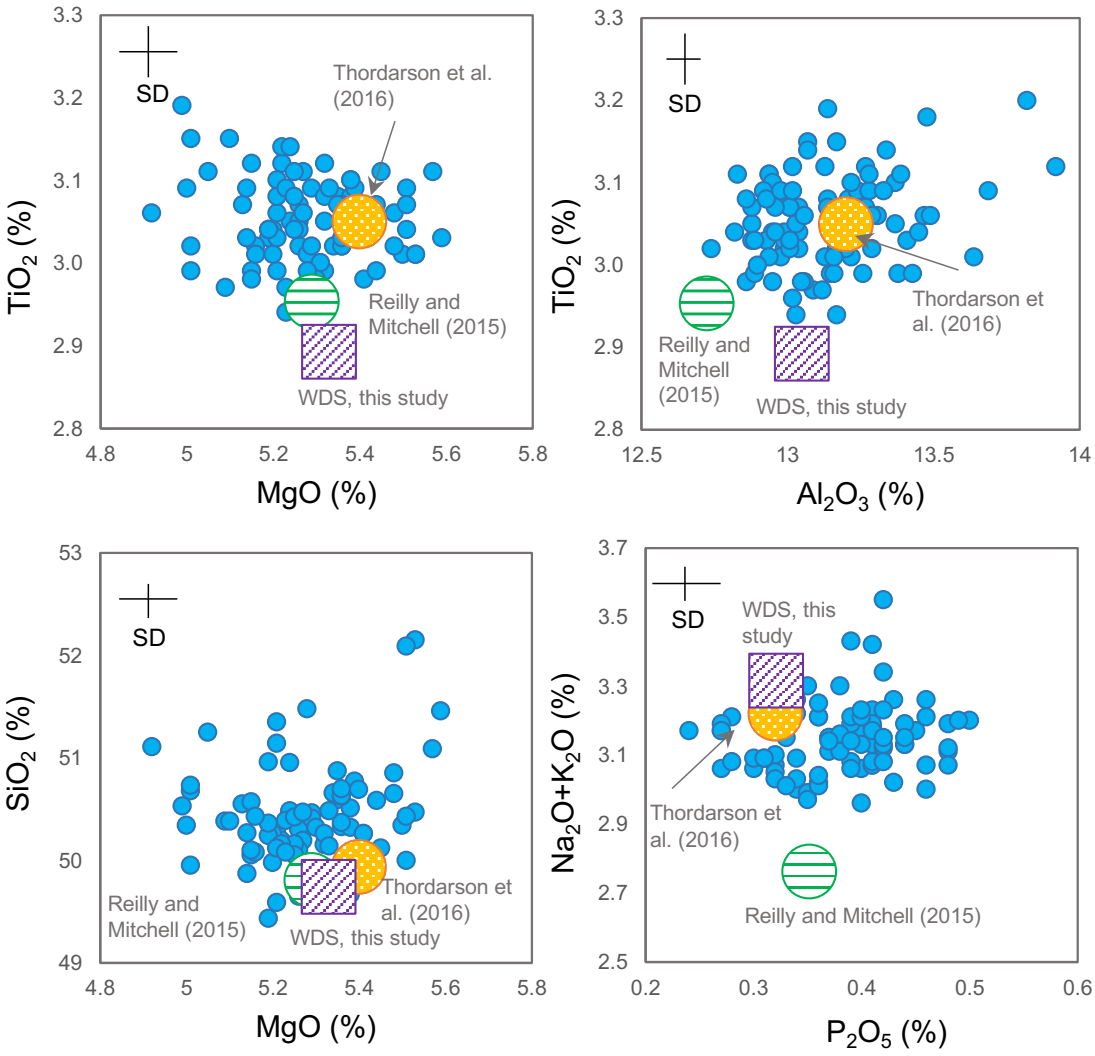


Fig. 3: Binary plots of selected major oxide compositions of Laki 1783-4 cryptotephra shards. Blue points represent all data acquired which includes several analyses per shard. Average compositions of Reilly and Mitchell (2015) and Thordarson et al. (1996) are shown for comparison. Average 1SD for the tephra analysed with the FE-SEM-EDS technique are shown.

The trace element composition obtained for five individual shards is presented in Table 2 and normalised to the values of upper continental crust (UCC) of McLennan (2001) in Figure 5a for comparison. With exception of Pb, which is slightly more enriched in the shards investigated in this study (but also have a higher uncertainty), the values are within the data obtained by Maruyama et al. (2016), which may demonstrate the accuracy of both datasets (Fig. 5a). The strombolian-type tephra is characterised by UCC-normalised slight enrichments in V (3-4) and Zn (1.3-2.9), as well as negative concentration anomalies in Rb (0.07-0.1), Cs (0.02-0.17), Pb (0.03-0.16), Th (0.08-0.1), U (0.08-0.18), and Hf (0.6-0.8). The rare earth element (REE) patterns are characterised by a depletion in the light rare earth elements (LREE) and relatively flat medium- and heavy REE (MREE, HREE) signatures (Fig. 5a, and 6a - blue lines) relative to UCC (McLennan et al., 2001) and MuQ (Mud from Queensland, prototype for modern upper continental crust, after Kamber et al., 2005). This is a common feature in N-MORB-type basalts (Hofmann, 1988), in agreement with mantle sources tapped by the Icelandic volcanoes. Based on these data, we interpret the cryptotephra found at 13-15 cm from the surface in the *Sphagnum* moss dominated woodland peat from the Brackloon wood as the volcanic products of the Laki 1783-4 eruption. Although it is now well documented that the different phases of the eruption (strombolian and phreatomagmatic) emitted chemically variable ash fragments to the atmosphere (e.g., Thordarson et a., 1996), only the least evolved fraction from the strombolian activity was found at this site.

Figure 4.

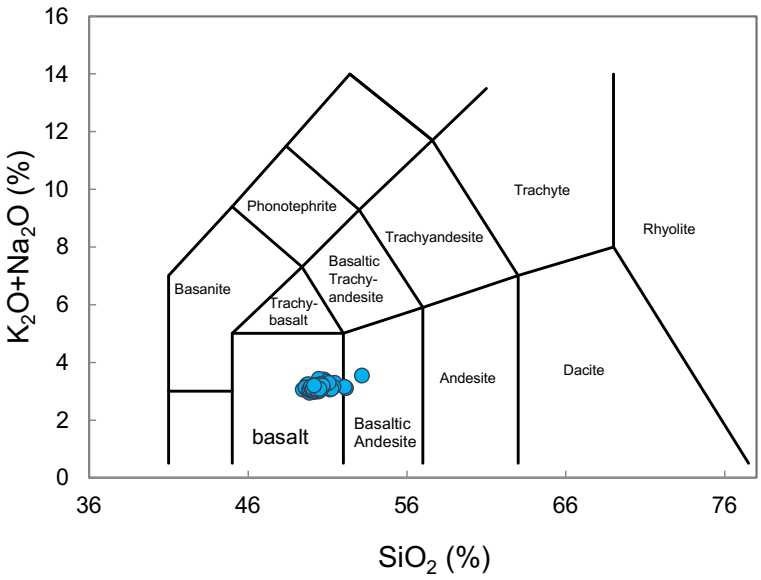


Fig. 4: TAS (total alkali vs. silica diagram) after Le Bass (1986) showing the characterisation of the cryptotephra shards as basaltic – basaltic andesite.

Figure 5.

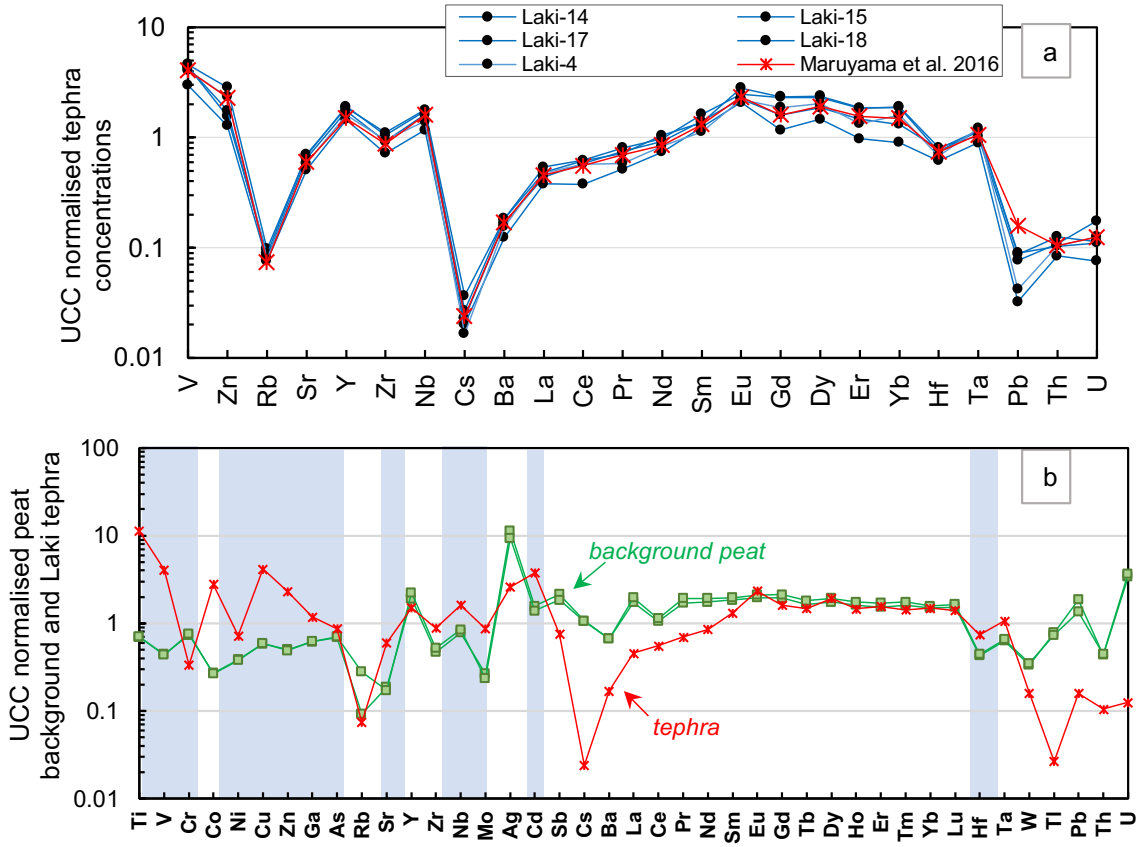


Fig. 5: a) upper continental crust (UCC, McLennan et al., 2001) normalised trace element data of cryptotephra shards obtained with the LA-ICP-MS technique. Literature values (Maruyama et al. 2016) are plotted for comparison; b) extended UCC normalised trace element patterns of background peat (green lines, BW2.18 and BW2.34) obtained with solution analyses together with tephra data (red line, Maruyama et al. 2016) for comparison. Blue shaded areas show the elements which are higher concentrated in tephra with respect to the peat.

5.3. The background composition of the peat

A possibility to resolve the volcanic signal deposited onto the peat is to correct the excess composition for the background. This requires first a general understanding of the nature of geogenic dust entering the bog through aeolian transport. As discussed in Chapter 5, the upward element enrichment observed from ca. 10 cm depth in this core is indicative of significant anthropogenic influence, more precisely, combustion of solid fossil fuels (coal). This excludes the peat composition of the uppermost 10 cm to be representative of a natural background. Also, as described in Chapter 3, the physical properties on the wood peat change from approx. 18-20 cm from the surface, seen in the ash contents. This may lead to further complications potentially leading to an under- or overcorrection of the background signal if the composition at this depth is used as background.

Consequently, the peat layers bracketing the tephra, i.e., 11-12 cm (BW2.18) and 16-17 cm (BW2.34) from the surface were considered as most appropriate approximation of the background.

Rare earth elements and Y (REY) are commonly used to trace sources of geogenic material as they show process-specific behaviour during rock formation, and conservative behaviour during weathering at the Earth's surface (Taylor and McLennan, 1985). For example, during partial melting of the mantle, the relatively incompatible LREE are preferentially enriched in the melt fraction, ultimately resulting in LREE enrichment in the crust and a LREE depletion relative to HREE in the residual mantle (Palme and O'Neill, 2013). Conversely, carbonate rocks are often characterised by a LREE depleted and relative HREE enriched signal with substantially negative Ce, and positive Y anomalies, respectively (the latter occasionally also for La, Eu, Gd, and Lu), which is genetically inherited from the composition of the seawater (Byrne and Kim, 1990; Tostevin et al., 2016; Webb and Kamber, 2000). The MuQ normalised REE composition of the background is presented in Figure 6a, together with the REE patterns of individual tephra shards for comparison, and in Figure 6b along with potential dust sources from relevant distance (mostly carbonates as well as quartz arenite and river sand from Gill et al., 2018). Shown are also MuQ normalised compositions of a typical quartzite from Schilling et al. (2014) to represent potential influx from Croagh Patrick on the west. The peat background is characterised by slight elevations in Y/Ho ratios up to 33-34 (usually 25-27 in siliceous rocks, Kamber et al., 2005), as well as negative Ce (0.6-0.7) and positive Y (1.25-1.27) anomalies, which are calculated as follows:

$$Y/Y^* = Y_N/\sqrt{(Dy_N * Ho_N)^2}$$
$$Ce/Ce^* = Ce_N/\sqrt{(La_N * Pr_N)^2}$$

where $_N$ are the MuQ values of Kamber et al. (2005).

Thus, the background composition of the peat points towards a carbonate source that contributes to the geogenic component in the bog. In addition, subtle enrichments in LREE relative to HREE $(La/Yb)_N$= 1.6-1.8 ($_N$= normalised to the MuQ values of Kamber et al., 2005), coupled with fluctuations in the magnitude of a negative Ce anomaly, together with good correlations between REE and lithophile elements Ti, Sr, Nb (0.7-0.9), point towards additional influx of siliciclastic material, such as sand detritus and possibly quartzite (Fig. 6b.). A systematic increase of carbonate with decrease of sand detritus, or vice versa, is not observed in the background, suggesting that the geogenic component is composed of a heterogeneous mixture from two different sources. In view of the known anthropogenic activity in the area, it is plausible that the detected carbonate signal in the

bog could emerge through occasional distribution of lime, applied in order to fertilise the agricultural areas close by (Cunningham, 2005). Somewhat irregular mechanical or manual distribution of this fertiliser to variable sand detritus-bearing environment would explain the heterogeneous mixture of these two components in the peat. Thus, the plausibility of another explanation renders the peat composition rather unaffected by groundwater disturbance and hence suitable as background signature.

5.4. Calculating excess metal enrichment

Figure 6.

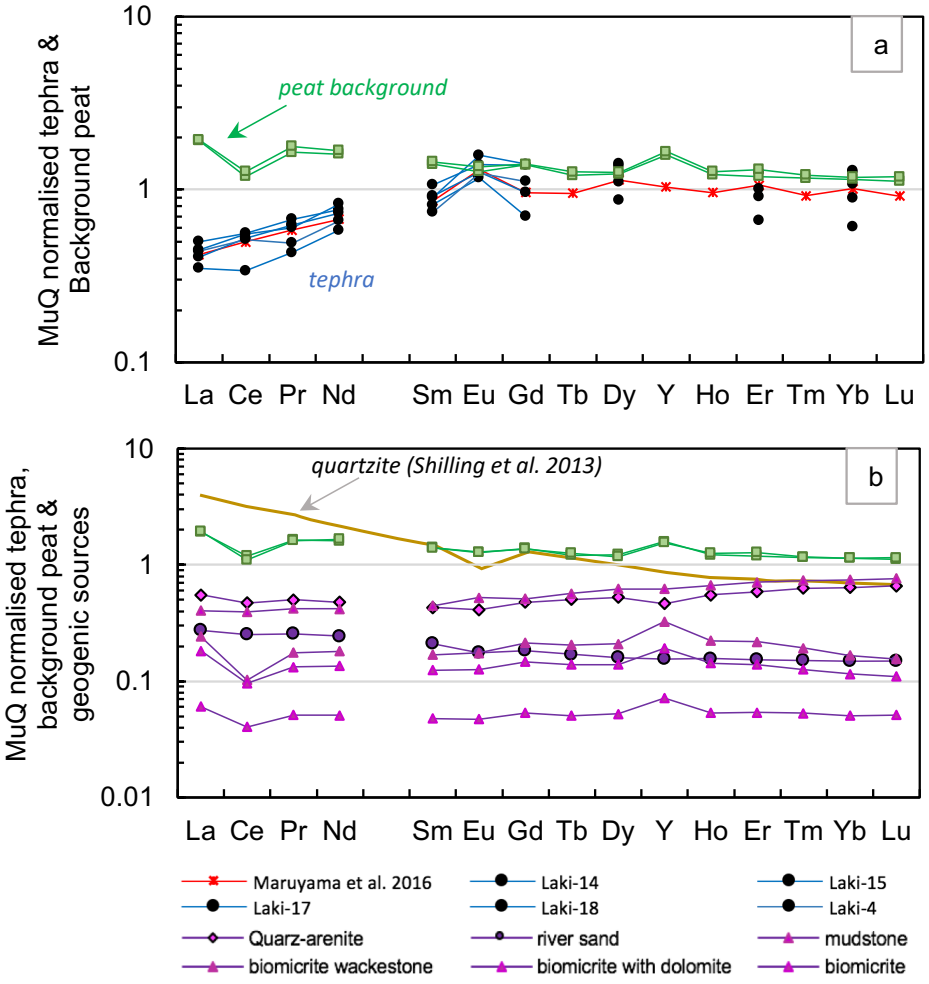


Fig. 6. Mud of Queensland (endmember for modern crust values by Kamber et al., 2005) normalised Rare Earth elements and Yttrium (REY) for: a) Laki 1783-4 tephra (blue lines), red line for the data of Maruyama et al. (2016), and background peat composition (BW2.18 and BW2.34), green lines; b) background peat composition (green lines) and other potential sources of geogenic material influx into the bog (biomicrites, quartz arenites, mudstone, and river sand) data from Gill et al. (2018) shown as differently shaded violet lines, and literature data for quartzite from Shilling et al. (2013), brown line.

In order to identify potential volcanic signals, the composition of tephra-bearing bulk peat is compared to a background for which we take the average composition of bracketing bulk peat layers. An additional advantage of selecting these two bracketing layers as background is that it takes into account and corrects for potentially anthropogenic element enrichment such as charcoal production during the 17th and 18th century (Cunningham, 2005).

In order to highlight any potential signal of volcanic input, an additional correction was applied by using Metal/Ta ratios of the background. The Ta normalisation accounts for fluctuations in the geogenic influx, as the main origin of Ta in peat bogs is of sedimentary and not volcanic origin. Excess enrichments were calculated as follows:

$$Metal_{excess} = Metal_{measured} - (Metal/Ta)_{measured} / (Metal/Ta)_{background}$$

where $Metal_{excess}$ is the background corrected concentration of the metal, $Metal_{measured}$ is the analysed concentration in the sample, $Metal/Ta_{measured}$ is the ratio in the analyses sample and $Metal/Ta_{background}$ is the ratio in the background.

By applying this correction, we can distinguish volcanic signals from primary geogenic element input at this depth. Indeed, some enrichments in Ti, Fe, Ce, V (13-14 cm), and to minor extents in Cd, Cu, Pb and Th (14-15 cm) can be identified in bulk peat at the depth of tephra deposition (Fig. 7). The enrichment in these elements might be indicative of inputs from tephra or volcanic aerosols. In order to further distinguish these two types of volcanic sources we examine the composition of the tephra with respect to the background peat in more detail.

Figure 7.

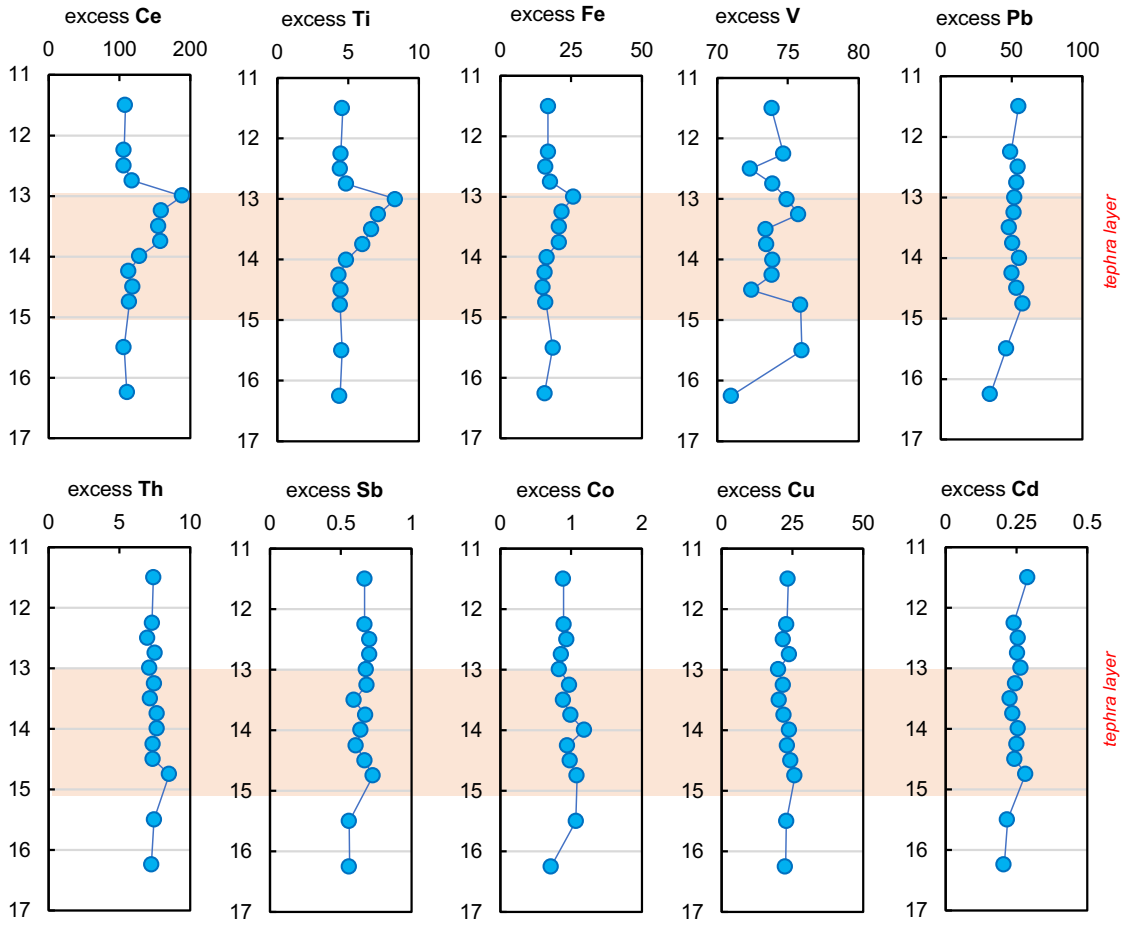


Fig. 7: Ta normalised excess element enrichments with respect to the background (BW2.18, 11-12 and BW2.34, 16-17cm). Red shaded areas indicate the tephra bearing peat segment.

5.5. The role of tephra in modifying bulk peat signatures

Laki 1783-4 tephra shows strong enrichments in Ti, V (Fig. 5b) and Fe relative to background peat. A possible relation between the Ti, Fe, Ce, and V enrichments observed at the depth of tephra deposition (see section 5.4) and the Laki 1783-4 tephra itself is examined next. For this, a simple calculation is performed to verify if a potential addition of this might theoretically contribute to the subtle shift in the composition of the bulk peat at this depth. In a first step, we determine the mass of a single shard from average volume (6µm*30µm*40µm obtained through microscopy investigations and LA-ICP-MS), and the known density of a basaltic shard (2.5 g/cm^3). The average mass of a cryptotephra shard, calculated at 0.0178 µg, was then multiplied with the respective concentration of each element obtained by the LA-ICP-MS technique to calculate the total amount of each metal contained per tephra shard. For instance, the results suggest that one shard could

contribute an average of 0.32 ng to the total Ti contained in 1 g peat. Owing to the high background in this core (2791 µg/g), an admixture of 24 shards is rather negligible. Moreover, in order for tephra alone to produce resolvable background-corrected excess (5%) Ti concentrations, ca. 3837 shards per g peat would be required. This is an unrealistic number as the observed cryptotephra abundance does not come close to these values in this core. This scenario becomes even more improbable for other elements such as Ce and V, which show even smaller enrichments in tephra compared to background peat.

It is further observed that the ratios of these elements in the Laki 1783 tephra (e.g., Ti/V= 42, Fe/Ti= 0.16, Ti/Ce= 519), are significantly different than those in the background peat (Ti/V= 61, Fe/Ti= 269, Ti/Ce= 41) and even more different than those in corrected tephra-bearing peat (Ti/V= 70-111, Fe/Ti= 275-320, Ti/Ce= 38-43). This is mostly due to highly variable Fe-Ti concentrations between and within the respective materials (tephra: Ti= 18364 ppm, Fe= 112787 ppm; tephra bearing peat: Ti= 3000-5799 ppm, Fe= 11-18 ppm). Hence, tephra addition to bulk peat should produce intermediate ratios of these elements in the tephra-bearing layer compared to background and tephra shards ratios. This is clearly not the case here (not shown), providing a further argument against tephra to account for the excess Ti and Fe peak observed at the tephra deposition depth. Owing to the fact that both Ti and Fe are refractory elements (Lodders, 2003), a partitioning of these two elements into the aerosol phase is unlikely, also casting doubt over this possibility as the origin of enrichment in peat. Thus, resolvable Fe and Ti peaks within the tephra layer cannot unequivocally be attributed to the presence of tephra, although higher enrichments of these elements in the tephra would make it seem so. However, although unlikely for refractory Fe and Ti, Laki aerosol deposition could theoretically account for enrichments of other incompatible, volatile (S, Zn, Cd, Pb) and moderately volatile elements (Cu) in peat.

5.6. Composition of the Laki 1783-4 volcanic aerosols deposited onto Brackloon wood peat at the west coast of Ireland

5.6.1. Sulphur enrichment patterns along the peat monolith

Concentrations of C-N-S (Table 3) were determined for tephra-bearing bulk peat as well as the bracketing layers to obtain a general understanding of S distribution along the critical depth profile. In general, concentrations of sulphur and nitrogen remain extremely high throughout the core with values ranging between 3600 and 4000 ppm for S, and N concentrations fluctuating between 1.2 and 1.8%. No striking S peak is observed in this core at the depth of tephra deposition; at least not as obvious as documented in ice cores

(e.g., Hong et al., 1996). There are two main explanations for this. The first is the high organic-related S background in peat bogs. Focused studies of N and S distribution and accumulation in peat bogs have demonstrated the high affinity of S to organic matter in wetland ecosystems (e.g., Moore et al., 2005; Novák and Wieder, 1992 and references therein). This results in successful S sequestration onto the decomposed organic matter (humic acids). Sulphur concentrations vary between 0.1 and 0.5% in pristine peat bogs (e.g., Moore et al., 2005). These values are significantly higher than ~1200 ng/g in ice cores (maximum concentration value in connection with the Laki S-peak reported by Hong et al., 1996 in Greenland ice). Hence, compared to ice cores, the high backgrounds in our investigated peat are responsible for less (if any) obvious volcanogenic S and N spikes. The second reason for the absence of a striking S peak is potential influence from oceanic aerosols. Sea-spray and sea-salts were shown to be highly enriched in sulphate (SO_4^{2-}) and nitrate (NO_3^-) concentrations, which vary between few and hundreds of ppm depending on the site (e.g., Neumann, 2016; Pernigotti et al., 2016). Archives situated in the vicinity of maritime and/or oceanic areas, such as Brackloon wood, are subjected to constant influx of N and S, ultimately creating elevated backgrounds in the respective bodies at the Earth's surface.

Because of the above-mentioned circumstances, the S peak accompanying the Laki 1783-4 volcanic eruption is nearly unidentifiable from average S values measured in the 0-17 cm peat section. Nevertheless, a closer observation of the S concentrations as shown in Figure 8 reveals the presence of minor S and N peaks in the tephra-bearing segment relative to the average background concentration provided by the bracketing layers. The presence of a non-lithogenic source at this depth is further supported by the weak correlations between S and LOI (R^2= 0.35), which are usually rather well correlated in archives dominated solely by soil and sediment dust input. Moreover, the background corrected excess S values in the tephra-bearing layer range between 110 and 170 ppm. As a matter of fact, these excess concentrations turn out to be significantly higher than the maximum Laki S signal of 1.12 ppm observed in Greenlandic ice (Hong et al., 1996). These findings suggest a stronger S peak over Ireland (i.e., north Europe) compared to Greenland, provided that a simultaneous release of S to the atmosphere from anthropogenic activities can be ruled out. This evaluation regarding the true origin of the S peak now benefits from assessment of other volatile element enrichments in the same peat.

Figure 8.

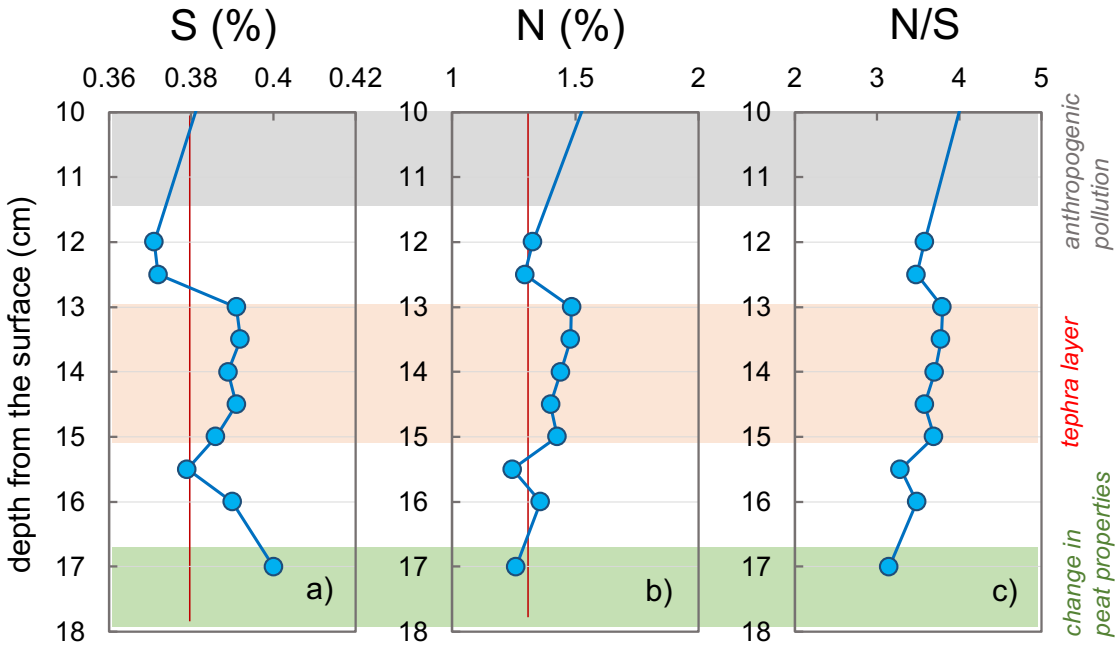


Fig. 8: Sulphur, nitrogen, and their ratios in the peat segment from 10 to 18 cm in the Brackloon wood monolith. Indicated are also the depth where the upward enrichment of the elements starts (anthropogenic pollution, grey shaded area), and the area where the acrotelm starts to transform into the catotelm leading to a change in the physical properties of the peat (green shaded area). Average background values are shown as vertical red lines.

5.6.2. Enrichments of other metals by Laki aerosol deposition

Subtle enrichment of Co, Ni, Cu, Zn, Mo, Cd is observed in background corrected tephra-bearing peat at 14-15 cm. Previous studies also reported pronounced Cd, Pb, Cu, and Zn aerosol peaks in ice following the Laki 1783-4 eruption (Greenland, Hong et al., 1996). This provides external evidence for an existence of such deposits in the first place and proves the consideration of this source to account for the enrichment in our peat core reasonable. As discussed above, the background-corrected element peaks in the ice core may be higher than those in our peat, yet absolute concentrations are much lower in the former, ultimately limiting absolute concentration-related comparisons between these two archives. Hence, in pursuing the scenario of a possible aerosol source in the background corrected element ratios, the relevant elements are compared with those in the ice archive from Greenland (Hong et al., 1996). A clear advantage of applying metal ratios instead of concentrations is the exclusion of uncertainties that will emerge due to different element accumulation rates at the two sites (peat vs. ice). The results are shown in Figure 9.

Figure 9.

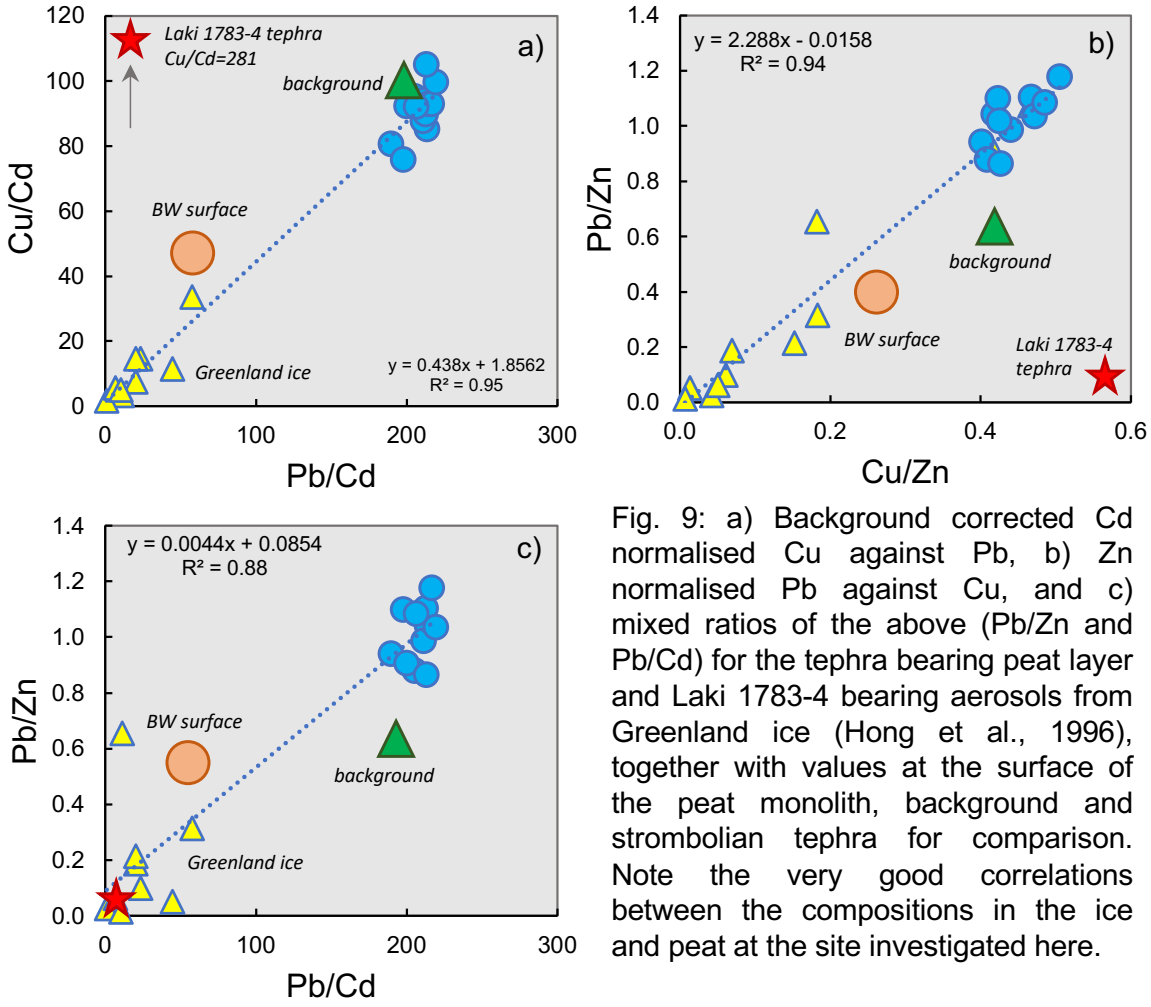


Fig. 9: a) Background corrected Cd normalised Cu against Pb, b) Zn normalised Pb against Cu, and c) mixed ratios of the above (Pb/Zn and Pb/Cd) for the tephra bearing peat layer and Laki 1783-4 bearing aerosols from Greenland ice (Hong et al., 1996), together with values at the surface of the peat monolith, background and strombolian tephra for comparison. Note the very good correlations between the compositions in the ice and peat at the site investigated here.

A first observation revealed by the illustration of element ratios is that the composition of the Laki tephra in our peat differs considerably from that of the Laki-bearing aerosols in Greenlandic ice (Fig. 9a-b). In particular, the much higher Cu contents in Laki tephra results in higher Cu/Cd (281 vs. max. 34 in ice) and Cu/Zn (0.6 vs. max. 0.2 in ice) compared to ice-hosted aerosols. Ratios of Cd-Zn-Pb between Laki tephra (values from Maruyama et al. 2016) and ice-hosted aerosols do not agree well. One reason for this difference in accordance between Cu and Cd-Zn-Pb may be the different condensation temperatures of the elements which follow the sequence: Cu>>Pb=Zn>Cd (Lodders, 2003). This means that during a volcanic eruption, the volatile elements Cd, Zn, and Pb will enter the vapour/aerosol phase already at lower temperatures (400-450°C) compared to the moderately volatile element Cu (>700°C), resulting in disproportional relative distribution of these elements between molten lava - tephra - and aerosols. A further evaluation of relative element fractionation is complicated by the fact that in this study we

investigate bulk aerosol composition, but only one end-member of the tephra products - the strombolian (basaltic) ejecta. The eruption is, however, also known for its destructive phreatomagmatic phase (Thordarson, 2003) during which, geochemically distinct tephra with significantly higher volatile element contents, and especially sulphur, was produced (Thordarson et al., 1996). Hence further investigations are necessary to assess all processes leading to this discrepancy in enrichments between Cu and Cd-Zn-Pb.

Another important observation is that inter-element ratios of Zn-Cd-Cu-Pb display generally good correlations (R^2=0.88-0.94) between the aerosols deposited individually in ice and in Brackloon woodland peat. Note that the deviation from these correlations for ratios involving Pb are explained by the ca. 30 percent difference between upper and lower bracketing background Pb content which makes the average background Pb content used for correction less representative and more susceptible to variations. This ultimately introduces an additional variation and slight offset towards the respective background ratios involving Pb. Most apparent is the illustration involving Pb in both ratios (Fig. 9c), whereas ratios of Zn-Cd-Cu are less affected by this bias owing to smaller variations and similar contents of these elements in the two bracketing peat layers used for each average background ratio.

Altogether, apart for a minor effect for Pb, these inter-element ratios are likely unrelated to additional influx of geogenic component (e.g., UCC: Cu/Cd= 255, Zn/Cd= 725). This reveals the co-enrichment as well as a common source of these elements. Most importantly, the composition of the peat at the depth of tephra deposition is different from the recently accumulated peat onto BW (e.g. 2-3 cm), interpreted to show anthropogenic influence from combustion of solid fossil fuels (Chapter 5), as well as from the peat underneath which serves for estimation of the background. Instead, the Cu/Cd, Pb/Cd, Pb/Zn, and Cu/Zn values at 13-15 cm depth can be explained through a 3 to 6 times stronger Laki 1783-4 aerosol signal deposited at the west coast of Ireland compared to the Greenlandic ice core investigated by Hong et al. (1996). The inferred proportionally higher aerosol metal concentration deposited in Ireland in comparison to Greenland, is in line with the modelled dispersal of the main ash/aerosol plume in south-east direction towards northern and central Europe (Fig. 10, e.g., Highwood and Stevenson, 2003; Sigurdsson, 1982; Thordarson, 2003). However, additional investigations in other cores at the west coast of Ireland are necessary to test this hypothesis.

Figure 10.

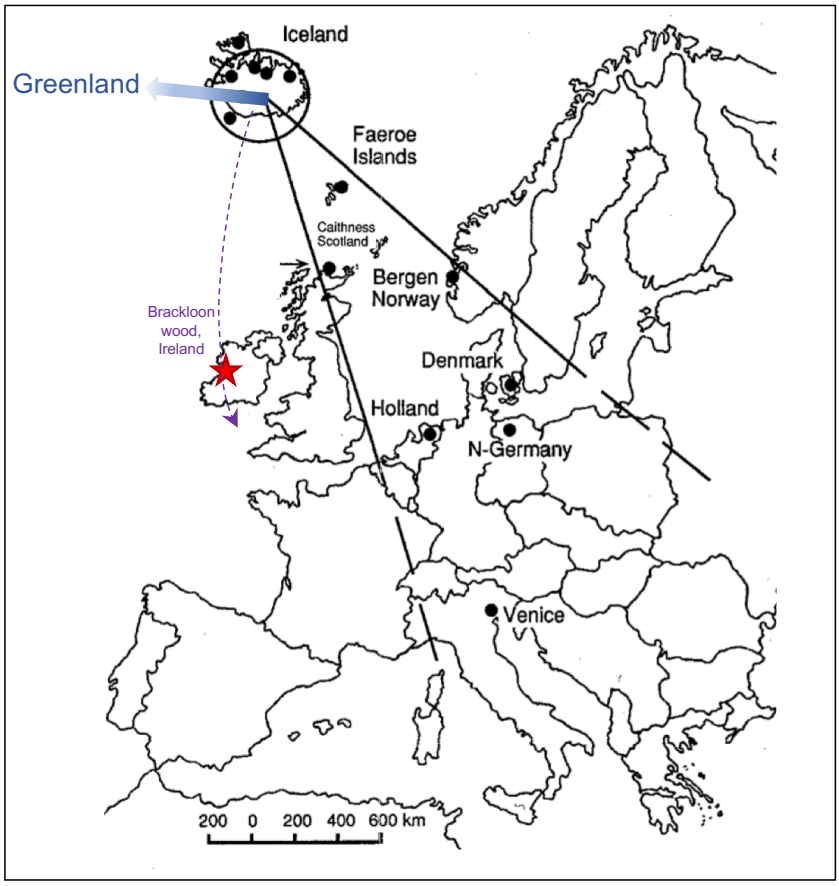


Fig. 10. Known dispersal of Laki 1783-4 volcanic ash from reports in different locations (black dots) compiled by Thordarson and Self (1993). The location of the strombolian Laki tephra in the peat monolith at the west coast of Ireland is also shown.

The possibility that Irish peat records a higher total aerosol deposition than Greenland ice would be in conjunction with a higher total S content observed in our peat compared to ice-hosted S (see above). Correlations between excess S and Cu, Cd, Pb, and/or Zn are not visible at the tephra depth, which complicates the interpretation of the subtle S peak. There are two main explanations for this finding: i) the sulphur signal is not exclusively volcanic, and that enrichments from sources such as oceanic aerosols and/or anthropogenic activities may play a significant role at this site, ii) it is possible that highly volatile S (<400°C, Lodders, 2003) has a higher residence time in the atmosphere with respect to the heavy metals, resulting in a delayed and sporadic precipitation of S, eventually leading to a disturbed metal/S ratio of the aerosol in the peat. It would hence expand our range of disproportionally deposited elements in Irish peat by S, with a sequence: S>>>Cu>>Pb=Zn>Cd (in agreement with their relative condensation temepratures, Lodders, 2003). This reasoning is further based on findings from focused

studies in the Arctic, which have shown that the atmospheric residence time of S strongly depends on two factors: chemical conversion to sulphate and rate of dry deposition (Barrie and Hoff, 1984). It is now widely known that S-rich Laki aerosols were injected into the upper troposphere and lower stratosphere ultimately resulting in aerosol propagation around the northern hemisphere. For example, Thordarson (2003) have shown that ca. 175 Mt of H_2SO_4 aerosols were removed as acid precipitation during the first months of 1783 AD, while the remaining ca. 25 Mt stayed trapped at tropopause level for more than 1 year. Our findings and future investigations should thus be considered in the context of the different metal-specific atmospheric residence times following volcanic eruptions. This may not only contribute to elucidate the Laki aerosol signatures recorded in Irish peat bogs but also of other volcanic aerosol signatures in different archives worldwide.

6. Summary and conclusions

This pilot study aims to investigate if organic rich archives such as peat bogs record past volcanic aerosol compositions with a focus on volcanogenic metal enrichment relative to the site-specific background (natural, and anthropogenic). Specifically, investigations are directed towards the tephra and aerosol metal budget released to the atmosphere following the Icelandic Laki 1783-4 volcanic eruption from its depositions onto a woodland peat archive at the west coast of Ireland, Brackloon wood. The main findings of this investigation are:

1. Excess enrichments in V, Ti, and Fe in bulk peat at 13 to 15 cm from the surface cannot unequivocally be attributed to an addition of basaltic cryptotephra at this depth, although higher concentrations of these elements in the separately investigated tephra compared to background peat shards would suggest this.
2. The Laki 1783-4 volcanic eruption is known for significant atmospheric S release. However, no striking sulphur concentration peak at the depth of tephra deposition, linkable to the eruption is observed in this core. This is due to the generally high sulphur background in this bog (0.36-0.4%) and by analogy in all organic rich archives at the Earth's surface. Yet, excess concentrations of 110 and 170 ppm are significantly higher than the maximum Laki S signal of 1.12 ppm observed in Greenlandic ice. This suggests a more pronounced volcanic S deposition over Ireland (i.e., north Europe) compared to Greenland, although the high but ultimately unconstrained residence time of S additionally complicates the matter.

3. Aerosol-related absolute Cu, Cd, Pb, and Zn enrichments as in Greenland ice are not seen in peat from Ireland. This is, as for S, attributed to the enhanced background composition of the peat. However, remarkable correlations between Cu/Cd and Pb/Cd as well as Pb/Zn and Cu/Zn in the tephra-bearing layer and aerosols deposited in Greenland ice are observed. This suggests a link between the compositions and thus a potentially common volcanic aerosol signal originating from the Laki eruption.

Altogether, the results of this study suggest that aerosols of the Laki 1783-4 volcanic eruptions have contributed to the heavy metal content (Cu, Cd, Pb, and Zn) in Brackloon wood peat archive at the west coast of Ireland. The total contribution of these metals from the same Icelandic Laki eruption is even higher than that for Greenland ice and attributed to the windward south-eastern dispersal of the volcanic cloud.

However, the initially high metal contents in the investigated peat constitute a background, which diminishes the difference and made it nearly untraceable. Peat bogs have potential as volcanic deposition archive that improves with lower background element contents.

References

Barrie, L.A., Hoff, R.M., 1984. The oxidation rate and residence time of sulphur dioxide in the arctic atmosphere. Atmos. Environ. 18, 2711–2722. https://doi.org/10.1016/0004-6981(84)90337-8

Blockley, S.P.E., Pyne-O'Donnell, S.D.F., Lowe, J.J., Matthews, I.P., Stone, A., Pollard, A.M., Turney, C.S.M., Molyneux, E.G., 2005. A new and less destructive laboratory procedure for the physical separation of distal glass tephra shards from sediments. Quat. Sci. Rev. 24, 1952–1960. https://doi.org/10.1016/j.quascirev.2004.12.008

Byrne, R.H., Kim, K.H., 1990. Rare earth element scavenging in seawater. Geochim. Cosmochim. Acta 54, 2645–2656. https://doi.org/10.1016/0016-7037(90)90002-3

Cunningham, D., 2005. Brackloon: The Story of an Irish Oak Wood.

Dugmore, A.J., Newton, A.J., 1992. Thin tephra layers in peat revealed by X-radiography. J. Archaeol. Sci. 19, 163–170. https://doi.org/10.1016/0305-4403(92)90047-7

Eggins, S.M., Woodhead, J.D., Kinsley, L.P.J., Mortimer, G.E., Sylvester, P.J., McCulloch, M.T., Hergt, J.M., Handler, M.R., 1997. n ! Zi- internal standardisation. Chem. Geol. 1, 311–326. https://doi.org/http://dx.doi.org/10.1016/S0009-2541(96)00100-3

Fiacco, R.J., Thordarson, T., Germani, M.S., Self, S., Palais, J.M., Whitlow, S., Grootes, P.M., 1994. Atmospheric aerosol loading and transport due to the 1783-84 Laki Eruption in Iceland, interpreted from ash particles and acidity in the GISP2 ice core. Quat. Res. 42, 231–240. https://doi.org/10.1006/qres.1994.1074

Gill, L.W., Babechuk, M.G., Kamber, B.S., McCormack, T., Murphy, C., 2018. Use of trace and rare earth elements to quantify autogenic and allogenic inputs within a lowland karst network. Appl. Geochemistry 90, 101–114. https://doi.org/10.1016/j.apgeochem.2018.01.001

Grattan, J., Durand, M., Taylor, S., 2003. Illness and elevated human mortality in Europe coincident with the Laki Fissure eruption. Geol. Soc. London, Spec. Publ. 213, 401–414. https://doi.org/10.1144/GSL.SP.2003.213.01.24

Highwood, E.J., Stevenson, D.S., 2003. Atmospheric impact of the 1783–1784 Laki Eruption: Part II Climatic effect of sulphate aerosol. Atmos. Chem. Phys. Discuss. 3, 1599–1629. https://doi.org/10.5194/acpd-3-1599-2003

Hofmann, A.W., 1988. Chemical differentiation of the Earth: the relationship between mantle, continental crust, and oceanic crust. Earth Planet. Sci. Lett. 90, 297–314. https://doi.org/10.1016/0012-821X(88)90132-X

Hong, S., Candelone, J.-P., Boutron, C.F., 1996. Deposition of atmospheric heavy metals to the Greenland ice sheet from the 1783–1784 volcanic eruption of Laki, Iceland. Earth Planet. Sci. Lett. 144, 605–610. https://doi.org/10.1016/S0012-821X(96)00171-9

Jacoby, G.C., Workman, K.W., D'Arrigo, R.D., 1999. Laki eruption of 1783, tree rings, and disaster for northwest Alaska Inuit. Quat. Sci. Rev. 18, 1365–1371. https://doi.org/10.1016/S0277-3791(98)00112-7

Jarosewich, E., 2002. Smithsonian Microbeam Standards. J. Res. Natl. Inst. Stand. Technol. 107, 681. https://doi.org/10.6028/jres.107.054

Jochum, K.P., Stoll, B., Herwig, K., Willbold, M., Hofmiann, A.W., Amini, M., Aarburg, S., Abouchami, W., Hellebrand, E., Mocek, B., Raczek, I., Stracke, A., Alard, O., Bouman, C., Becker, S., Dücking, M., Brätz, H., Klemd, R., De Bruin, D., Canil, D., Cornell, D., De Hoog, C.J., Dalpé, C., Danyushevshy, L., Eisenhauer, A., Gao, Y., Snow, J.E., Groschopf, N., Günther, D., Latkoczy, C., Guillong, M., Hauri, E.H., Höfer, H.E., Lahaye, Y., Horz, K., Jacob, D.E., Kasemann, S.A., Kent, A.J.R., Ludwig, T., Zack, T., Mason, P.R.D., Meixner, A., Rosner, M., Misawa, K., Nash, B.P., Pfänder, J., Premo, W.R., Sun, W.D., Tiepolo, M., Vannucci, R., Vennemann, T., Wayne, D., Woodhead, J.D., 2006. MPI-DING reference glasses for in situ microanalysis: New reference values for element concentrations and isotope ratios. Geochemistry, Geophys. Geosystems 7. https://doi.org/10.1029/2005GC001060

Kamber, B.S., Greig, A., Collerson, K.D., 2005. A new estimate for the composition of weathered young upper continental crust from alluvial sediments, Queensland, Australia. Geochim. Cosmochim. Acta 69, 1041–1058. https://doi.org/10.1016/j.gca.2004.08.020

Kamber, B.S., Greig, A., Schoenberg, R., Collerson, K.D., 2003. A refined solution to Earth's hidden niobium: Implications for evolution of continental crust and mode of core formation, in: Precambrian Research. pp. 289–308. https://doi.org/10.1016/S0301-9268(03)00100-1

Le Bas, M.J., Le Maitre, R.W., Streckeisen, A., Zanettin, B., 1986. A chemical classification of volcanic rocks based on the total alkali silica diagram. J. Petrol. 27, 745–750. https://doi.org/10.1093/petrology/27.3.745

Lodders, K., 2003. Solar System Abundances and Condensation Temperatures of the Elements. Astrophys. J. 591, 1220–1247. https://doi.org/10.1086/375492

Maruyama, S., Hattori, K., Hirata, T., Suzuki, T., Danhara, T., 2016. Simultaneous determination of 58 major and trace elements in volcanic glass shards from the INTAV sample mount using femtosecond laser ablation-inductively coupled plasma-mass spectrometry. Geochem. J. 50, 403–422. https://doi.org/10.2343/geochemj.2.0436

Mather, T. a., Pyle, D.M.M., Oppenheimer, C., 2003. Tropospheric volcanic aerosol. Volcanism Earth's … 189–212. https://doi.org/10.1029/139GM12

McConnell, J.R., Edwards, R., 2008. Coal burning leaves toxic heavy metal legacy in the Arctic. Proc. Natl. Acad. Sci. 105, 12140–12144. https://doi.org/10.1073/pnas.0803564105

McLennan, S.M., 2001. Relationships between the trace element composition of sedimentary rocks and upper continental crust. Geochemistry, Geophys. Geosystems 2. https://doi.org/10.1029/2000GC000109

Mikutta, C., Rothwell, J.J., 2016. Peat Bogs as Hotspots for Organoarsenical Formation and Persistence. Environ. Sci. Technol. 50, 4314–4323. https://doi.org/10.1021/acs.est.5b06182

Moore, T., Blodau, C., Turunen, J., Roulet, N., Richard, P.J.H., 2005. Patterns of nitrogen and sulfur accumulation and retention in ombrotrophic bogs, eastern Canada. Glob. Chang. Biol. 11, 356–367. https://doi.org/10.1111/j.1365-2486.2004.00882.x

Neumann, D., 2016. The impact of sea salt emissions on the air quality in the North Sea and Baltic Sea regions at Hamburg.

Novak, M., 1994. Sulfur during early diagenesis in Sphagnum peat: insights from delta 34-S

profiles in 210-Pb-dated peat cores. Limnol. Oceanogr. 39, 1172–1185.

Novák, M., Wieder, R.K., 1992. Inorganic and organic sulfur profiles in nine Sphagnum peat bogs in the United States and Czechoslovakia. Water, Air, Soil Pollut. 65, 353–369. https://doi.org/10.1007/BF00479898

Nriagu, J.O., 1989. A global assessment of natural sources of atmospheric trace metals. Nature 338, 47–49. https://doi.org/10.1038/338047a0

Oman, L., Robock, A., Stenchikov, G.L., Thordarson, T., Koch, D., Shindell, D.T., Gao, C., 2006. Modeling the distribution of the volcanic aerosol cloud from the 1783-1784 Laki eruption. J. Geophys. Res. Atmos. 111. https://doi.org/10.1029/2005JD006899

Palme, H., O'Neill, H., 2013. Cosmochemical Estimates of Mantle Composition, 2nd ed, Treatise on Geochemistry: Second Edition. Elsevier Ltd. https://doi.org/10.1016/B978-0-08-095975-7.00201-1

Pernigotti, D., Belis, C.A., Spanó, L., 2016. SPECIEUROPE: The European data base for PM source profiles. Atmos. Pollut. Res. 7, 307–314. https://doi.org/10.1016/j.apr.2015.10.007

Reilly, E., Mitchell, F.J., 2015. Establishing chronologies for woodland small hollow and mor humus deposits using tephrochronology and radiocarbon dating. Holocene 25, 241–252. https://doi.org/10.1177/0959683614557571

Schilling, J., Reimann, C., Roberts, D., 2014. REE potential of the Nordkinn Peninsula, North Norway: A comparison of soil and bedrock composition. Appl. Geochemistry 41, 95–106. https://doi.org/10.1016/j.apgeochem.2013.12.004

Schmidt, A., Leadbetter, S., Theys, N., Carboni, E., Witham, C.S., Stevenson, J.A., Birch, C.E., Thordarson, T., Turnock, S., Barsotti, S., Delaney, L., Feng, W., Grainger, R.G., Hort, M.C., Höskuldsson, Á., 2015. Satellite detection, long-range transport, and air quality impacts of volcanic sulfurdioxide from the 2014-2015 flood lava eruption at Bardarbunga (Iceland). J. Geophys. Res. Atmos. 120, 9739–9757. https://doi.org/10.1002/2015JD023638.Received

Sigmarsson, O., Condomines, M., Grönvold, K., Thordarson, T., 1991. Extreme magma homogeneity in the 1783–84 Lakagigar Eruption: Origin of a large volume of evolved basalt in Iceland. Geophys. Res. Lett. 18, 2229–2232. https://doi.org/10.1029/91GL02328

Sigurdsson, H., 1982. Volcanic pollution and climate: The 1783 Laki eruption. Eos, Trans. Am. Geophys. Union 63, 601–602. https://doi.org/10.1029/EO063i032p00601

Taylor, S.R., McLennan, S.., 1985. The continental crust: Its composition and evolution. McClennan, Blackwell Sci. Publ. 21, 85–86. https://doi.org/10.1002/gj.3350210116

Thordarson, T., 2003. Atmospheric and environmental effects of the 1783–1784 Laki eruption: A review and reassessment. J. Geophys. Res. 108, 4011. https://doi.org/10.1029/2001JD002042

Thordarson, T., Self, S., 1993. The Laki (Skaftár Fires) and Grímsvötn eruptions in 1783-1785. Bull. Volcanol. 55, 233–263. https://doi.org/10.1007/BF00624353

Thordarson, T., Self, S., Óskarsson, N., Hulsebosch, T., 1996. Sulfur, chlorine, and fluorine degassing and atmospheric loading by the 1783-1784 AD Laki (Skaftár Fires) eruption in Iceland. Bull. Volcanol. 58, 205–225. https://doi.org/10.1007/s004450050136

Tostevin, R., Shields, G.A., Tarbuck, G.M., He, T., Clarkson, M.O., Wood, R.A., 2016. Effective use of cerium anomalies as a redox proxy in carbonate-dominated marine settings. Chem.

Geol. 438, 146–162. https://doi.org/10.1016/j.chemgeo.2016.06.027

Ulrich, T., Kamber, B.S., Woodhead, J.D., Spencer, L.A., 2010. Long-Term Observations of Isotope Ratio Accuracy and Reproducibility Using Quadrupole ICP-MS. Geostand. Geoanalytical Res. 34, 161–174. https://doi.org/10.1111/j.1751-908X.2010.00046.x

Webb, G.E., Kamber, B.S., 2000. Rare earth elements in Holocene reefal microbialites: A new shallow seawater proxy. Geochim. Cosmochim. Acta 64, 1557–1565. https://doi.org/10.1016/S0016-7037(99)00400-7

Witham, C.S., Oppenheimer, C., 2004. Mortality in England during the 1783-4 Laki Craters eruption. Bull. Volcanol. 67, 15–26. https://doi.org/10.1007/s00445-004-0357-7

Chapter 7

Synthesis

1. Summary and major findings of the thesis

In this project the geochemical signature of various metal sources emitted to the Irish atmosphere is investigated from their deposition onto ombrotrophic peat bogs. This includes the first application of Zn isotopes to reconstruct sources of atmospheric pollution recorded in Irish peat bogs. Three main parts are summarized, each with a distinct focus:

1) The atmospheric record of elemental and Pb isotope evolution in response to local mining, industrial activities and leaded gasoline pollution in eastern Ireland during the 19^{th}-20^{th} century is inferred from ombrotrophic peat bog investigation from the Wicklow mountains (Liffey Head Bog). For this, a chronology for the relevant segment of the monolith could be established via radionuclide dating (^{210}Pb-^{241}Am). Peat sub-samples were investigated for trace element and Pb isotope composition at high spatial resolution (1 cm).
2) Pollution sources of atmospheric Zn and accompanying metals (Ni, Cu, Cr, V) during the last 150 years are investigated in peat bogs from two contrasting settings of a near-urban (Liffey Head Bog, Co. Wicklow) and rural area in Ireland (Brackloon wood, Co. Mayo). Specifically, Zn isotopes in the uppermost part of the near-urban bog trace the origin of the most recent Zn enrichment.
3) Metal release into the atmosphere following the Icelandic Laki 1783-4 volcanic eruption are recorded in specific horizons of woodland peat (Brackloon wood) at the west coast of Ireland. Trace element and S contents of tephra shards and tephra-bearing peat horizons are used to assess if such organic rich peat bogs are suitable geochemical archives of aerosols released from historic volcanic eruptions.

The main findings of this PhD can be summarised as follows:

- The mining and smelting activities in the Wicklow mountains resulted in high perturbations not only in the targeted metals Pb and Zn, but also in other heavy metals and especially Cu, Ag, Cd, Sn, and Sb. These metals occur as impurities

within the mineralisation. In addition, the enrichment of Cu and Cd can be further attributed to the wide use of solid fossil fuels and especially coals during the major mining and smelting period.

- The composition of Pb isotopes in this bog precisely documents the shift from a radiogenic, mining-dominated (19th century-first half of 20th century) to a leaded-gasoline dominated signal (1940-2000 AD), recognized through significantly less radiogenic values between 1970 and 1980 AD.
- Unlike at other sites within the northern hemisphere, the introduction and use of leaded gasoline during the 20th century is not associated with a major peak of Pb pollution at this site. Rather, historical Pb-Zn mining and smelting of local ores were significant. It is thus important to combine trace element and (Pb) isotope information in order to reconstruct historic pollution patterns. This is especially important when two contrasting activities and sources (mining and leaded gasoline) occur simultaneously as it is the case in the Wicklow uplands.

- Peat monoliths from both rural site Brackloon wood and near-urban site Liffey Head, display increasing upward enrichments in Zn, Cr, Ni, V, Cu, and Mo which cannot be attributed to element mobility or plant recycling, but instead mirror increasing aerial injections of these elements from recent human activities. In detail, distinctive metal ratios (Zn/Cd, Ni/Cd, V/Cd, Cu/Cd) together with mixing models point to contrasting sources of these pronounced metal depositions at the two sites: a signal dominated by solid fossil fuels and especially coal in rural areas and a liquid (petrol, oil, diesel) fossil fuel pollution close to the near-urban area of Dublin.
- Zinc isotope analyses of peat subsamples from the near-urban archive (Liffey Head bog) show an evolution from heavy values during the mining period ($\delta^{66/64}$Zn= 0.53 ±0.03‰) to significantly lighter compositions ($\delta^{66/64}$Zn= 0.18±0.03‰) of recently deposited particulate matter. Zinc isotopes correlate with Pb isotopes that are commonly accepted to be highly immobile within peat bogs. This also suggests restricted mobilisation of Zn in the investigated peat section. The light Zn isotope signature in the upper part of the Liffey Head bog is similar to that of road traffic particulates identified elsewhere (Barcelona, London). This can be attributed to an increasing influence of liquid fossil fuel combustion and more recent (past 20 years) diesel use in Ireland. This is analogous to all urban areas in Europe.
- Combined with other information such as obtained from Pb isotope signatures and metal ratios, Zn isotopes are an additional tracer of the atmospheric signal in the Anthropocene.

- Calculated excess enrichments in V, Ti, and Fe in Laki 1783-4 tephra-bearing peat from the Brackloon wood archive cannot unequivocally be attributed to an addition of basaltic cryptotephra at this depth, although higher concentrations of these elements in the separately investigated tephra compared to background peat shards point to this scenario.
- Strong aerosol-related absolute Cu, Cd, Pb, and Zn enrichments as in Greenland ice are not observed in peat. This is attributed to the enhanced background composition of the peat. However, minor enrichments and particularly remarkable correlations between ratios of these elements such as Cu/Cd, Pb/Cd, Pb/Zn and Cu/Zn in the tephra-bearing layer and aerosols deposited in Greenland ice are observed. This suggests a link between the compositions and thus a potentially common volcanic aerosol signal originating from the Laki eruption.
- No striking sulphur concentration peak at the depth of tephra deposition, linkable to the eruption is observed in the Brackloon wood core. This is due to the generally high sulphur background in this bog (0.36-0.4%) and by analogy in all organic rich archives at the Earth's surface. However, excess concentrations of 110 and 170 ppm are still significantly higher than the maximum Laki S signal of 1.12 ppm observed in Greenlandic ice. This may be due to the wind-related direction of the eruptive cloud, which favoured more pronounced volcanic S deposition over Ireland compared to Greenland. The high but ultimately unconstrained atmospheric residence time of S, however, complicates this interpretation.
- Peat bogs have potential as volcanic deposition archives and improve with lower background element contents.

2. Suggestions for future studies

Considering the widespread occurrence of peat across the landscape of Ireland, the number of environmental studies employing peat bogs as natural archives of atmospheric composition is surprisingly scarce. There is thus significant potential to extract further historical and recent geochemical information from these archives. The following topics are suggested for further research:

- To investigate the Zn isotope composition in the Brackloon wood peat bog from the west coast of Ireland, interpreted as emission sink of solid fossil fuel combustion and especially coal combustion. The results can then be compared to the Zn isotope signature in Liffey Head bog, which clearly trace recent pollution from liquid fossil fuels. This investigation would explore the possibilities and

limitations of using Zn isotopes as pollution tracer from different, but genetically related anthropogenic sources.

- Geochemical characterisation of peatlands from the Midland basin to establish a potential E-W pollution transect emerging from anthropogenic activities across the island. Likewise, these investigations would benefit from studies conducted in ombrotrophic peat bogs from the south coast of Ireland. It is expected that these archives will be influenced from long-range metal pollution from continental Europe (i.e., Spain, France).
- Geochemical investigation of peat bogs located along the western coast of Ireland. Investigations of this kind could potentially reveal the timing and magnitude of long-range pollution originating from the North American continent. However, our study has shown that the peat bogs at the west coast are relatively pristine in terms of anthropogenic pollution, possibly an advantage for the next point.
- To explore the geochemical signal of tephra in bulk peat at other sites. This is of particular interest for the tephrostratigrapic community because, i) cryptotephra is usually not visible with the naked eye, and ii) the separation and characterization of the tephra shards from the peat matrix is a very time-consuming process. Beyond these practical reasons, investigating the tephra layer and aerosols of past volcanic eruptions may help us to understand the circulation of volcanic products within the atmosphere, and their local impact. Therefore, our approach was to test this hypothesis in an archive where the presence of a particular tephra layer was previously confirmed (LAKI 1783-4 volcanic eruption). We obtained some interesting results, which are the first of this kind for peat embedded Laki 1783-4 cryptotephra, but we also encountered some difficulties as explained in more detail in Chapter 6. Overall, the high metal background in peat hindered a clear depiction of the tephra signal, and this is likely one of the main reasons for the scarcity of such studies in general. It is suggested that similar studies could be conducted in pristine bogs from e.g., central Sweden, Norway, or Scotland. A central site should minimize the influence of marine aerosols which can be a significant source of metals such as S, Se, Cd, and Zn. As of to date, Laki 1783-4 tephra layer(s) has(ve) been described and investigated in ice cores only. However, the known trajectory of the ash plume clearly indicates that aerosols have also entered the atmosphere of almost all northern European countries. There is thus a huge potential to investigate the footprint of this massive volcanic event at other sites and to compare the findings with those in peat bogs from Ireland (this study). The outcome of such studies could help and/or complement

those investigating atmospheric plume pathways based on computational modelling only.

- To examine the aerosol composition of historic and more recent volcanic eruptions deposited onto ombrotrophic peat bogs growing at the north and west coast of Ireland, which are in the trajectory of Icelandic volcanic plumes directed towards continental Europe. The detection of an eruption-specific geochemical signal (including distinctive metal ratios) in bulk peat could potentially serve as a chronostratigraphic tool if found and correlated to other archives. This however requires a rather pristine environment of the peat archive with little influence from human activities. This criterion becomes increasingly difficult to meet.